Scuola Internazionale Superiore di Studi Avanzati – SISSA

Trieste, Italy

METAL ION REGULATION IN THE CENTRAL NERVOUS SYSTEM AND IN GLUTAMATERGIC SYNAPSES:

ROLE OF THE CELLULAR PRION PROTEIN

Thesis submitted for the degree of Phylosophy Doctor

CANDIDATE

Lisa Gasperini

SUPERVISORS

Prof. Giuseppe Legname, Ph.D.

Dr. Federico Benetti, Ph.D.

Academic year 2011/2012

A Pietro

Declaration

The work described in this thesis has been carried out at Scuola Internazionale Superiore di Studi Avanzati (SISSA), Trieste, Italy, from November 2008 to October 2012.

During my Ph.D. course I have contributed to two publications, a review and a research article, which are included in the *Appendix* section.

INDEX

LIST OF ABBREVIATIONS

Aβ: amyloid β

AD: Alzheimer's disease

ALS: amyotrophic lateral sclerosis

AMPA: α-amino-3-hydroxy-5-methyl-4-isoxazolepropionate

APP: amyloid precursor protein

ATP: adenosine triphosphate

BCA: bicinchoninic acid

BSA: bovine serum albumin

BSE: bovine spongiform encephalopaty

BBB: blood–brain barrier

CA1: *Cornu Ammonis* 1

CA3: *Cornu Ammonis* 3

CaM-BD: calmodulin binding domain

CamkII: Ca^{2+}/calmodulin-dependent protein kinase II

Casp3: caspase 3

CC: charged cluster

Cco: cytochrome C oxidase

Ccs: copper chaperon for superoxide dismutase

CD: central domain

CDP: chronic demyelinating polyneuropathy

CHAPS: 3-[(3-cholamidopropyl)dimethylammonio]-1-propanesulfonate

CICR: calcium-induced calcium release

CJD: Creutzfeldt-Jakob disease

CNS: central nervous system

Cp: ceruloplasmin

Creb: cyclic adenosine monophosphate response element binding protein

CSF: cerebrospinal fluid

Ctr1: copper transporter 1

CWD: chronic wasting disease

DAPI: 4',6-diamidino-2-phenylindole

DG: dentate gyrus

DIV: days *in vitro*

DMF: dimethylformamide

Dmt1: divalent metal transporter 1

Dpl: Doppel

fALS: familial amyotrophic lateral sclerosis

FFI: fatal familial insomnia

Fpn1: ferroportin 1

FtH: ferritin heavy chain

FtL: ferritin light chain

Gapdh: glyceraldehyde 3-phosphate dehydrogenase

GFAP: glial fibrillar acidic protein

GluN(1, 2A-D, 3A-B): NMDA receptor subunit (1, 2A-D, 3A-B)

GPI: glycosylphosphatidylinositol

GSS: Gerstmann, Sträussler and Scheinker syndrome

HC: hydrophobic core

HIF: hypoxia-inducible factor

IRE: iron response element

IRP: iron regulatory protein

MMTS: methyl methanthiosulfonate

MNK: Menkes's disease protein

MPT: mitochondrial permeability transition

Mt: metalothionein

MW: molecular weight

Ncx1: Na+/Ca2+ exchanger

NeuN: neuronal nuclei

NMDA: N-methyl-D-aspartate

NMDAR: NMDA receptor

NO: nitric oxide

nNOS: neuronal nitric oxide synthase

OHC: organotypic hippocampal cultures

OR: octapeptide repeat

PFA: paraformaldehyde

Pka: protein kinase A

Pkc: protein kinase C

Pmca: plasma membrane Ca^{2+} ATPase

PNS: periferal nervous system

PrP^{C}: cellular prion protein

PrP^{Sc}: scrapie prion protein

RBC: red blood cells

RES: reticuloendothelial system

RNS: reactive nitrogen species

ROS: reactive oxygen species

SERCA2: sarco(endo)plasmic reticulum Ca^{2+} ATPase 2

SNO: S-nitrosylation

Sod1: Cu,Zn-dependent superoxide dismutase

Sod2: Mn-dependent superoxide dismutase

Steap3: six transmembrane epithelial antigen of the prostate 3

Tf: transferrin

TfR1: transferrin receptor 1

TGN: *trans*-Golgi network

TSE: transmissible spongiform encephalopathies

WB: Western blot

WND: Wilson's disease protein

WT: wild-type

ZnT: zinc transporter

ABSTRACT

Despite many efforts, the molecular mechanisms underlying the pathophysiology of neurodegenerative disorders have not been fully understood. Results published in literature highlight that different neurodegenerative diseases share common features: protein aggregation in neuronal tissue; oxidation of neuronal tissue mediated by redox-active metal ions interaction with a target protein; and functional demise. So, unveiling the physiological function of protein that aggregate in neurodegenerating tissues, as well as their interplay with metal ions, becomes a prominent issue, in order to understand the etiological trigger and to define a possible therapeutic strategy.

Metal ions are essential elements for cellular processes, but at the same they are potentially dangerous since they can give rise to Fenton reaction and oxidative/nitrosative stress. So, their homeostasis is strictly regulated in each district of the organism, but in particular in the brain. The brain, having the highest metabolic rate and depending predominantly on oxidative metabolism for its energy, has developed fine mechanisms to compartmentalize, distribute, uptake and excrete the different ionic species. Alterations in one of these mechanisms can lead to great neuronal damages, and maybe neurodegenerative disorders.

This work has been focused on the cellular prion protein (PrP^{C}), whose conformational isoform, the scrapie prion protein (PrP^{Sc}) is the causative agent of prion disordes and whose function has not been clearly defined, yet. Metal ions are a common denominator to all the cellular pathways in which PrP^{C} seems to be actively involved. In particular, metal ions homeostasis maintainance, neuroprotection in excitotoxic condition and ionotropic receptor modulation have been studied.

In the first part of the project, PrP^{C} role in metal ion homeostais maintainance has been investigated. To this aim, copper, manganese, zinc and iron content, as well as metal binding proteins expression have been measured in a PrP knockout murine model, compared to wild-type. The results describe the global rearrangement occurring in the expression of metal binding proteins to maintain trace metals homeostasis, trying to compensate PrP^{C} absence. At the same time, a pronounced decrease in Ceruloplasmin ferroxidase activity has been detected in PrP null mouse serum, pointing out a global impairment in copper metabolism in PrP^{C} absence.

In the second part of the project, the importance of the interaction between PrP^{C} and copper ions in excitotoxic conditions and in synapses functionality has been studied. It has been published that PrP null mice show higher levels of neuronal cell death in stressful conditions and when subjected to toxic treatment with glutamate receptor agonists. Moreover, these mice show altered kinetics of N-methyl-D-aspartate (NMDA) receptor current. These alterations appears to be due to an inhibitory regulation that PrP^{C} exerts on NMDA receptors via copper ions, lacking in PrP null hippocampi. First, the

enhanced suceptibility to excitotoxicity of PrP knockout mice has been verified and characterised in organotypic hippocampal cultures upon treatment with NMDA. Higher neuronal cell death levels have been detected in all the investigated hippocampal regions. To identify which cellular regulatory mechanism is alterd in PrP^C absence, the expression of the proteins mainly involved in excitotoxicity has been compared between PrP knockout and wild-type hippocampi. Among other minor differences, a different modulation of calcium transporters expression has been identified in PrP knockout hippocampi and brains. This global alteration appears to be necessary to maintain calcium homeostasis, since calcium content measurements did not reveal any strong difference between PrP null and wild-type samples.

NMDA receptors can be S-nitrosylated on extracellular cysteines and this reaction is always inhibitory. S-nytrosilation requires an electron acceptor to occur, for this reason copper ions are often involved in these kind of reactions. Moreover, copper ions are known to modulate NMDA receptor activity, but the precise mechanism has not been described, yet. Since PrP^C is known to support the S-nitrosylation of other membrane proteins, the S-nitrosylation levels of NMDA receptor subunits GluN1 and GluN2A have been measured in PrP knockout hippocampi from adult mice and compared to wild-type ones. Results show that the S-nitrosylated fractions of both GluN1 and GluN2A are reduced in PrP absence. So, this reveals that PrP^C modulates NMDA receptor activity providing the copper ions necessary to support their inhibitory S-nitrosylation reaction. Through this mechanism, PrP^C contributes to inhibit NMDA receptor currents, as well as to protect neurons in excitotoxic conditions.

INTRODUCTION

During last century, neurodegenerative diseases have become a prominent health issue because of their increasing impact on modern society. Despite many efforts, the molecular mechanisms responsible for the pathophysiology of this group of disorders have not been fully understood. In a review published in the year 2000, it was observed that all neurodegenerative diseases share common features: protein aggregation in neuronal tissue; oxidation of neuronal tissue mediated by redox-active metal ions interaction with a target protein; and functional demise (Bush, 2000). The author proposed that at least certain disorders, like Alzheimer's disease (AD), familial amyotrophic lateral sclerosis (fALS) and Creutzfeldt-Jakob disease (CJD), are caused by abnormal interaction of metals that are enriched in neuronal tissue with specific proteins that are vulnerable to such interactions. According to the author's opinion, these abnormal metal-protein interactions are the etiological trigger of such disorders, together with the generation of microanatomical stress that triggers the damage of the cell site where the abnormal metal-protein interaction occurs. The author's theory is summarized in Table 1 (modified from (Bush, 2000)).

Cu/Fe-mediated degenerative diseases				
Specific protein		Adverse metal	Specific tissue	Specific disease
Non-pathological	Pathological			
APP	Aβ	Cu, Fe, possible loss of Zn	Neocortex	AD
PrP^{C}	PrP^{Sc}	Cu	Neocortex	CJD
SOD1	SOD1	Cu, loss of Zn	Motor neuron	fALS
α-Crystallin	α-Crystallin	Cu, Fe	Lens	Cataracts

Table 1. List of the neurodegenerative diseases that share the same molecular pathogenic mechanism proposed in (Bush, 2000). Amyloid precursor protein (APP), Amyloid β (Aβ), cellular Prion Protein (PrP^{C}) scrapie Prion Protein (PrP^{Sc}), Superoxide dismutase 1 (SOD1).

Among all, prion disorders represent a prominent biological and pathological question. This class of diseases also known as transmissible spongiform encephalopaties (TSEs) can be either sporadic or genetic or infective (Prusiner, 2001). Infectivity is properly the peculiar characteristic of prions. Prion diseases include bovine spongiform encephalopaty (BSE) in cattle, scrapie in ovine, chronic wasting disease (CWD) in deer, moose and elk, and Kuru, CJD, fatal familial insomnia (FFI) and Gerstmann, Sträussler and Scheinker syndrome (GSS) in humans (Table 2 (Aguzzi et al., 2004)).

Spectrum of prion diseases of humans and animals

Prion disease	Natural host species	Etiology
sCJD	Humans	Unknown (somatic *PRNP* mutation?)
Familial Creutzfeldt-Jakob disease (fCJD)	Humans	Familial (germ line *PRNP* mutation)
Iatrogenic Creutzfeldt-Jakob disease (iCJD)	Humans	Surgical procedures (infection)
vCJD	Humans	Ingestion of BSE-contaminated food; transfusion medicine (infection)
Kuru	Humans	Ingestion, ritualistic cannibalism (infection)
Fatal Familial Insomnia (FFI)	Humans	Familial (germ line *PRNP* mutation)
Gerstmann-Sträussler-Scheinker Syndrome	Humans	Familial (germ line *PRNP* mutation)
Scrapie	Sheep, goats	Infection, natural; mode of transmission unclear
Chronic Wasting Disease (CWD)	Deer, Elk	Infection; mode of transmission unclear
BSE	Cattle	Ingestion of BSE-contaminated feed (infection)
Transmissible mink encephalopathy	Mink	Ingestion (infection); Origin unclear
Feline spongiform encephalopathy	Cats	Ingestion of BSE-contaminated feed (infection)
Spongiform encephalopathy of zoo animals	Zoologic bovids, primates	Ingestion of BSE-contaminated feed (infection)

Table 2. Spectrum of prion diseases of human and animals (Aguzzi et al., 2004)

All prion diseases affect primarly the nervous system, but the clinical features can be variable according to the different TSEs forms. These differences regard the etiology (whether sporadic, genetic or infective), the incidence of the disease, the brain region affected by replicating prions deposits, the manifested clinical symptoms and the disease time-course (Prusiner, 1992; Prusiner and DeArmond, 1994). Despite these differences, all TSEs are generally characterized by spongiosis, resulting in brain tissue vacuolated appearance, neuronal loss and diffused astrocytic gliosis (Figure 1 (Aguzzi et al., 2001)). At the present, all prions diseases are fatal, progressive and without cure, dramatic features shared by all others neurodegenerative disorders.

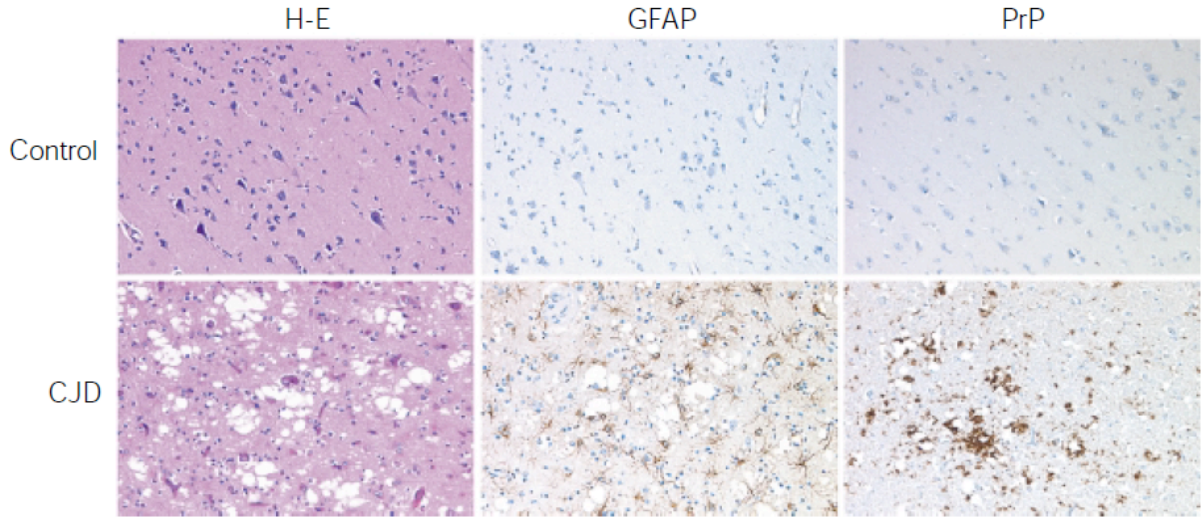

Figure 1. Neuropathological features of TSEs. Histological and immunohistochemical analysis of frontal cortex samples from the brain of a patient who died of non-cerebral causes (upper row) and a patient suffering from CJD (lower row). Brain sections were stained with hematoxylin-eosin (H-E, left panels), with antibodies against glial fibrillar acidic protein (GFAP, middle panels) and with antibodies against the prion protein (PrP, right panels). Neuronal loss and prominent spongiosis are visible in the H-E stain. Strong proliferation of reactive astrocytes (gliosis) and perivacuolar prion protein deposits are detectable in the GFAP and PrP immunostaining of the CJD brain samples (from Aguzzi et al., 2001).

PRION CONCEPT

The term "prion" was coined by Prusiner in 1982 and stands for "proteinaceus infectious particle", to underline the exclusively proteinaceous property of these disorders causative, infective agent: this proposition lead to the so called "protein-only hypothesis" (Prusiner, 1982). According to Prusiner's theory, the infective particle responsible for scrapie disease is primarily composed of a protein able to transmit the infection and replicate itself without requirement of nucleic acids. The protein identification and the sequencing revealed it was encoded by an endogenous cellular gene (in mouse *Prnp*, in humans *PRNP*) whose translational product was called cellular prion protein (PrP^{C}) (Oesch et al., 1985). Prions are the product of a posttranslational conformational remodelling event converting PrP^{C} into the disease-associated infectious form PrP^{Sc}. PrP^{C} and PrP^{Sc} differ for some biochemical characteristics: PrP^{C} is mainly α-helical, while PrP^{Sc} is highly enriched in β-sheet (Caughey et al., 1991; Gasset et al., 1993). In prion disease inherited forms, a genetic mutation in the PrP encoding gene occurs and destabilizes the protein tertiary structure, promoting its conversion to the scrapie form as well as the aggregation process. In infective forms, a preformed PrP^{Sc}-aggregate directly triggers the conversion of endogenous PrP^{C}. In sporadic disease, PrP^{C} tertiary structure is likely to be perturbed by unknown biochemical modifications, favouring PrP^{Sc} formation. However, the mechanisms underlying sporadic TSEs are yet to be clarified (Prusiner, 1991, 1994).

PRION TOXICITY

The mechanism by which prions damage the central nervous system (CNS) remains unknown. The infectious particle may correspond to either a single molecule of a prion or a small PrP^{Sc} oligomer, but which species triggers the toxic effects is still under debate (Aguzzi and Falsig, 2012). In the case of prion diseases, it is known that PrP^{C} is required for the pathology development (Bueler et al., 1993; Watts and Westaway, 2007). Nevertheless, mice expressing low levels of glycosylphosphatidylinositol (GPI) lacking PrP^{C}, named PrP(ΔGPI), remained healthy and exhibited little or no neuropathologic changes, while neuronal expression of PrP(ΔGPI) at 1.7× levels compared with PrP^{C} expression in wild-type mice resulted in late-onset, spontaneous neurologic illness accompanied by a profound CNS amyloidosis resembling GSS (Chesebro et al., 2005; Stohr et al., 2011). Moreover, the pathology can be reversed by acute PrP^{C} ablation *in vivo* during the neurotoxic phase of prion replication (Mallucci et al., 2003) leading to a hypothetical switch off of PrP^{C} endogenous expression as a cure to prion diseases. In light of all these findings, it is still unclear whether prion toxicity is due either to a gain-of-function of oligomeric species or to a lack-of-function of PrP^{C}. To answer all these questions, it is crucial to understand which is PrP^{C} physiological function.

THE CELLULAR PRION PROTEIN - PrP^C

The cellular prion protein, PrP^C, is an endogenously encoded protein composed of 254 amino acids in mouse. As described in Figure 2, it is a sialoglycoprotein that is attached to the outer leaf of the plasma membrane via a C-terminal GPI anchor (Stahl et al., 1990). It can be expressed in un-, mono- or di-glycosilated forms, corresponding to the variable occupancy of the residues Asn180 and Asn196 in mice (Haraguchi et al., 1989). The globular domain of the protein contains three α-helices interspersed with an antiparallel β-sheet. One disulfide bridge is present between Cys178 and Cys213. The N-terminal portion is a flexible, unstructured domain containing the octapeptide repeat (OR) that is preceded and followed by two positively charged clusters, CC_1 and CC_2. The N- and the C-terminals are linked by a hydrophobic amino acidic stretch, also named hydrophobic core (HC) (Zahn et al., 2000).

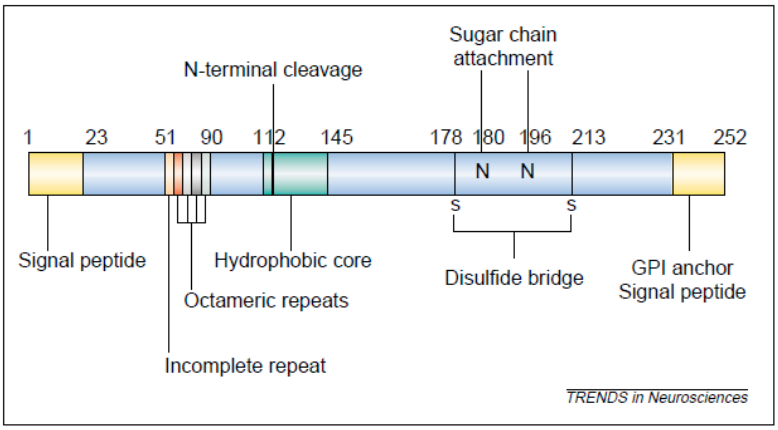

Figure 2. Mouse prion protein scheme. This protein is anchored to the cell membrane by a glycosylphosphatidylinositol (GPI) anchor. The signal peptide for entry into the endoplasmic reticulum and the GPI signal peptide are cleaved before the protein reaches the cell surface. Glycosylation can occur on one, two or none of the Asn residues indicated. A hydrophobic region envelops a cleavage point (N-terminal cleavage) where the protein is cleaved during normal metabolic breakdown. A disulfide bridge links two regions of the protein that form separate α-helices in the three dimensional structure of the protein. The complete octameric repeats can bind up to four copper atoms, most mammals also have an incomplete repeat located upstream of this (Brown, 2001).

COPPER- BINDING TO PrP^C

One of the most salient features of PrP^C is its ability to bind divalent cations such as copper (Cu) ions (Arena et al., 2012). The major Cu binding site has been identified at the N-terminus OR domain composed of four sequential repeats of the sequence PHGGGWGQ between residues 59-90, while 51-58 residues constitute a nonarepeat lacking the histidine residue (Brown et al., 1997a; Hornshaw et al., 1995). Cu binding importance for PrP^C physiological function is reflected in the high OR conservation degree among different mammalian and avian species (Vassallo and Herms, 2003). Beside Cu, the OR

region is able to bind other divalent cations like Zn, Ni, Fe and Mn (Jackson et al., 2001; Singh et al., 2010; Stockel et al., 1998). However, at physiological pH Cu shows the highest binding affinity and specific Cu concentrations are sensed by transitioning from a multi-His binding mode at low Cu levels to a single-His, amide nitrogen bond at high Cu levels (Chattopadhyay et al., 2005; Liu et al., 2011). The OR region cooperatively binds up to four Cu ions with 5-8μM affinity (Kramer et al., 2001; Whittal et al., 2000). These values are compatible with the physiological Cu concentration released in the synaptic cleft during synaptic vesicle release (15μM) and during neuronal depolarization (100-300μM) (Hartter and Barnea, 1988). Moreover, histidines at positions 96 and 111 create a high affinity Cu binding site (10^{-14}M) (Jackson et al., 2001; Jones et al., 2004). Both the low and high occupancy copper binding mode support the reduction of Cu(II) to Cu(I), thus, protecting against the production of reactive oxygen species from unregulated Fenton type reactions (Liu et al., 2011). Despite many studies trying to understand the physiological relevance of PrP^C Cu binding, a defined consensus has been elusive.

PrP^C Expression and Subcellular Localization

Though PrP^C is mostly expressed in the nervous system, it is also present in many non-neuronal tissues, for instance blood lymphocytes, gastroepithelial cells, heart, kidney and muscles (Fournier et al., 1998; Horiuchi et al., 1995). This pattern of expression implies that PrP^C function is not limited to the nervous tissue, despite the fact that the high expression in the CNS suggests a special relevance for neurons. The protein PrP^C is particularly abundant in the developing and in the mature nervous system and it is expressed in both neuronal and glial cells. PrP^C expression starts from early embryonic stages and is developmentally regulated (Benvegnu et al., 2010; Lazarini et al., 1991; Manson et al., 1992; Mobley et al., 1988; Sales et al., 2002). In the brain, its expression increases during the initial postnatal weeks up to the synaptogenetic process completion (coincident with one month of age), and afterwards it remains stable at plateau during adulthood. In particular, the olfactory bulb and the hippocampus, which are both characterized by neuronal renewal also in adulthood, show the higher PrP^C expression levels (Sales et al., 2002). The protein levels may decrease with aging.

The polypeptide expression levels vary among distinct brain regions, cell types and neurochemical phenotypes (Benvegnu et al., 2010; Linden et al., 2008). While several controversial results concerning PrP^C subcellular localization (cell body, axonal, dendritic, synaptic compartment) have been reported, it is widely accepted that its expression is concentrated at synapses, both presynaptically and postsynaptically (Fournier et al., 1998; Haeberle et al., 2000; Herms et al., 1999; Linden et al., 2008; Moya et al., 2000; Sales et al., 1998). Many lines of evidence suggest that PrP^C transport along the axon to the presynaptic or the postsynaptic bouton depends on the different glycoforms of the protein (Rodolfo et al., 1999). Moreover, the diglycosilated PrP^C can be isolated in detergent insoluble rafts

(Naslavsky et al., 1997). These are specialized plasma membrane areas enriched in cholesterol, sphingolipids and proteins, functioning in membrane trafficking and signalling (Simons and Ikonen, 1997). Accumulating evidence has shown that both the presynaptic and postsynaptic sites are highly enriched in lipid rafts, which are likely to organize and maintain synaptic proteins in their precise localization. For example, both ionotropic and metabotropic glutamate receptor are specifically localized in rafts (Sebastiao et al., 2013).

PrP KNOCKOUT AND TRANSGENIC MURINE MODELS

To understand PrP^C physiological function, several knockout and transgenic murine lines for the *Prnp* gene have been created. The first generation of knockout mice, namely $Prnp^{0/0}$ (ZurichI) and $Prnp^{-/-}$ (Edimburgh) (Bueler et al., 1992; Manson et al., 1994) showed normal development as well as no pathological signs during their lifespan. Subsequently, other three $Prnp^{0/0}$ were created, namely Ngsk $Prnp^{-/-}$ (Nagasaki), Rcm0 and $Prnp^{-/-}$(Zurich II), which revealed loss of Purkinje cells and cerebellar degeneration (Moore et al., 1999; Rossi et al., 2001; Sakaguchi et al., 1996). These results were due to another gene, *Prnd*, located 16kb downstream to *Prnp* gene, which resulted to be overexpressed in Ngsk, Rcm0 and ZurichII, but not in ZurichI and Edimburgh (Moore et al., 1999). This gene encodes for a protein, named Doppel (Dpl, *Mus musculus* nomenclature), which is not usually expressed in the brain and resulted expressed in the second generation of PrP knockout mice, because of an accidental deletion of a splice acceptor site, leading to exon skipping phenomenon and, in turn, to the generation of chimeric *Prnp-Prnd* mRNA. This brought Dpl expression under the control of *Prnp* promoter, so highly expressed in the brain. Dpl ectopic expression in the brain causes cerebellar granule ataxia and degeneration that could be rescued by *Prnp* gene re-introduction (Nishida et al., 1999). This latter result shows PrP^C acting as an antagonist of Dpl, counteracting its neurotoxic effects *in vivo* and *in vitro* (Didonna et al., 2012).

Additionally, murine models carrying PrP^C deletion mutants have been created aiming at identifying functional domains of the protein (Figure 3). For example, an initial report of $Prnp^{0/0}$ mice expressing PrP^C lacking amino acid residues 32-121 or 32-134 (PrPΔ32-121 and PrPΔ32-134) revealed how the expression of these truncated PrP caused severe ataxia and neuronal cell death limited to the granular layer of the cerebellum, as well as widespread gliosis and demyelination in the brain stem, similar to the phenotype elicited by Dpl ectopic expression (Shmerling et al., 1998). Gliosis and demyelination could be rescued by oligodendrocyte-specific PrP^C expression, but not cerebellar neurodegeneration. Viceversa, neuron-specific PrP^C expression can partially rescue cerebellar granule cell degeneration, but not demyelination (Radovanovic et al., 2005). Thus, white matter disease and cerebellar granule cell degeneration are independent and distinct in these models and wild-type PrP^C expression is required in

both neurons and glia to completely revert the degenerative phenotype. Neurodegeneration and myelin damage are two distinct pathological phenotypes induced by distinct PrP mutants. Mice on a *Prnp*$^{0/0}$ background and expressing PrP^{C} lacking amino acid residues 32-93 (PrPΔ32-93) within the OR region do not show pathological phenotypes: this may indicate that the lack of the central domain (CD, residues 94-134) creates a toxic protein isoform. The CD domain includes the positively charged CC2 cluster and the HC core, previously described. To analyse the two domains different contributions to the pathological phenotype, other *Prnp* transgenic models have been created deleting the entire central domain, PrPΔ94-134 (Baumann et al., 2007). Mice entirely lacking CD showed a drastic neuropathological phenotype with vacuolar degeneration, astrogliosis, extensive central and peripheral nervous system (PNS) and death within 20-30 days (Baumann et al., 2007). Despite the similar myelin damage, this model lacks cerebellar degeneration observed in PrPΔ32-121 and PrPΔ32-134 expressing mice. Furthermore, mice lacking residues 105-125 (referred to as ΔCR) develop an even more dramatic phenotype, developing a severe neurodegeneration that becomes lethal within the first post-natal week (Li et al., 2007). Expression of ΔCR PrP induces a strong ion channel activity in transfected cells that can be detected by patch-clamping techniques (Solomon et al., 2010; Solomon et al., 2011). Each of these phenotypes can be rescued co-expressing the wild-type PrP^{C} in a dose-dependent manner according to the mutant PrP expression level and the severity of the pathology elicited (Baumann et al., 2007; Li et al., 2007). According to the model proposed by Baumann and colleagues and shown in Figure 4, PrP^{C} and its deletion mutants can compete for a common ligand, maybe a receptor that regulate signal transduction.

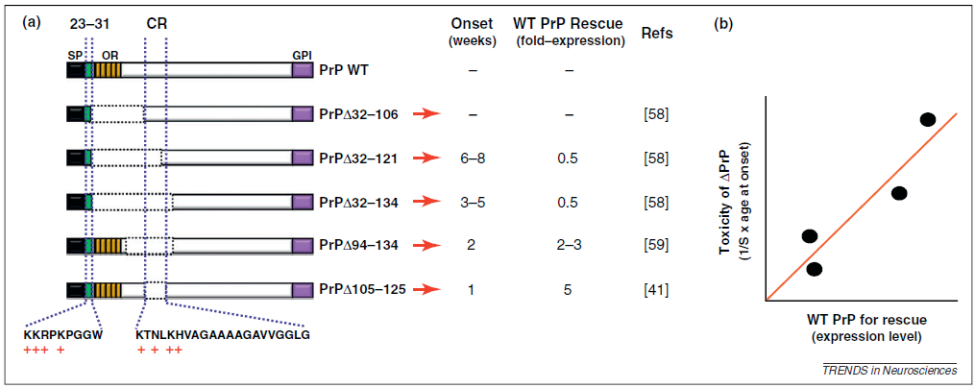

Figure 3. Deletions within the central region of the prion protein (PrP) are associated with neurotoxicity in transgenic mice. (a) Deletions up to residue 106 have no adverse effect (Shmerling et al., 1998), whereas deletions extending to residues 121 or 134 cause spontaneous neurodegenerative illness in the absence of endogenous PrP^{C} (Shmerling et al., 1998). Additional deletions (Δ94-134 (Baumann et al., 2007) and Δ105-125 (Li et al., 2007)) narrow the critical neurotoxicity-determining region to a highly conserved segment of 21 amino acids in the central region (105-125). Schematics show the structures of wild-type (WT) mouse PrP and each of the deletion mutants (with the deleted region indicated by broken lines). The column labelled "Onset" gives the age (in weeks) at which spontaneous neurological illness occurs in mice expressing the corresponding deletion mutant. The column labelled "WT PrP rescue" gives the fold expression WT PrPC needed to prevent the appearance of neurological illness. A minus symbol (-) indicated that no spontaneous disease is observed. (b) The graph, which is a representation of the data shown in the first two columns, shows the inverse correlation between age of onset in the different mouse lines and the amount of WT PrP expression required for rescuing the neurological phenotype (Biasini et al., 2012).

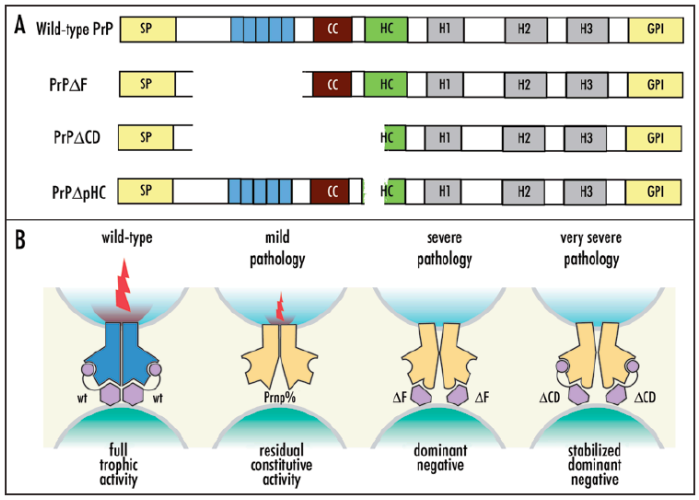

Figure 4. A model showing the effects of PrP^{C} deletion mutants. (A) Schematic diagram of wild-type PrP^{C} and its several deletion mutants. SP, signal peptide; octarepeats are indicated in blue; CC, charged cluster; HC, hydrophobic core; H1, H2, H3 Helix 1, 2 and 3, respectively; GPI, GPI-anchor addition sequence (B). PrP (purple) consist of a globular C-terminal domain (hexagon) and a N-terminal flexible tail (arch) encompassing the octapeptide repeats (circle). The model rests on the following assumptions: (1) PrP activates a hitherto unidentified receptor (PrP_R) which transmits myelin maintainence signal (flashes); (2) in the absence of PrP, PrP_R exerts some residual activity, either constitutively or by recruiting a surrogate ligand; (3) the activity of PrP and its mutants requires homo- or heterodimerization, and induces dimerization of PrP_R; and (4) PrP dimers containing PrPΔCD or PrPΔCD trap PrP_R in an inactive dominat-negative state (from (Steele et al., 2007)).

PHYSIOLOGICAL FUNCTION OF PrP^C

Though the precise PrP^C role in cellular physiology has not properly been established, this protein has been linked to many cellular processes in the nervous system: neuronal survival, neurite outgrowth, synapse formation, maintenance and functionality, as well as formation and maintenance of myelinated fibers (Figure 5 (Aguzzi et al., 2008) and Table 3 (Caughey and Baron, 2006)). Another function that has been proposed for PrP^C concerns a role in metal ion homeostasis and metabolism (Singh et al., 2009b; Singh et al., 2010).

Hereafter, some of the proposed functions of PrP^C will be described, according to the topic and the aim of this Ph.D. project and thesis.

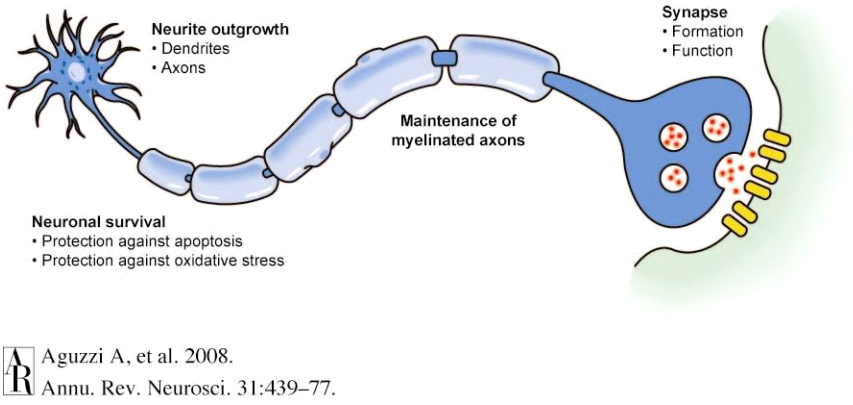

Aguzzi A, et al. 2008.
Annu. Rev. Neurosci. 31:439–77.

Figure 5. Physiological processes involving PrP^C. Several processes in the nervous system have been influenced by PrP^C. Neurite ougrowth, including growth of axons and dendrites, was observed to be reuced in neurons lacking PrP^C. PrP^C has often been reported to promote neuronal survival, in particular following apoptotic or oxidative stress. Cerebellar granule cell apoptosis was observed in mice expressing toxic N-terminal deletion mutants of PrP. In addition, tha latter transgenic mice show an impaired maintenance of myelinated axons in the white matter. Another site of PrP^C action might be the synapse, which is often affected in the first stage of prion diseases and whose formation was found to be reduced in neuronal cultures devoid of PrP^C. Furthermore, electrophysiological studies indicate a role of PrP^C in synapse function, especially in neurotrasmitter release (Aguzzi et al., 2008).

Table 1 | The cellular distribution and activities of PrP^C in cell types in which known or putative functions have been described

Cell type	Process	Function	Mechanisms, ligands and pathways
Neuron	Neuritogenesis	Adhesion, signalling	Recruits NCAM into rafts to allow it to activate Fyn kinase[35], which mediates intracellular signalling pathways
			STI-1 binding induces activation of mitogen-activated protein kinase[36]
			Binds LRP/LR and HSPG by means of separate sites[60]
			Binds laminin[74]
	Synaptogenesis, polarization	Signalling	PrP^C acts as a growth factor, activating multiple pathways[38]
	Survival, trophic effects	Anti-apoptotic	Interacts with BAX[31], STI1 (ref. 36) and NCAM[75]
		Pro-apoptotic	Binds to anti-apoptotic Bcl-2 (for a review, see ref. 31)
			Crosslinks with anti-PrP antibody[76]
			Increases levels of p53 (reviewed in ref. 31)
	Copper binding	Copper endocytosis	Induces PrP^C to aggregate, exit from rafts and undergo clathrin-dependent endocytosis[77]
		Copper homeostasis	Maintains appropriate copper levels at the presynaptic membrane and during conditions of oxidative stress (reviewed in ref. 34)
		SOD activity*	Copper-bound PrP^C has SOD activity (reviewed in ref. 34)
	Redox homeostasis	Signalling	Induces NADPH-oxidase dependent ROS through Fyn activation[78]
Neural stem cells	Neurogenesis	Unknown	Increases cell proliferation in neurogenic regions[46]
	Differentiation	Unknown	PrP^C levels positively influence differentiation[46]
Haematopoietic stem cells	Long-term renewal	Anti-apoptotic? Homing?	Possible mechanisms: transduce cell survival signals; cell-adhesion activity targets cells to appropriate environment; or function as co-receptors for hormones affecting HSC activity[45]
T cells	Activation	Signalling?	PrP^C upregulation upon mitogen-induced activation[79]
	Development	Antioxidant	Copper binding in thymus[80]
Leukocytes	Differentiation	Unknown	PrP^C expression by lymphocyte/monocyte lineage[81]
	Phagocytosis	Unknown	PrP^C modulates phagocytosis[44]
	Inflammatory response	Homing	PrP^C alters leukocyte recruitment to site of inflammation[44]

*Some argue that PrP does not exhibit SOD activity.

Table 3. The cellular distribution and activities of PrP^C in cell types in which known or putative functions have been described (Caughey and Baron, 2006).

FUNCTIONS OF PrP^C AND METALS INTERACTION

The importance of understanding the interaction between PrP^C and metals relies on the physiological and pathological implications it has. In normal conditions, PrP^C mediates Cu and Fe uptake (Brown, 2003; Singh et al., 2009b). PrP^{Sc} has a higher affinity for Ni, decreasing the binding of Zn and Mn (Jackson et al., 2001). All essential metals metabolic pathways are strictly related and interconnected. So, for instance, it is likely that Cu and Fe uptake is impaired in prion disease due to this shift in metal binding affinity of PrP^{Sc}.

The PrP^C-Cu interaction is the best characterized, as described above. Observations from neuroblastoma cells suggest that PrP^C contributes to Cu uptake since it binds extracellular Cu ions and delivers them to the endocytic compartment, thus increasing antioxidant enzymes activity (Brown and Harris, 2003; Pauly and Harris, 1998; Rachidi et al., 2003). Moreover, the OR region plays a role in the reduction of Cu(II) to Cu(I) before transporting the metal across the endosomal membrane to the cytosol (Miura et al., 2005). Thus, PrP^Cmay function as a Cu uptake and delivery protein, although results concerning Cu content in the brain of wild-type, PrP^C null, PrP^C overexpressing and scrapie infected mice reported in literature are discordant, leaving PrP^C influence on the global brain Cu

content an unsettled matter (Singh et al., 2010). For instance, some results show no differences in Cu content upon PrP^C ablation (Giese et al., 2005; Waggoner et al., 2000), but others highlight a reduced Cu amount in the CNS of PrP^C null mice (Brown et al., 1997a; Brown et al., 1998). Concerning the role of the protein at the synapses, it has been proposed by Vassallo and Herms in 2003 that PrP^C acts as a buffer of Cu(II) ions released in the synaptic cleft. In this way, PrP^C protects synapses from Fenton redox reaction that Cu(II) can produce. Furthermore, in the presynaptic bouton, PrP^C has a role in the redistribution of Cu ions that are released together with neurotransmitters, contributing to synaptosomal Cu concentration maintenance. This likely occurs by transferring of Cu to membrane transporters that have higher affinity compared to PrP^C. A similar mechanism may occur in the postsynaptic bouton where PrP^C is also expressed (Moya et al., 2000) and Cu ions are released from the *trans*-Golgi network (TGN) upon activation of glutamate ionotropic receptors (Schlief et al., 2005; Schlief et al., 2006). Vassallo and Herms hypothesis explains why Cu content in *Prnp*$^{0/0}$ mice is almost unchanged: PrP^C absence affects Cu distribution but not its overall content (Vassallo and Herms, 2003).

Using cells expressing PrP^C mutants and *Prnp*$^{0/0}$ mice, it has been shown that the protein has a fundamental role in Fe metabolism (Singh et al., 2009b; Singh et al., 2009c). PrP null cells have a lower Fe content as well as a lower ferritin saturation level. Even increasing Fe concentration in the extracellular medium, Fe uptake and storage remains unchanged, thus indicating a dominant effect of PrP^C ablation. On the contrary, cells overexpressing PrP^C increase the intracellular Fe pool, saturating ferritin molecules. In addition, *Prnp*$^{0/0}$ mice show a lower Fe content in the brain, probably due to an impaired intestinal absorption, while, re-establishing PrP^C expression in PrP^C null mice, the phenotype is reversed indicating the specificity of PrP^C functional role (Singh et al., 2009b). Presently, it has not been clarified whether PrP^C mediates Fe uptake by using a novel pathway or by interacting with conventional Fe uptake and transport pathways (Singh et al., 2010). It has been proposed that it can interact with the transferrin/transferrin receptor pathway or functions as a ferric reductase, facilitating the transport of Fe(III) from endosomes to cytosolic ferritin (Singh et al., 2009c). However, since Fe content is just mildly affected in *Prnp*$^{0/0}$ mice, it is likely that PrP^C absence modulates others Fe uptake proteins or compensatory mechanisms occur. Concerning a direct binding between PrP^C and Fe, results are still contradictory and preliminary (Singh et al., 2010).

In 2010, Aguzzi's group reported that PrP^C expression on neuronal cells, but not on Schwann's cells, is fundamental to maintain myelination and prevent chronic demyelinating polyneuropathy (CDP) in the PNS (Bremer et al., 2010). Their results better characterised what previously observed by Nishida and colleagues (Nishida et al., 1999). It has been known that metal ions, in particular Cu and Fe are necessary to both myelin formation and maintainance (Benetti et al., 2010; Skripuletz et al., 2008). So, it

is likely that PrP^C function in these processes can be due to both a direct molecular mechanism, as suggested in (Benvegnu et al., 2011), and to an alteration in Cu and Fe homeostasis that triggers CDP.

Though with a lower affinity, PrP^C also binds Zn. However, in cell models Zn is able to alter the distribution of PrP^C-Cu complex (Watt and Hooper, 2003), indicating that, given the relevant Zn concentration in the brain, PrP^C-Zn interaction may be more significant than expected (Kenward et al., 2007; Qin et al., 2002; Walter et al., 2007; Watt and Hooper, 2003). Concerning PrP^C role in Zn uptake, controversial results has been published. Rachidi and colleagues observed that PrP^C protects from Zn toxicity in cell cultures without affecting Zn uptake. Thus, a Zn re-localization effect of PrP^C expression together with an increased expression of metallothioneins (Mt) were supposed to mediate protection from Zn toxicity (Rachidi et al., 2009). On the contrary, Watt and colleagues recently reported that PrP^C enhances the uptake of zinc into neuronal cells (Watt et al., 2012). The transport requires PrP^C ORs and amino-terminal polybasic region, but not its endocytosis. PrP^C-mediated Zn uptake occurs upon activation of α-amino-3-hydroxy-5-methyl-4-isoxazolepropionate (AMPA) receptors. Evidences of a physiological consequence of this process were also provided: Zn-sensitive intracellular tyrosine phosphatase activity is decreased in wild-type cells and increased in the brains of PrP^C null mice. Moreover, PrP^C-mediated Zn uptake is ablated in cells expressing familial associated mutants of the protein and in prion-infected cells. These data suggest that alterations in Zn uptake may contribute to neurodegeneration in prion and other neurodegenerative diseases.

Recombinant PrP has been shown to bind Mn in place of Cu with the same or weaker affinity on the N-terminal OR region, and Mn^{2+} binds also at a second site near His 96 or His111 (Brown et al., 2000; Jackson, 2001). However, after binding, Mn switches PrP^C conformation into a PrP^{Sc} similar form with increased β-sheet content and reduced antioxidant activity (Brown et al., 2000; Tsenkova et al., 2004). A switch of PrP^C to a protease-resistant and detergent-isoluble conformation has been also observed after Cu addition to PrP^C extracted from transgenic mouse brain and transfected cells (Quaglio et al., 2001). As in case of Mn, Cu-treated PrP^C resulted to be structurally distinct from PrP^{Sc}. The authors observed that metal binding to the N-terminal region of PrP affects its biochemical properties. This suggests a potential roles in prion diseases and in the physiological function of PrP^C.

ESSENTIAL METALS METABOLISM AND HOMEOSTASIS

Biometals are essential for a wide range of biological functions, from electrochemical gradients generation to enzyme active sites formation. Based on instability constant values of their complexes with biological ligands, metals are classified as weak (e.g. sodium and potassium, $K_{inst} \geq 10^{-1}$ M), moderate (e.g. calcium and magnesium, $K_{inst} \geq 10^{-8}$ M) and strong (e.g. transition metals, $K_{inst} \leq 10^{-15}$

M). Both alkali metals and alkaline earth metal, also called *hard* ions, generates weak and moderate complexes because of their poor polarizability. They give rise to highly dynamic complexes, preferring oxygen over nitrogen and sulphur ligands. On the contrary, transition metals, also called *soft* ions and characterized by multiple valences, present an incomplete inner electron shell that is highly polarizable, allowing stable complexes formation, such as those of prosthetic groups. That is the reason why transition metals prefer nitrogen and sulphur ligands. While *hard* ions are indicated as macronutrients because of their large amounts in biological systems, *soft* ions are known as micronutrients. However, iron, copper, zinc, manganese, cobalt, nickel, chromium and molybdenum provide essential biochemical activities and structural scaffolding to a multitude of proteins including enzymes and other cellular constituents. Moreover, free ionic or exchangeable Zn and Cu are released in the glutamatergic synaptic cleft of hippocampus and cortex to inhibit N-Methyl-D-Aspartate (NMDA) receptor activity (Schlief et al., 2005). At the same time, increasing evidences suggest that Zn can be a second messenger, like calcium (Frederickson et al., 2005).

Iron is the most abundant transition metal and it is used by both Fe-sulphur cluster and porphyrin conjugates containing proteins, primarily heme. Fe-containing proteins include haemoglobin and myoglobin which function in oxygen transport, cytochromes which are necessary for both respiration and detoxification, aconitase and other proteins which are required for oxidative metabolism, ribonucleotide reductase which catalyzes the rate-limiting step in DNA synthesis, and many others (Hower et al., 2009). Iron is required in different CNS metabolic processes as neurotransmitter production or nitric oxide metabolism (Ponka, 1999). Its oxidation states range from –II to +VI, though the two most biologically relevant are Fe(II) and Fe(III) (Bleackley and Macgillivray, 2011). Iron, as the other transition metals, is a redox active element and it can promote free radicals formation through the Fenton reaction, with potential highly toxic effects. To minimize this risk, organisms have developed efficient systems for properly uptake, transport, load on proteins and store Fe ions, summarized in Figure 6 (Kambe et al., 2008). Considering the whole organism, Fe homeostasis is regulated at absorption, utilization and storage sites; no regulated excretion pathways have been developed (De Domenico et al., 2008). Major sites of regulation are: duodenum for dietary Fe absorption; bone marrow for red blood cells production; liver for Fe storage; spleen and other cells of the reticuloendothelial system (RES) for red blood cells catabolism and Fe recycling. Cell types involved in Fe homeostasis are the enterocyte in the duodenum, reticulocyte in the bone marrow, and macrophages in the spleen, liver and RES (De Domenico et al., 2008). Briefly, Fe is oxidized to Fe^{3+} in the intestinal lumen and in the serum, but to be transported into cells it needs to be reduced to Fe^{2+}, likely by DCytb. So, upon extracellular reduction, Fe^{2+} is transported into enterocytes by divalent metal transporter 1 (Dmt1), it is exported by ferroportin (Fpn) and subsequently oxidized to Fe^{3+} by membrane bound copper-dependent ferroxidases hephaestin and ceruloplasmin (Cp). In the serum,

Fe^{3+} is bound to transferrin (Tf) that delivers it to cells. Upon transferrin receptor (TfR) binding, the Fe^{3+}–Tf complex is internalized and iron is released from Tf in acidified endosomes, reduced by a six transmembrane epithelial antigen of the prostate (Steap) metalloreductase and then transported into the cytoplasm by Dmt1. Apo-Tf and the TfR are returned to circulation and plasma membrane, respectively, via the recycling endosome pathway. Cytosolic Fe is translocated into mitochondria via mitoferrin and loaded into Fe-S cluster by frataxin. Fe-S cluster is released into cytoplasm by ATP-binding cassette transporter Abcb7. In the cytoplasm, Fe is stored as a complex with ferritin. In erythroblast, mitochondrial Fe is primarily used for heme synthesis. Fe recycling occur via reticulo-endothelial macrophages, which engulf aged red blood cells and release it in the extracellular environment via Fpn. Released Fe is newly oxidized by GPI-linked Cp and loaded on Tf (Kambe, Weaver, & Andrews, 2008).

Copper is an essential nutrient for all eukaryotic organisms due to its function as cofactor in a broad range of critical processes that include respiration (cytochrome C oxidase), neuropeptide maturation (peptidyl-α-mono-oxygenase), protection from oxidative stress (Cu,Zn-dependent superoxide dismutase, Sod1), neurotransmitter biogenesis (dopamine β-hydroxylase), pigmentation (tyrosinase), Fe absorption (Cp), connective tissue maturation (lysyl oxidase), and other key biological functions (Gupta and Lutsenko, 2009; Nose et al., 2006). Copper oxidation states range from +I to +III, though the biologically relevant oxidation states are +I and +II. Cuprous ions (Cu^{+}) prefer sulphur atoms as a ligand, while cupric ions (Cu^{2+}) prefer nitrogen ones. Copper is also able to generate free radical species, and its homeostasis is strictly regulated. The metabolic pathway responsible for Cu homeostasis is summarized in Figure 7 (Kambe et al., 2008). Copper is oxidized in the intestinal lumen and serum, but it requires to be reduced to Cu^{+} before transport into cells. The Steap ferric/cupric reductases (Steaps 2, 3, and 4) are essential for the Cu reduction, as well as for Fe reduction (Ohgami et al., 2006). Although mechanisms involved in enterocytes Cu uptake are not completely defined, several studies suggested a role for the high-affinity copper-transporter 1 (Ctr1). From enterocytes, Cu is exported into the bloodstream by Atp7a for further distribution to tissues (Gupta and Lutsenko, 2009). So, Cu can reach the liver, the primary copper homeostasis organ. In the hepatocyte, Atp7b is devoted both to the excess Cu excretion into the bile and to Cu translocation into the TGN where it is loaded on Cp, the primary copper-binding protein in serum. In the cytoplasm, Cu serves copper chaperones, Cox17/19, Atox1 and Ccs, which deliver it respectively to: mitochondria and cytochrome C oxidase; Atp7a in the TGN for activation of lysyl oxidase, tyrosinase, peptidylglycine α-amidating mono-oxygenase; and Sod1.

Zinc is one of the most abundant elements within cells (King, 2011). It serves structural and/or catalytic roles in hundreds of proteins involved in cellular metabolism and gene expression, such as

metalloproteases and zinc finger proteins (Bleackley and Macgillivray, 2011; Tapiero and Tew, 2003). Since Zn^{2+} ion has a full d orbital, it does not give rise to multiple valences under physiological conditions and it does not participate in redox reactions (Williams, 1987). Twenty four different genes encode proteins that may be involved in Zn uptake (Zip genes) or efflux (ZnT genes) in a cell-specific, developmentally regulated, and Zn-regulated manner (Figure 8 (Kambe et al., 2008)). Dietary Zn absorption is mainly mediated by Zip4, though other transporters should have important roles. ZnT1 is responsible for Zn export into the portal blood or into the conceptus being localized on the basolateral membrane. Other ZnT proteins (eg. ZnT4) likely play a role in this process. Zip5 is localized on enterocytes, endoderm cells and pancreatic acinar cells basolateral membranes, where it may serve to remove Zn from the blood when it is abundantly supplied. In peripheral tissues, various plasma membrane Zip transporters likely mediate Zn uptake. Inside the cell, free Zn levels are kept low through Mt binding or transport into secretory vesicles, endosomes/lysosomes or zincosomes by ZnT2 and ZnT4. To control excess content, Zn activates Zn-sensing transcription factors. ZnTs2–7 participate in Zn delivery to the secretory pathway, whereas Zip7 may transport zinc out of the Golgi apparatus into the cytoplasm. ZnT3 transports Zn into glutamate containing vesicles in the brain whereas ZnT8 transports zinc into pancreatic β-cell insulin secretory granules.

Manganese is an essential metal that is found in all tissues and is required for normal amino acid, lipid, protein, and carbohydrate metabolism. Manganese is fondamental for immune system functioning, for blood sugars and cellular energy regulation, bone growth, defense against free radicals, and, together with vitamin K, blood clotting. Manganese functions as a cofactor in several enzymes: arginase (urea formation), glutamine synthetase (critical for brain ammonia metabolism), phosphoenolpyruvate decarboxylase (gluconeogenesis), and manganese superoxide dismutase (antioxidant, Sod2) (Erikson et al., 2005). In humans and animals, Mn is a cofactor of several enzymes necessary for neuronal and glial cell function, as well as enzymes involved in neurotransmitter synthesis and metabolism (Bowman et al., 2011). Manganese oxidation states range from –III to +VII, though the three major biologically-relevant oxidation states are Mn(II), Mn(III) and Mn(IV) (Bleackley and Macgillivray, 2011). When bound to enzymes, Mn(III) is predominant, while Mn(II) and Mn(IV) are the most commonly taken into the body. Ceruloplasmin oxidases Mn(II) to Mn(III), resulting in a shift of Mn bound to α_2-macroglubulin to Tf, that is relevant since Mn bound to α_2-macroglubulin is more rapidly cleared compared to the Tf-bound form (Aschner, 2006; Gibbons et al., 1976). Manganese oxidation/reduction rate and its association to proteins are a key determinants for its retention and delivery in the body (Davidsson et al., 1989). Yeast Mn metabolism is summarized in Figure 9 (Bleackley and Macgillivray, 2011). In the large intestine Mn is transported by simple diffusion, while it is absorbed by active transport in the small intestine. Excess of Mn is eliminated via bile. A plethora of plasma proteins or ligands have been implicated as specific Mn carrier proteins, including

transglutaminase, β_1-globulin, albumin, and transferrin. In fact, approximately 80% of plasma Mn is bound to β_1-globulin. Several transporters are involved in cellular uptake and release of Mn, for instance Fpn1, Dmt1, TfR, Zip8 and voltage-gated Ca^{2+} channels, each one being also involved in other metal ions transport. Intracellular Mn is transported via Ca^{2+} uniporter to the mitochondria, where it is loaded onto Sod2. In the brain, Mn(III) enters via TfR, while Mn(II) is readly transported into the CNS either as a free ion species or as a nonspecific protein-bound species (Aschner and Gannon, 1994; Rabin et al., 1993). Also Dmt1 has been found to be involved in Mn uptake in the brain (Chua and Morgan, 1997). However, the main form entering the brain seems to be manganese citrate (Crossgrove and Yokel, 2004). Concerning its efflux, a lack of active Mn transport from the CNS to the systemic circulation has been suggested: a slow diffusion process likely occurs (Yokel and Crossgrove, 2004; Yokel et al., 2003).

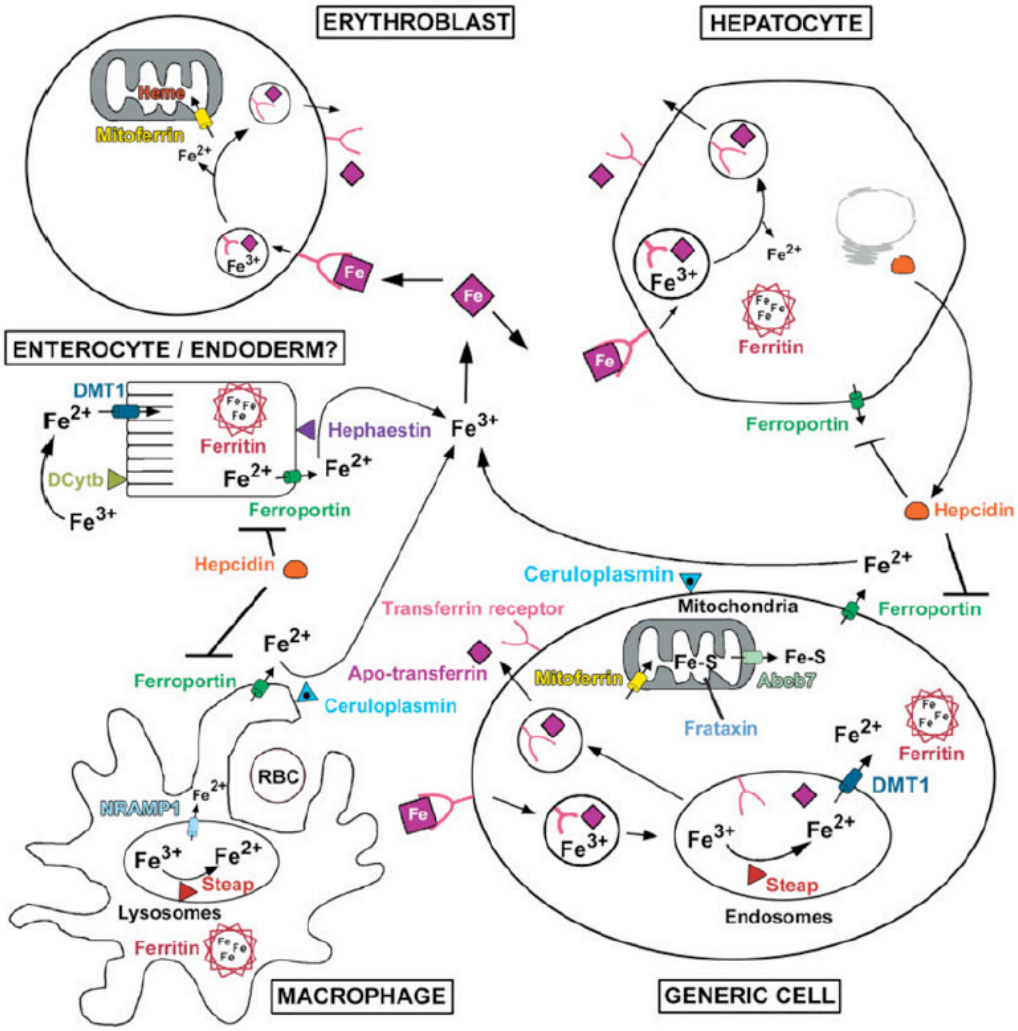

Figure 6. Overview of Fe homeostasis. Fe is oxidized in the intestinal lumen and in the serum, but is reduced before transport into cells. Fe is transported into enterocytes by Dmt1 after extracellular reduction perhaps by DCytb. Fe uptake by visceral endoderm cells is apparently not dependent on Dmt1 and could require the transferrin uptake system. Fe is transported out of cells by Ferroportin and is thought to be subsequently oxidized by membrane bound Hephaestin and Ceruloplasmin. Fe, inflammation and hypoxia regulate Hepcidin, a polypeptide hormone made by the hepatocyte. Hepcidin binds to Ferroportin resulting in degradation of the transporter. In the serum, Fe^{3+} binds to Transferrin. Developing erithrobrast and many other cell types take up Fe via the transferrin-mediated endocytic pathway. After binding to the transferrin receptor, the Fe–transferrin complex is internalized and Fe is released from transferrin in the acidified endosome, reduced by a Steap metalloreductase and then transported into the cytoplasm by Dmt1. Apo-transferrin and the transferrin receptor are returned to circulation and plasma membrane, respectively, via the recycling endosome pathway. All nonerythroid cells store Fe complexed with the ferritin heavy and light chains (Ferritin) which can store up to 4,000 atoms of Fe per molecule. Cytoplasmic Fe is transported into mitochondria by mitoferrin where it is loaded into Fe-S clusters in a process that requires Frataxin. A substrate essential for Fe-S assembly in the cytoplasm is transported out of the mitochondria by the ATP-binding cassette transporter Abcb7. In the erythroblast, mitochondrial Fe is primarily utilized for heme synthesis. A major fraction of Fe is recycled by the reticulo-endothelial macrophage which phagocytoses aged red blood cells (RBC). The Fe is solubilized in the lysosomes, reduced by a Steap metalloreductase and exported out of the lysosome by Nramp1. Fe is released from the macrophage by ferroportin, subsequently reoxidized by Ceruloplasmin, and conveyed again via transferrin through the systemic circulation. (Kambe et al., 2008)

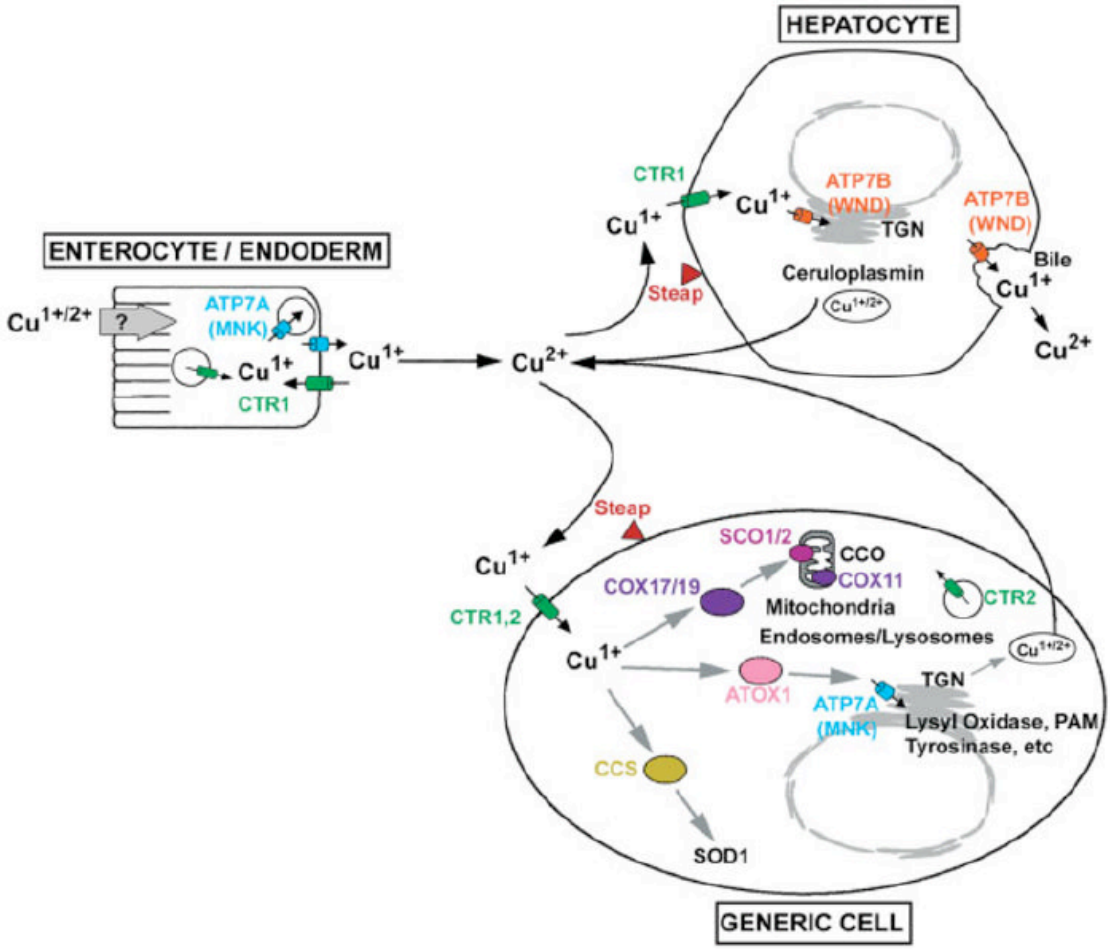

Figure 7. Overview of Cu homeostasis. Cu is oxidized in the intestinal lumen and in the serum, but is reduced to Cu^{1+} before transport into cells. The Steap ferric/cupric reductases (Steaps 2, 3, and 4) are localized to endosomes/lysosomes and the plasma membrane and may be essential for the reduction of Cu, as well as the reduction of iron (Ohgami et al., 2006). Cu is transported into enterocyte/endoderm cells by unknown mechanisms (endocytosis?). Ctr1 is essential for the acquisition of dietary Cu but its function in the enterocyte is unknown. In many other cell types, Cu is taken up by Ctr1 localized to the plasma membrane and perhaps also by Ctr2 (Slc31a2). Cu taken up by enterocyte/endoderm is exported into portal blood/conceptus, respectively, by Atp7a (Menkes's disease protein, MNK) which is localized to vesicles trafficking toward the basolateral membrane and to the basolateral membrane. Cu exported to portal blood is taken up into the liver, the primary organ that regulates Cu homeostasis. In the hepatocyte, Atp7b (Wilson's disease protein, WND) effluxes excess Cu into the bile and puts Cu into the trans-Golgi network (TGN) where it is loaded into ceruloplasmin, a ferroxidase that is the primary Cu binding protein in serum. Inside the cell, Cu is distributed to cytoplasmic Cu chaperones (Cox17/19, Atox1, Ccs) which, in turn, deliver Cu to mitochondrial inner membrane and ultimately cytochrome C oxidase (Cco) or to Atp7a in the TGN, and cytoplasmic Sod1, respectively. Atp7a transports Cu into the TGN and activates Cu containing secretory and membrane-bound proteins [lysyl oxidase, tyrosinase, peptidylglycine α-amidating monooxygenase (PAM)]. It should be noted that the cellular localization and abundance of Ctr1, Atp7a, and Atp7b are dynamically regulated by Cu availability, which is not reflected in this static cartoon. (Kambe et al., 2008).

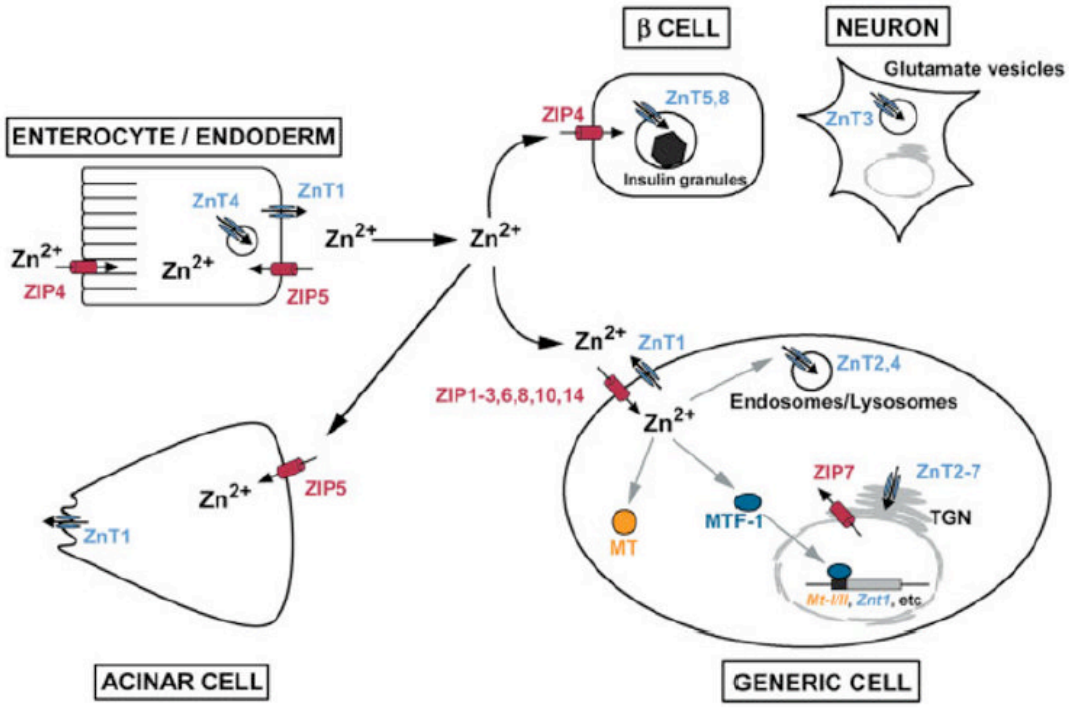

Figure 8. Overview of Zn homeostasis. Twenty four different genes encode proteins that may be involved in the uptake (Zip genes) or efflux (ZnT genes) of this metal in a cell-specific, developmentally regulated, and Zn-regulated manner. The functions of many of these genes remain to be determined. Therefore, this cartoon provides only a superficial and static view of Zn homeostasis. Zip4 plays a critical role in the absorption of dietary Zn by enterocyte/endoderm cells when Zn is limiting, but other transporters must also play important roles. Zn is thought to be exported into portal blood or into the conceptus by ZnT1 localized on the basolateral membrane. Other ZnT proteins (i.e. ZnT4) also likely play a role in this process. Zip5 is localized to the basolateral membranes of enterocytes, endoderm cells and pancreatic acinar cells where it may serve to remove Zn from the blood when Zn is replete. In peripheral tissues, Zn is probably taken up by various Zip transporters localized on the plasma membrane. To date ZIPs1, 2, 3, 6, 8, 10, and 14 have each been shown to have Zn transport activity in transfection or oocyte injection studies, and most show tissue-specific patterns of expression. Inside the cell, free Zn levels are kept low and Zn can be bound to Mt or transported into secretory vesicles, endosomes/lysosomes or Znosomes by ZnT2 and ZnT4. Zn activates the Zn-sensing transcription factor Mtf-1 which regulates transcription of the mouse Mt-I/II and Znt1 genes and represses expression of Zip10 in an effort to control excess Zn. ZnTs2–7 participate in the delivery of Zn into the secretory pathway, whereas Zip7 may transport Zn out of the Golgi apparatus into the cytoplasm. ZnT3 transports Zn into glutamate containing vesicles in the brain whereas ZnT8 transports Zn into pancreatic β-cell insulin secretory granules. ZIP4 is expressed in β-cells, but its localization in those cells has not been reported (Kambe et al., 2008).

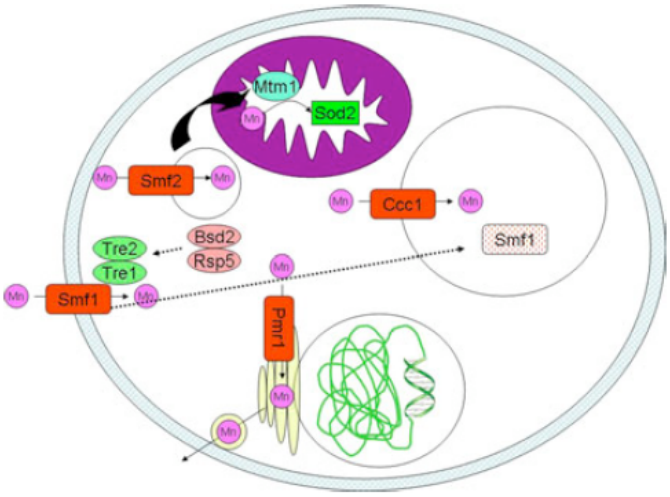

Figure 9. Manganese homeostasis in *S. cerevisiae*. Transporters are shown in red. (Bleackley and Macgillivray, 2011)

Although metals are often considered individually, there are significant interactions between them and alterations of each metal metabolism can affect the others. Interferences among transition metals occur at different levels: absorption inhibition, compartmental displacement and enzymatic impairment, including both competition for the binding site, as well as catalytic functionality. This can be understood also by the fact that they share several common transporters. Fe and Cu metabolisms are intricately interconnected (Cherukuri et al., 2005; Ohgami et al., 2006). Cu has a dual effect on iron metabolism: a synergistic one due to its requirement for ferroxidases (Cp, hephaestin) activity, but a competitive one, due to common absorption mechanisms, when Cu is in excess. Competitive inhibition of Fe absorption by Zn and Mn has also been shown (Rossander-Hulten et al., 1991). Zn exerts its antagonistic effect also on Cu absorption (Fischer et al., 1981; L'Abbe and Fischer, 1984). High Zn dietary levels cause a reduction of Cu-dependent enzymes activity similar to that observed during Cu deficiency. Competition between Mn and Fe at the gastrointestinal tract has been documented, and it is most likely mediated by Dmt1. Moreover, a small fraction of Mn^{3+} is also bound to the Tf (Aschner, 2006). These interferences can also lead to enzymatic impairment, with subsequent alterations of biological processes.

METAL IONS AND NEURODEGENERATION

For a long time, it has been commonly thought that the neurological syndromes in which metals are implicated are hypothetically caused either by toxicological exposure or by deficiency. For functioning, the brain requires high concentrations of metal ions and its oxidative metabolic rate is elevated. Therefore, the brain must have efficient homeostatic mechanisms and buffering systems to prevent the abnormal discompartmentalization of metal ions and control their availability (Bush, 2000). Also, the

blood–brain barrier (BBB) is relatively impermeable to fluctuating levels of plasma metal ions. It is known that several of the metal regulatory transport systems are energy dependent (e.g. Atp7b). Therefore, damage to the BBB or energy compromise in the brain are two characteristics of several neurodegenerative disorders that could perturb metal levels and lead to deranged protein behavior (Bush, 2000). In principle, two main generic reactions relevant to neurodegenerative disease can occur. First, a metal–protein association leads to protein aggregation; this reaction can involve redox-inert metal ions such as Zn^{2+}, or redox-active metal ions such as Cu^{2+} and Fe^{3+}. Second, a metal-catalyzed protein oxidation leads to protein damage and denaturation; this reaction involves a redox-active metal ion such as Cu^{2+}, Fe^{3+}, or Mn^{2+} (Bush, 2000). Copper and iron can accept or donate electrons, triggering radical formation, reactive nitrogen species (RNS) and reactive oxygen species (ROS) formation and oxidative attack of tissue components contributing to disease and aging. On the contrary, Zn generally acts as an antioxidant, maintaining its valence, but it can give several toxic effects, e.g. Aβ precipitation (Bertoni-Freddari et al., 2008; Frederickson et al., 2005). Concerning Mn, its neurotoxicity seems to be primarily due to oxidation of important cellular component by Mn^{3+}. In fact, intracellularly Mn^{2+} is oxidized to Mn^{3+} reacting with the superoxide anion produced by the mitochondrial electron transport chain. In the mitochondria, Mn can inhibit the complex I, leading to altered oxidative phosphorylation. In particular, Mn^{3+} toxic effects are likely to occur in dopaminergic cells (Archibald and Tyree, 1987; Aschner, 2006). Paradoxically, both metal ions loss and accumulation can bring to neurological diseases (Lovell, 2009). For this reason, their content in the brain is tightly regulated and no passive flux of metals through the BBB occurs. However, Fe, Cu and Zn involvement in several interactions with the major protein components of neurodegenerative diseases is not due to increased exposure to metals, but rather to a breakdown in the homeostatic mechanisms that compartmentalize and regulate them (Barnham and Bush, 2008).

The dominant risk factor associated with neurodegeneration is ageing increasing. It has been reported that brain Cu levels rise from youth to adulthood, then from middle age onwards they drops markedly, leading to a loss of Cu-dependent enzymes activity, e.g. Sod1 and Cp (Adlard and Bush, 2006; Religa et al., 2006). Moreover, Fe levels increase in the brain in an age-related manner (Hardy et al., 2005; Suh et al., 2005) and failure of ubiquitous ferroxidases Cp, FtH and frataxin cause neurodegenerative disorders (Chinnery et al., 2007; Mantovan et al., 2006; Zecca et al., 2004).

Different neurodegenerative disorders, due to genetic origin, involve mutations in metal ion metabolism proteins. An example is the Menkes' disease that is caused by loss-of-function mutations in the Atp7a encoding gene (Chelly et al., 1993; Mercer et al., 1993; Vulpe et al., 1993). The disease results from the impaired activity of specific cuproenzymes caused by the impaired Atp7a function. Moreover, as will be better described in next paragraph, without Cu release in synapses upon NMDA receptor

activation, excitotoxic events are likely to occur (Schlief et al., 2005). Systemic Cu treatment is not effective in patients with Menkes disease because Cu transport into the brain is dependent on Atp7a (Madsen and Gitlin, 2007). Another pathology resulting from Cu transporter loss-of-function is Wilson's disease. It involves mutations in the Atp7b encoding gene, resulting in biliary Cu excretion impairment and consequent hepatocyte Cu accumulation. This accumulation damages the liver and activates cell-death pathways, inducing Cu leakage into the plasma and following overload in all tissues. Even though Atp7b is expressed in some brain regions, the disease results from liver accumulation of Cu (Gitlin, 2003; Tao et al., 2003). Moreover, in absence of Atp7b activity, Cu will not be delivered to Cp. Apo-ceruloplasmin is rapidly degraded in the plasma, resulting in a lack of ferroxidase activity and consequently alterations in Fe metabolism. Wilson's disease affected patients develop severe Parkinsonian symptoms, due to basal ganglia Cu accumulation and neuronal cell death, together with behavioural problems and psycosis (Dening, 1991; Oder et al., 1991). These symptoms are the result of Cu accumulation, since treatment with Cu chelators improve the neuropathology (Schlief and Gitlin, 2006). A further example of genetic disorder due to loss-of-function of a metal binding protein is aceruloplasminemia. As the name indicates, this autosomal recessive disorder is caused by a mutation in the Cp encoding gene (Harris et al., 1995). So, Cp is absent in the serum, as well as serum Fe levels are decreased inducing anemia and brain Fe accumulation (Kono and Miyajima, 2006). Loss of Cp results also in non-Tf bound Fe that rapidly accumulates in liver, pancreas and other tissue after Dmt1 removal from plasma membrane (Andrews, 2002; Hentze et al., 2004). Accumulation of Fe in the brain is unique to aceruloplasminemia, suggesting that the GPI-anchored Cp isoform present in astrocytes is a ferroxidase that facilitates the rate of Fe release from storage cells in the CNS (Madsen and Gitlin, 2007).

PrP^C Antioxidant Activity

An overlap between systems controlling redox-active metals homeostasis and oxygen radicals metabolism has been extensively documented (Avery, 2001). The physiological connection between transition metals and oxidative stress is exemplified by the activities of metal-detoxifying proteins and antioxidant enzymes (Vassallo and Herms, 2003). It has been suggested that PrP^C is associated with cellular systems that control redox balance and protects from oxidative stress (Brown et al., 2002). Lack of PrP^C results in increased neuronal sensitivity to oxidative stress (Brown et al., 1997b; Rachidi et al., 2003). PrP^C knock down decreased Sod1 activity because of a reduced Cu incorporation, not linked to alterations in the copper chaperon for superoxide dismutase (Ccs) (Brown and Besinger, 1998; Kralovicova et al., 2009). Moreover, *Prnp*$^{0/0}$ brains present higher levels of lipids and protein oxidation (Wong et al., 2001). Indeed, PrP^C expression is increased in a variety of stress related conditions, including heat shock, hypoxia, ischemia and hypoglycaemia, as well as in stroke models (McLennan et

al., 2004; Mitsios et al., 2007; Shyu et al., 2005; Shyu et al., 2000; Shyu et al., 2004). Moreover, a knock down of any Sod proteins triggers PrP^C expression, on the contrary shutting down PrP^C increases extracellular-Sod expression and Sod2 activity (Brown and Besinger, 1998; Kralovicova et al., 2009). This connection between PrP^C and Sod proteins indicates a common cell protection pathway. Furthermore, *in vitro* experiments revealed that PrP^C has Sod-like activity with a dismutation constant rate similar to Sod2's one (Brown et al., 2001; Brown et al., 1999; Cui et al., 2003; Treiber et al., 2007). Sod activity is dependent on Cu(II) incorporation and it probably involves Cu(II) reduction (Brown et al., 2001). It should be also noted that PrP^C is cleaved at the end of its Cu-binding OR through the action of ROS, a process termed β-cleavage. β-cleavage is considered an early and critical event in the mechanism by which PrP^C protects cells against oxidative stress. If a PrP construct lacks the OR, the protein will fail to undergo ROS-mediated β-cleavage, as occurs with the two mutant forms of PrP, PG14, and A116V, associated with human prion diseases (Watt et al., 2005).

In their review, Vassallo and Hermes state that the most likely candidate as intracellular messenger for PrP^C-mediated protection is calcium. Intracellular calcium is a critical component of the signalling pathways that lead to neuron structural and functional changes. The calcium signal usually corresponds to an elevation of the intracellular calcium concentration as a consequence of synaptic activity-induced depolarization. Indeed, in PrP null conditions neuron calcium homeostasis is impaired (Krebs et al., 2007). Hence, PrP^C may influence both neuron survival and synaptic physiology regulating calcium homeostasis (Vassallo and Herms, 2003). The model proposed is reported in Figure 10.

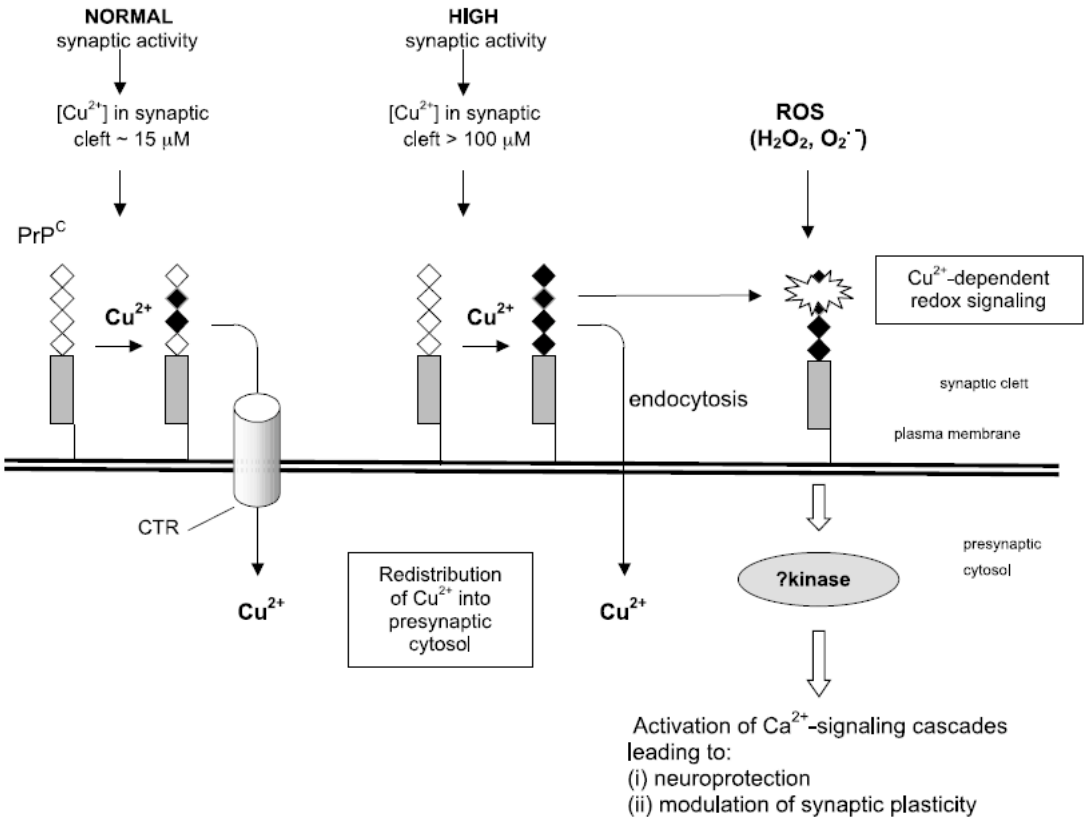

Figure 10. Schematic representation of the physiological role of prion protein (PrP^C) in copper homeostasis and redox signalling. Cu^{2+} ions released during neurotransmitter vesicles exocytosis are buffered by PrP^C, and subsequentially returned to the pre-synaptic cytosol. This can occur either by transfer of copper to copper transporter proteins (CTR) within the membrane, or in case of high copper concentrations in the synaptic cleft, via PrP^C-mediated endocytosis (◇represent an octarepeat; ◆represent an octarepeat bound to copper(II) ion). Further, copper-loaded PrP^C may interact with ROS, including H_2O_2 and $O_2^{\bullet-}$, triggering redox signalling and subsequently activation of Ca^{2+}-dependent signalling cascade. Changes in the intracellular Ca^{2+} levels lead to a modulation of synaptic activity and neuroprotection. (from (Vassallo and Herms, 2003)).

PrP^C AND SYNAPTIC FUNCTIONALITY

Electrophysiology studies suggest a role for PrP^C in the regulation of ion channels and neuronal excitability. PrP^C localizes at synapses, together with a plethora of ion channels, and evidence supports that this is important for normal synaptic development and functionality (Kanaani et al., 2005; Moya et al., 2000). A variety of electrophysiological abnormalities have been observed in cerebellum or hippocampus of PrP null mice (Carleton et al., 2001; Colling et al., 1996; Collinge et al., 1994; Fuhrmann et al., 2006; Herms et al., 2001; Lazzari et al., 2011; Maglio et al., 2004; Mallucci et al., 2002; Manson et al., 1995; Prestori et al., 2008). However, the most compelling evidence for a functional interaction between PrP^C and ion channels concerns glutamate excitatory receptors, in particular NMDARs (Khosravani et al., 2008b; You et al., 2012). First, Zamponi's group reported that adult PrP

null mice exhibit greater basal excitability in the CA1 region of the hippocampus. In particular, synaptic NMDAR-mediated current was altered, showing slowed deactivation kinetics. They obtained the same results also in neuronal cultures transfected with PrP^C siRNA, confirming that PrP^C is a negative regulator of NMDAR function in hippocampal neurons. In the same work, they showed that *Prnp*$^{0/0}$ neurons are also more susceptible to NMDAR-mediated cell death, both *in vitro* and *in vivo* (Khosravani et al., 2008b). More recently, the same group published an article concerning the crucial role of Cu, PrP^C and NMDAR in mediating amyloid β (Aβ) neurotoxic effect. Their interdependent role consists in the induction of a pathologically large non-desensitizing steady-state NMDAR current. They also showed that the same electrophysiologial alteration is observed in both PrP null hippocampus and in wild-type hippocampus treated with a Cu chelator. Copper addition re-establishes NMDAR current in both Aβ-treated and PrP null neurons, meaning that PrP-mediated modulation of NMDAR occurs via Cu ions and Aβ oligomers block this modulation, maybe interfering with Cu-PrP^C binding. The authors propose that PrP regulates NMDARs by decreasing glycine affinity for the receptor, so diminishing its agonistic effect (You et al., 2012).

NMDA Receptors: Function, Subunit Composition and Regulation

NMDARs, together with other glutamate ionotropic receptors, are key mediators of the excitatory synaptic transmission in the brain. These glutamate-gated cation channels convert a chemical signal (glutamate released from the presynaptic terminal) into an electric signal (a membrane voltage change due to cation flow through the channels) (Yashiro and Philpot, 2008). NMDARs have critical roles in excitatory synaptic transmission, plasticity and excitotoxicity in the CNS. The involvement of NMDARs in these diverse processes reflects their unique features, which include voltage-sensitive block by extracellular Mg^{2+}, a high permeability to Ca^{2+} and unusually slow 'activation/deactivation' kinetics. Moreover, the co-agonist glycine binding is required for NMDAR activation, whereas physiological levels of protons suppress receptor's opening (Cull-Candy et al., 2001). Several and distinct NMDAR subtypes have been identified in CNS, differing in their sensitivity to endogenous and exogenous ligands, permeation and block by divalent ions, kinetic properties, and interaction with intracellular proteins. So NMDARs functional properties are determined by their subunit composition (Cull-Candy et al., 2001). A variety of NMDAR subunits have been identified: the ubiquitously expressed GluN1 subunit (formerly known as NR1); a family of four distinct GluN2A-D subunits (formerly NR2A-D); and two GluN3A-B subunits (formerly NR3A-B) (Das et al., 1998; Moriyoshi et al., 1991; Sugihara et al., 1992). The diversification is also increased by the different splicing isoforms each subunit presents (Dingledine et al., 1999). *In situ* hybridization studies have shown that mRNAs

for NMDAR subunits are differentially distributed throughout the brain, with patterns of expression that change strikingly during development (Akazawa et al., 1994; Monyer et al., 1994). GluN2B and GluN2D subunits predominate in the neonatal brain, but over the course of development these are supplemented with, or replaced by, GluN2A and in some regions GluN2C subunits. All NMDARs appear to function as heteromeric assemblies composed of multiple GluN1 subunits in combination with at least one type of GluN2. The GluN3 subunit does not form functional receptors alone, but can co-assemble with GluN1/GluN2 complexes (Das et al., 1998; Perez-Otano et al., 2001). As each of the constituent subunits confers distinct properties to the receptor assembly, to a greater or lesser extent, many of the important functional attributes of the native receptors are determined by the expression of the various subunits and isoforms, as it is shown in Figure 11 (Cull-Candy et al., 2001). NMDARs are found both at synaptic and extrasynaptic sites including the cell soma and the dendritic shaft. Extrasynaptic NMDARs are activated not only at pathological situations, but also by burst of activity that can occur under physiological conditions (Hardingham et al., 2002; Harris and Pettit, 2008). Therefore, extrasynaptic NMDARs are involved in stimulus-dependent synaptic modifications, and they are likely activated in a manner that is distinct from the activation of synaptic NMDARs. The possibility that NMDARs subunit composition differs between synaptic and extrasynaptic sites is also controversial. It has been proposed that GluN2A-containing NMDARs occupy the central portion of synapses, while GluN2B-containing ones are preferentially targeted to peripheral portions of synapses or to extrasynaptic sites (Cull-Candy et al., 2001). Although diheteromeric GluN2A-, GluN2B- and GluN2C-containing NMDARs participate in synaptic transmission, there is no evidence for GluN1/GluN2D-containing receptors at any central synapse. Distinct single-channel properties of GluN1/GluN2D receptors have enabled their identification in the extrasynaptic membrane of several cell types. As reviewed by Cull-Candy et al., in 2001, many studies led to conclude that GluN2D-containing NMDARs are absent from synaptic sites.

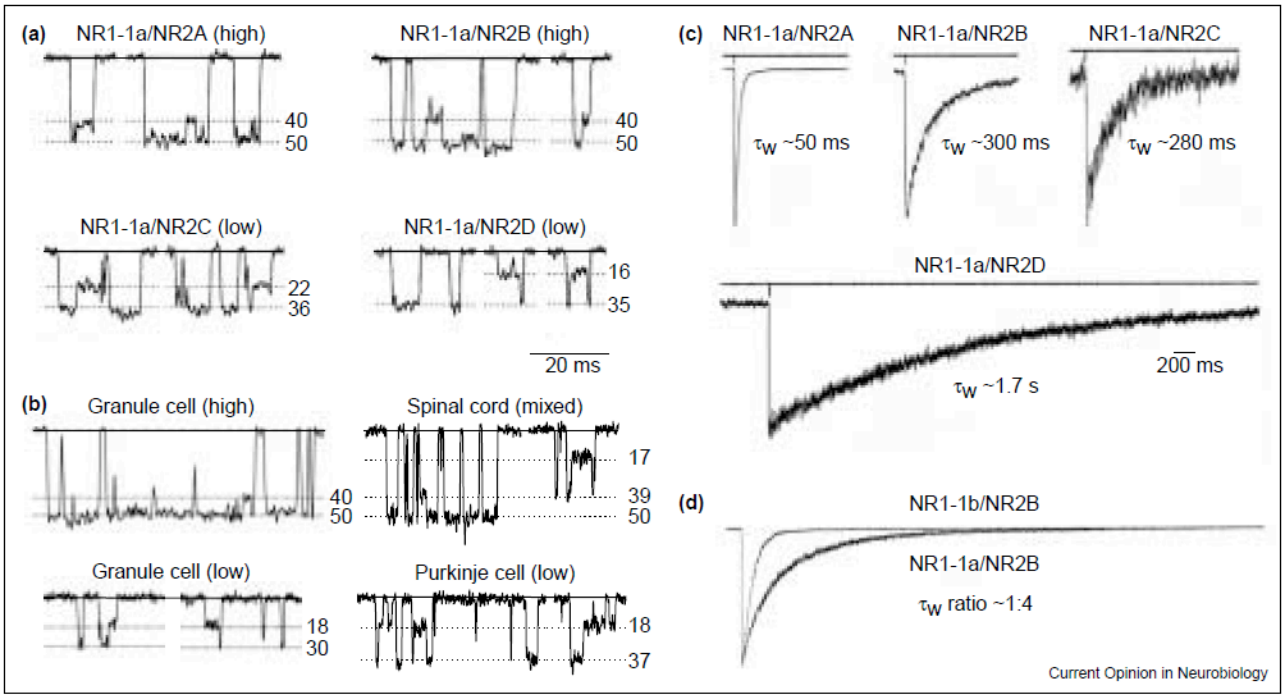

Figure 11. Functional properties of NMDARs conferred by specific subunits. (a) Representative single-channel records of recombinant NMDARs expressed in Xenopus oocytes, showing the high-conductance openings of NR2A- and NR2B-containing receptors, and the low-conductance openings of NR2C- and NR2D-containing receptors. Solid lines indicate the closed state, and dotted lines indicate open states. Numbers indicate conductance in picosiemens (Behe et al., 1999). (b) Example of single-channel records of native NMDARs from cerebellar granule cells, a dorsal horn neuron of the spinal cord, and a cerebellar Purkinje cell, showing openings of high- and low-conductance (Farrant et al., 1994; Momiyama et al., 1996). In these examples, the high-conductance channels are thought to arise from NR1/NR2B receptors and the low-conductance channels from GluN1/GluN2D receptors in spinal cord and Purkinje cells, and from NR1/NR2C receptors in granule cells. (c) Macroscopic currents from recombinant NMDARs expressed in HEK293 cells, illustrating the NR2 subunit-dependent deactivation seen in response to 1-ms applications of 1 mM glutamate (Vicini et al., 1998). (d) Macroscopic currents from recombinant NMDARs illustrating the influence of NR1 splice varaiants on deactivation (4-ms applications of 1 mM glutamate; (Rumbaugh et al., 2000)). τ_w is the weighted deactivation time constant.

Since NMDARs play crucial roles in physiological processes, like learning and memory (Collingridge, 1987), as well as in the pathophysiology of CNS disorders, like ischemia, epilepsy, many neurodegenerative diseases and even also neuropsychiatric disorders, such as schizofrenia (Aarts et al., 2002; Lipton and Rosenberg, 1994; Loftis and Janowsky, 2003), several regulatory mechanisms have been identified, reviewed by (Dingledine et al., 1999). For example, activating phosphorylation can occur on serine and threonine residues by mean of protein kinase A (Pka), protein kinase C (Pkc) and Ca^{2+}/calmodulin-dependent protein kinase II (CamkII), while deactivating dephosphorylation occurs via Ca^{2+}/calmodulin-dependent phosphatase calcineurin. Activating phosphorylation can occur also on tyrosine residues, by mean of Src and Fyn kinases. Other regulatory mechanisms involve glycosylation, covalent bound to lipids, as well as proteolytic degradation mainly mediated by calpain.

In 1996, it was published that in hippocampal neurons Cu can modulate NMDARs (Vlachova et al., 1996). In fact, upon depolarization ionic Cu is released into the cleft reaching 100μM concentration (Kardos et al., 1989). Copper release is dependent on Ca^{2+} influx from NMDARs that activates TGN vesicles containing Cu accumulated by the Atp7a (Schlief et al., 2005; Schlief et al., 2006). Vlachova and colleagues showed that Cu ions are high-affinity, voltage-dependent, NMDAR antagonists. The inhibitory properties of Cu suggest an extracellular binding site, out of the membrane electric field. However, this binding site has not been discovered, and also the precise mechanism of Cu inhibition on NMDARs has not currently been defined.

Lipton and colleagues have argued that modulation of NMDAR activity involves sulfhydryl reactions of at least seven cysteine residues with redox reagents, Zn^{2+} or nitric oxide (NO) (Lipton et al., 2002) (see Box 1). The various involvement of these cysteine residues (some involve a single protein thiol group, whereas others involve the recruitment of multiple thiol groups to the reaction mechanism) can be summarized in a Venn diagram that shows each cysteine residue can influence high-affinity Zn^{2+} inhibition, redox modulation or S-nitrosylation (reaction with NO) of the NMDA receptor (Figure 12). Because a single sulfhydryl group can, in some cases, react with an oxidizing agent, NO or Zn^{2+}, these thiol groups are capable of multiple tasks. Upon transport into vesicles by mean of ZnT3, Zn ions are released from the presynaptic bouton together with glutamate (Assaf and Chung, 1984; Howell et al., 1984). However, Zn-mediated modulation does not occur via a direct binding to cystein thiols. In fact, it was shown that the thiol groups enhance high-affinity Zn^{2+} inhibition of the NMDA receptor when in their oxidized state (i.e. when part of a disulfide bond). Hence, it can be concluded that the redox status of these thiol groups modulates the effect of Zn^{2+} allosterically, rather than by direct binding to Zn^{2+}. In fact, high-affinity Zn^{2+}-coordination site involves three histidines and one glutamate, rather than cysteine, residues (Choi and Lipton, 1999; Fayyazuddin et al., 2000; Low et al., 2000; Paoletti et al., 2000). Five cysteine thiol groups are involved in S-nitrosylation: Cys744 and Cys798 of GluN1, and Cys87, Cys320 and Cys399 of GluN2A (Choi et al., 2000). In all cases, S-nitrosylation of receptor thiol is inhibitory – that is, it decreases the amplitude of NMDA-evoked responses by decreasing the number of channel openings. The allosteric inhibition is mediated by a single crucial thiol group (Cys399 of GluN2A) while the other four cysteine residues only contribute to this reaction when they are in a free thiol conformation (i.e. in their chemically reduced state) and have not been oxidized to disulfide (Choi et al., 2000). Moreover, Cys399 on GluN2A also plays a role in Zn^{2+} inhibition that is mechanistically distinct from those of the other four cysteine residues (Paoletti et al., 2000). Exposure to NO enhances GluN1/GluN2A receptor sensitivity to high-affinity Zn^{2+}-mediated inhibition, and this effect is completely abrogated in the GluN1/GluN2A Cys399Ala mutant. Furthermore, it has been shown that the inhibitory effect of Zn^{2+} is exerted by enhanced glutamate affinity that results in receptor desensitization (Zheng et al., 2001). Based on all these findings, together with the analogy to the effects

of S-nitrosylation on hemoglobin, Lipton and colleagues proposes a model in which S-nitrosylation of Cys399 on GluN2A allosterically affects the quaternary organization of the receptor, resulting in enhanced glutamate binding and receptor desensitization (Lipton et al., 2002).

Box 1. Potential reactions of protein thiol with nitric oxide, Zn^{2+} and redox reagents

Competing reactions of the sulfhydryl (thiol) groups of cysteine residues with nitric oxide (NO), Zn^{2+} and redox reagents can regulate protein function. Note that, for simplicity, the following reactions have not been balanced for charge and electron transfer.

Competitive reactions of NO and Zn^{2+} for cysteine thiol groups (RS-H) on proteins:

RS-H + NO ↔ RS-NO + H
RS-H + Zn ↔ RS-Zn + H
RS-Zn + NO ↔ RS-NO + Zn

Redox reactions of cysteine residues:

RS-SR + DTT(2H) ↔ 2RS-H + oxDTT
2RS-H + DTNB ↔ RS-SR + 2TNB + 2H, or
RS-H ↔ RS-TNB + H

Disulfide can be reduced to free thiol – for example, by dithiothreitol (DTT), which in the process becomes oxidized itself (oxDTT). Conversely, free thiol groups can be oxidized by 5,5′-dithio-*bis*(2-bisnitrobenzoic acid) (DTNB) to form disulfide, with resulting reduction of DTNB to 2TNB or to thiobenzoate protein derivatives (RS-TNB).

S-Nitrosylated protein can be reduced to free thiol and NO by reducing agents, such as DTT:

2RS-NO + DTT(2H) ↔ 2RS-H + 2NO + oxDTT

Box 1. Potential reactions of protein thiol with nitric oxide, Zn^{2+} and redox reagents (Lipton et al., 2002).

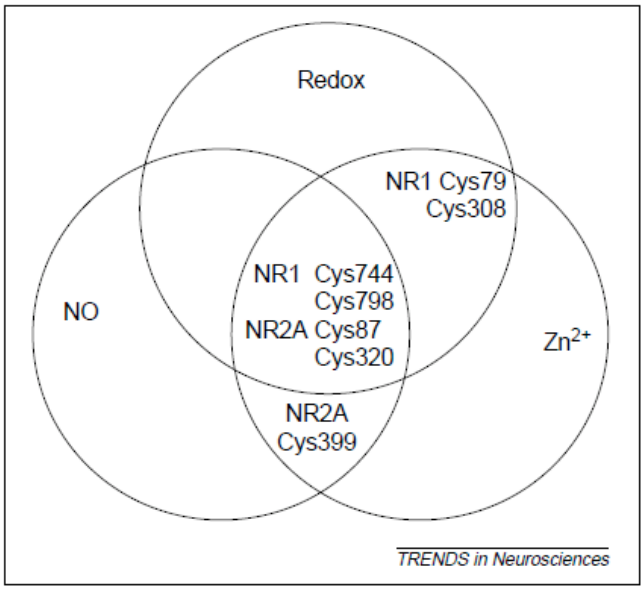

Figure 12. Effect of individual cysteine residues on the NMDA receptor. Depending on the exact site on the receptor, various individual cysteine residues can react with redox reagents, undergo S-nitrosylation or influence high-affinity Zn^{2+} inhibition. The Venn diagram summarizes the effect of each cysteine residue on the NR1 (currently named GluN1) and NR2A (currently named GluN2A) subunits, based on site-directed mutagenesis experiments. (Modified from (Lipton et al., 2002))

PrP^C AND EXCITOTOXICITY

The PrP-medited regulation of NMDARs is confirmed by the enhanced susceptibility reported for PrP null mice in excitotoxic conditions. It has been reported that PrP ablated mice are more susceptible to excitotoxic stimulation (Rangel et al., 2007; Spudich et al., 2005; You et al., 2012). Following intraluminal middle cerebral artery occlusion, PrP null mice showed a 200% increased infarct size,

together with enhanced levels of active caspase 3 (Casp3) (Spudich et al., 2005). A similar result was obtained both *in vivo* and *in vitro* with organotypic hippocampal cultures (OHCs) following stimulation with kainic acid. In particular, mice injected with kainic acid showed higher seizure behaviour together with increased neuronal cell death. Using OHCs they confirmed the increased susceptibility in the pyramidal layer cells. Moreover, they found an involvement of NMDARs in the apoptotic process since adding the synaptic NMDARs antagonist MK-801 neuronal cell death was significantly reduced (Rangel et al., 2007).

EXCITOTOXICY AND MAJOR PLAYERS INVOLVED IN ITS MECHANISMS

Excitotoxicity is a pathological process that kills or damages neurons following an excessive excitatory stimulation and that occurs in spinal cord injury, stroke, traumatic brain injury, hearing loss (through noise overexposure or ototoxicity) and in neurodegenerative diseases of the CNS such as multiple sclerosis, Alzheimer's disease, amyotrophic lateral sclerosis (ALS), Parkinson's disease, alcoholism or alcohol withdrawal, and Huntington's disease. As illustrated in Figure 13, excitotoxicity is caused by glutamate overstimulation of its ion channel receptors that provokes an intracellular calcium overload. The massive Ca^{2+} entrance activates a cascade that leads to neuronal cell death. In fact, two paradoxical roles are played by Ca^{2+}: one in physiological states and another one in CNS disease. Glutamatergic neurotransmission is dependent upon cytosolic and nuclear Ca^{2+}-dependent signaling by Ca^{2+}/calmodulin-dependent kinase IV, ras-extracellular signal–regulated kinase 1/2 pathway, and cyclic adenosine monophosphate response element binding protein (Creb)-dependent transcription of brain-derived neurotropic factor. This signalling pathway is essential for neuronal survival. Thus, it is important to differentiate between physiological Ca^{2+} transients mediated by synaptic glutamatergic neurotransmission needed for survival, antagonism of which causes cell death by apoptosis, and the more sustained and larger Ca^{2+} increases that result from pathological activation of extrasynaptic and synaptic glutamatergic receptors (Dong et al., 2006; Hardingham and Bading, 2003). The most common disease paradigm is stroke, where increased glutamate synaptic vesicular release, failure of cellular transporters, and glutamate release from dying cells lead to high extracellular glutamate, high glutamate receptors activation, and massive Na^{+} and Ca^{2+} influx (Dong et al., 2006)

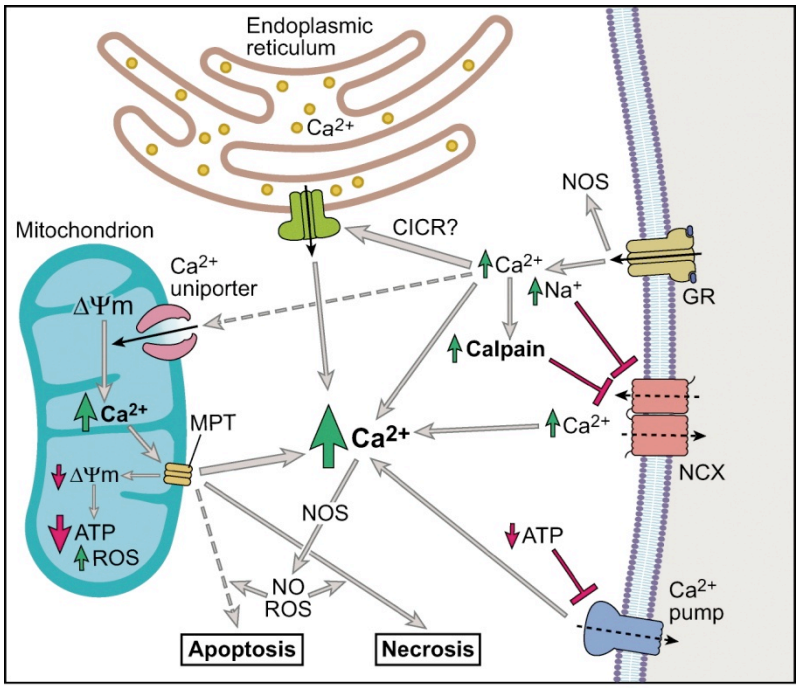

Dong Z, et al. 2006.
Annu. Rev. Pathol. Mech. Dis. 1:405–34

Figure 13. Excitotoxic injury in neurons. Binding of glutamate results in Na^+ and Ca^{2+} influx through plasma membrane glutamate receptors (GR). Consequently, cytosolic Na^+ and Ca^{2+} increase. Increased cytosolic Na^+ results in the consumption of adenosine triphosphate (ATP), and therefore decreases of the nucleotide. Increased Ca^{2+} leads to the activation of hydrolytic enzymes such as calpain. Ligation of glutamate to GR also stimulates production of nitric oxide (NO) by nitric oxide synthase (NOS). From the cytosol, Ca^{2+} is transported across the mitochondrial inner membranes through a Ca^{2+} uniporter into the mitochondrial matrix. This requires a proton-motive force (mitochondrial potential, $\Delta\psi m$) across the inner membrane. As long as $\Delta\psi m$ remains above threshold levels, and cytosolic Ca^{2+} is high, Ca^{2+} continues to be transported into the mitochondrial matrix. Increasing accumulation of Ca^{2+} leads to the formation of calcium precipitates within mitochondria, generation of reactive oxygen species (ROS), phospholipid hydrolysis, and, eventually, decrease of $\Delta\psi m$ and ATP, formation of mitochondrial permeability transition (MPT) pores in the inner membrane, and leakage of the accumulated Ca^{2+} back into the cytosol. Together with the failure of ATP-dependent Ca^{2+} pumps, and possibly with the participation of calcium-induced calcium release (CICR) from the endoplasmic reticulum, mitochondrial release of accumulated Ca^{2+} causes a catastrophic, delayed Ca^{2+} increase, which kills the cell. Increased cytosolic Na^+ may also be expected to inhibit Na^+ and Ca^{2+} exchange across the plasma membrane through the Na^+/ Ca^{2+} exchanger (NCX) in the physiological mode, and, in addition, drive reverse exchange of Na^+ and Ca^{2+} and thus exacerbate Ca^{2+} increase in the cytosol. Proteolysis of the exchanger by calpain may also inhibit Na^+/ Ca^{2+}exchange. Depending on the intensity and speed of Ca^{2+}-dependent injury, determined in part by oxidant damage through ROS generation and concomitant NO production, cell death occurs by necrosis or apoptosis (from (Dong et al., 2006).

As described in Figure 14, in excitotoxic conditions neuronal nitric oxide synthase (nNOS) is activated, leading to an increased generation of NO. NO interacts with many intracellular targets and triggers a variety of signal transduction pathways, resulting in stimulatory or inhibitory output signals. Upon excitotoxic insult, NO can play a neuroprotective function, for example inhibiting NMDAR by S-nitrosylation. However, NO becomes noxious whether produced in excess and, if a cell is in a pro-

oxidant state, NO can undergo oxidative-reductive reactions to form toxic compounds, RNS. In the last decade, the term "nitrosative stress" has been used to indicate the cellular damage elicited by excessive NO and RNS (Calabrese et al., 2007). NO and RNS have been implicated in the pathogenesis of neurodegenerative disorders. In fact, extreme nitrosative/oxidative stress can facilitate protein misfolding and aggregation, and very likely viceversa. The mechanism underlying this phenomenon is still elusive. It has been proposed that NO-related species may significantly participate in the protein misfolding process through S-nitrosylation (and nitration, also) under degenerative conditions (Gu et al., 2010). Moreover, together with the production of toxic species like peroxynitrite, high levels of NO are thought to stimulate neurotoxic pathways through the S-nitrosylation of a number of targets, activating neuronal cell death, as described in Figure 14 (Nakamura and Lipton, 2011).

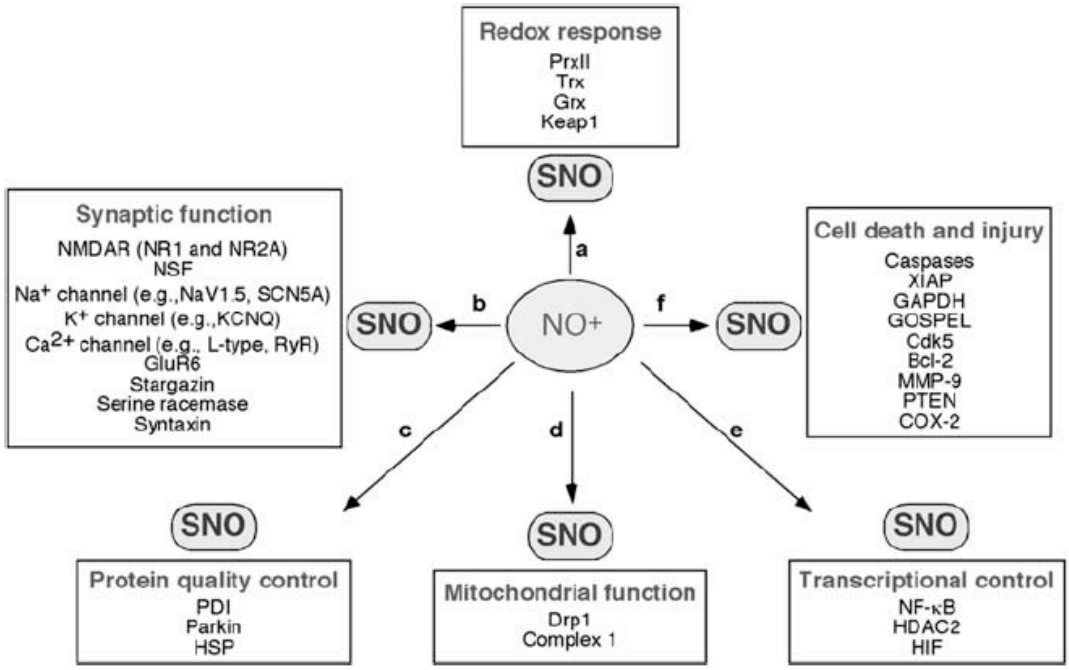

Figure 14. Representative examples of S-nitrosylated proteins that can regulate neuronal function. NO generated in the nervous system modulates the activity of various proteins via S-nitrosylation (or further oxidation) controlling (a) redox responses, (b) synaptic function, (c) protein quality control, (d) mitochondrial function, (e) transcriptional regulation, and (f) cell death and injury. Depending on the level of NO, S-nitrosylation of these proteins can mediate either neuroprotective or neurodestructive pathways (Nakamura and Lipton, 2011).

Other key proteins in excitotoxic mechanisms are calcium trasporters. In the resting excitable cell, when intracellular Ca^{2+} concentrations rise and the cell requires the return to resting levels, this exchange transport mechanism couples the uphill extrusion of Ca^{2+} to the influx of Na^{+} ions into the cells down their electrochemical gradient (Carafoli, 1985). This mode of operation, defined as forward mode, keeps the 10^4-fold difference in Ca^{2+} concentrations across the cell membrane (Blaustein and

Santiago, 1977). Several studies indicate that seizure-induced changes are accompanied by changes in the expression and/or function of calcium extrusion proteins (Garcia et al., 1997; Keele et al., 2000; Parsons et al., 2000). Three calcium pumps have been analyzed for this Ph.D. project: Na^+/Ca^{2+} exchanger 1 (Ncx1), plasma membrane Ca^{2+} ATPase (Pmca) and sarco(endo)plasmic reticulum Ca^{2+} ATPase 2 (Serca2).

The Ncx family if composed of three identified members: Ncx1, Ncx2 and Ncx3. As reviewed by Carafoli in 1987 (Carafoli, 1987), Ncx is particularly active in excitable plasma membranes where an electrically exchange of 3 Na^+ per 1 Ca^{2+} occurs (Baker et al., 1969; Blaustein and Hodgkin, 1969). The antiporter is activated in the range of submicromolar concentrations (0.1-0.3μM) of intracellular Ca^{2+} (DiPolo, 1979). Ncx has a low affinity and it does not bind very tightly to Ca^{2+}. However, it has high capacity, so it can move ions rapidly, transporting up to five thousand Ca^{2+} ions per second. Therefore, it requires large concentrations of Ca^{2+} to be effective, but it is useful for ridding the cell of large amounts of Ca^{2+} in a short time, as it is needed in a neuron after an action potential (Carafoli et al., 2001).

The Ca^{2+} pumps belong to the family of P-type ATPases, which is characterized by the temporary conservation of ATP energy in the form of a phosphorylated enzyme intermediate (hence P-type) formed between the γ-phosphate of hydrolized ATP and an invariant D-residue in a highly conserved sequence in P-type ATPases (Pedersen and Carafoli, 1987). This pumps are high-affinity enzymes, which interact with Ca^{2+} with a K_m well below 1μM, but which transport Ca^{2+} with a low total capacity: about 0.5nmoles of Ca^{2+} transported per mg of membrane per sec (Caroni and Carafoli, 1981). The first ATP-driven Ca^{2+} transport system, which was later identified as the Serca pump, was discovered in 1961-1962 in a skeletal muscle fraction, known at the time as the Marsh relaxing factor. Studies in the early period showed that the pump transports 2 Ca^{2+} ions per ATP hydrolized and that it countertransports H^+ in exchange for Ca^{2+}. As reviewed in 2008 by Carafoli and colleagues, contrary to Serca, Pmca can transport 1 Ca^{2+} ion per ATP hydrolized, per 1 H^+(Di Leva et al., 2008). One of its major characteristics is the stimulation by calmodulin, not via phosphorylation, but through a direct interaction that moves the autoinhibitory domain calmodulin binding domain (CaM-BD) and that can lower Pmca affinity for Ca^{2+} from 20μM to 1μM (Brodin et al., 1992). Interestingly, the most potent activator of Pmca is phosphatidylinositol biphosphate (PIP2), the only acidic phospholipid whose concentration in the plasma membrane may change rapidly in response to external stimulation (Carafoli and Zurini, 1982; Choquette et al., 1984). Pmca can also be constitutively activated by calpain cleavage that definitely removes CaM-BD (James et al., 1989). All the mechanism cooperate to lower Pmca K_d to values as low as about 100-200nM (Di Leva et al., 2008).

AIM

Despite many efforts, the mechanisms underlying the pathophysiology of neurodegenerative disorders have not been clarified, yet, though a crucial point seems to be represented by metals and protein aggregation (Bush, 2000). Understanding the physiological function of the involved proteins represents a central question, since this is fundamental to characterize the pathological mechanisms, as well as to find a curative strategy. A peculiar case is represented by prion diseases, also known as Transmissible Spongiform Encephalopathies (TSEs). In fact, besides having genetic and sporadic origins, like the other neurodegenerative disorders, prion diseases are transmissible (Prusiner, 2001). In 1982, Prusiner defined the concept of prions, stating that the disorder causative infective agent has exclusively proteinaceous properties (Prusiner, 1982). This etiological agent derives from PrP^{C}, the endogenously encoded protein (Oesch et al., 1985), that triggers the pathology upon conformational conversion, giving rise to the prion, or PrP^{Sc}, enriched in β-sheets and prone to aggregate (Caughey and Raymond, 1991; Gasset et al., 1993). Despite being highly conserved among species, PrP^{C} physiological function has not been completely defined (Aguzzi et al., 2008). A striking property of PrP^{C} is its high affinity binding for divalent cations, in particular Cu, but also Zn and Mn (Jackson et al., 2001; Singh et al., 2010; Stockel et al., 1998). Concerning Cu ion, PrP^{C} is also able to support the ion reduction, being able of binding both Cu(I) and Cu(II) (Liu et al., 2011). To unveil PrP^{C} function, several knockout and transgenic murine lines for the *Prnp* gene have been created. These knockout lines are viable and fertile, showing no gross disturbancies (Bueler et al., 1992; Manson et al., 1994). However, a few phenotypic traits have been identified, suggesting a role for PrP^{C} in synapses. In fact, PrP null mice show increased excitability (Maglio et al., 2004) and reduced afterhyperpolarizarion potentials in hippocampal neurons (Mallucci et al., 2002), together with a slowed deactivation kinetic of NMDARs currents, likely due to PrP^{C}-bound Cu ions (Khosravani et al., 2008b; You et al., 2012). Moreover, PrP ablation provokes high neuronal cell death upon excitotoxic insults, such as *in vitro* kainate or NMDA tratements and *in vivo* stroke (Rangel et al., 2007; Spudich et al., 2005; You et al., 2012). It has been proposed that PrP^{C} functions in hippocampal glutamatergic synapses–where it is highly expressed–as an inhibitory modulator of NMDA receptors (NMDARs) activity, and this role seems to be crucial in stressful conditions. However, the precise mechanism through which PrP^{C} carries on this function has not been defined. Can PrP^{C} role in glutamatergic synapses, as well as in stressful conditions, be due to its metal ion binding property? Metal ions are essential for many biochemical reactions and they play key roles in embryonic, fetal and postnatal development in higher eukaryotes central nervous system. In the brain,

different mechanisms have developed to sense and regulate tightly transition metals concentration. Alteration in metal ion homeostasis, due to altered supply or protein loss of function, strongly impairs neuronal functionality: deficiencies during prenatal or early postnatal life result in profound development disturbances, while accumulation or dyshomeostasis is toxic because metal ions support Fenton reaction leading to free radicals production (Kambe et al., 2008). Essential metals are crucial synaptic function regulators: for example, Zn and Cu, released in the synaptic cleft, modulate NMDARs (Choi and Lipton, 1999; Fayyazuddin et al., 2000; Low et al., 2000; Paoletti et al., 2000; Vlachova et al., 1996). Besides being a metal binding protein, increasing evidences suggest that PrP^C is involved in metal ion homeostasis maintenance and in their metabolism (Brown, 2003; Brown et al., 2001; Singh et al., 2009a; Singh et al., 2009b; Singh et al., 2010). Moreover, *Prnp*$^{0/0}$ mice show impairments in synaptic functionality and neuronal excitability in the hippocampus, increased susceptibility in stressful conditions, as well as demyelination in aging, and metal ions play fundamental roles in all these cellular mechanisms. The aim of the first part of this project was the characterization of PrP^C role in metal ions metabolism and homeostasis. To do this, *Prnp*$^{+/+}$ and *Prnp*$^{0/0}$ brains and hippocampi have been compared concerning their Cu, Fe, Zn and Mn content, as well as the expression levels of the major proteins involved in their metabolism. The hippocampus has been chosen as a brain area of major interest for two reasons: first, it displays very high levels of PrP^C expression (Benvegnu et al., 2010; Sales et al., 1998); second, many hippocampal impairments have been observed in *Prnp*$^{0/0}$ mouse models (Colling et al., 1996; Collinge et al., 1994; Criado et al., 2005; Khosravani et al., 2008b; Maglio et al., 2004; Mallucci et al., 2002; Rangel et al., 2007). Particular attention has been paid to ceruloplasmin (Cp) since it is expressed in two isoforms–i.e. a secreted one and a membrane-anchored one–that allow Cp to be at the same time the major Cu carrier in the serum and a Cu-dependent oxidase with key functions in Fe and Mn absorption and distribution (Harris et al., 1995). The aim of the second part of the project was the understanding of the exact mechanism through which PrP^C inhibits NMDARs, exerting a neuroprotective role in stressful conditions. PrP^C is localized in lipid rafts of the postsynaptic terminal, close to NMDARs (Fournier et al., 2000; Haeberle et al., 2000; Herms et al., 1999; Linden et al., 2008; Naslavsky et al., 1997; Sales et al., 1998). Their opening, upon glutamate release from the presynaptic bouton, activates the protein of the *trans*-Golgi network: the Cu transporter Atp7a is one of them. This event provokes the release of Cu into the synaptic cleft, reaching 100μM concentration (Schlief et al., 2005; Schlief et al., 2006). Released Cu ions are able to modulate NMDARs activity, but the precise mechanism has not been understood and no binding sites have been identified, yet (Vlachova et al., 1996). Ca^{2+} influx through NMDARs activates also neuronal nitric oxide synthase (nNOS). The produced NO can cross plasma membrane and play functions in the synaptic cleft, for example it can modulate proteins by mean of cysteine residues S-nitrosylation (Jaffrey and Snyder, 2001; Lipton et al., 2002). NMDAR subunits GluN1 and GluN2A are

S-nitrosylated on extracellular cysteines and this reaction is always inhibitory (Choi et al., 2000). This posttranslational modification requires an electron acceptor that is reduced upon cysteine thiol oxidation: this electron acceptor is usually Cu. As above described, a high amount of Cu ions is available in the synaptic cleft after NMDARs opening. However, to prevent Fenton reaction and oxidative stress production, Cu is immediately bound by metal-binding proteins: one of them is PrP^C that can bind both Cu(II) and Cu(I) and even supports the reduction. Moreover, it has been published that PrP^C-bound Cu ions support the S-nitrosylation of another membrane protein (Mani et al., 2003) and that PrP^C modulation of NMDARs is dependent on Cu ions (You et al., 2012). To summarize, the aim of the project was to study the neuroprotective role of PrP^C in glutamatergic synapses mediated by the inhibitory S-nitrosylation of NMDARs. First, the enhanced susceptibility to excitotoxic stimulus in a *Prnp*$^{0/0}$ murine model was studied in organotypic hippocampal cultures treated with NMDA by comparing neuronal death, as the appearance of pyknotic nuclei, in three different regions: *Cornu Ammonis* 1 (CA1), *Cornu Ammonis* 3 (CA3) and the Dentate Gyrus (DG). Second, the expression levels of proteins involved in the excitotoxic mechanism was established (Dong et al., 2006), in particular, NMDA receptor subunits GluN1, GluN2A and GluN2B, nNOS, Casp3 and calcium transporters, Ncx1, Pmca and Serca2 (the isoforms Ncx1 and Serca2 were chosen according to their expression pattern in the CNS). Since some alterations in Ncx1, Pmca and Serca2 expression have been detected, Ca^{2+} concentration was measured and compared to establish whether PrP null mice increased susceptibility was due to Ca^{2+} overload in the CNS. Third, GluN1 and GluN2A S-nitrosylation levels were compared in *Prnp*$^{+/+}$ and *Prnp*$^{0/0}$ hippocampi from adult mice. To do this, the biotin switch assay was set up (Jaffrey and Snyder, 2001).

MATERIALS AND METHODS

ANIMALS

Inbred FVB/N *Prnp*$^{+/+}$ and FVB *Prnp*$^{0/0}$ mice were used in these experiments. The FVB *Prnp*$^{0/0}$ mice were obtained by backcrossing the original *Prnp*$^{0/0}$ mice (ZurichI (Bueler et al., 1992)) to FVB/N inbred mice for more than 20 generations (Lledo et al., 1996). All experiments were carried out in accordance with European regulations [European Community Council Directive, November 24, 1986 (86/609/EEC)] and were approved by the local authority veterinary service. After the animal sacrifice, brains were extracted and hippocampi were isolated in phosphate buffered saline pH 7.4 (PBS). Dissected structures were immediately frozen in liquid nitrogen and stored at -80°C. Samples were collected at the following developmental stages: P1 (post-natal day 1), P7, P30, P90, P180, P365. P1 and P7 were considered early developmental stages, P30 the end of synaptogenesis, P90 adulthood, P180 late adulthood, P365 aging.

PROTEIN EXPRESSION ANALYSIS

Proteins expression was measured by Western blot (WB). Brains and ippocampi, extracted from male mice, were homogenized and briefly sonicated in lysis buffer containing: 50mM TrisHCl pH 7.5, 150mM NaCl, 1mM EDTA, 0.5% 3-[(3-cholamidopropyl)dimethylammonio]-1-propanesulfonate (CHAPS, Sigma-Aldrich, St Louis, MO, USA), 10% glycerol, proteases inhibitors cocktail (Inhibitor complete mini, Roche Diagnostics Corp., Mannheim, Germany). After samples cleaning by centrifugation (10 min, 2000g, 4°C), protein concentration was determined by bicinchoninic acid (BCA) assay (Pierce, Rockford, IL, USA). For each sample, the same protein amount (30-60μg) was separated on SDS–PAGE. On each gel, *Prnp*$^{+/+}$ and *Prnp*$^{0/0}$samples of the same age were loaded, in order to compare them. Commonly, proteins were boiled in loading buffer (10% glycerol, 50mM TrisHCl pH 6.8, 2% w/v SDS, 4M Urea, 0.005% bromophenol blue). However, for a few proteins analysis (Ncx, Serca2, Pmca), denaturation was performed at 30°C for 30 min with a different loading buffer (72mM NaCl, 1.9M Urea, 5mM DTT, 3% w/v SDS, 10% w/v glycerol, 62.5mM TrisHCl pH 6.8, 0.004% bromophenol blue). The acrylamide concentration was chosen depending on the protein molecular weight (MW). Proteins were transferred on nitrocellulose and after 1h in blocking solution membranes were incubated overnight at 4°C with the primary antibody, except anti-β-Tubulin III, anti-β-Actin,

anti-PrP, anti-Atp7b and anti-Fp1, which were incubated 1h at room temperature. After incubation with the secondary antibody, membranes were developed with ECL detection reagent (GE Healthcare, Waukesha, WI, USA) and recorded by the digital imaging system Alliance 4.7 (UVITEC, Cambridge, UK). Bands quantification was performed with Uviband 15.0 software (UVITEC, Cambridge, UK). Each protein signal was normalized against either β-Actin or β-Tubulin III, depending on the protein MW, the signal intensity and the secondary antibody.

ANTIBODIES

The following primary antibodies were used in TBST + 5% milk: monoclonal [5F10] to Calcium Pump pan Pmca ATPase 1:2000 (ab2825 Abcam, Cambridge, UK); anti-Ctr1 1:500 (ab123105 Abcam); anti-Sod1 1:1000 (ab13499 Abcam); anti-ZnT3 1:1000 (197002 Synaptic System, Goettingen, Germany); monoclonal anti-PrP SHA31 1μg/ml (A03213 BertinPharma, Montigny le Bretonneux, France); Fab D18 fragment raised against PrP 1μg/ml, InPro Biotech; anti-Atp7b 1:1000 (NB100-360 Novus Biologicals, Littleton, CO, USA); anti-nNOS 1:1000 (4234 Cell Signaling, Beverly, MA, USA); anti-GluN2A 1:1000 (ab1555 Millipore, Billerica, MA, USA); anti-TfR1 1:500 (13-6800 Invitrogen, Paisley, UK); anti-Sod2 1:1000 (SAB2102261 Sigma-Aldrich); anti-β-Tubulin III 1:5000 (T2200 Sigma-Aldrich); anti-β-Actin Peroxidase (AC-15) 1:10000 (A3854 Sigma-Aldrich); anti-GluN1 1:2000 (G8913 Sigma-Aldrich); anti-GluN2A 1:2000 (G9038 Sigma-Aldrich); anti-Steap3 1:3000 (AV43515 Sigma-Aldrich); anti-Atp7a 1:2000 (AV33797 Sigma-Aldrich); anti-Ccs (FL-274) 1:400 (sc-20141 Santa Cruz Biotechnology, CA, USA); anti-Ncx (H-300) 1:200 (sc-32881 Santa Cruz); anti-GluN2B (C-20) 1:200 (sc-1469 Santa Cruz).

The following primary antibodies were used in TBST + 5% BSA: anti-Cp 1:250 (611488 BD Transduction Laboratories, Milan, Italy); anti-Tf 1:2000 (GTX21223 GeneTex, Texas, USA); anti-human ferritin 1:1000 (F5012 Sigma-Aldrich); anti-ferritin heavy chain (H-53) 1:200 (sc-25617 Santa Cruz); anti-Metallothionein (FL-61) 1:200 (sc-11377 Santa Cruz).

The following primary antibodies were used in TBST + 3% BSA + 5% milk: anti-Fp1 1:1000 (NBP1-21502 Novus Biologicals); anti-Serca2 (N-19) 1:500 (sc-8095 Santa Cruz).

METAL IONS MEASUREMENTS

Brains and ippocampi from male mice were dissected in bidistilled water (ddH_2O), to maximally reduce metal ions contamination, and completely dried in vacuum conditions before weighing them. Samples were dissolved in 5 volumes of 65% nitric acid (30709, Sigma Aldrich) overnight at 70°C, except P1 and P7 hippocampi which were dissolved in 10 volumes of 65% nitric acid. Calcium content was

measured by a Perkin-Elmer atomic absorption spectrophotometer (model AAnalyst 100), while copper, iron, manganese and zinc were measured by inductively coupled plasma mass spectroscopy (ICP-MS, NexION 300D, PerkinElmer).

CERULOPLASMIN ACTIVITY

Ceruloplasmin is a Cu-dependent ferroxidase and the major Cu transporter in the blood. Its enzymatic activity was measured from *Prnp*$^{+/+}$ and *Prnp*$^{0/0}$serum. Serum samples were prepared as follows: male mice were deeply anesthetized with 2g/kg urethane (Sigma-Aldrich), blood was taken directly from the heart and was left 30 min at room temperature to finally isolate serum by centrifugation at 900g for 10 minutes. Cp activity was measured following the protocol published by (Schosinsky et al., 1974). Briefly, 50µl serum (50µl ddH_2O for the blank) were added to 750µl acetate buffer (100mM sodium acetate·3H_2O, pH 5) and heated for 5 min at 30°C. The substrate, *o*-dianisidine dihydrochloride (D3252, Sigma-Aldrich), was prepared 7.88mM in ddH_2O and heated at 30°C for 5 min. 200µl 7.88mM *o*-dianisidine were added to the each tube and the reaction was stopped and stabilized adding 2ml 9M sulfuric acid. Differently from the published protocol, set up on human serum, in which the reaction was stopped after 15 minutes, in our experimental conditions this timing was not enough to get a good absorbance (Abs) peak at 540nm. Performing a reaction time course, we observed that the peak signal was strong and not at plateau after 2.5 hours reaction (Figure 15). So 2.5 hours was the reaction time used for the comparison between *Prnp*$^{+/+}$ and *Prnp*$^{0/0}$serum samples Cp activity. The enzymatic activity of ceruloplasmin is expressed in International Units, in terms of substrate consumed: Ceruloplasmin oxidase activity = Abs x 0.416 U/ml. The factor 0,0416 was obtained as follows: Concn of substrate oxidized = (absorbance x 3 x 20)/(9. 6 x 150) µmol/ml per minute, where: 9.6 is the molar absorptivity of colored solution in terms of substrate consumed (ml µmol^{-1} cm^{-1}); 3.0 = correction factor for the final measured solution volume; 20 correction for serum volume used (0.05 ml); and 150 incubation time (min) (Schosinsky et al., 1974).

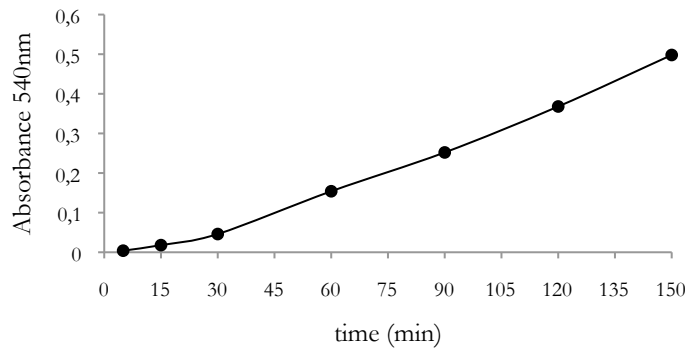

Figure 15. Cp activity reaction time-course.

RNA EXTRACTION AND REAL TIME PCR

To check Cp mRNA levels, hippocampi from P15 male mice were investigated. This developmental stage was chosen because it is in the middle between P7 and P30, which are two ages showing high protein level difference between *Prnp*$^{+/+}$ and *Prnp*$^{0/0}$. Four *Prnp*$^{+/+}$ and four *Prnp*$^{0/0}$hippocampi were immediately taken after sacrifice into TRIzol reagent (15596018, Invitrogen), frozen in liquid nitrogen and stored at -80°C. Total RNA from the samples was extracted following the TRIzol reagent manufacturer's instructions. To limit genomic DNA contamination, samples were treated with RNase free DNase set (79254, Qiagen, Germantown, MD, USA) and purified using the RNeasy mini kit (74104, Qiagen). Total RNA quality was assessed by observing on 1% agarose gel the two characteristic bands corresponding respectively to 28S, 18S rRNA, together with a lower and less intense band likely corresponding to tRNA and 5S rRNA. RNA quantification was performed using an ND-1000 Nanodrop spectrophotometer (Thermoscientific). For each sample, 4µg of RNA were retrotranscribed by using SuperScriptIII RT (18080, Invitrogen) and oligodT primer (5′-GCT GTC AAC GAT ACG CTA CGT AAC GGC ATG ACA GTG$(T)_{24}$-3′).

To check genomic contamination, RT- reactions were performed, i.e. retrotranscription reaction without the SuperScriptIII RT enzyme. Quantitative real time PCR was performed using iQ SYBR Green Supermix (170-8880, Bio-Rad, Hercules, USA) and an iCycler IQ Real Time PCR System (Bio-Rad). Expression of the gene of interest was normalized to housekeeping gene βIII-Tubulin and glyceraldehyde 3-phosphate dehydrogenase (Gapdh), and the initial amount of the template of each sample was determined as relative expression versus housekeeping gene chosen as reference. The relative expression of each sample was calculated by the formula $2exp^{-\Delta\Delta Ct}$ (User Bulletin 2 of the ABI Prism 7700 Sequence Detection System) (Livak and Schmittgen, 2001). Housekeeping gene expression is not modified under the present experimental conditions (data not shown). Primer sequences for secreted Cp (sec_Cp), GPI-anchored Cp (GPI_Cp), βIII-Tubulin (βTub) and Gapdh are shown in Table 4. Real time PCR products were also analyzed on a 2% agarose gel.

Primer		*Primer sequence (5'-3')*	*Base pairs*	*Annealing temperature (°C)*	*Accession no.*	*Reference*
sec_Cp	sense	TCCCTGGAACATACCAAACC	157	60	NM_007752	(Stasi et al., 2007)
	antisense	ATTTATTTCATTCAGCCAGACTTAG				
GPI_Cp	sense	TCCCTGGAACATACCAAACC	158	60	AK086999	(Stasi et al., 2007)
	antisense	CCAGGTCATCCTGTAACTCTGA			AK043248	
βTub	sense	CGCCTTTGGACACCTATTC	240	60	NM_023279	(Simonetti et al., 2008)
	antisense	TACTCCTCACGCACCTTG				
Gapdh	sense	TTCACCACCATGGAGAAGGC	236	60	NM_008084	(Chen et al., 2003)
	antisense	GGCATGGACTGTGGTCATGA				

Table 4. Experimental parameters used for real time PCR experiments

BIOTIN SWITCH ASSAY

The biotin switch assay was performed as described by Jaffrey and Snyder (Jaffrey and Snyder, 2001) with a few modifications. Hippocampal samples were collected as described above from adult male mice and homogenized in 400µl HEN buffer (250mM HEPES pH 7.5, 1mM EDTA, 0.1mM Neocuproine (Sigma-Aldrich) containing proteases inhibitors and centrifuged at 2000g, 10 minutes at 4°C. Protein concentration in the supernatant was determined by BCA assay. For each sample, 1mg of proteins was used for the further steps of the protocol. Samples were diluted to 0.8µg/µl in HEN buffer + 0.4% CHAPS (Sigma Aldrich) and incubated in 4 volumes of blocking solution (9 volume of HEN, 1 volume of 25% w/v SDS in ddH_2O, 20mM methyl methanthiosulfonate (MMTS, Sigma-Aldrich) from the 2M stock solution in dimethylformamide (DMF)) at 50°C for 1 hour. MMTS was removed by acetone-precipitation and the protein pellet was resuspended in 100µl of HENS buffer (HEN+1%SDS). 30mM ascorbate was added to samples and the reaction was carried out for 3 hours at 25°C (Giustarini et al., 2008). Ascorbate was removed by acetone-precipitation and the protein pellet was resuspended in 100µl of HENS buffer. EZ-Link HPDP-biotin (Thermoscientific, Waltham, MA, USA) was added 1:3 to the samples. After 1 hour incubation at 25°C, HPDP-biotin was removed by dialysis in HENS buffer. To purify biotinilated proteins, 2 volumes of neutralization buffer (20mM HEPES pH 7.5, 100mM NaCl, 1mM EDTA, 0.5% Triton X-100) and 15µl of Immobilized NeutrAvidin Protein (Thermoscientific) were added to the samples and incubated for 2 hours at room temperature. Resin was washed 5 times with neutralization buffer adjust to 600mM NaCl, biotinilated proteins were eluted directly in SDS-PAGE sample buffer boiled and loaded on 8% acrylamide gel for protein immunodetection.

ORGANOTYPIC HIPPOCAMPAL CULTURES PREPARATION

Organotypic hippocampal culture (OHC) preparation protocol was set up based on Gahwiler (Gahwiler et al., 1997). Briefly, in aseptic condition P5 mice hippocampi were dissected in dissection medium (Gey's balanced salt solution, 5.6mM D-Glucose, 1mM kynurenic acid) and sliced by means of a tissue chopper into 300μm thick sections. After washing in dissection medium for 40 min at 4°C, slices showing an intact hippocampal cytoarchitecture were selected, singularly attached to a coverslip by embedding in a chicken plasma (Sigma-Aldrich) and thrombin (Aurogene, UK) cloth and maintained at 37°C in roller tubes with a medium composed by 50% basal medium Eagle (BME, Gibco, Life Technologies, UK), 25% horse serum (Gibco), 25% Hank's balanced salt solution (Gibco), 5.6mM D-Glucose, 2mM L-Glutamine.

EXCITOTOXIC TREATMENT

To compare susceptibility to excitotoxicity in *Prnp*$^{+/+}$ and *Prnp*$^{0/0}$cultures, after 13 days *in vitro* (DIV) OHCs were treated in serum-free medium for 3h with 5μM NMDA (Tocris biosciences, UK). NMDA was dissolved 1mM in sterile ddH_2O and stored at -20°C. In control slices, serum-free medium was added with corresponding volume of ddH_2O. One slice for each group was taken after the treatment to assess the immediate effect, while the remaining slices were in left 24h wash out in culture medium. Afterwards, all the slices were processed for immunofluorescence.

IMMUNOFLUORESCENCE

To evaluate neuronal cell death, slices were fixed in 4% paraformaldehyde (PFA, Sigma Aldrich) in PBS pH 7.4 overnight at 4°C. To improve the nuclear staining, slices were treated as follows: 5 min for 3 times washing in PBS-1% TritonX-100, 10 min in 0.1N HCl at 4°C, 10 min in 0.2N HCl at room temperature, 20 min in 0.2N HCl at 37°C, 12 min in borate buffer pH 8.4 (77mM boric acid, 6.6mM borax) at room temperature, 5 min for 3 times washing in PBS-1%TritonX-100. Slices were incubated for 2h at room temperature in blocking solution (1M glycin, 5% normal goat serum, PBS-1%TritonX-100) and overnight at 4°C with anti-Neuronal Nuclei antibody 1:500 (NeuN clone A60mab377 Millipore) in blocking solution. After washing 5 min for 3 times in PBS-1%TritonX-100, slices were incubated with Alexa Fluorophore-conjugated secondary antibodies (1:500) and 4',6-diamidino-2-phenylindole (DAPI, 1:500) in blocking solution for 2h at room temperature. Slices were washed in PBS, rinsed in water, and mounted with VectaShield (Vector Laboratories, Burlingame, CA, USA).

To evaluate PrP distribution, sliceswere fixed in 4% PFA in PBS pH 7.4 for 30 min at room temperature, cryoprotected in 10% sucrose in PBS for 1h at room temperature and in 20% sucrose in

PBS overnight at 4°C. To expose the antigen, slices were frozen (5 min) and thawed (5 min) 3 times in 100% ethanol using dry ice. Slices were incubated in blocking solution (10% BSA, 5% normal goat serum, PBS-0.1 % TritonX-100) 4h at room temperature, then overnight at 4°C with anti-PrP SHA31 1:500 in 5% BSA, 0.1% Triton X-100, 1% normal goat serum, PBS/tween 0.05%. After washing 30 min in 5% BSA, 1% normal goat serum in PBS, slices were incubated 3h at room temperature with Alexa Fluorophore-conjugated secondary antibodies (1:500) and DAPI (1:500) in the same solution used for the primary antibody. Slices were washed in PBS, rinsed in water, and mounted with VectaShield (Vector Laboratories).

CONFOCAL MICROSCOPY AND IMAGE ANALYSIS

Hippocampal cultures were examined on a Leica DMIRE2 confocal microscope (Leica Microsystem GmbH, Germany) equipped with DIC and fluorescent optics, Diode laser 405nm, Ar/ArKr 488nm and He/Ne 543/594nm lasers. The fluorescence images (1024x1024 pixels) were acquired with either a 63×1.4 NA or a 40×1.4 NA oil immersion objective additionally zoomed 1.5-fold, with 200Hz acquisition speed. Stacks of z-sections with an interval of 3μm were sequentially scanned. The CA1, CA3 and DG were the regions selected for the analysis (Figure 16).

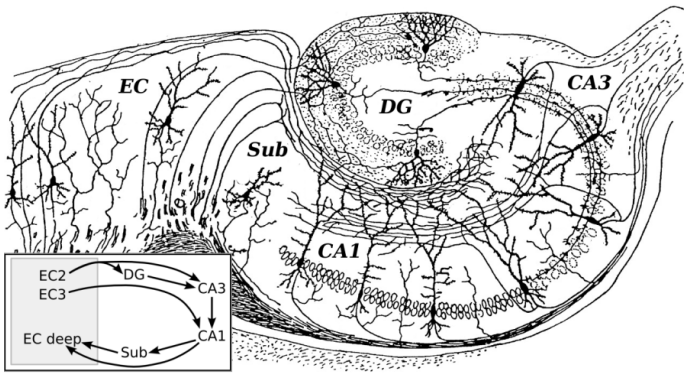

Figure 16. Scheme of hippocampus architecture (modified from Santiago Ramón and Cajal, 1911).

The total nuclei number was evaluated in singular frames (1 each 6μm) with DAPI staining using the Volocity 5.4 3D imaging software (PerkinElmer, Coventry, UK). Pyknotic nuclei were counted in the same frames by mean of ImageJ software by W. Rasband (developed at the U.S. National Institutes of Health and available at http://rsbweb.nih.gov/ij/).

STATISTICAL ANALYSES

Metal ion content, WB, Cp activity, real time PCR and pyknotic nuclei count results were compared between $Prnp^{+/+}$ and $Prnp^{0/0}$ samples performing the Student's T test setting two-tailed distribution and

two-sample unequal variance. For OHC experiments, each culture preparation (resulting from 3 mice dissection) was considered as one sample, so the average neuronal cell death percentage was calculated and compared by mean of the T test with the other culture preparations, for a final sample size of three. Concerning the biotin switch assay, in each experiment one *Prnp*$^{+/+}$ and one *Prnp*$^{0/0}$ sample were contemporary processed. Therefore, the statistics of all the experiments was performed by the paired Student's T test setting two-tailed distribution.

RESULTS

PrP^C ROLE IN ESSENTIAL METAL IONS HOMEOSTASIS MAINTENANCE

ESSENTIAL METALS CONTENT

The total content of essential metal ions (Cu, Mn, Zn and Fe) was measured in both brains and hippocampi of *Prnp*$^{+/+}$ and *Prnp*$^{0/0}$ mice at different developmental stages: P1 (newborn), P7 (early post-natal), P30 (end of synaptogenesis), P90 (adulthood), P180 (late adulthood), P365 (aging). These measurements allowed comparing trace metal ions content both in corresponding ages and in their developmental trend in *Prnp*$^{+/+}$ and *Prnp*$^{0/0}$ conditions.

Figure 17 shows metal ions content in total brain extracts, while Figure 18 illustrates results in the hippocampus. In the brain, copper content is quite constant in both wild-type and PrP null mouse conditions and rises in aging (Figure 17A). Compared to *Prnp*$^{+/+}$ samples, *Prnp*$^{0/0}$ brains show many alterations in Cu content, in particular at P1 their Cu content is half the wild-type's one. In both *Prnp*$^{+/+}$ and *Prnp*$^{0/0}$ samples, Mn trend decreases from P1 to P30, then it is kept almost constant (Figure 17B). However, its content is lower in PrP null samples at early post-natal stage and again at P180, whileit is higher at P30. Similarly to Mn, Zn content decreases from P1 to P30, then it is almost constant (Figure 17C). Also Zn concentration is lowered by PrP ablation at P1 and P180, while it is higher al P30. Concerning Fe, its content also decreases from P1 to P30, then it is constant in the adulthood and it slightly rises in aging (Figure 17D). Concerning *Prnp*$^{0/0}$ brains, Fe content is lower at P1 and P7, then higher at P30. In the hippocampus, Cu content increases during the development, but *Prnp*$^{0/0}$ samples have a lower content at the different stages with the exception of P90 (Figure 18A). Considering Mn, its concentration is lower at P180 in *Prnp*$^{0/0}$ samples (Figure 18B). Similarly to Cu, Zn content is lowered by PrP ablation at P1 and P180, but it is higher at P90 (Figure 18C). Like in the brain, Fe content show a slightly decreasing trend between P1 and P30, then it is constant and it rises in the aging. *Prnp*$^{0/0}$ samples show lower levels at P7 and P180, but a higher level at P90 compared to *Prnp*$^{+/+}$(Figure 18D).

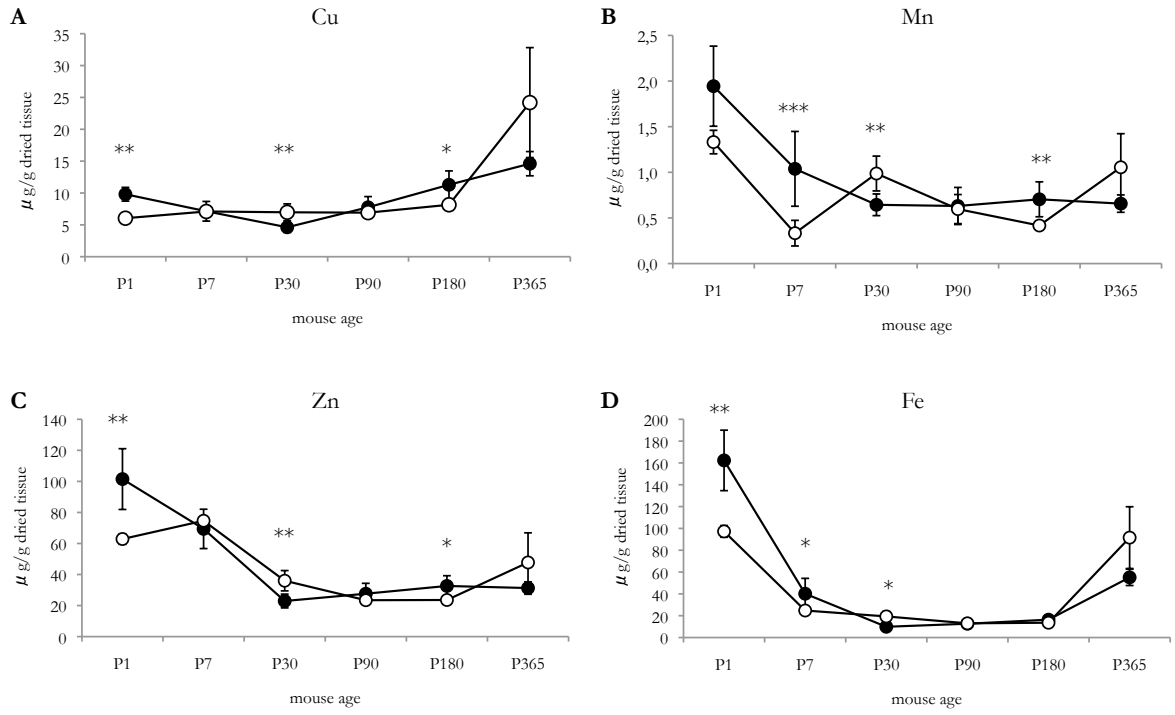

Figure 17. Transition metals content in *Prnp*$^{+/+}$ and *Prnp*$^{0/0}$ brains at different developmental stages. Filled circles (●) represent *Prnp*$^{+/+}$ values, while empty circles (○) indicate *Prnp*$^{0/0}$ values. (A) Copper; (B) Manganese; (C) Zinc; (D) Iron. Sample size: P1 n=4; P7 n=4; P30 n=6; P90 n=5; P180 n=6; P365 n=4. * p<0.05; ** p<0.01; *** p<0.001.

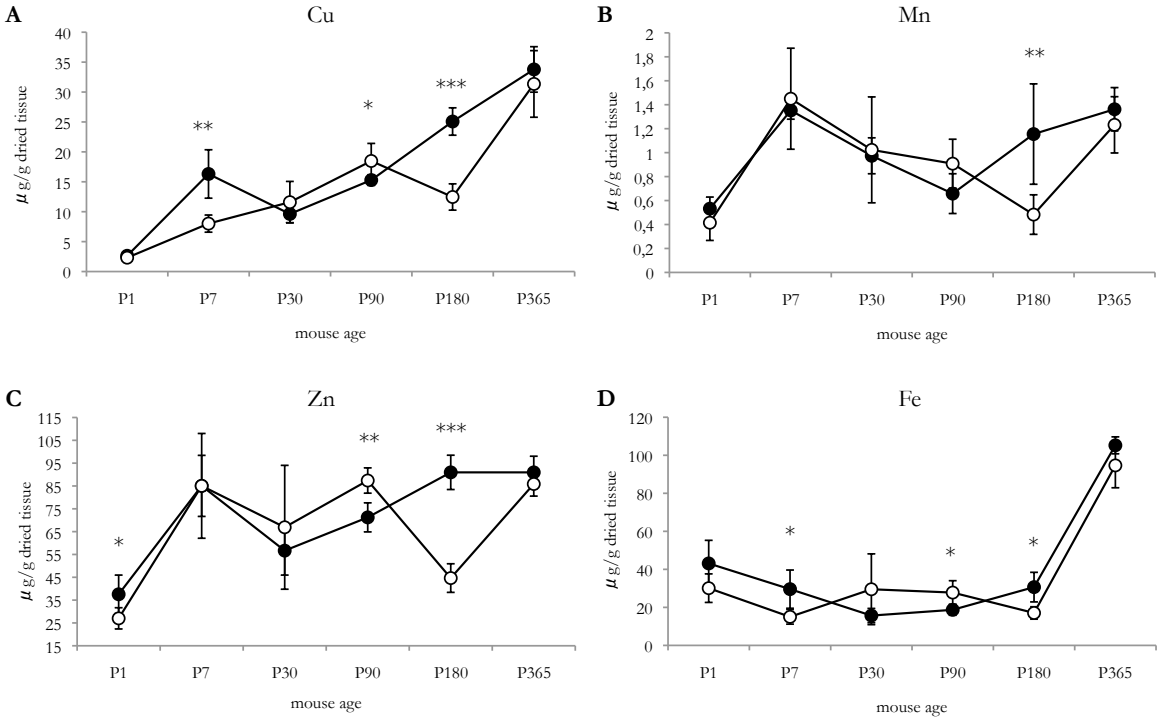

Figure 18. Transition metals content in *Prnp*$^{+/+}$ and *Prnp*$^{0/0}$ hippocampal samples at different developmental stages. Filled circles (●) represent *Prnp*$^{+/+}$ values, while empty circles (○) indicate *Prnp*$^{0/0}$ values. (A) Copper; (B) Manganese; (C) Zinc; (D) Iron. Sample size: P1 n=4; P7 n=4; P30 n=6; P90 n=5; P180 n=6; P365 n=4.. * p<0.05; ** p<0.01; *** p<0.001.

ESSENTIAL METALS HOMEOSTASIS PROTEINS EXPRESSION ANALYSIS

The expression of proteins with a relevant role in metal ions metabolism was analyzed in both *Prnp*$^{+/+}$ and *Prnp*$^{0/0}$ brains and hippocampi. β-III Tubulin and β-Actin were chosen as housekeeping proteins after verifying no differences in their expression levels between *Prnp*$^{+/+}$ and *Prnp*$^{0/0}$samples at the different considered developmental stages (Figure 19).

Concerning copper metabolism and homeostasis, the following proteins were measured: Ceruloplasmin (Cp), Six-Transmembrane Epithelial Antigen of Prostate 3 (Steap3), Cu,Zn-Superoxide Dismutase (Sod1), Copper chaperon for Sod1 (Ccs), Copper Transporter 1 (Ctr1), Atp7a and Atp7b. In Figure 20, representative images of bands obtained from WB experiments in brain and hippocampus are shown for each protein, including housekeeping proteins and PrP. Considering brain samples, in Figure 21 graphs representing proteins expression in *Prnp*$^{+/+}$ and *Prnp*$^{0/0}$ mice at the different developmental stages are reported. During development Cp expression rises and in PrP null conditions its presence is increased (Figure 21A). Steap3 expression decreases during the development but PrP absence does not affect its levels (Figure 21B). The expression of Sod1 increases with the age, but without differences induced by PrP ablation (Figure 21C). Concerning Ccs expression, it increases with the age and in *Prnp*$^{0/0}$ samples it has lower levels at P1 and P365 (Figure 21D). Considering three Cu transporters, the expression levels of Ctr1 (Figure 21E), Atp7a (Figure 21F) and Atp7b (Figure 21G) are generally not affected by PrP absence, though a increased Atp7b level in P1 mice. In Figure 22 graphs showing proteins expression in *Prnp*$^{+/+}$ and *Prnp*$^{0/0}$ hippocampal samples at the different developmental stages are shown. Cp expression increases during development, but in the hippocampus PrP absence generally lowers its levels compared to *Prnp*$^{+/+}$, though at P1 and at P365 no differences were detected (Figure 22A). As in the brain, Steap3 expression broadly decreases during the development and it does not show differences in PrP null conditions compared to *Prnp*$^{+/+}$ (Figure 22B). Again similarly to the brain, Sod1 expression increases with the age without differences between *Prnp*$^{+/+}$ and *Prnp*$^{0/0}$ samples (Figure 22C). On the contrary, Ccs expression in *Prnp*$^{0/0}$ hippocampi is lowered at some developmental stages: P1, P30 and P90 (Figure 22D). Concerning Cu transporters, Ctr1 and Atp7a expression levels rise with the age and both are generally higher in *Prnp*$^{0/0}$ samples, while, as in the brain, Atp7b expression is increased by PrP ablation just at P1 (Figure 22E-G).

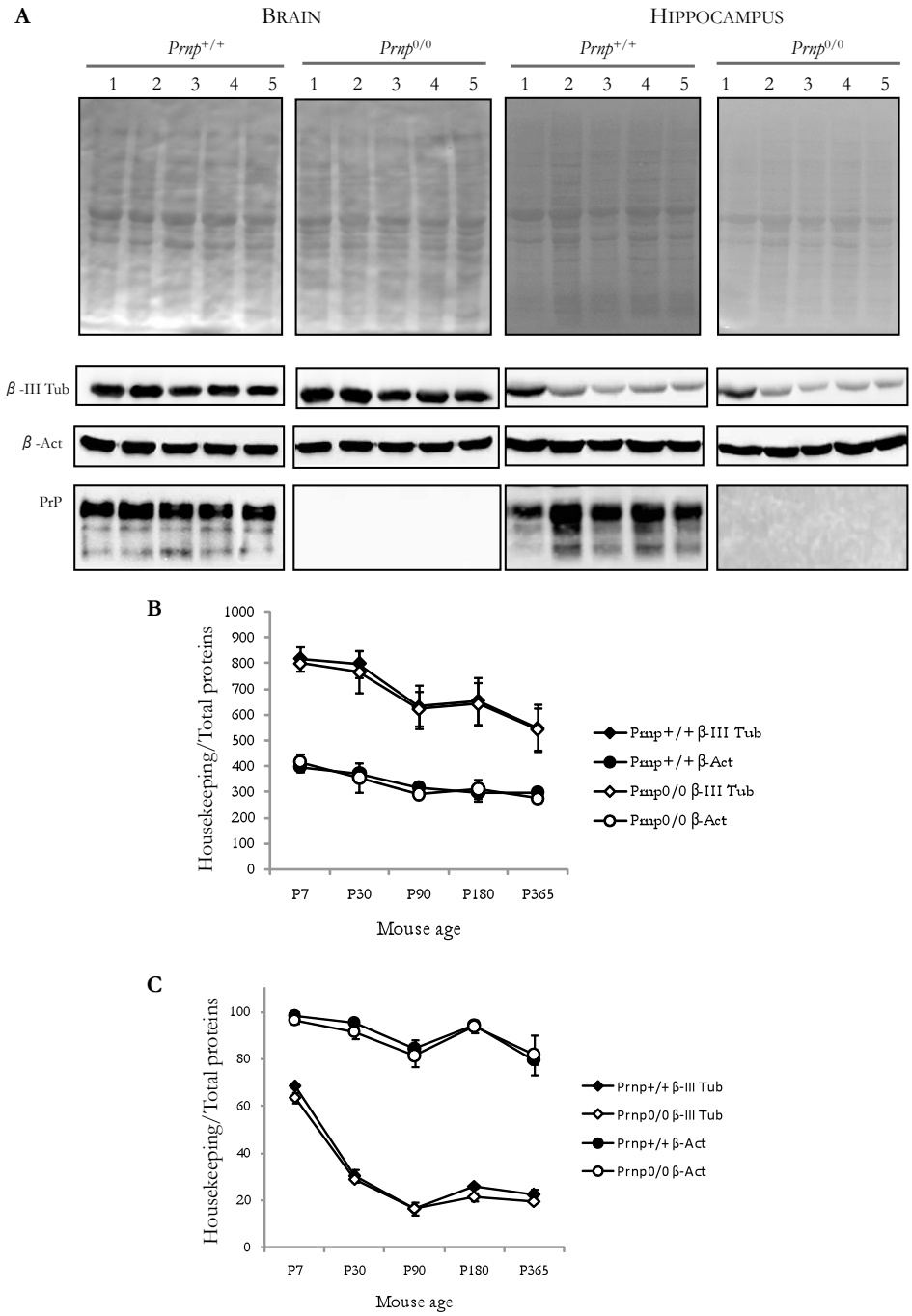

Figure 19. Comparison of housekeeping genes –β-III Tubulin and β-Actin – expression levels between *Prnp*$^{+/+}$ and *Prnp*$^{0/0}$ brain and hippocampus. (A) Top: from left to right, Ponceau staining of *Prnp*$^{+/+}$ and *Prnp*$^{0/0}$ brain and hippocampus blots, lines from 1 to 5 represent respectively P7, P30, P90, P180, P365 mouse ages; Bottom: from left to right, immunodetection of β-III Tubulin, β-Actin and PrP in *Prnp*$^{+/+}$ and *Prnp*$^{0/0}$ brains and hippocampi; (B) Graphs showing β-III Tubulin and β-Actin optical density normalized on total proteins (Ponceau staining optical density) in *Prnp*$^{+/+}$ and *Prnp*$^{0/0}$ brain (n=3); (C) Graphs showing β-III Tubulin and β-Actin optical density normalized on total proteins (Ponceau staining optical density) in *Prnp*$^{+/+}$ and *Prnp*$^{0/0}$ hippocampus (n=3).

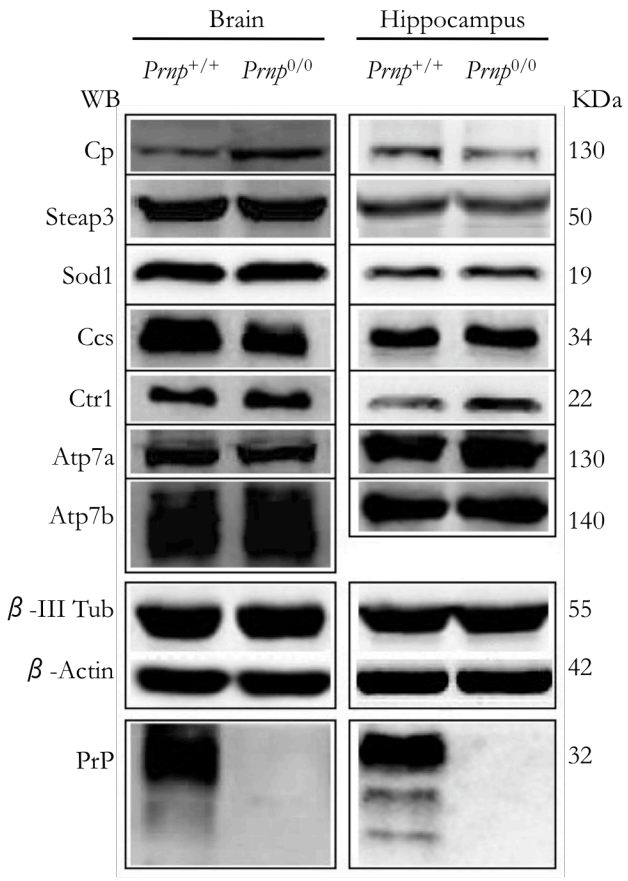

Figure 20. Copper metabolism proteins. Representative immunoblot of each analyzed protein in the whole brain and in the hippocampus in *Prnp*$^{+/+}$ and *Prnp*$^{0/0}$ mice. Housekeeping proteins – β-III Tubulin and β-Actin – are also shown. *Prnp*$^{+/+}$ and *Prnp*$^{0/0}$ genotypes were confirmed by PrP immunodetection.

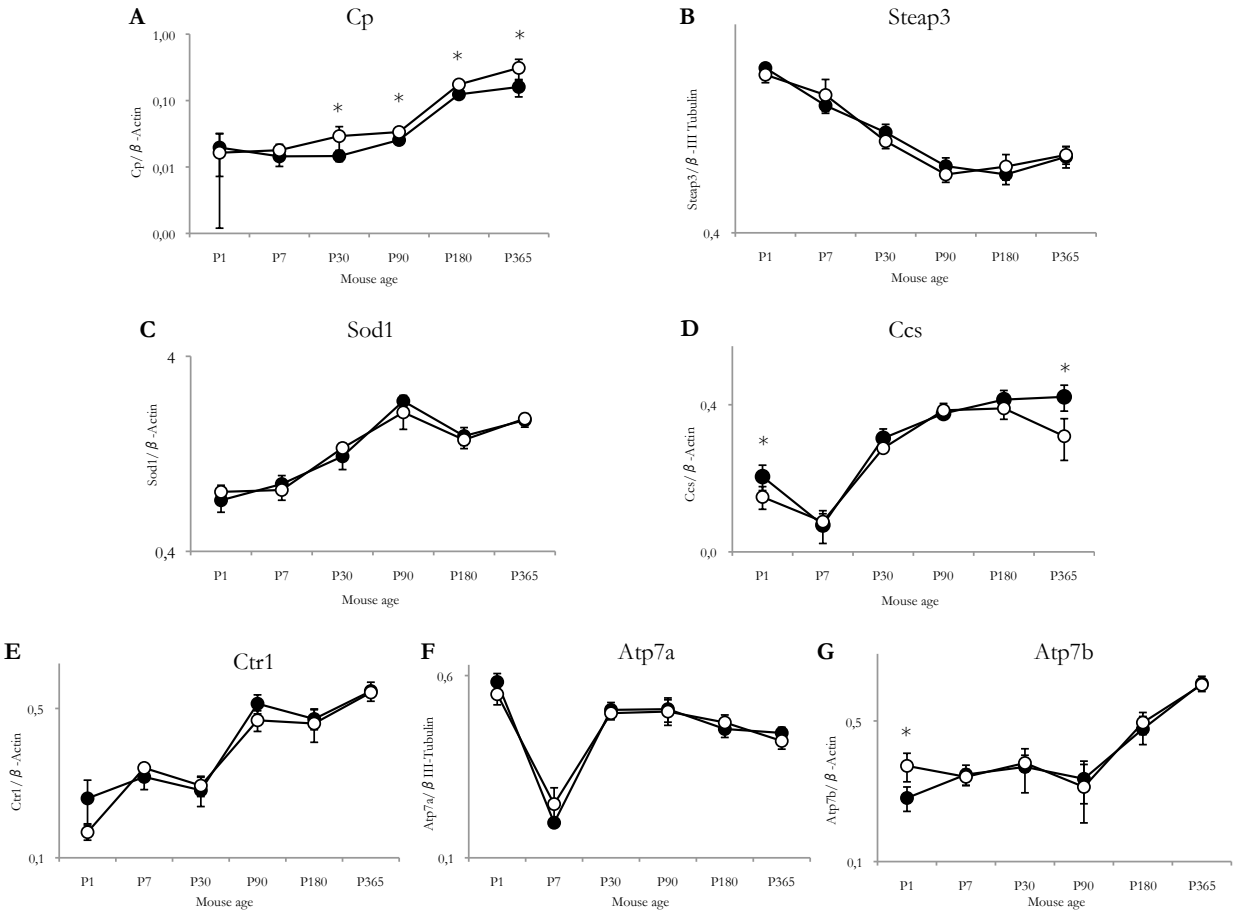

Figure 21. Copper-binding proteins expression levels in *Prnp*$^{+/+}$ and *Prnp*$^{0/0}$ brains at different developmental stages. For each protein, the optical density value was normalized on a housekeeping protein. Filled circles (●) represent *Prnp*$^{+/+}$ values, while empty circles (○) indicate *Prnp*$^{0/0}$ values. (A) Ceruloplasmin (Cp); (B) Six-Transmembrane Epithelial Antigen of Prostate 3 (Steap3); (C) Cu,Zn-Superoxide Dismutase (Sod1); (D) Copper chaperone for Sod1 (Ccs); (E) Copper Transporter 1 (Ctr1); (F) Atp7a; (G) Atp7b. Minimum sample size: n=4; * $p<0.05$, ** $p<0.01$, *** $p<0.001$

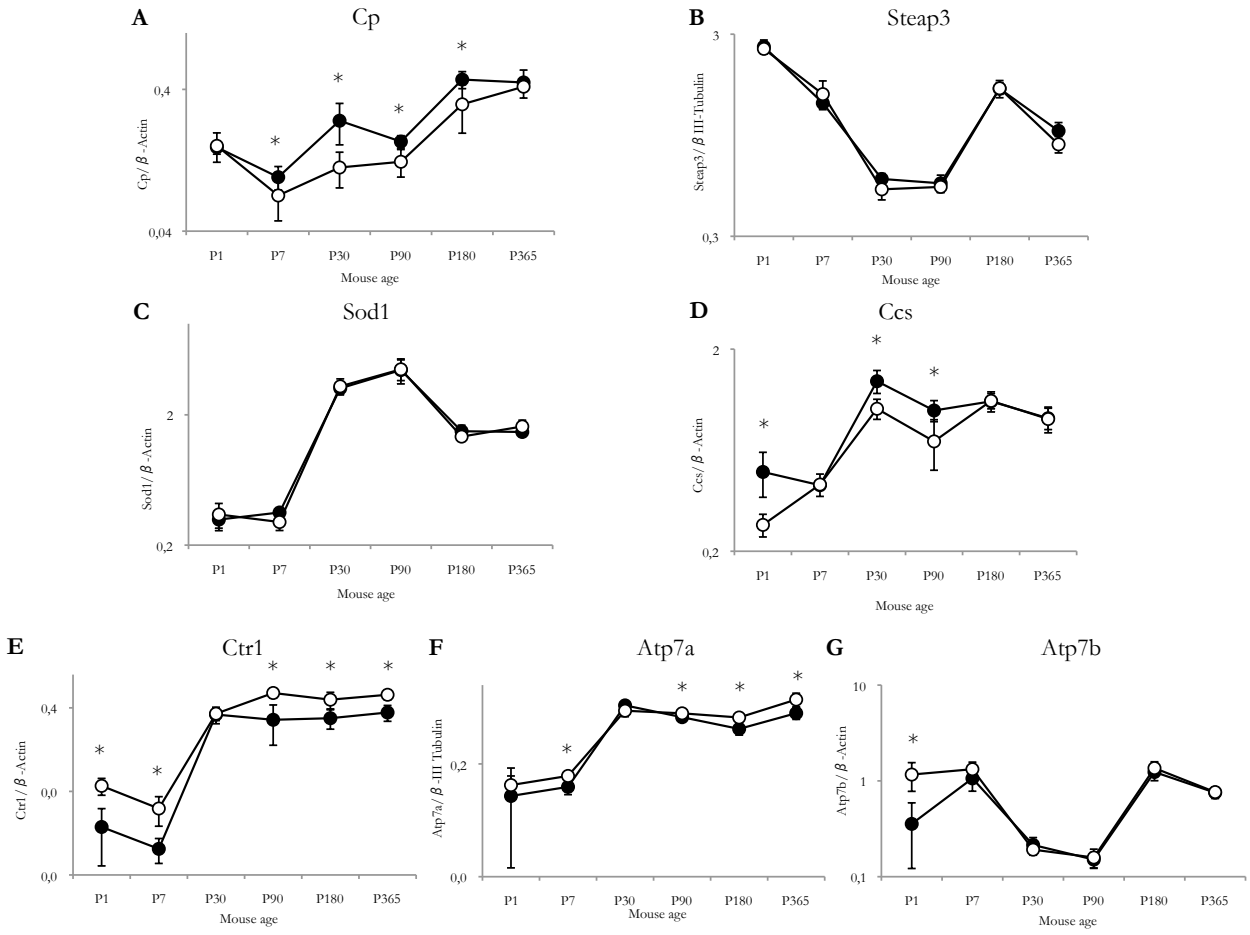

Figure 22. Copper-binding proteins expression levels in *Prnp*$^{+/+}$ and *Prnp*$^{0/0}$ hippocampi at different developmental stages. For each protein, the optical density value was normalized on a housekeeping protein. Filled circles (●) represent *Prnp*$^{+/+}$ values, while empty circles (○) indicate *Prnp*$^{0/0}$ values. (A) Ceruloplasmin (Cp); (B) Six-Transmembrane Epithelial Antigen of Prostate 3 (Steap3); (C) Cu,Zn-Superoxide Dismutase (Sod1); (D) Copper chaperone for Sod1 (Ccs); (E) Copper Transporter 1 (Ctr1); (F) Atp7a; (G) Atp7b. Minimum sample size: n=4; * p<0.05, ** p<0.01, *** p<0.001

To study Fe metabolism alterations due to PrP ablation, the following proteins were analyzed: Cp, Steap3, Transferrin (Tf), Transferrin Receptor 1 (TfR1). Ferroportin 1 (Fpn1), Ferritin heavy chain (FtH), Ferritin light chain (FtL). Figure 23 shows representative images of bands obtained from WB experiments in brain and hippocampus for each protein, including housekeeping proteins and PrP to confirm its absence in PrP null mice. In Figure 24, graphs representing proteins expression in *Prnp*$^{+/+}$ and *Prnp*$^{0/0}$ brains at the different developmental stages are reported. Though reported also in Figure 24A,B to facilitate a comprehensive analysis, brain Cp and Steap3 expression patterns were described in the previous paragraph. PrP null mice show higher expression levels of Fe uptake proteins, Tf and TfR1 at all the developmental stages analysed, with exception of P1 TfR1 which is lower in PrP null samples (Figure 24C,D). On the contrary, Fpn1 levels are lowered in *Prnp*$^{0/0}$samples starting from P30

(Figure 24E), while FtH levels are lowered from P1 to P30 and then slightly higher at P180 and P365 (Figure 24F). Concerning FtL expressions, no alterations were observed in *Prnp*$^{0/0}$ brains compared to *Prnp*$^{+/+}$ (Figure 24G). Figure 25 shows graphs corresponding to the expression patterns of the analyzed proteins at the different developmental stages in *Prnp*$^{+/+}$ and *Prnp*$^{0/0}$ hippocampi. Figure 25A-B shows Cp and Steap3 trends already described in the previous paragraph. As in the brain, Tf and TfR1 expression levels are broadly increases in PrP absence (Figure 25C,D). Differently from the brain, Fpn1 levels are not altered in PrP null hippocampi (Figure 25E), while FtL expression is lowered from P1 to P90 (Figure 25G). Concerning FtH expression, similarly to the brain, it is lower in *Prnp*$^{0/0}$ from P1 to P90 and at P180 and P365 slightly increased (Figure 25F).

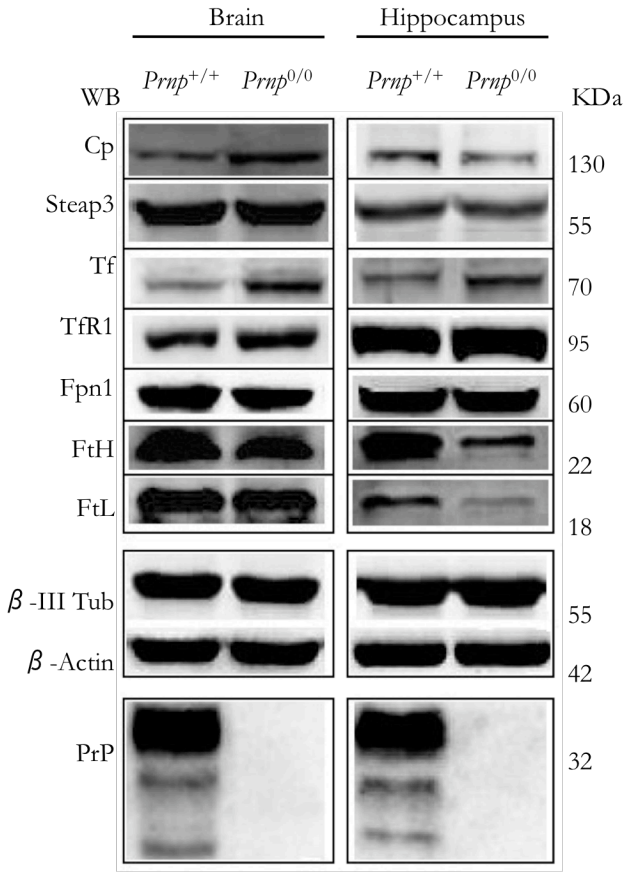

Figure 23. Iron metabolism proteins. Representative immunoblot of each analyzed protein in the whole brain and in the hippocampus in *Prnp*$^{+/+}$ and *Prnp*$^{0/0}$ mice. Housekeeping proteins – β-III Tubulin and β-Actin – are also shown. *Prnp*$^{+/+}$ and *Prnp*$^{0/0}$ genotypes were confirmed by PrP immunodetection.

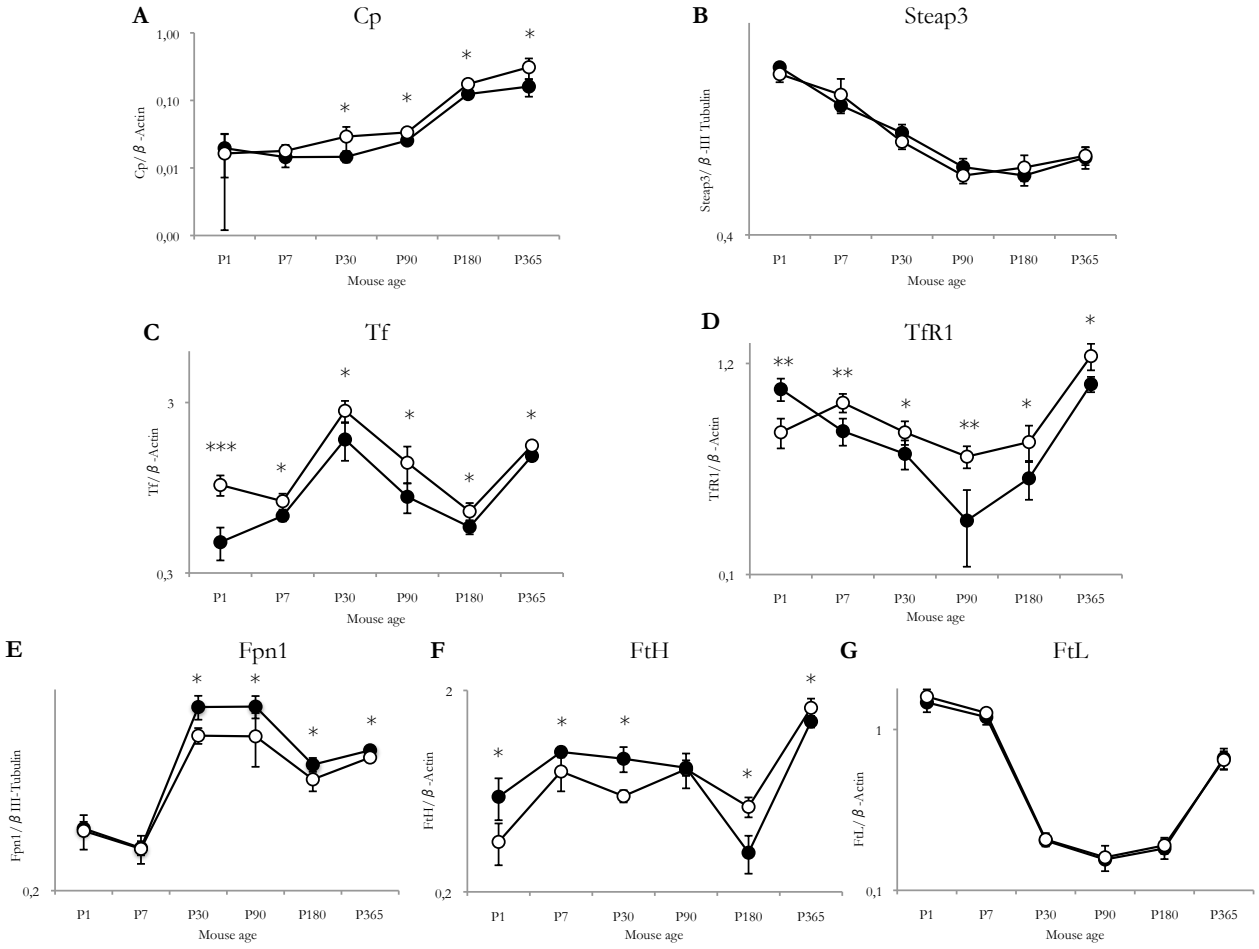

Figure 24. Expression levels of iron metabolism proteins in *Prnp*$^{+/+}$ and *Prnp*$^{0/0}$ brains at different developmental stages. For each protein, the optical density value was normalized on a housekeeping protein. Filled circles (●) represent *Prnp*$^{+/+}$ alues, while empty circles (○) indicate *Prnp*$^{0/0}$ values. (A) Ceruloplasmin (Cp); (B) Six-Transmembrane Epithelial Antigen of Prostate 3 (Steap3); (C) Transferrin (Tf); (D) Transferrin Receptor 1 (TfR1); (E) Ferroportin 1 (Fpn1); (F) Ferritin heavy chain (FtH); (G) Ferritin light chain (FtL). Minimum sample size: n=4; * $p<0.05$, ** $p<0.01$, *** $p<0.001$

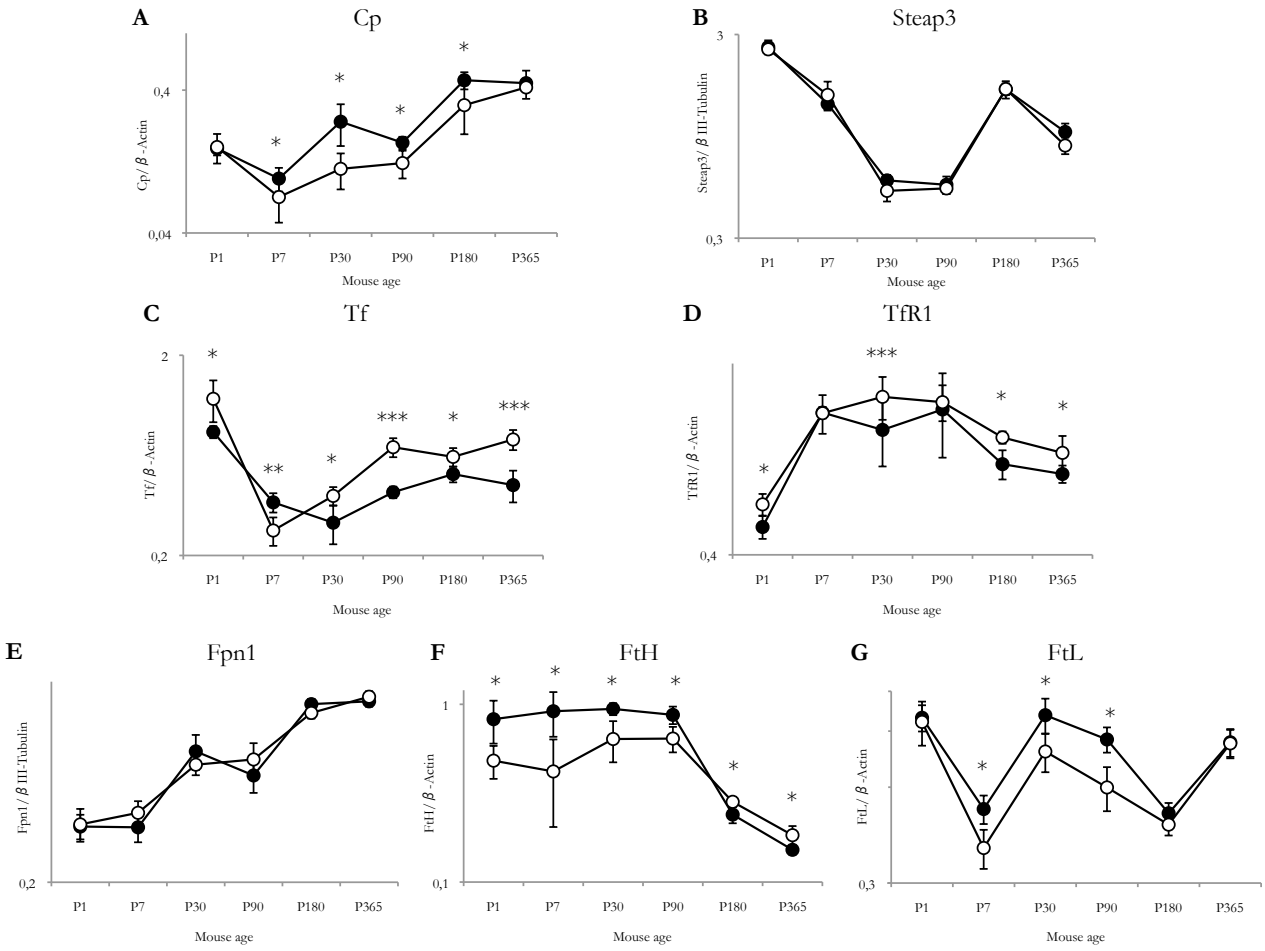

Figure 25. Expression levels of iron metabolism proteins in *Prnp*$^{+/+}$ and *Prnp*$^{0/0}$ hippocampi at different developmental stages. For each protein, the optical density value was normalized on a housekeeping protein. Filled circles (●) represent *Prnp*$^{+/+}$ values, while empty circles (○) indicate *Prnp*$^{0/0}$ values. (A) Ceruloplasmin (Cp); (B) Six-Transmembrane Epithelial Antigen of Prostate 3 (Steap3); (C) Transferrin (Tf); (D) Transferrin Receptor 1 (TfR1); (E) Ferroportin 1 (Fpn1); (F) Ferritin heavy chain (FtH); (G) Ferritin light chain (FtL). Minimum sample size: n=4; * $p<0.05$, ** $p<0.01$, *** $p<0.001$

To characterize Zn metabolism in PrP absence, the expression of the following protein was analyzed: Sod1, Metallothioneins (Mt) and Zn transporter 3 (ZnT3). Figure 26 shows representative bands obtained from WB experiments of brains and hippocampi for each protein including housekeeping and PrP to confirm *Prnp*$^{+/+}$ and *Prnp*$^{0/0}$ samples. In Figure 27 graphs displaying Zn metabolism proteins expression in *Prnp*$^{+/+}$ and *Prnp*$^{0/0}$ brains at the different developmental stages are reported. As previously reported for Cu metabolism, Sod1 expression is not altered in PrP null condition (Figure 27A). Concerning Mt expression, though a lower level in *Prnp*$^{0/0}$ at P7, it is quite constant during development then it decreases in the aging. However, at P180 and P365 PrP absence keeps Mt levels slightly higher compared to *Prnp*$^{+/+}$ (Figure 27B). ZnT3 expression rises during development reaching a plateau at the end of synaptogenesis without showing any difference between *Prnp*$^{+/+}$ and *Prnp*$^{0/0}$ brains (Figure 27C). Figure 28 reports graphs describing Zn metabolism proteins expression at the different

ages in *Prnp*$^{+/+}$ and *Prnp*$^{0/0}$ in hippocampal samples. Figure 28A reports the same Sod1 pattern already described for Cu metabolism. Mt and ZnT3 expression levels increase from P1 to P30 where they reach a peak and then Mt decreases towards aging while ZnT3 is constant, both without revealing any difference in PrP null conditions compared to *Prnp*$^{+/+}$ (Figure 28B,C).

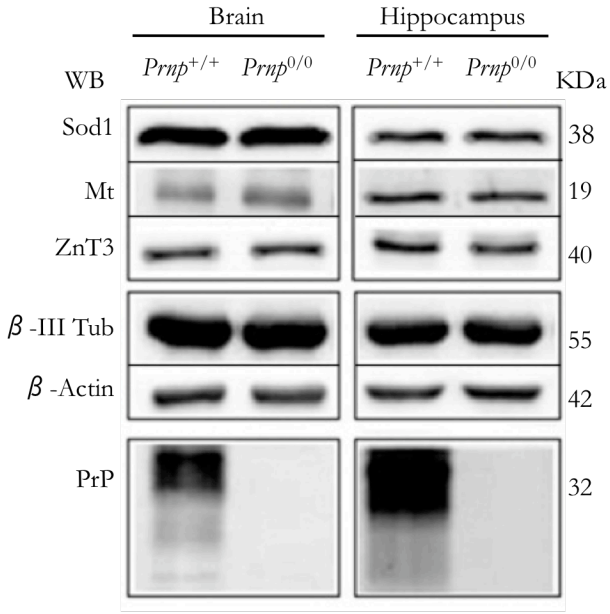

Figure 26. Zinc metabolism proteins. Representative immunoblot of each analyzed protein in the whole brain and in the hippocampus in *Prnp*$^{+/+}$ and *Prnp*$^{0/0}$ mice. Housekeeping proteins – β-III Tubulin and β-Actin – are also shown. *Prnp*$^{+/+}$ *and Prnp*$^{0/0}$ genotypes were confirmed by PrP immunodetection.

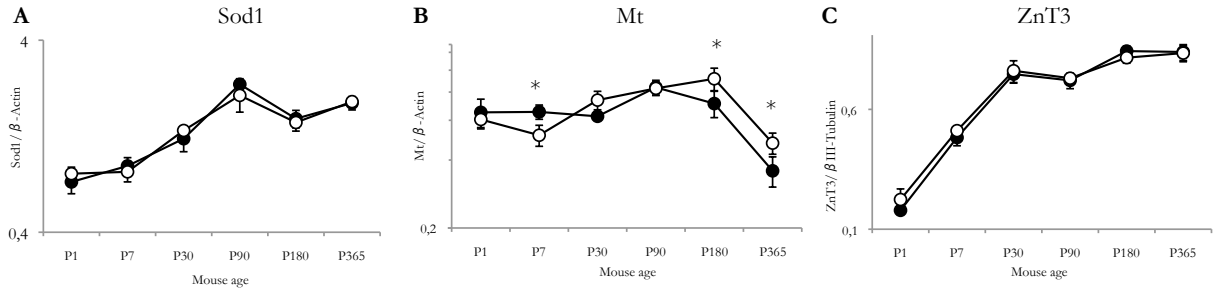

Figure 27. Zinc-binding proteins expression levels in *Prnp*$^{+/+}$ and *Prnp*$^{0/0}$ brains at different developmental stages. For each protein, the optical density value was normalized on a housekeeping protein. Filled circles (●) represent *Prnp*$^{+/+}$ values, while empty circles (○) indicate *Prnp*$^{0/0}$ values. (A) Cu,Zn-Superoxide Dismutase (Sod1); (B) Metallothioneins (Mt); (C) Zinc Transporter 3 (ZnT3). Sample size: n=4; * $p<0.05$, ** $p<0.01$, *** $p<0.001$

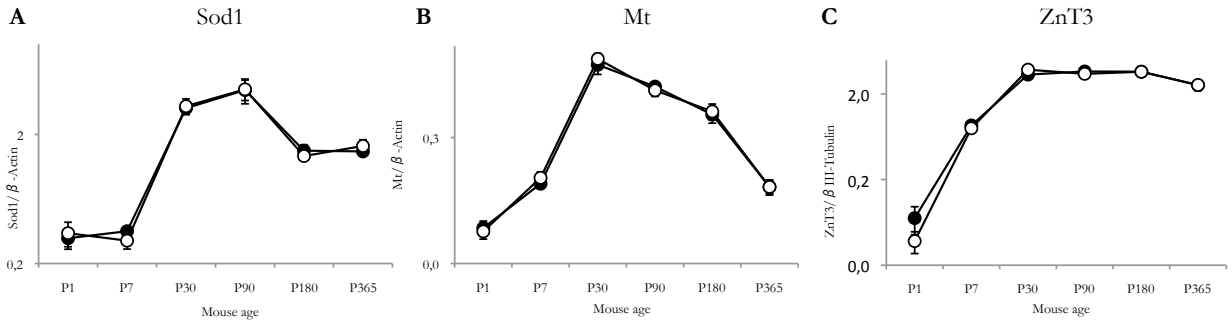

Figure 28. Zinc-binding proteins expression levels in *Prnp*$^{+/+}$ and *Prnp*$^{0/0}$ hippocampi at different developmental stages. For each protein, the optical density value was normalized on a housekeeping protein. Filled circles (●) represent *Prnp*$^{+/+}$ values, while empty circles (○) indicate *Prnp*$^{0/0}$ values. (A) Cu,Zn-Superoxide Dismutase (Sod1); (B) Metallothioneins (Mt); (C) Zinc Transporter 3 (ZnT3). Sample size: n=4; * p<0.05, ** p<0.01, *** p<0.001

Concerning Mn metabolism, just Mn, Superoxide dismutase (Sod2) expression was evaluated. Figure 29 shows representative bands obtained from brain and hippocampus protein extracts WB after detection of Sod2, the housekeeping and PrP to confirm *Prnp*$^{+/+}$ and *Prnp*$^{0/0}$ samples. In Figure 30A,B graphs displaying Sod2 expression levels in *Prnp*$^{+/+}$ and *Prnp*$^{0/0}$ brains and hippocampi at the different developmental stages are reported. In the brain, Sod2 expression increases up to P30 then it slowly decreases (Figure 30A), while in the hippocampus it increases with the age (Figure 30B). No differences between *Prnp*$^{+/+}$ and *Prnp*$^{0/0}$ samples were detected with exception of a little increase in P90 brain in *Prnp*$^{0/0}$.

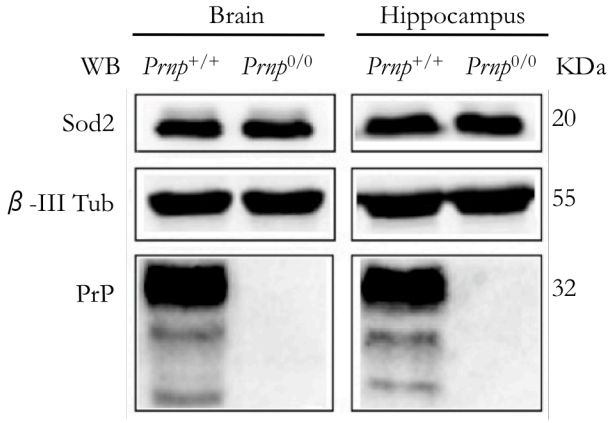

Figure 29. Manganese metabolism protein. Representative immunoblot of Sod2 in the whole brain and in the hippocampus in *Prnp*$^{+/+}$ and *Prnp*$^{0/0}$ mice. Housekeeping protein – β-III Tubulin – is also shown. *Prnp*$^{+/+}$ and *Prnp*$^{0/0}$ genotypes were confirmed by PrP immunodetection.

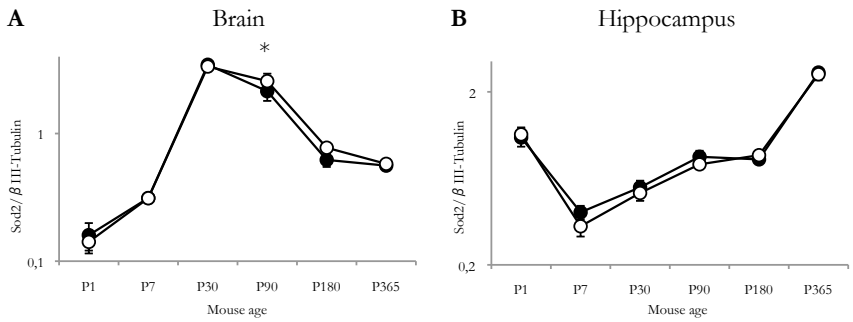

Figure 30. Manganese-binding protein expression levels in *Prnp*$^{+/+}$ and *Prnp*$^{0/0}$ brains and hippocampi at different developmental stages. For Sod2, the optical density value was normalized on a housekeeping protein – β-III Tubulin-. Filled circles (●) represent *Prnp*$^{+/+}$ values, while empty circles (○) indicate *Prnp*$^{0/0}$ values. (A) brain samples; (B) hippocampus samples. Sample size: n=4; * $p<0.05$, ** $p<0.01$, *** $p<0.001$

CERULOPLASMIN TRANSCRIPTION AND FUNCTIONALITY

As it has been described in the previous section, *Prnp*$^{0/0}$ mice showed alterated Cp levels compared to *Prnp*$^{+/+}$, and, in particular, they exhibit lower Cp presence in the hippocampus. To understand if this was due to a transcriptional regulation, real time PCR experiments were performed on hippocampal total RNA, extracted from mice showing altered protein levels, measuring both the secrete and the GPI-anchored form of the protein which were differentiated using specific primers (Stasi *et al.*, 2007). The results were normalized on two housekeeping genes (GAPDH and βIII-Tubulin) whose expression levels are not different in *Prnp*$^{+/+}$ and *Prnp*$^{0/0}$ samples (data not shown). Figure 31 reports a representative image of the real time PCR amplification products agarose gel. The non template control (NTC) did not give any amplification result, as well as the reaction performed using RT- template.

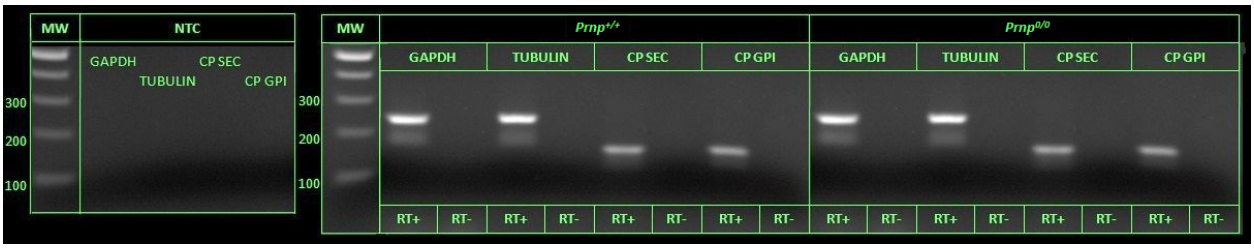

Figure 31. Real time PCR amplification products bands visualized on a 2% agarose gel. Starting from the left: non template control (NTC) amplification products for all the used primers; GAPDH, βTub, sec_Cp, GPI_Cp amplification products from *Prnp*$^{+/+}$RT+ and RT- templates; GAPDH, βTub, sec_Cp, GPI_Cp amplification products from *Prnp*$^{0/0}$RT+ and RT- templates.

As can be seen from Figure 32, no differences between *Prnp*$^{+/+}$ and *Prnp*$^{0/0}$were detected both for the secreted and the GPI-anchored form of Cp. The same result was obtained normalizing either with

GAPDH or βIII-Tubulin. So, different Cp protein levels in brains and hippocampi of *Prnp*$^{+/+}$and *Prnp*$^{0/0}$ mice are not due to differential transcriptional regulation.

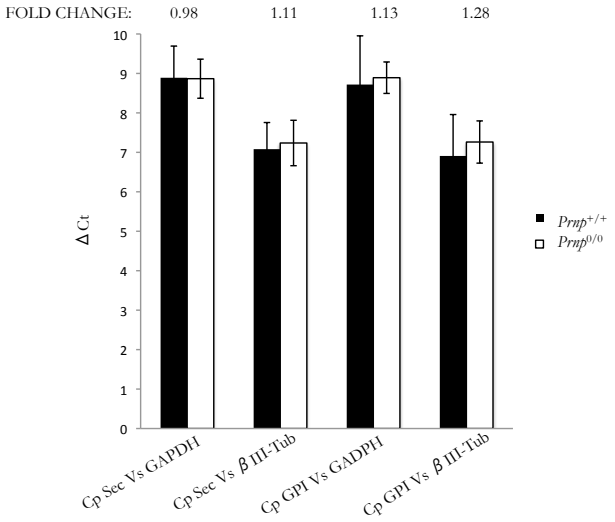

Figure 32. Cp mRNA levels comparison between *Prnp*$^{+/+}$ and *Prnp*$^{0/0}$ samples. In the graph, the results normalized against both the housekeeping genes are shown for secreted and GPI-anchored Cp mRNA. The relative expression of each sample was calculated by the formula $2exp^{-\Delta\Delta Ct}$ the fold change values are reported on the top of each column. Sample size n=4.

Biosynthesis of liver-secreted Cp does not seem to depend on the availability of copper, which is evidenced by the presence of apo-Cp in plasma under conditions of copper deficiency or when some protein needed to provide copper for biosynthesis of Cp is invalid, as in the case of mutated Atp7b Wilson's disease (Vassiliev et al., 2005). However, if Cu ions are not properly loaded on Cp, its ferroxidase activity is impaired (Vassiliev et al., 2005). Circulating Cp Cu-loading and ferroxidase activity are independent to astrocytes- and neurons-synthetised Cp ones, since they derive from two different systems. However, if plasma circulating Cp ferroxidase activity is impaired, it results in increased oxidative stress levels that can lead to neurodegeneration. Plasma Cp ferroxidase activity was measured following the protocol published in (Schosinsky et al., 1974), and adapted to mice. As can be seen in Figure 33, in normal conditions serum Cp activity increases with the age, while in PrP absence this increase is not detected. In fact, *Prnp*$^{0/0}$ sera show impaired Cp ferroxidase activity and the difference increases with the age ($p<0.05$ at P15 and P180, $p<0.01$ at P365). The similar level observed at P30 can be reconducted to a general different situation of metal ion homeostasis, previosly described concerning metal content. At P90, impairments in PrP null serum Cp activity are detectable, though not statistically significant ($p=0.075$).

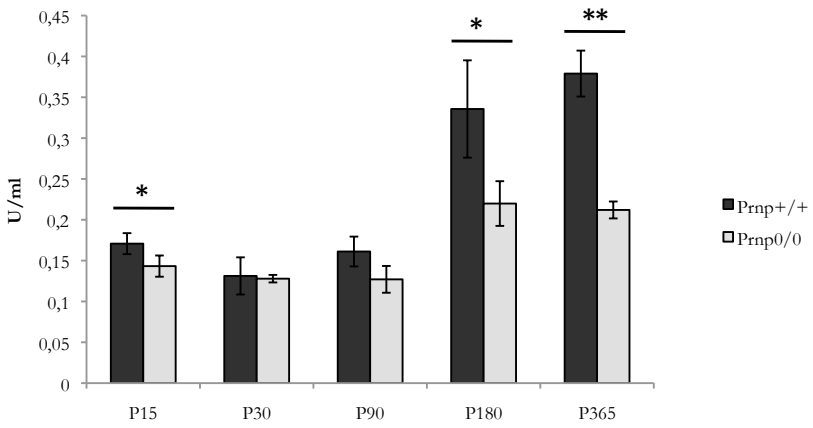

Figure 33. Cp functionality comparison between *Prnp*$^{+/+}$ and *Prnp*$^{0/0}$ samples. The graph shows the results obtained from sera samples of different mouse ages (P15, P30, P90, P180 and P365). Cp activity was calculated as U/ml according to Schosinsky et al. in 1974. Sample size: P15, P30, P180 n=4; P90, P365 n=3. * $p<0.05$; ** $p<0.01$.

PrP^{C} Neuroprotective Role in Excitotoxicity: NMDARs Activity Regulation.

Excitotoxicity in *Prnp*$^{+/+}$ and *Prnp*$^{0/0}$ Organotypic Hippocampal Cultures

To study PrP role in excitotoxic conditions, OHCs were prepared from *Prnp*$^{+/+}$ and *Prnp*$^{0/0}$ pups. OHCs were treated after 13 DIV, since at this stage cultures appear flattened, thin and with a well-defined cytoarchitecture. Figure 34 shows an example of a control slice, after 13 DIV, stained with DAPI and NeuN, a neuronal nuclei marker that better highlights hippocampal regions CA1, CA3 and DG.

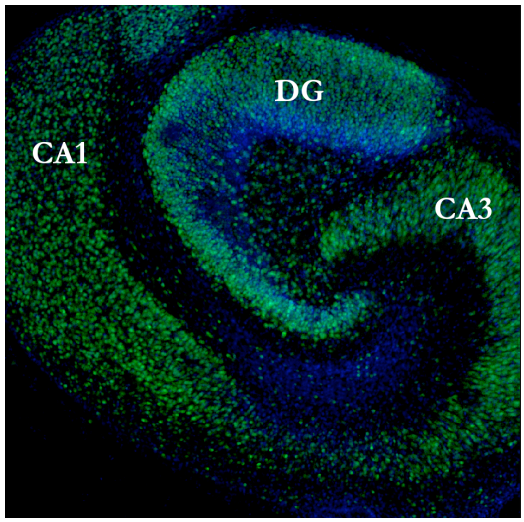

Figure 34. Organotypic hippocampal cultures at 13 DIV stained with DAPI (blue) and NeuN antibody (green). The three hippocampal regions analysed in the following experiments are highlighted: *Cornu Ammonis 1* (CA1), *Cornu Ammonis 3* (CA3), Dentate Gyrus (DG).

PrP^C expression was assesed in OHCs: a strong staining was observed in both CA1 and CA3 areas and a mild staining was detected in the DG (Figure 35, top row). In *Prnp*$^{0/0}$ OHCs no immunoreactivity for PrP^C was observed, confirming the specificity of the antibody (Figure 35, bottom row).

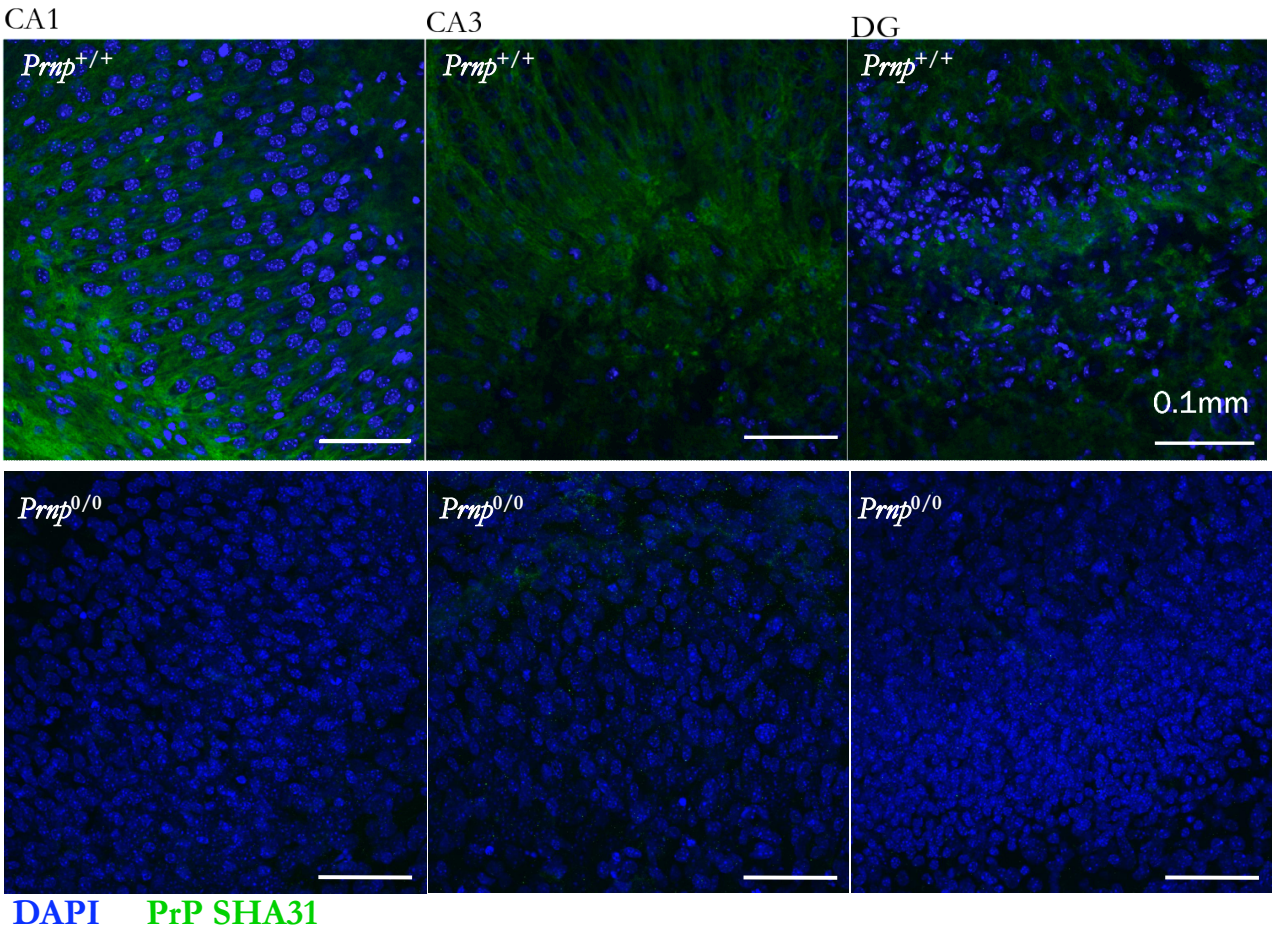

Figure 34. PrP^C immunofluorescent staining using PrP SHA31 antibody on OHCs. Confocal microscope fluorescence images were acquired using a 40×1.4 NA oil immersion objective. SHA31 is displayed in green and DAPI in blue. Staining for *Prnp*$^{+/+}$ and *Prnp*$^{0/0}$ OHCs is shown respectively in top and bottom row.

After 13 DIV, cultures were treated for 3 hours with 5µM NMDA and processed for immunofluorescence after 24 hours wash out. The combination of NeuN and DAPI staining resulted to be a good experimental procedure to evaluate neuronal cell death, as it is shown in Figure 36: DAPI staining allows discriminating healthy nuclei, which are big and contain distinguishable nucleoli, from pyknotic ones, which are smaller and fully condensed; NeuN immunostaining is localized in the nucleus in healthy neurons, while it is dispersed around condensed chromatin or completely lost in pyknotic nuclei. The NeuN staining was not quantified, but it was used on a quality level, mergd with DAPI stainig, to verify that counted pyknotic nuclei corresponded to neuronal cells (Figure 36).

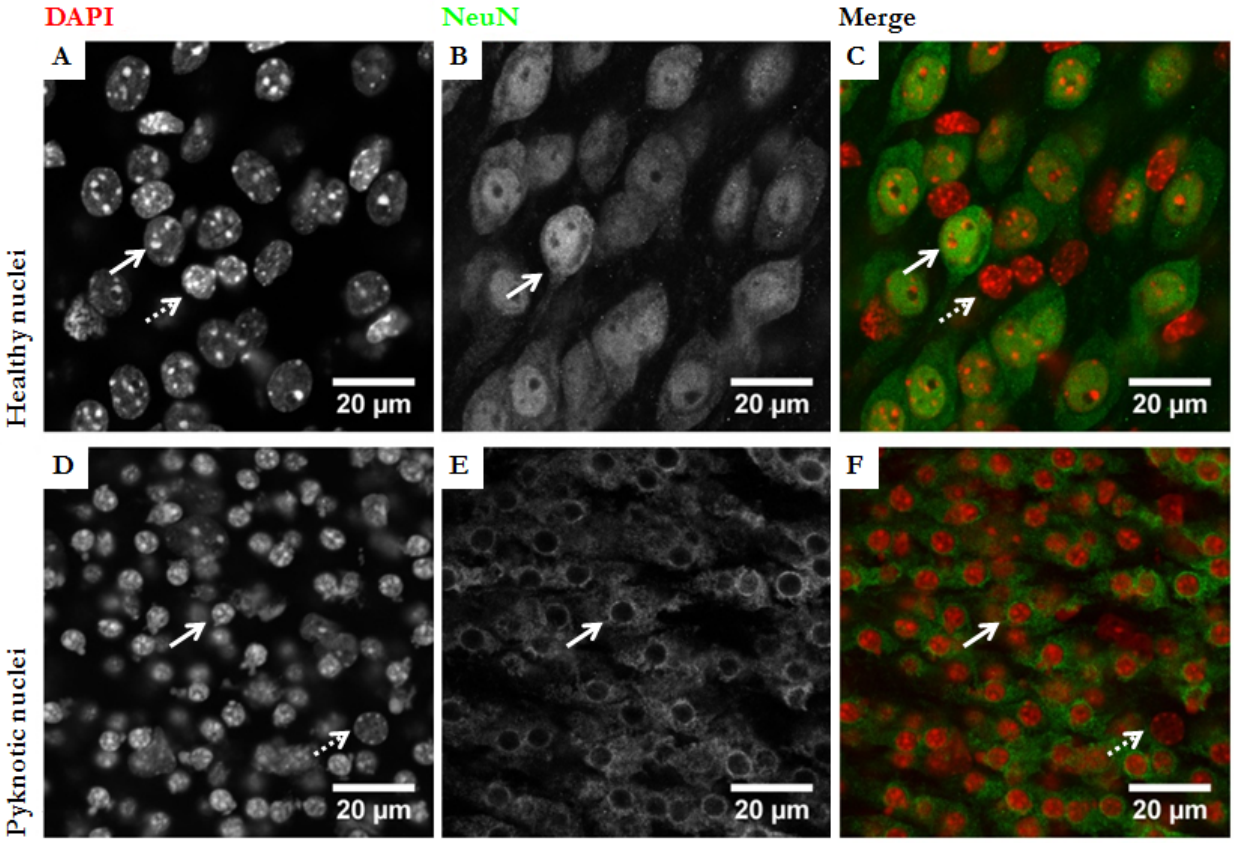

Figure 36. Combination of NeuN and DAPI immunostaining to evaluate neuronal cell death. Confocal microscope fluorescence images were acquired using a 63×1.4 NA oil immersion objective. In A-C panels healthy nuclei from untreated OHCs are shown: (A) DAPI staining, (B) NeuN immunostaining, (C) merge. In D-F panels pyknotic nuclei from NMDA treated OHCs are shown: (D) DAPI staining, (E) NeuN immunostaining, (F) merge. Solid arrows indicate neuronal nuclei; dashed arrows indicate glial nuclei. In the merge images, NeuN staining is displayed in green and DAPI one in red.

The NMDA treatment (5µM for 3 hours) was chosen based on results published in literature (Bunk et al., 2010; Kristensen et al., 2001). This NMDA stimulation turned out to be optimal for comparing susceptibility between *Prnp*$^{+/+}$ and *Prnp*$^{0/0}$ cultures since in *Prnp*$^{+/+}$ it induced low levels of neuronal cell death, but high levels in *Prnp*$^{0/0}$preparations. As it can be seen in Figure 37, 3 hours 5µM NMDA triggers spread neuronal cell death just in CA1 region in *Prnp*$^{+/+}$ OHCs, but not in the CA3 and in the DG. On the other hand, in PrP null preparations neuronal cell death was observed at high levels also in the CA3 and in the DG. These observations were confirmed by quantification (Figure 38). In fact, the statistical analysis revealed that 3 hours 5µM NMDA induced significant neuronal cell death in *Prnp*$^{+/+}$ CA1 ($p<0.05$), as well as in *Prnp*$^{0/0}$ CA1 ($p<0.05$), but with higher levels in PrP absence ($p<0.05$). Considering CA3 and DG, the treatment was not able to induce significant neuronal cell death in *Prnp*$^{+/+}$ OHCs, but it did on *Prnp*$^{0/0}$ samples (both $p<0.05$). So, CA3 and DG neuronal cell death in PrP null condition was significantly higher compared to *Prnp*$^{+/+}$ (both $p<0.01$).

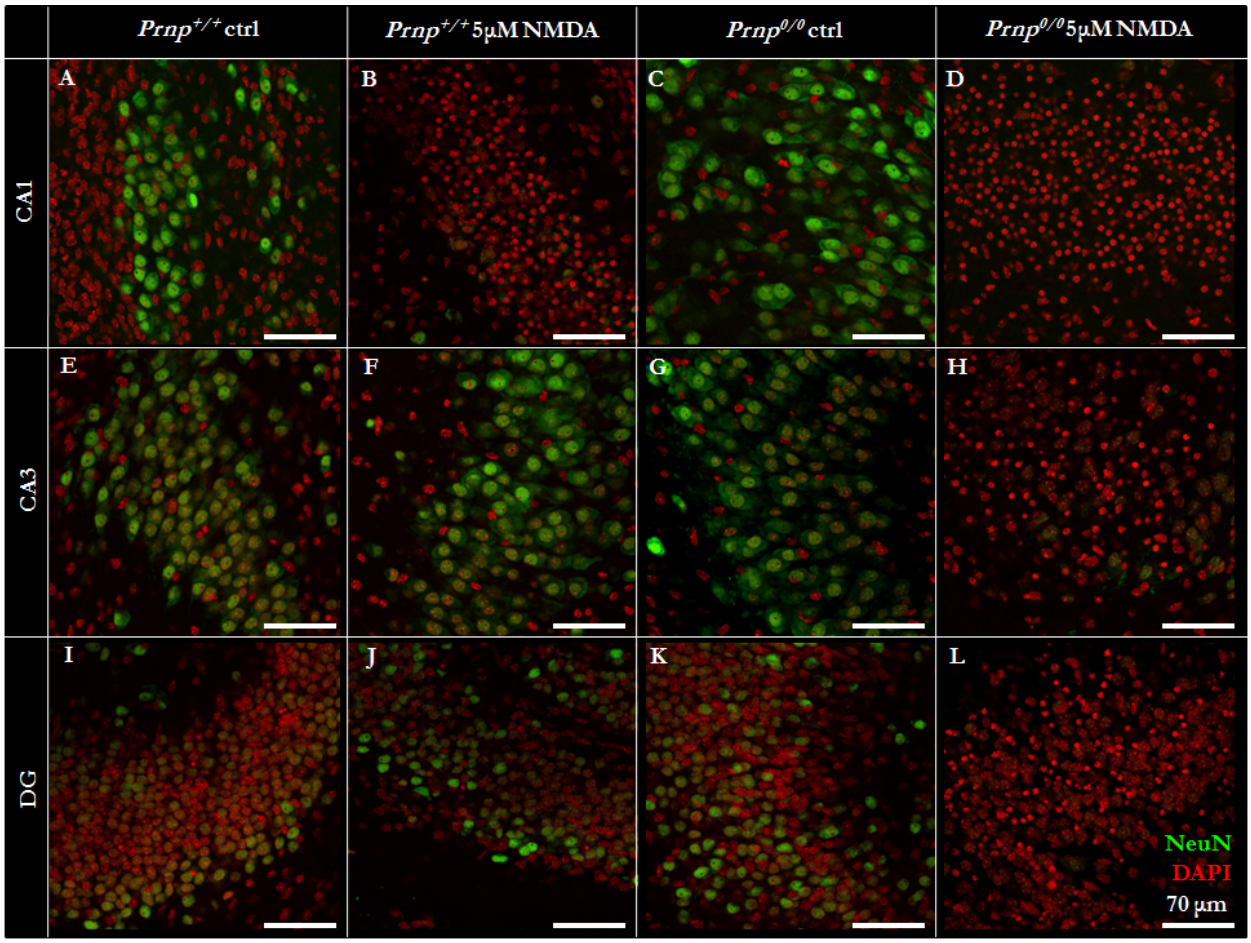

Figure 37. Comparison between *Prnp*$^{+/+}$ and *Prnp*$^{0/0}$ OHCs regional susceptibility to NMDA treatment. Confocal microscope fluorescence images were acquired using a 40×1.4 NA oil immersion objective. In rows, three different hippocampal regions are shown: (A-D) CA1, (E-H) CA3, (I-L) DG. In columns, four different experimental conditions are shown: (A, E, I) *Prnp*$^{+/+}$ control, (B, F, J) *Prnp*$^{+/+}$ 5µM NMDA, (C, G, K) *Prnp*$^{0/0}$ control, (D, H, L) *Prnp*$^{0/0}$ 5µM NMDA. NeuN staining is displayed in green and DAPI one in red.

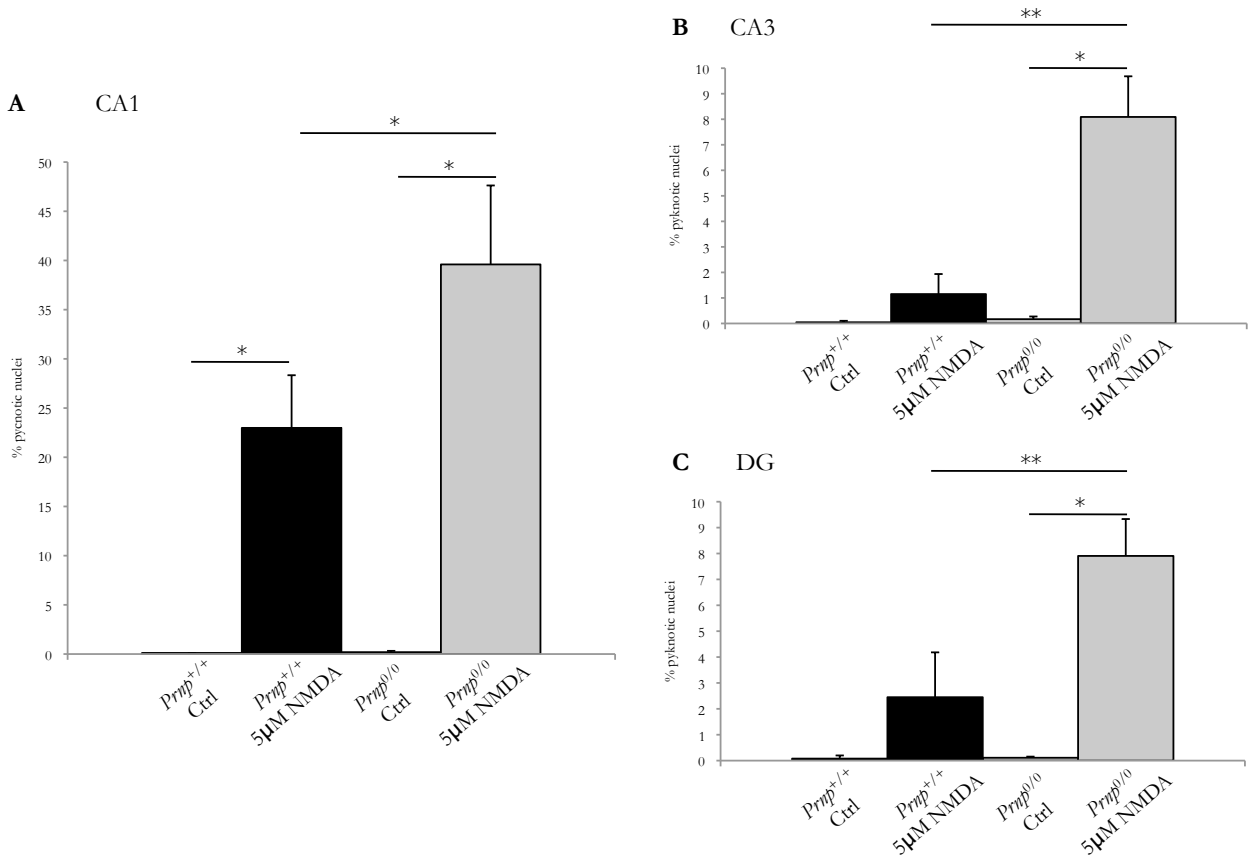

Figure 38. Comparison between *Prnp*$^{+/+}$ and *Prnp*$^{0/0}$ OHCs regional susceptibility to NMDA treatment. Quantification was calculated as the percentage of neuronal pyknotic nuclei on the total cell number considering separately three hippocampal areas: (A) CA1, (B) CA3, (C) DG. Sample size: n=3, i.e. 3 independent experiments, each one prepared from 3 mice dissection resulting in an average number of 15 control cultures and 15 NMDA-treated cultures. * $p<0.05$; ** $p<0.01$

EXCITOTOXICITY MAJOR PLAYERS ANALYSIS

To understand the reason why in *Prnp*$^{0/0}$neurons are more susceptible to excitotoxic conditions, the expression levels of proteins involved in the molecular mechanism underlying NMDA toxic effect was analyzed in *Prnp*$^{+/+}$ and *Prnp*$^{0/0}$ samples at different ages (P30, P90, P180, P365). In the same samples, total calcium content was measured. Concerning proteins, the expression levels of NMDA receptor mostly esxpressed subunits, nNOS and Casp3 were assessed in the hippocampus, while calcium pumps and calcium content were measured both in the hippocampus and in the brain. Figures 39 and 41 show representative images of Western blotting experiments for each protein. For the NMDAR subunits GluN1, GluN2A and GluN2B expression levels, in general *Prnp*$^{0/0}$ hippocampi showed higher levels, in particular from adulthood to aging (Figure 40). Regarding nNOS expression levels, generally PrP ablation does not play a role, except for a minor difference at P30 (Figure 40D). Caspase3 expression analysis revealed a lower level at P30 but a higher one at P365 in *Prnp*$^{0/0}$ mice (Figure 40E).

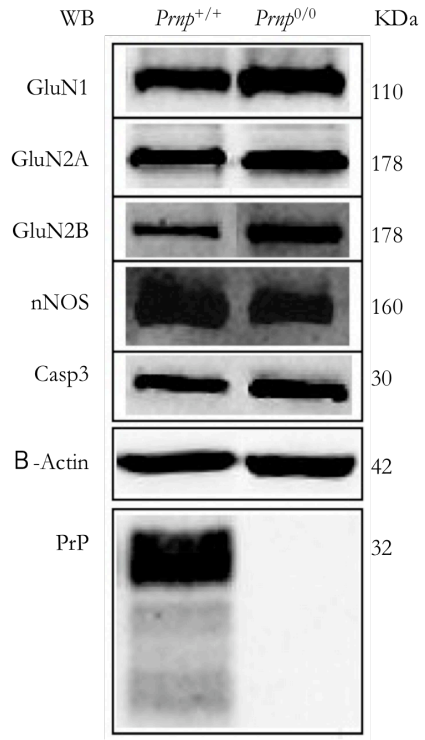

Figure 39. Expression levels of some proteins involved in excitotoxicity. Representative immunoblot of each analyzed protein in *Prnp*$^{+/+}$ and *Prnp*$^{0/0}$ hippocampus. Housekeeping protein – β-Actin – is also shown. *Prnp*$^{+/+}$ and *Prnp*$^{0/0}$ genotypes were confirmed by PrP immunodetection.

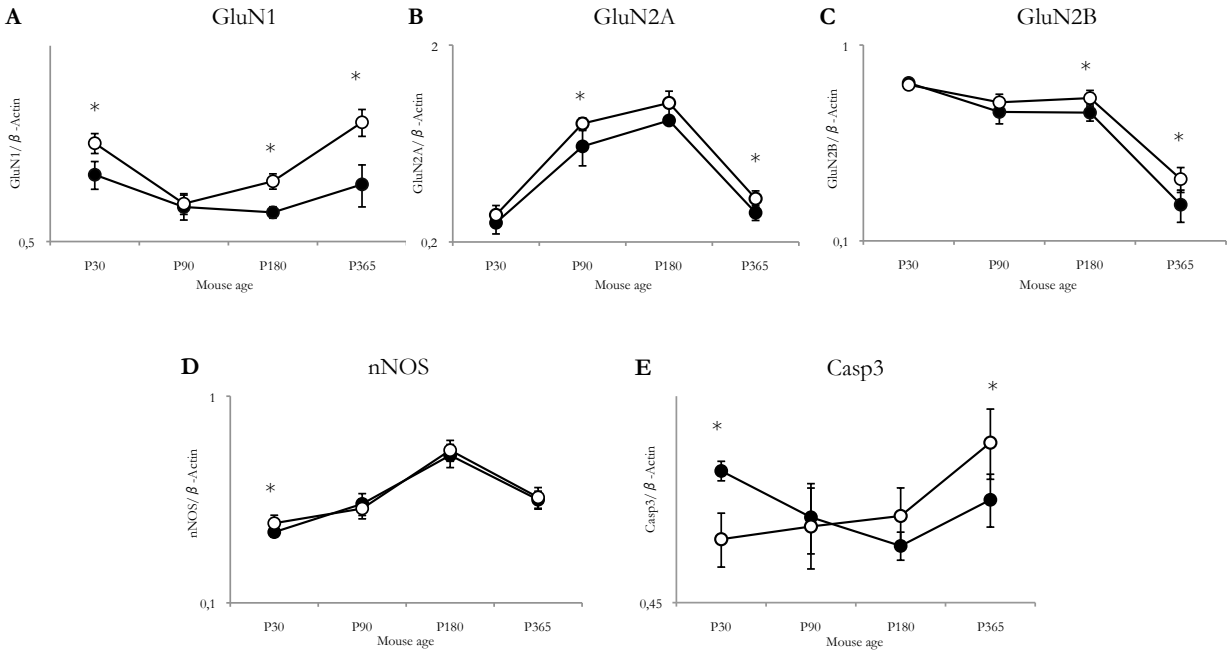

Figure 40. Expression levels of some proteins involved in excitotoxicity in *Prnp*$^{+/+}$ and *Prnp*$^{0/0}$ hippocampi at different developmental stages. For each protein, the optical density value was normalized on a housekeeping protein – β-Actin-. Filled circles (●) represent *Prnp*$^{+/+}$ values, while empty circles (○) indicate *Prnp*$^{0/0}$ values. (A) NMDA receptor subunit 1 (GluN1); (B) NMDA receptor subunit 2A (GluN2A); (C) NMDA receptor subunit 2B (GluN2B); (D) neuronal nitric oxide synthase (nNOS); (E) Caspase 3. Sample size: n=4; * $p<0.05$, ** $p<0.01$, *** $p<0.001$

Calcium pumps expression in *Prnp*$^{0/0}$ resulted to be peculiar. In fact, in both brain and hippocampus, as shown in Figures 42A and 43A, the expression of the pump with low affinity but high capacity of transport, Ncx1, is increased just in the early post-natal stages P1 and P7, while the expression of pumps with high affinity and low capacity, Pmca and Serca2, is differently regulated. In the brain, Pmca expression is increased in PrP null mice from adulthood to aging (Figure 42B), while Serca2 is not affected except a marked increase at P1 (Figure 42C). In the hippocampus, Pmca expression is increased starting from P30; at P1 and P7 it is even lower compared to *Prnp*$^{+/+}$ (Figure 43B). A similar behavior was detected also for Serca2: diminished levels at P7, and increased levels starting from P30 in *Prnp*$^{0/0}$ compared to *Prnp*$^{+/+}$(Figure 43C).

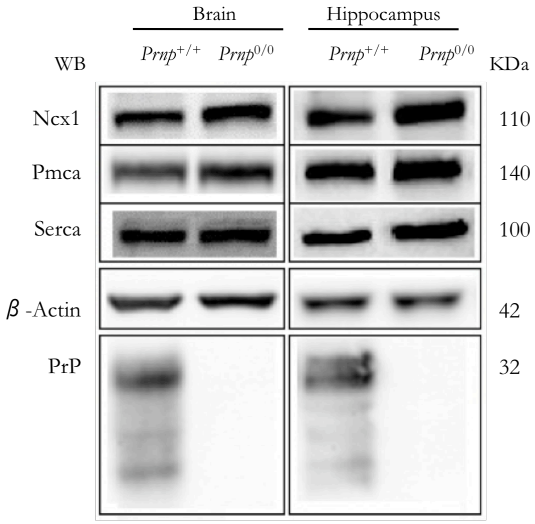

Figure 41. Calcium pumps expression levels. Representative immunoblot of each analyzed protein in *Prnp*$^{+/+}$ and *Prnp*$^{0/0}$ hippocampus. Housekeeping protein – β-Actin – is also shown. *Prnp*$^{+/+}$ and *Prnp*$^{0/0}$ genotypes were confirmed by PrP immunodetection.

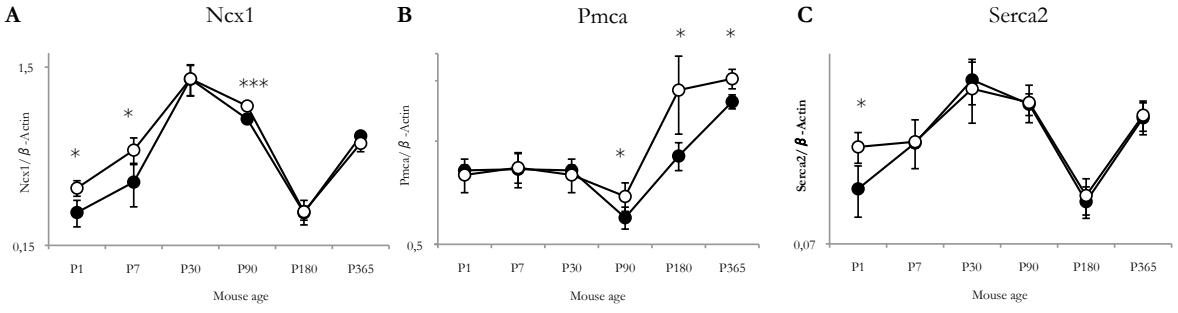

Figure 42. Calcium pumps expression levels in *Prnp*$^{+/+}$ and *Prnp*$^{0/0}$ brains at different developmental stages. For each protein, the optical density value was normalized on a housekeeping protein – β-Actin-. Filled circles (●) represent *Prnp*$^{+/+}$ values, while empty circles (○) indicate *Prnp*$^{0/0}$ values. (**A**) Na^+/Ca^{2+} exchanger 1 (Ncx1); (**B**) Plasma Membrane Calcium ATPase (Pmca); (C) Sarco(Endo)plasmic Reticulum Calcium ATPase 2 (Serca2). Minimum sample size: n=4; * $p<0.05$, ** $p<0.01$, *** $p<0.001$

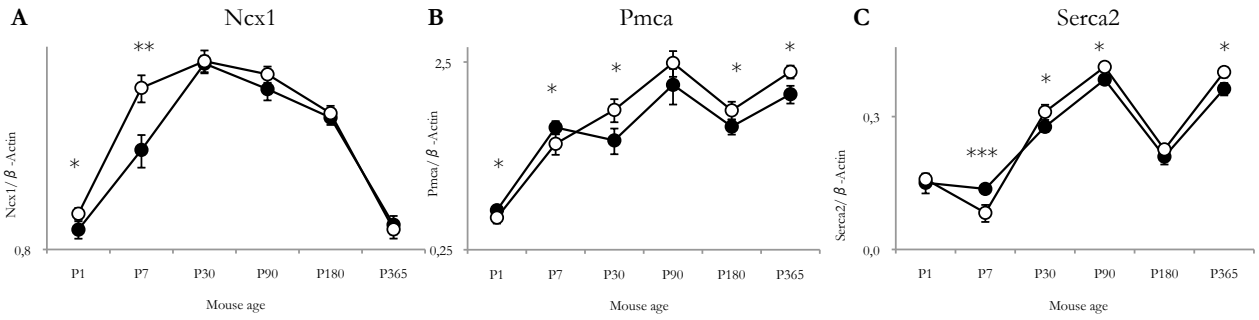

Figure 43. Calcium pumps expression levels in *Prnp*$^{+/+}$ and *Prnp*$^{0/0}$ hippocampi at different developmental stages. For each protein, the optical density value was normalized on a housekeeping protein – β-Actin-. Filled circles (●) represent *Prnp*$^{+/+}$ values, while empty circles (○) indicate *Prnp*$^{0/0}$ values. (**A**) Na^+/Ca^{2+} exchanger 1 (Ncx1); (**B**) Plasma Membrane Calcium ATPase (Pmca); (C) Sarco(Endo)plasmic Reticulum Calcium ATPase 2 (Serca2). Minimum sample size: n=4; * $p<0.05$, ** $p<0.01$, *** $p<0.001$

To understand whether this different expression of calcium transporters, occurring in the hippocampus and brain of *Prnp*$^{0/0}$, was due to maintainance of calcium to wild-type levels, Ca^{2+} ions concentration was measured in both brain and hippocampus during the development. The results are shown in Figure 44A,B. In the brain of *Prnp*$^{+/+}$ and *Prnp*$^{0/0}$ the same Ca^{2+} concentration is present, except at P30 in *Prnp*$^{0/0}$. In the hippocampus, no differences were observed up to P180. In fact, from late adulthood to aging Ca^{2+} homeostasis appears impaired, since oscillations occur affecting the total calcium content.

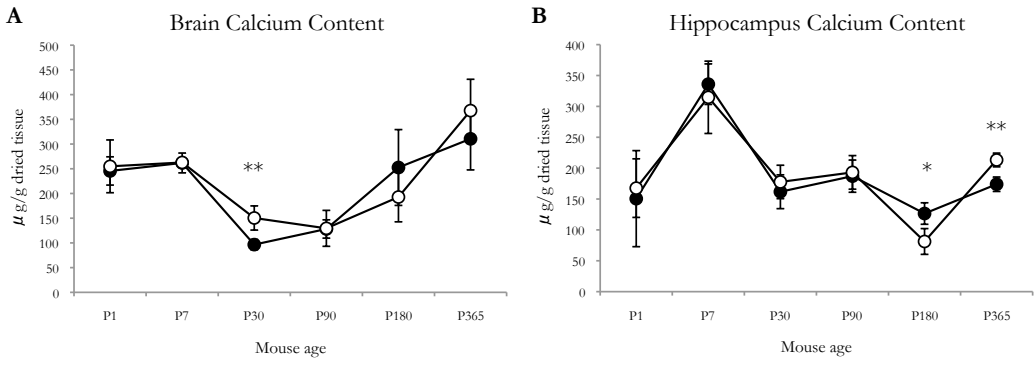

Figure 44. Calcium content *Prnp*$^{+/+}$ and *Prnp*$^{0/0}$ samples at different developmental stages. Filled circles (●) represent *Prnp*$^{+/+}$ values, while empty circles (○) indicate *Prnp*$^{0/0}$ values. (A) brain; (B) hippocampus. Minimum sample size n=5. * $p<0.05$; ** $p<0.01$; *** $p<0.001$.

NMDAR SUBUNITS S-NITROSYLATION LEVELS IN *Prnp*$^{+/+}$ AND *Prnp*$^{0/0}$ HIPPOCAMPI

To determine whether PrP neuroprotective function upon NMDA induced toxicity is due to a direct modulation of NMDARs by mediating the inhibitory S-nitrosylation reaction, SNO levels of NMDAR subunits GluN1 and GluN2A were measured. To this end, the biotin switch assay was applied to hippocampal protein extracts from adult *Prnp*$^{+/+}$ and *Prnp*$^{0/0}$ mice. In Figure 45A-B, the biotin switch assay output for SNO-GluN1 measurement is shown. In particular, Figure 45A displays the SNO fraction of both GluN1 and β-Actin in *Prnp*$^{+/+}$ and *Prnp*$^{0/0}$ samples, as well as in the control without biotin. As controls, GluN1, β-Actin and PrP were immunodetected also in the starting material (input) and in the supernatant after incubation with the Neutravidin resin (Figure 45B). In Figure 45C, a table reports the values obtained for SNO-GluN1 O.D. signal normalized on SNO-β-Actin from *Prnp*$^{+/+}$ and *Prnp*$^{0/0}$ samples for each experiment. In the same table, the p value indicating the statistical significance of the difference between *Prnp*$^{+/+}$ and *Prnp*$^{0/0}$ in the entire experimental set is reported (p=0.0002).

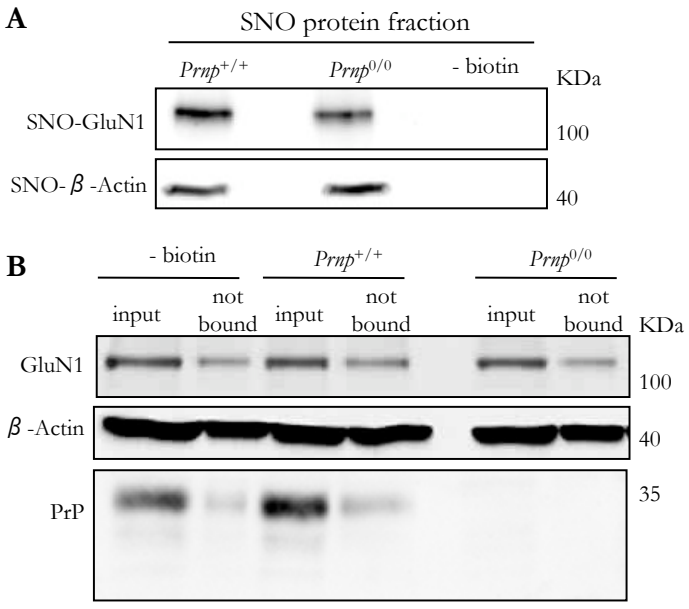

C

	ratio SNO-GluN1/SNO-β-actin							p value
Prnp$^{+/+}$	0.320	0.316	0.346	0.134	0.316	0.187	0.373	0.0002
Prnp$^{0/0}$	0.145	0.086	0.182	0.039	0.086	0.047	0.098	

Figure 45. SNO-GluN1 levels in *Prnp*$^{+/+}$ and *Prnp*$^{0/0}$ hippocampal samples. The biotin switch assay was performed to detect SNO-proteins levels starting from 1mg protein extract. (A) SNO-GluN1 and SNO-β-Actin in *Prnp*$^{+/+}$ and *Prnp*$^{0/0}$ hippocampi and in the control without biotin; (B) GluN1, β-Actin and PrP immunodetection in the starting material (input) and in the supernatant after incubation with the Neutravidin resin (not bound); (C) table reporting the values of SNO-GluN1 normalized on SNO-β-Actin obtained for each experiment performed in *Prnp*$^{+/+}$ and *Prnp*$^{0/0}$ samples and the p value calculated with the paired T test formula.

Considering SNO-GluN2A detection and measurement, Figure 46A-C reports as example the biotin switch assay output. In particular, Figure 46A shows the SNO fraction of GluN2A and β-Actin in two *Prnp*$^{+/+}$ and two *Prnp*$^{0/0}$ samples, as well as in the control without biotin. To check samples quality, Figure 46B display the result of the immunodetection of GluN2A, β-Actin and PrP in the supernatant after incubation with the Neutravidin resin, while Figure 46C shows the same on the input material. The table in Figure 46D reports the quantification values for SNO-GluN2A, normalized on SNO-β-Actin, obtained in each experiment with *Prnp*$^{+/+}$ and *Prnp*$^{0/0}$ samples. The resulting p value indicating the significance of the difference between *Prnp*$^{+/+}$ and *Prnp*$^{0/0}$ condition is also reported (p=0.0368).

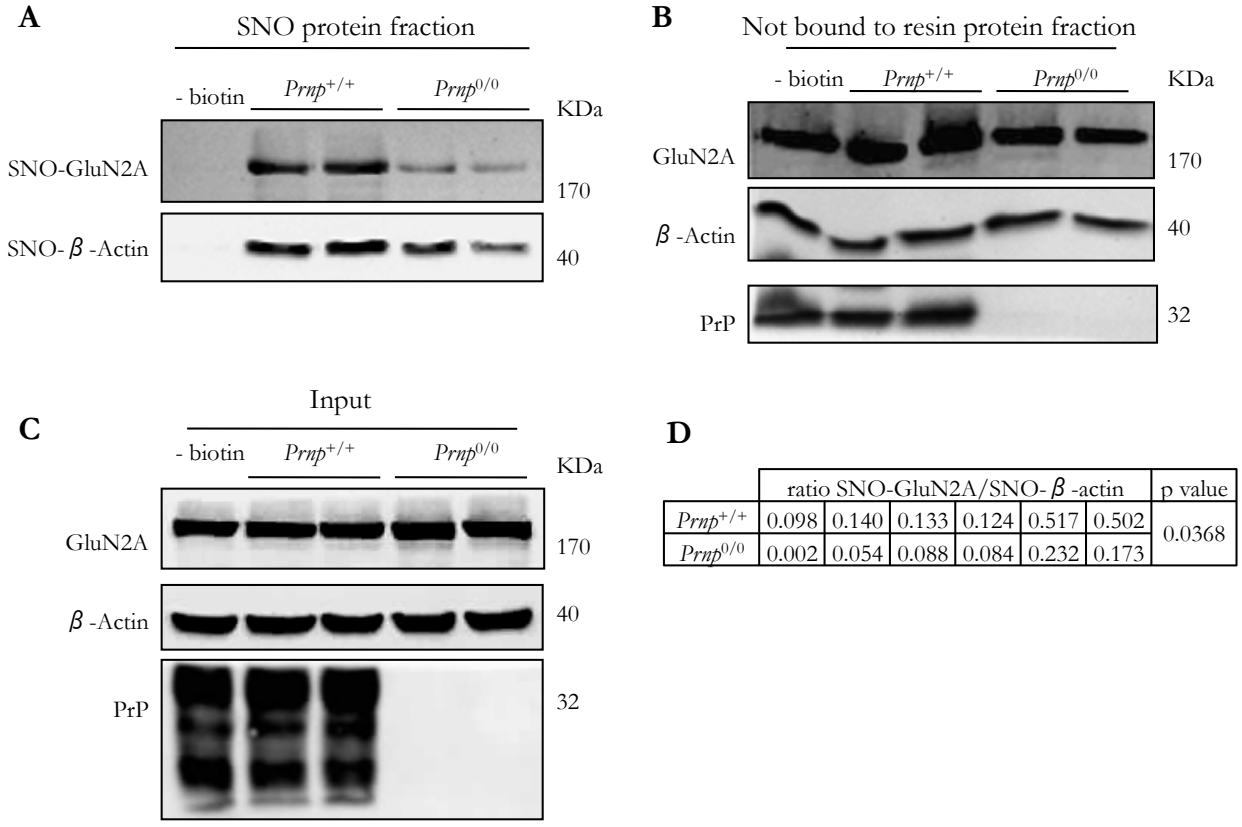

	ratio SNO-GluN2A/SNO-β-actin						p value
Prnp$^{+/+}$	0.098	0.140	0.133	0.124	0.517	0.502	0.0368
Prnp$^{0/0}$	0.002	0.054	0.088	0.084	0.232	0.173	

Figure 46. SNO-GluN2A levels in *Prnp*$^{+/+}$ and *Prnp*$^{0/0}$ hippocampal samples. The biotin switch assay was performed to detect SNO-proteins levels starting from 1mg protein extract. (A) SNO-GluN2A and SNO-β-Actin in *Prnp*$^{+/+}$ and *Prnp*$^{0/0}$ hippocampi and in the control without biotin; (B) GluN2A, β-Actin and PrP immunodetection in the fraction that did not reacted with Neutravidin resin; (C) GluN2A, β-Actin and PrP immunodetection in the starting material (input); (D) table reporting the values of SNO-GluN2A normalized on SNO-β-Actin obtained for each experiment performed in *Prnp*$^{+/+}$ and *Prnp*$^{0/0}$ samples and the p value calculated with the paired T test formula.

DISCUSSION

Among different neurodegenerative diseases, altered concentration in metal ions, protein aggregation, RNS and ROS have been identified as common traits (Bush, 2000). However, the precise mechanism that gives rise to these pathologies has not been defined. Table 1 shows the neurodegeneration characteristics of aggregating proteins, like Aβ, Sod1 and PrP, that share a crucial property of being metal-binding proteins. The focus of this study has been PrP^C. This endogenously encoded protein has a wide range of interesting characteristics. The protein is very well conserved in different mammalian species, although its ablation in several knockout mouse models seem to compromise neither vitality nor fertility and does not produce gross phenotypic disturbances (Bueler et al., 1992; Manson et al., 1994). The protein is expressed in different tissues, showing the highest level in the CNS synapses, in particular in the hippocampus (Benvegnu et al., 2010; Fournier et al., 1998; Horiuchi et al., 1995; Linden et al., 2008). The polypeptide is GPI-anchored to plasma membrane and targeted to lipid rafts, like most of the GPI-anchored proteins (Naslavsky et al., 1997; Simons and Ikonen, 1997). The PrP^C is able to bind divalent cations with higher affinity for Cu and lower for Mn and Zn (Jackson et al., 2001; Singh et al., 2010; Stockel et al., 1998), it supports the reduction of Cu(II) to Cu(I) and, upon this reaction, it is internalized, so that it can pass Cu(I) to Cu transporters and chaperons (Liu et al., 2011). Different processes have been found to be affected by PrP^C ablation: synaptic formation and functionality, myelin sheets formation and maintenance, metal ions absorption and distribution, oxidative stress control, among others (Aguzzi et al., 2008; Bremer et al., 2010). However, its cellular function has not been established. To define the pathological mechanism leading to prion neurodegeneration, it is very important to understand PrP^C mechanism of action in physiological conditions. In fact, the loss-of-function of PrP^C is likely implied in prion diseases, since aggregates spreading removes functional PrP^C molecules.

The first part of the project has been dedicated to understanding the influence that PrP^C exerts on metal ions metabolism through the characterization of alterations occurring when PrP^C is absent. Metal ions are crucial elements for cellular processes, since they are involved as co-factors in many protein functions, but at the same they are potentially dangerous for the cell itself because they can give rise to Fenton reaction and oxidative/nitrosative stress. For these reasons, they are subjected to a strictly regulated homeostasis and metabolism in each district, but in particular in the brain. In fact, since brain activity has the highest metabolic rate of all organs and depends predominantly on oxidative metabolism for its energy, it has developed fine mechanisms to compartmentalize, distribute, uptake,

excrete and control the different ionic species it contains. Both in development and in aging, alterations in one of the mechanism listed above can easily provoke great neuronal damages, and maybe neurodegenerative disorders. Metal ions are a common denominator to all the cellular pathways in which PrP^C seems to be actively involved, for example ionotropic receptor modulation and response to stressful conditions and excitotoxic insults.

First, Cu, Zn, Fe and Mn total concentrations were measured in brains and hippocampi. *Prnp*$^{0/0}$ mouse samples were compared to *Prnp*$^{+/+}$ ones at different developmental stages: neonatal (P1), early postnatal (P7), synaptogenesis completion (P30), adulthood (P90), late adulthood (P180), aging (P365). Table 5 summarises the results obtained concerning brain measurements, showed in detail in Figure 17. Zn and Fe brain total content seem to be less affected by PrP ablation. In fact, *Prnp*$^{+/+}$ and *Prnp*$^{0/0}$ show similar decreasing trend during the development. The only main difference occurs at P1, where *Prnp*$^{0/0}$ mice reveal a striking lower content compared to *Prnp*$^{+/+}$ brains. This observation suggests that PrP^C role in Zn and Fe metabolism is predominant at this developmental stage and other mechanisms cannot compensate. Cu and Mn concentrations are more altered by PrP ablation. In *Prnp*$^{+/+}$ brains, Cu concentration decreases from the early postnatal stages to the end of synaptogenesis, then it increases up to aging. In *Prnp*$^{0/0}$, instead, Cu content is much lower in P1 samples, it is kept almost constant with slight variations up to P180, then it suddenly rises, although at not statistically significant levels due to biological variance of the samples. Mn concentration shows completely different trends in *Prnp*$^{+/+}$and *Prnp*$^{0/0}$. In normal conditions, Mn content decreases from the early postnatal stages to synaptogenesis completion, afterwards it is quite constant. In *Prnp*$^{0/0}$ brains, Mn concentration has a similar general trend, but at P1 and P7 it is lower compared to *Prnp*$^{+/+}$ and from P30 to the aging the values oscillate around the *Prnp*$^{+/+}$ ones, likely because compensatory mechanisms continuously need to arrange and re-organize to balance PrP^C absence.

	P1	P7	P30	P90	P180	P365
Cu	- -	**#**	++	#	-	#
Mn	#	**- -**	++	#	-	#
Zn	**- -**	#	++	#	-	#
Fe	- -	+	+	#	#	#

Table 5. Summary of brain metal content measurements results. (-): *Prnp*$^{0/0}$ metal content is significantly lower than *Prnp*$^{+/+}$; (+): *Prnp*$^{0/0}$ metal content is significantly higher than *Prnp*$^{+/+}$; (#): no statistically significant difference.

Table 6 summarizes the results obtained from hippocampal samples and showed in detail in Figure 18. PrP ablation highly affects Cu and Fe concentrations, which are lower at both P7 and P180, critical

stages that seem to be particularly susceptible to PrP^C function, while in adulthood their content is brought to normal levels by compensatory mechanism. In both *Prnp*$^{+/+}$ and *Prnp*$^{0/0}$, Zn and Mn contents have not a well-defined trend in the development. However, they both are decreased by PrP absence at P180 that is confirmed to be a stage in which PrP^C function is particularly predominant over the other mechanisms.

	P1	P7	P30	P90	P180	P365
Cu	#	- -	#	+	- -	#
Fe	#	- -	#	+	-	#
Zn	-	#	#	++	- - -	#
Mn	#	#	#	#	- -	#

Table 6. Summary of hippocampus metal content measurements results. (-): *Prnp*$^{0/0}$ metal content is significantly lower than *Prnp*$^{+/+}$; (+): *Prnp*$^{0/0}$ metal content is significantly higher than *Prnp*$^{+/+}$; (#): no statistically significant difference.

For each analyzed transition metal, the major proteins responsible for its metabolism regulation were characterized according to their expression levels in the development and the results of the comparison have been schematised in Table 7.

Ceruloplasmin (Cp) can be expressed in two forms, a secreted one and a GPI-anchored one, by the liver, which provides for the higher portion, but also by the brain, lung, spleen and testis (Aldred et al., 1987; Fleming and Gitlin, 1990; Klomp and Gitlin, 1996). The GPI-anchored form is present on astrocytes and leptomeningeal cells (Mittal et al., 2003; Patel and David, 1997). Cp is a α_2-globulin that carries 95% of serum copper (Harris and Gitlin, 1996). It functions as a Cu-dependent ferroxidase and in its GPI-anchored form provides for Fe mobilization promoting, for example, Fe efflux from astrocytes (Hellman et al., 2002; Jeong and David, 2003). In fact, in case of Cp hypofunctionality, Fe accumulates inside astrocytes. The ferroxidase activity confers Cp an antioxidant function (Goldstein et al., 1979a, b). GPI-anchored Cp is responsible for Fe oxidation that is necessary for loading apo-Tf with Fe^{3+}, this allows to prevent Fenton reaction as well as to transport Fe to neurons (Patel and David, 1997). Cp expression is not dependent upon Cu availability, as checked by apo-Cp presence in the serum of patients affected by Wilson's disease, a pathology in which copper is accumulated but not available (Vassiliev et al., 2005).

The six-transmembrane epithelial antigen of the prostate 3 (Steap3) belongs to the family of Steap protein. Steap3 is expressed in a wide range of tissues as a transmembrane metalloreductase. It seems to

be the most important metalloreductase of the Steap family, playing crucial role in both Fe and Cu uptake (Knutson, 2007). In particular, its function is linked to the Tf/TfR cycle.

The Cu,Zn-Superoxide Dismutase (Sod1) catalyzes the disproportionation of superoxide anion to oxygen and hydrogen peroxide (McCord and Fridovich, 1969). Each unit contains a Cu ion and a Zn ion, the latter is not essential for the dismutation reaction, but stabilyzes the protein (Furukawa et al., 2004). To function, Sod1 requires to be loaded with metal ions by Ccs, since this reaction cannot be achieved spontaneously in the cell (Culotta et al., 1997). If the posttranslational activation of Sod1, including Cu and Zn, binding is defective, Sod1 can even be toxic producing aggregates, like in ALS (Banci et al., 2010).

The copper chaperone for superoxide dismutase (Ccs) contains a Cu binding domain that serves to load Sod1 with the Cu ion it requires for functioning. Moreover, Ccs contains also a Zn binding site that is not essential but contributes to protein stabilization, as for Sod1. Actually, it has been proposed that Ccs can function also as a Zn chaperone, but this mechanism has not been proved, yet (Banci et al., 2010). Ccs seems to be the preferred route of Sod1 activation, but it is not the only one.

Copper transporter 1 (Ctr1) is a plasma membrane protein with a homotrimeric pore essential for Cu(I) uptake in all cells. Cu(II) is thought to be reduced to Cu(I) by various Steap proteins on the cell surface before uptake by Ctr1. Cu uptake by Ctr1 is (i) energy dependent, (ii) stimulated by acidic extracellular pH and high K^+ concentrations, and (iii) time dependent and saturable (Gaggelli et al., 2006). Evidence suggests that Ctr1 may be posttranslationally regulated by intracellular Cu availability. Elevated intracellular Cu levels stimulate the rapid endocytosis and degradation of Ctr1 from the cell membrane, resulting in attenuated Cu uptake and thus preventing the cellular overload (Gaggelli et al., 2006). Ctr1 has been shown to be present in the BBB, choroid plexus, as well as the brain parenchyma (Choi and Zheng, 2009; Kuo et al., 2006). Recent data show that chronic exposure to Mn in rats leads to the subcellular relocation of Ctr1, rendering a highly concentrated Ctr1 in the apical brush boarder of the choroidal epithelia facing the cerebrospinal fluid (CSF). The exact implication of this intracellular trafficking of Ctr1 in response to Mn exposure remains to be determined. However, it seems that in the brain Ctr1 uptake function is predominantly from the CSF and minor from the blood (Kuo et al., 2006).

Two intracellular ATPases, Atp7a and Atp7b, are involved in ATP-dependent transport of Cu across the brain barriers. Genes that encode for these proteins are mutated in the inherited disorders of Cu metabolism, Menkes and Wilson diseases. Menkes disease is a fatal X-linked Cu deficiency syndrome that arises from defective Atp7a-driven transport of Cu from the intestine into the portal circulation, and aberrant distribution of Cu in the body. Wilson disease is an autosomal recessive Cu toxicity

disorder that results from disruption of Atp7b-mediated Cu export from liver hepatocytes into bile, and consequently liver and brain Cu accumulation. Atp7a is expressed in the majority of tissues except for the liver. Atp7b expression is more restricted, with highest expression in the liver. Both proteins possess eight transmembrane domains and contain six Met–X–Cys–X–X–Cys Cu binding motifs at the N-terminus (Lutsenko et al., 2007). Both are expressed in the brain capillary endothelial cells, in the choroidal epithelial cells (Choi and Zheng, 2009; Nishihara et al., 1998), in the BBB and in blood CSF barrier. Both ATPases are localized to the TGN, where they are utilized in the Cu secretory pathway, delivering Cu for incorporation into cuproenzymes. When intracellular Cu levels rise, both Atp7a and Atp7b are translocate from the TGN and carry Cu to the cellular membrane for efflux from the cell. This function is not only necessary for Cu trans-barrier transport, but also important for preventing excess Cu accumulation inside the barrier cells. The same mechanism, mediated by Atp7a, is activated in the postsynaptic terminal upon activation of NMDAR leading to Cu release in the synaptic cleft (Schlief et al., 2006). The localization, regulation and directional trafficking of both these Cu exporters at the brain barriers, and their respective roles in CNS Cu homeostasis, remain largely unknown.

Transferrin (Tf) binds Fe^{3+} in the circulation and brings it to the different site of use. Fe release from holo-Tf occurs after binding to its receptor, internalization in vesicles, acidification of the vesicles and reduction Fe^{3+} to Fe^{2+} by Steap3. The protein is essentially synthesized in hepatocytes, but also in Sertoli cells, in the epithelial cells of the choroid plexus in rodents and in oligodendrocytes (Zakin et al., 2002). Tf expression is regulated also by the hypoxia-inducible factor-1(HIF-1)/hereditary hemochromatosis gene product interaction (Rolfs et al., 1997). Moreover, diferric Tf levels have been suggested to modulate the expression of other proteins involved in Fe metabolism (Anderson et al., 2007).

Transferrin receptor 1 (TfR1) is a disulfide bonded, homodimeric receptor that is found on the surface of most body cells. TfR1 deficiency leads to embryonic lethality in mice, an indication of its physiological essentiality (Levy et al., 1999). The receptor binds diferric Tf with 10-fold higher affinity than monoferric Tf at physiological pH, and 2,000-fold higher affinity than apo-Tf. Since Tf binds Fe with such a high affinity, it is likely that Fe release also requires reduction, and takes advantage of a conformational change in Tf that accompanies its binding to TfR1 (Bali et al., 1991; Tsunoo and Sussman, 1983; Watkins et al., 1992). TfR1 expression is modulated in response to Fe abundance as described in Figure 47 (Zecca et al., 2004).

Ferroportin 1 (Fpn1) is a plasma membrane Fe export protein. Fpn is expressed at particularly high levels on the surface of cells with a high capacity to export iron, such as macrophages and enterocytes, but it appears to be present on almost all cells. Mutations in the Fpn gene create severe alterations in Fe metabolism: tissue Fe overloading occurs, but a systemic anemia is induced as reduced Fe export into

the plasma means reduced Fe supply to erythroid progenitors. Fpn deletion is not compatible with postnatal life. Its mechanism is not properly characterized, but it is known that it binds Fe^{2+}. GPI-anchored Cp is devoted to the oxidation of Fe^{2+} exported by Fpn to load Fe^{3+} on apo-Tf. Fpn transcription regulation occurs with the same mechanism described for ferritin in Figure 47, so in low Fe conditions its expression is diminished (Anderson et al., 2007).

The storage protein ferritin (Ft) is a 24-subunit protein shell enclosing a hollow interior, in which large Fe amounts are stored in a soluble, non-toxic, but bioavailable form. Mammalian Ft contains variable amounts of two types of polypeptide chain, heavy (H) and light (L), which have different functions. FtH chains have a ferroxidase centre, which can catalyse the rapid oxidation from Fe^{2+} to Fe^{3+}, whereas FtL chains are thought to function in the nucleation of the mineral core within the protein shell. L-rich Ft is associated to Fe storage, while H-rich Ft is associated to stress response (Zecca et al., 2004). Ft expression is regulated according to Fe availability in the opposing way with respect to TfR1 expression (Figure 47).

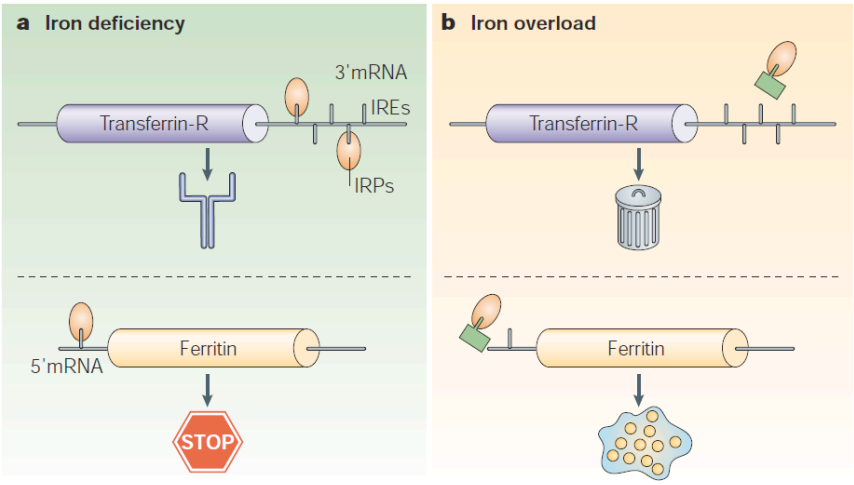

Figure 47. Production of the transferrin receptor (TfR) and ferritin is regulated at the level of mRNA by iron regulatory proteins (IRPs), which bind to iron response elements (IREs) on the 3'- and 5'- untranslated regions of their respective mRNAs. (a) In iron deficiency, the IRPs bind to the IREs, protecting the TfR mRNA from nuclease digestion and preventing the synthesis of ferritin. (b) When iron is abundant, the modified IRP no longer binds to the IREs — in IRP1 the IRE binding site is blocked by a 4Fe–4S cluster (green rectangle), whereas in IRP2 the protein is targeted for destruction in the proteasome — allowing TfR mRNA to be destroyed and allowing the expression of ferritin (Zecca et al., 2004).

Metallothioneins (Mt) are very small proteins containing highly conserved cystene residues that allow them to bind seven divalent metal ions (e.g. Zn) and up to twelve monovalent Cu ions (Bogumil et al., 1998; Faller et al., 1999). Mt expression is regulated in response to a range of stimuli, including metals, hormones, cytokines, oxidative agents, inflammation and stress. This complex regulation is mediated by

metal responsive elements, glucocorticoid responsive element, antioxidant response elements. Mt expression occurs in both CNS and PNS, particularly in reactive astrocytes. In neurons Mt promote neuronal survival and regeneration upon injury (Chung et al., 2007; Chung and West, 2004). There are a number of ways that MtI/II potentially enhance the ability of astrocytes to promote neuronal regeneration, for example by Zn binding, with roles in metal homeostasis or free radicals scavenging (Hidalgo et al., 2001; West et al., 2004). Mt likely acts within astrocytes, maybe to handle toxic intermediates. Moreover MtI/II and MtIII expressions are differently regulated in response to brain insults (West et al., 2008). Mt proteins also represent a source of Zn ions. In fact, they can rapidly release it by nitrosylation or oxidation of the thiol ligands (Maret, 1994, 2000). MtIII Zn release in the CA1 region of the hippocampus contributes to cell injury (Lee et al., 2003), but the opposite effect is observed in the CA3 where presynaptic release of Zn is neuroprotective (Takeda et al., 1999).

Zinc transporter proteins (ZnT) are responsible for Zn export and sequestration. Eight ZnT types have been characterized (Lovell, 2009). ZnT3 was analyzed in this project because it is the one responsible for Zn sequestration into vesicles in the hippocampal dentate granule cells, pyramidal and intraneurons (Palmiter et al., 1996). These vesicles contain Zn that is released with glutamate and that modulates NMDAR activity.

Specifically concerning Mn metabolism, just Mn-superoxide dismutase (Sod2) was analyzed in this study. It has been shown by Fridovich and colleagues that Sod2 is a ubiquitous metalloenzyme, essential for the survival of all aerobic organisms from bacteria to humans (Fridovich, 1974, 1995). Like Sod1, Sod2 catalyses the dismutation of superoxide anion radical to hydrogen peroxide and molecular oxygen. Sod2 is encoded by a nuclear gene and is transported across two mitochondrial membranes to the matrix. In mice, the lack of Sod2, or the complete elimination of its expression, causes dilated cardiomyopathy and neurodegeneration leading to early postnatal death. Sod2 is able to modulate some gene transcription through the HIF-1: at lower levels of Sod2, HIF-1α levels are elevated, but are suppressed at higher Sod2 levels. The biphasic influence of Sod2 on activation of HIF-1α is H_2O_2-dependent, as removal of peroxides reverses the effect (Miriyala et al., 2012).

Table 7 summarises all the obtained results concerning both metal ion content and protein expression measurements. As described in the *Introduction*, essential metals metabolisms cannot be considered individually: they are strictly interconnected and an alteration occurring in one of them is likely to alter all the others. As an example, if Cu content is altered or if it is miscompartimentalized, Fe uptake and distribution will be impaired, since Fe metabolism is regulated by Cu-dependent oxidases and reductases.

Brain							Hippocampus						
Copper metabolism													
	P1	P7	P30	P90	P180	P365		P1	P7	P30	P90	P180	P365
Cu	- -	#	++	#	-	#	Cu	#	- -	#	+	- - -	#
Cp	#	#	+	+	+	+	Cp	#	-	-	-	-	#
Steap3	#	#	#	#	#	#	Steap3	#	#	#	#	#	#
Sod1	#	#	#	#	#	#	Sod1	#	#	#	#	#	#
Ccs	-	#	#	#	#	-	Ccs	-	#	-	-	-	#
Ctr1	#	#	#	#	#	#	Ctr1	+	+	#	+	+	+
Atp7a	#	#	#	#	#	#	Atp7a	#	+	#	#	+	+
Atp7b	+	#	#	#	#	#	Atp7b	+	#	#	#	#	#
Iron metabolism													
	P1	P7	P30	P90	P180	P365		P1	P7	P30	P90	P180	P365
Fe	- -	-	+	#	#	#	Fe	#	-	#	+	-	#
Cp	#	#	+	+	+	+	Cp	#	-	-	-	-	#
Steap3	#	#	#	#	#	#	Steap3	#	#	#	#	#	#
Tf	+++	+	+	+	+	+	Tf	+	- -	+	+++	+	+++
TfR1	- -	++	+	++	+	+	TfR1	+	#	++	#	+	+
Fpn1	#	#	-	-	-	-	Fpn1	#	#	#	#	#	#
FtH	-	-	-	#	+	+	FtH	-	-	-	-	+	+
FtL	#	#	#	#	#	#	FtL	#	-	-	-	#	#
Zinc metabolism													
	P1	P7	P30	P90	P180	P365		P1	P7	P30	P90	P180	P365
Zn	- -	#	++	#	-	#	Zn	-	#	#	++	- - -	#
Sod1	#	#	#	#	#	#	Sod1	#	#	#	#	#	#
Mt	#	-	#	#	+	+	Mt	#	#	#	#	#	#
ZnT3	#	#	#	#	#	#	ZnT3	#	#	#	#	#	#
Manganese metabolism													
	P1	P7	P30	P90	P180	P365		P1	P7	P30	P90	P180	P365
Mn	#	- - -	++	#	- -	#	Mn	#	#	#	#	- -	#
Sod2	#	#	#	+	#	#	Sod2	#	#	#	#	#	#

Table 7. Summary of Cu metabolism proteins expression comparison between *Prnp*$^{+/+}$ and *Prnp*$^{0/0}$. The results are reported as *Prnp*$^{0/0}$ Vs *Prnp*$^{+/+}$. (-): significantly lower; (+): significantly higher; (#): no statistically significant difference.

To characterize essential metal metabolism in PrP null condition, for each metal ion both membrane transporters and cytosolic binding proteins expression has been investigated. Observing all the obtained data, it emerges that transporters and metal uptake proteins are generally upregulated in PrP absence, while exporters and storage proteins are downregulated. These overall protein expression re-arrangement is in agreement with metal ion levels measured in *Prnp*$^{0/0}$ brains and hippocampi, which resulted to be decreased compared to wild-type in particular in the early postnatal stages. In fact, Fe, and also Mn, uptake proteins (TfR1 and Tf) are generally increased in *Prnp*$^{0/0}$ brains and hippocampi, as well as Fe exporter (Fpn1) and storage proteins (FtH and FtL) are broadly decreased, in agreement with the results already published (Singh et al., 2009b). However, from late adulthood to aging, FtH expression is increased and this is likely to represent a response to a stressful condition (Zecca et al.,

2004). This does not agree with what previously published (Singh et al., 2009b), since their results show lower FtH levels in 6 months-old mouse brains. The same modulation can be observed concerning Cu binding proteins, though mainly in the hippocampus. In fact, Cu transporters (Ctr1 and Atp7a) are generally upregulated, while cytosolic proteins (Sod1 and Ccs) are either not affected or downregulated.

A protein showing strong expression alterations in PrP null samples is Cp, whose levels are increased in the brain and decreased in the hippocapus of *Prnp*$^{0/0}$ mice. Since the ratio between blood and brain volumes is very low, it is likely that the Cp revealed in the measurements is mainly synthetised by neurons and astrocytes. No Cp transcriptional regulation in response to Cu concentration has been described in literature and the same was confirmed by real time PCR on hippocampal mRNA extracts results reported in Figure 33. However, its degradation rate might be affected by Cu concentration, delivery and availability, thus resulting in the different Cp levels detected in brain and hippocampus.

Considering the observed Fe metabolic situation in PrP null brains, how can this global reorganization be justified in lack of a Cu-binding protein, like PrP^{C} is? In the finely tuned and very well orchestrated metal ion homeostasis mechanism, PrP^{C} functions as a player whose role, even if not strictly essential, needs to be compensated, in case of absence, through a deep reorganization of the other players, to reach the final goal which corresponds to homeostasis. This is confirmed also on Mn metabolism. In fact, as Fe and Zn, Mn levels are lowered in *Prnp*$^{0/0}$ brains in the early postnatal stages, while they are increased at P30. Mn shares with Fe the same transporters, in particular TfR1 and Fpn1. So, the rearranged TfR1 and Fpn1 expressions, beside rising Fe levels, likely increase Mn content. Moreover, since Tf and Cp are increased, a higher portion of Mn should be bound to Tf, since, as previously described, Mn oxidation operated by Cp promotes its binding to Tf, slowering its clearance. So, as for Cu and Fe, after P30 Mn content alterations are diminished and, though oscillation, mechanisms continue to re-organize maintaining its homeostasis as close to wild-type conditions as possible. Though a slight increase at P90, Sod2 expression is not altered. Since it was reported that in PrP absence Sod2 activity is triggered to face and prevent ROS formation (Brown and Besinger, 1998; Kralovicova et al., 2009), it is possible that the increased expression in adulthood is due to an increased requirement of Sod2 activity in particular in this stage. However, if really Sod2 activity is increased, it means that Mn homeostasis and metabolism are efficiently balanced in PrP null conditions, so Mn ions are effectively delivered to Sod2, otherwise it would not be able to catalyse the dismutase reaction. The content of Zn ions is lower in P1 PrP null brains compared to wild-type ones, it increases at P30 and it is again lowered at P180. So, it seems that Zn content follows more or less the same trend of Cu, Fe and Mn. It may be that transporters that were not analyzed in this study are subjected to expression modulations in *Prnp*$^{0/0}$ brains. Interestingly, Mt expression is increase from P180 to P365: this may represent a response to a stressful condition, as it was supposed for FtH.

In the hippocampus, Cu content is highly affected by PrP absence at P7 and at P180, stages showing a great lowering of its concentration. Differently from brain samples, alterations in Cu transporters expressions occur. At P7, both Ctr1 and Atp7a expressions are increased: this modulation may be caused by low Cu content. Impairments in Cu metabolism may also induce Cp decreased levels: if Cu is not properly stored or delivered in PrP null conditions, it cannot be load on Cp, resulting in lower Cp levels maybe due to apo-Cp higher degradation rate. In fact, as real time PCR results show in Figure 33, lower Cp levels are not consequent to decreased transcription.

The hypothesis of a condition of Cu miscompartmentalization, affecting the entire organism, thus, leading to impaired Cu loading on Cp, was assessed and confirmed by measuring Cp activity in sera. Circulating Cp is produced and Cu-loaded in the liver, and it represents the major Cu carrier in the entire body. So, its Cu-dependent ferroxidase activity is a good marker of Cu availability and homeostasis. Different ages were tested, P15, P30, P90, P180 and P365, revealing that Cp activity increases with age. However, this is true for *Prnp*$^{+/+}$ mice, but not for *Prnp*$^{0/0}$ ones. In fact, *Prnp*$^{0/0}$ Cp activity is lower compared to wild-type one, and the difference increases in the aging. This means that, at the systemic level, Cu homeostasis is impaired in such a way that its availability for Cp loading cannot be increased after a certain level, resulting in decreased ferroxidase activity. The peculiarity of P30 metal ion condition is confirmed also in this experiment where P30 results to be the only stage with comparable levels of Cp activity in wild-type and PrP null mice: given the importance of synaptogenesys completion, it is likely that many compensatory effect occur in this stage to maintain metal ion homeostasis and metal-dependent enzymes functionality. It would be interesting to measure Fe plasma levels at P365. In fact, it has been published that PrP null 6 months-old mice show mild anemia (Singh et al., 2009b). This, according to the results here shown, can be consequent to lower Cp activity that triggers lower plasma Fe levels, inducing anemia. If this is the case, anemia should increase in aging, with Cp activity becoming lower and lower. According to what has been observed in Wilson's disease and aceruloplasminemia conditions, diminished Cp functionality should cause brain Fe accumulation (Qian and Wang, 1998). In the results previously showed, this was not strikingly detected because in the aging brain Fe levels increases in *Prnp*$^{0/0}$ mice, but the difference with *Prnp*$^{+/+}$ samples is not significant - maybe the gap can get more pronounced in further aging stages -, while in the aging hippocampus, Fe concentration increases in both *Prnp*$^{+/+}$ and *Prnp*$^{0/0}$ mice in the same manner. Going back to the other analysed proteins, also in the hippocampus Sod1 expression is not impaired, but it is likely less functional (Brown and Besinger, 1998; Kralovicova et al., 2009), also because lower Ccs levels were detected at different developmental stage, maybe due to impairments in Cu delivery pathways. Though the existence of others mechanisms that deliver Cu to Sod1, this is the prevalent one, so its decrease must contribute to the diminished Sod1 functionality. Concerning Fe homeostasis, the same phenotype observed in the brain, typical of Fe deficiency conditions, was confirmed in the

hippocampus of PrP null mice. In fact, Fe uptake proteins Tf and TfR1 showed increased expression levels, though a lower Tf level at P7 was detected concomitant with the major drop in Fe concentration. Moreover, FtH was decreased up to adulthood, confirming the transcriptional regulation model in Figure 47, but going towards aging, like in the brain, FtH is increased, confirming that a stress condition is occurring at higher levels compared to wild-type hippocampi. Moreover, since Ft is expressed in oligodendrocytes, being the major Fe source, the occurring stressful conditions may be related to a demyelinating phenomenon (Todorich et al., 2011). Differently from the brain, Fpn1 expression was not affected, indicating either that Fe metabolic impairment in PrP null hippocampi is less pronounced compared to the entire brain or that it cannot be rescued decreasing the export. Another difference, suggesting a different situation compared to the brain, is the lower FtL expression detected in the hippocampus. These findings suggest that Fe homeostasis compensation occurs with different mechanism in the hippocampus with respect to the total brain. It may be that these differences between PrP null brains and hippocampi regulation of Fe metabolism are linked to the lower Cp levels observed in the hippocampus. The same considerations done about Mn homeostasis in the brain can be transposed to the hippocampus. Largely sharing the same transporters and the same Tf-loading upon Cp oxidation, Mn concentration is affected by PrP ablation in a way similar to Fe one. However, at P180 its content is lowered in a more pronounced manner compared to Fe. This suggests that, in Cp deficiency conditions, Mn oxidation is more affected than Fe one. Concerning Zn metabolism, though its concentrations was affected by PrP ablation, in particular at P1 and P180, the latter one showing an astonishing reduced content, the proteins analysed did not reveal any difference compared to wild-type hippocampal samples, indicating that, if some protein expression alteration occurs, it involves others Zn metabolic pathway players.

In general, known that many transporters and enzymes function for different cations, metal ions occupancy of binding sites is dependent on both the relative abundance of the competitor ions and the protein binding site affinity for each ion. So, if one metal exceeds, the binding, as well as the uptake, the distribution and the availability, of the others ions will be diminished. This corresponds, for example, to the situation theoretically occurring in case of Fe or Mn excess: if Fe overload occurs, Mn content will be likely decreased, and vice versa, since they share transporters, like TfR1 and Dmt1, but also oxidation by Cp is required for both ionic species homeostasis. On the contrary, in Fe deficiency, Mn uptake is likely to be increased, and vice versa. However, in case of Cu deficiency, consequences on other metals are completely different. In fact, instead of being a competitor for transporter sites, Cu is essential for other Mn and Fe uptake since it is the cofactor of oxidases (Cp) and reductases (Steap) responsible for Mn and Fe loading on, passage among and release from transporters. According to what emerges from the results here presented, this is likely the situation induced by PrP absence. PrP binds metal ions, like Cu, Zn, Mn and also Fe. However, its affinity for Cu is definitely higher,

especially in biological conditions (Chattopadhyay et al., 2005; Liu et al., 2011). It is likely that the PrP-bound Cu represent a prominent fraction of the total Cu content. As a consequence, in PrP absence, at the absorption sites, Cu can occupy proteins not primarily devoted to its metabolism. This can have different consequences: first, alteration in Cu absorption itself; second, interferences with other cations absorption, impairing it; third, altered compartmentalization of Cu ions, which will not be as available as they are in normal conditions for enzymes loading and cofactor functioning. Both these consequences lead to diminished cations absorption and distribution. However, metal ions pathways can be so finely regulated, by transcriptional, translational, posttranslational and translocation regulation of soluble and membrane transporters, that a compensation occurs, even though just partial. This is the reason why, in *Prnp*$^{0/0}$ mice, even if not dramatically, metal ions content is altered: this is likely to be the common denominator to the phenotypes observed in *Prnp*$^{0/0}$ mouse CNS, for example demyelination, which has been reported in PrP null conditions (Bremer et al., 2010) and which is caused by Cu and Fe impaired metabolism (Benetti et al., 2010; Skripuletz et al., 2008), and also impaired synaptic plasticity and alteration in oxidative stress response.

In *Prnp*$^{0/0}$ mice, phenotypes related to synaptic functionality impairments have been reported (Criado et al., 2005; Maglio et al., 2004; Mallucci et al., 2002). In particular, excitatory glutamatergic synapses appear to be the major site in which PrP^{C} plays an important role. In fact, it has been reported in literature that NMDAR currents are altered upon PrP ablation: NMDARs show slowed deactivation kinetics (Khosravani et al., 2008a), as well as a large non-desensitizing steady-state (You et al., 2012). This increased steady-state length, of course, damages neurons: in fact, *Prnp*$^{0/0}$ neurons are more susceptible to excitotoxic insult. The alteration of NMDAR activity observed in PrP^{C} absence can be induced in wild-type conditions adding a Cu chelator, on the contrary, PrP^{C} null neurons can approach the wild-type current upon Cu addition (You et al., 2012). How PrP^{C}-bound Cu can inhibit NMDAR was not clarified, neither it has been described in literature the general mechanism through which Cu inhibits NMDARs (Vlachova et al., 1996). However, it is known that NMDARs can be modulated by extracellular cysteines S-nitrosylation and that this reaction is always inhibitory (Choi and Lipton, 2000; Choi et al., 2000; Lipton et al., 2002). As described in Box1 in the *Introduction*, S-nitrosylation reaction requires one-electron oxidation from the free radical NO to NO^{+} that is mediated by a transition metal, in particular Cu. Since PrP^{C} can bind up to five Cu ions and supports its reduction, it can represent the link between free synaptic Cu and NO^{+} production. In fact, Cu is released by TGN vesicles after glutamatergic stimulation of NMDAR and Ca^{2+} intracellular influx, as well as nNOS is activated to produce NO. Therefore, PrP^{C}-bound Cu could contribute to NMDAR inhibition promoting S-nitrosylation of extracellular cysteines, as it does for glypican-1 (Mani et al., 2003). To validate this hypothesis, first the increased susceptibility to NMDA stimulation in our murine model was assessed by mean of OHCs: a very potent system that allows to operate *in vitro* maintaining the organ

cytoarchitecture. Treating OHCs with 5μM NMDA for three hours induced very low neuronal cell death levels in *Prnp*$^{+/+}$ hippocampus, allowing an easier comparison with *Prnp*$^{0/0}$ cultures. The results obtained confirmed that *Prnp*$^{0/0}$ hippocampus is more susceptible to excitotoxic treatment. As shown in Figures 37 and 38, *Prnp*$^{+/+}$ neurons were affected by the treatment in a significant manner almost only in the CA1 region, which is known to be the first responding to insults (Bunk et al., 2010; Kristensen et al., 2001), while in the CA3 and in the DG neuronal cell death levels were very low. On the contrary, *Prnp*$^{0/0}$ hippocampus, beside showing a higher death levels in the CA1 compared to *Prnp*$^{+/+}$, revealed significant pyknotic nuclei percentages also in the CA3 and in the DG, confirming what previously published with propidium iodide staining on OHCs (Rangel et al., 2007). Moreover, neuronal cell death was accompanied by loss of NeuN staining, which appeared fading around pyknotic nuclei. By expression analysis of the proteins playing major roles in excitotoxicity, it was observed that no alterations occur in nNOS expression, meaning that RNS should not be increased in *Prnp*$^{0/0}$ hippocampus because of an increased enzyme expression level. The analysis of Casp3 expression levels revealed that it is expressed at lower levels at P30 and at higher levels at P365. The decrease at P30 may be one cause of the impairments in learning and memory processes observed in PrP ablated mice (Criado et al., 2005). In fact, during the CNS developlment, Casp3, has non-apoptotic functions in neurons and, if mutated, provokes synaptic alterations including learning and memory deficits (D'Amelio et al., 2010). Casp3 higher expression at P365 may be due to increased stress condition occurring in aging *Prnp*$^{0/0}$ hippocampus: in fact, it has been shown that Casp3 mRNA and protein levels are increased after apoptosis-promoting insults, like ischemia (Chen et al., 1998). However, NMDAR subunits expression was highly increased in PrP null conditions: GluN2A, GluN2B, as well as the ubiquitous GluN1 showed higher expression levels, confirming what previously published in literature (Maglio et al., 2004). The reason why this alteration occurs cannot be explained in light of the data collected in this work. An increased expression in NMDARs, whether functional, may lead to impaired Ca^{2+} homeostasis. To address this point, Ca^{2+} transporters were analysed according to their expression. Alterations in Ncx1, Pmca and Serca2 were detected both in the brain and in the hippocampus of *Prnp*$^{0/0}$ mice. In general, it came out that in the early postnatal stages *Prnp*$^{0/0}$ mice upregulate the expression of transporters with low affinity, but high capacity (Ncx1), likely to move huge amount of Ca^{2+}. In adulthood and aging, on the contrary, the expression of pumps with high affinity, but low capacity (Pmca and Serca2) was enhanced, indicating that a finer regulation is required, maybe to sense small Ca^{2+} concentration oscillations. To check whether these alterations were aimed to maintain Ca^{2+} homeostasis, or whether, on the contrary, these modifications induced impairments in the homeostasis, Ca^{2+} total content was measured in both brain and hippocampus at the different developmental stages. Results showed that Ca^{2+} is almost not affected by PrP ablation, suggesting that modulation of Ca^{2+} transporters likely occurs to solve a situation in which Ca^{2+} homeostasis would be impaired. Taken

together these results explain neither why *Prnp*$^{0/0}$ hippocampus is more susceptible to excitotoxicity nor how PrP^{C}-bound Cu ions modulate NMDAR functionality. The measurements of S-nitrosylation levels of GluN1 and GluN2A subunits provided the answer. In fact, in *Prnp*$^{0/0}$ hippocampus both the subunits showed lower S-nitrosylation levels compared to *Prnp*$^{+/+}$ samples. This result explains why NMDAR currents are altered by PrP ablation, as well as why PrP null mice are more susceptible to excitotoxic insults. The model in Figure 48, confirmed by these results, describes the neurochemical mechanism through which PrP^{C} exerts its neuroprotective function: upon Cu binding in the synaptic cleft, PrP^{C} bring the electron acceptor that supports the inhibitory S-nitrosylation of NMDARs.

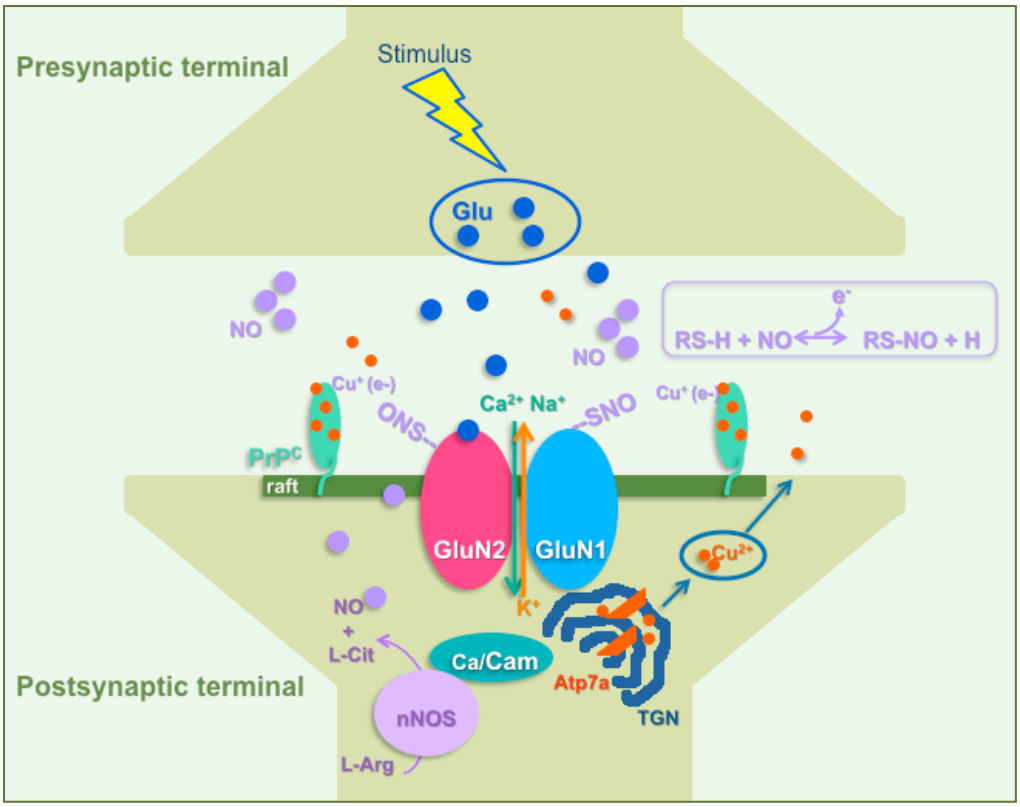

Figure 48. Mechanism of PrP^{C}-medited inhibition of NMDA receptor.

CONCLUSIONS

Define the physiological function of the proteins involved in neurodegenerative disorder is crucial for understanding pathological mechanisms underlying these disorders. Concerning proteins that aggregate in neurodegenerating neurons, like PrP, their function may be lost upon oligomerization, and this could contribute to the disease progression.

The work described in this thesis has been focused on PrP^C physiological function in the context of CNS metal ions homeostasis and glutamatergic synapses regulation. What links these two apparently separated aspects is PrP^C ability to bind metal ions. Copper is an essential metal with the highest binding affinity for PrP^C and an interesting point is represented by PrP^C ability to support its reduction. Results obtained studying PrP null mice indicate that the essential metals homeostasis is affected by PrP ablation mainly in the early postnatal stages. Starting from synaptogenesis completion, the set of pathways devoted to metals metabolism rearrange the expression, the activity and, likely, the localization of transporters and enzymes in order to re-establish a condition as much close to normal one as possible. PrP^C absence corresponds to the lack of a protein that is so widely and highly expressed that likely binds a high percentage of copper ions. This induces copper dys-homeostasis, triggering two main consequences: (i) alteration in the binding rate of the others divalent cations, impairing their absorption, delivery and excretion; (ii) not proper copper delivery and compartmentalisation. Copper miscompartmentalisation can occur for two reasons: (i) the binding to other proteins will bring it to other cellular district; (ii) the delivery, occurring when PrP^C-mediated reduction of Cu(II) to Cu(I) induce endocytosis and Cu(I) passes to other transporters, is completely missing. Even if in adulthood and aging the metal ions content is almost re-established, these set of results do not indicate where ions are localized, where they are stored and which proteins they are bound to. As a consequence, loading on copper-dependent enzymes will be impaired: an example is ceruloplasmin, which shows decreased ferroxidase activity, consequently impairing Fe homeostasis. Being metal ions so important in the organism physiology, these set of alterations, even if not apparently so huge, triggers consequences, as the demyelination observed in aged mice. Concerning the exact PrP^C role in metal ions homeostasis, the situation here presented suggests that PrP^C is an important copper buffering protein and that PrP^C-mediated copper uptake in the cell and delivery to intracellular transporters is necessary for the correct functioning of all essential metals homeostasis pathways.

Copper binding confers PrP^C another important function that in this work has been clarified. Evidence reported in literature describe NMDAR activity and regulation impairments in PrP null conditions, as well as an increased susceptibility to excitotoxic stimuli, such as NMDA and kainate treatment. Both NMDARs current alteration and neuronal cell death upon insult were rescued by copper adding, or, on the contrary, were induced in wild-type hippocampus upon copper chelator adding, suggesting that PrP^C-mediated modulation of NMDARs is mediated by copper. In this work, a more detailed characterization of hippocampal susceptibility to NMDA treatment was described using OHCs as a system and evaluating neuronal cell death by pyknotic nuclei counting and neuronal marker staining, instead of primary hippocampal cultures or propidium iodide staining. The results obtained show that, while in wild-type sample low NMDA exposure (5μM for three hours) can induce significant neuronal cell death just in the CA1 region, in PrP absence high pyknosis levels are triggered also in the CA3 and in the DG, beside having enhanced mortality in the CA1. Excitotoxicity major players expression levels were measured in PrP null hippocampi, revealing the more interesting differences in calcium transporters. In fact, the results show that, to properly maintain calcium homoestasis, PrP null mice require a specific up-regulation of the transporters: (i) high capacity but low affinity transporters (Ncx1) are over-expressed in the early postnatal stages, likely because massive movements of calcium are required in these stages; (ii) high affinity but low capacity calcium pumps (Pmca and Serca2) are up-regulated from adulthood to aging, likely because a finest sensing of calcium concentration oscillations is required in these stages. Increased NMDAR subunits expression was also revealed in PrP null hippocampus; however, a higher expression cannot account for the slowed deactivation kinetics and the increased steady-states reported in literature. The mechanism here hypothesised and also confirmed claims that PrP^C mediates NMDAR inhibition bringing the copper ion that functions as electron acceptor for the S-nitrosylation of GluN1 and GluN2A extracellular cysteines. In fact, in PrP null hippocampus lower levels of S-nitrosylated GluN1 and GluN2A were detected, meaning that PrP^C promotes this inhibitory reaction that occurs at lower levels in its absence. This explains, also, at least one way of copper-mediated inhibition of NMDARs, since, even if this modulation has been described many years ago, no binding sites have been detected and no mechanisms have been described.

These results highlight the importance of metal ions homeostasis in the CNS and in glutamatergic synapses, as well as the central role PrP^C plays in maintaining the homeostasis and in bringing copper ions where they are required and in the oxidation state they are required in synapse.

ACKNOWLEDGEMENTS

The development of this work has been possible thanks to Prof. Legname who accepted me in his group four years ago. I would like to thank him for his constant guide, for his suggestions, for the discussions, for trusting me, for allowing me to be independent and to decide how to move inside this project. I would like to thank him also for all opportunities he gave me in these years, I recognize that it is not obvious and I really appreciate this. I have learned a lot from this experience!

I shared the path of this project with Dr. Federico Benetti who chose me for working on it. I am totally and sincerly grateful to you, Federico, for the work you have done with me in these years, for all the things you taught me, for the patience you had, for all the laughs, for not abandoning me after your moving, for trusting me first as a person and then as a student. Sometimes it has not been easy, but we have been able to obtain good results, to work cooperatively (you one emisphere, and I the other one!) and to overcome the difficulties.

I would like to thank ALL the present and past members of the Prion Biology Lab, in particolar Andrea, Ilaria, Gabriele, Maura, Nhat, Thao, Silvia, Erica, Francesco, Stefano and Federica. However, my deepest thanks are for Elisa for working and supporting me during this last and hard year. I really hope you enjoyed and appreciated it as much as I did!! I also hope you to have a satisfying and enjoyable PhD course. Thanks for appreciating the work I was doing, for your patience, for being able to find all the things that I used to loose (my head included) and for being a good friend!! Call me whenever you need me…or even if you don't need me! Ste and Federica, you were the first friends I found here (you cannot imagine how much I appreciated this!), we shared great moments and staying here without you has not been easy at all…

An enormous aknowledgement is for all the members of the Common Molecular Biology Lab, in particular Aswini (a great teacher!), Giovanni, Fulvio (primario), Devendra&Lijo, Paola (our "scientific Mum"), Niels and Sandra. Enough words do not exist to thank Roby and Alessia… You have been my FRIENDS, my everyday support! During days (and nights) in lab we shared laughs, fun, suggestions, we helped each other in every moment, and you have to know that you are the best lab-friend I could ever imagine to find! I really love you, my "single ladies"!

A special thank also to all the SISSA staff, in particular Bea for all the work she did for me and my beloved cultures, for her friendship and psychological assistance, Jess for the precious help, for all the laughs and "pause cicchin" and Tullio for the help and his "kindness/rudeness" that we all love.

BIBLIOGRAPHY

Aarts, M., Liu, Y., Liu, L., Besshoh, S., Arundine, M., Gurd, J.W., Wang, Y.T., Salter, M.W., and Tymianski, M. (2002). Treatment of ischemic brain damage by perturbing NMDA receptor- PSD-95 protein interactions. Science *298*, 846-850.

Adlard, P.A., and Bush, A.I. (2006). Metals and Alzheimer's disease. J Alzheimers Dis *10*, 145-163.

Aguzzi, A., Baumann, F., and Bremer, J. (2008). The prion's elusive reason for being. Annu Rev Neurosci *31*, 439-477.

Aguzzi, A., and Falsig, J. (2012). Prion propagation, toxicity and degradation. Nat Neurosci *15*, 936-939.

Aguzzi, A., Heikenwalder, M., and Miele, G. (2004). Progress and problems in the biology, diagnostics, and therapeutics of prion diseases. J Clin Invest *114*, 153-160.

Aguzzi, A., Montrasio, F., and Kaeser, P.S. (2001). Prions: health scare and biological challenge. Nat Rev Mol Cell Biol *2*, 118-126.

Akazawa, C., Shigemoto, R., Bessho, Y., Nakanishi, S., and Mizuno, N. (1994). Differential expression of five N-methyl-D-aspartate receptor subunit mRNAs in the cerebellum of developing and adult rats. J Comp Neurol *347*, 150-160.

Aldred, A.R., Grimes, A., Schreiber, G., and Mercer, J.F. (1987). Rat ceruloplasmin. Molecular cloning and gene expression in liver, choroid plexus, yolk sac, placenta, and testis. J Biol Chem *262*, 2875-2878.

Anderson, G.J., Darshan, D., Wilkins, S.J., and Frazer, D.M. (2007). Regulation of systemic iron homeostasis: how the body responds to changes in iron demand. Biometals *20*, 665-674.

Andrews, N.C. (2002). A genetic view of iron homeostasis. Semin Hematol *39*, 227-234.

Archibald, F.S., and Tyree, C. (1987). Manganese poisoning and the attack of trivalent manganese upon catecholamines. Arch Biochem Biophys *256*, 638-650.

Arena, G., La Mendola, D., Pappalard, G., Sóvágód, I., and Rizzarelli, E. (2012). Interactions of Cu2+ with prion family peptide fragments: Considerations
on affinity, speciation and coordination. Coordination Chemistry Reviews *256*, 2202-2218.

Aschner, M. (2006). The transport of manganese across the blood-brain barrier. Neurotoxicology *27*, 311-314.

Aschner, M., and Gannon, M. (1994). Manganese (Mn) transport across the rat blood-brain barrier: saturable and transferrin-dependent transport mechanisms. Brain Res Bull *33*, 345-349.

Assaf, S.Y., and Chung, S.H. (1984). Release of endogenous Zn2+ from brain tissue during activity. Nature *308*, 734-736.

Avery, S.V. (2001). Metal toxicity in yeasts and the role of oxidative stress. Adv Appl Microbiol *49*, 111-142.

Baker, P.F., Blaustein, M.P., Hodgkin, A.L., and Steinhardt, R.A. (1969). The influence of calcium on sodium efflux in squid axons. J Physiol *200*, 431-458.

Bali, P.K., Zak, O., and Aisen, P. (1991). A new role for the transferrin receptor in the release of iron from transferrin. Biochemistry *30*, 324-328.

Banci, L., Bertini, I., Cantini, F., and Ciofi-Baffoni, S. (2010). Cellular copper distribution: a mechanistic systems biology approach. Cell Mol Life Sci *67*, 2563-2589.

Barnham, K.J., and Bush, A.I. (2008). Metals in Alzheimer's and Parkinson's diseases. Curr Opin Chem Biol *12*, 222-228.

Baumann, F., Tolnay, M., Brabeck, C., Pahnke, J., Kloz, U., Niemann, H.H., Heikenwalder, M., Rulicke, T., Burkle, A., and Aguzzi, A. (2007). Lethal recessive myelin toxicity of prion protein lacking its central domain. EMBO J *26*, 538-547.

Behe, P., Colquhoum, D., and Wyllie, D.J. (1999). Activation of single AMPA- and NMDA-type gluatamete-receptor channels. In Ionotropic glutamate receptors in the CNS, J. P., and M. H., eds. (Berlin, Springer), pp. 175-218.

Benetti, F., Ventura, M., Salmini, B., Ceola, S., Carbonera, D., Mammi, S., Zitolo, A., D'Angelo, P., Urso, E., Maffia, M.*, et al.* (2010). Cuprizone neurotoxicity, copper deficiency and neurodegeneration. Neurotoxicology *31*, 509-517.

Benvegnu, S., Gasperini, L., and Legname, G. (2011). Aged PrP null mice show defective processing of neuregulins in the peripheral nervous system. Mol Cell Neurosci *47*, 28-35.

Benvegnu, S., Poggiolini, I., and Legname, G. (2010). Neurodevelopmental expression and localization of the cellular prion protein in the central nervous system of the mouse. J Comp Neurol *518*, 1879-1891.

Bertoni-Freddari, C., Fattoretti, P., Casoli, T., Di Stefano, G., Giorgetti, B., and Balietti, M. (2008). Brain aging: The zinc connection. Exp Gerontol *43*, 389-393.

Biasini, E., Turnbaugh, J.A., Unterberger, U., and Harris, D.A. (2012). Prion protein at the crossroads of physiology and disease. Trends Neurosci *35*, 92-103.

Blaustein, M.P., and Hodgkin, A.L. (1969). The effect of cyanide on the efflux of calcium from squid axons. J Physiol *200*, 497-527.

Blaustein, M.P., and Santiago, E.M. (1977). Effects of internal and external cations and of ATP on sodium-calcium and calcium-calcium exchange in squid axons. Biophys J *20*, 79-111.

Bleackley, M.R., and Macgillivray, R.T. (2011). Transition metal homeostasis: from yeast to human disease. Biometals *24*, 785-809.

Bogumil, R., Faller, P., Binz, P.A., Vasak, M., Charnock, J.M., and Garner, C.D. (1998). Structural characterization of Cu(I) and Zn(II) sites in neuronal-growth-inhibitory factor by extended X-ray absorption fine structure (EXAFS). Eur J Biochem *255*, 172-177.

Bowman, A.B., Kwakye, G.F., Hernandez, E.H., and Aschner, M. (2011). Role of manganese in neurodegenerative diseases. J Trace Elem Med Biol *25*, 191-203.

Bremer, J., Baumann, F., Tiberi, C., Wessig, C., Fischer, H., Schwarz, P., Steele, A.D., Toyka, K.V., Nave, K.A., Weis, J.*, et al.* (2010). Axonal prion protein is required for peripheral myelin maintenance. Nat Neurosci *13*, 310-318.

Brodin, P., Falchetto, R., Vorherr, T., and Carafoli, E. (1992). Identification of two domains which mediate the binding of activating phospholipids to the plasma-membrane Ca2+ pump. Eur J Biochem *204*, 939-946.

Brown, D.R. (2001). Prion and prejudice: normal protein and the synapse. Trends Neurosci *24*, 85-90.

Brown, D.R. (2003). Prion protein expression modulates neuronal copper content. J Neurochem *87*, 377-385.

Brown, D.R., and Besinger, A. (1998). Prion protein expression and superoxide dismutase activity. Biochem J *334 (Pt 2)*, 423-429.

Brown, D.R., Clive, C., and Haswell, S.J. (2001). Antioxidant activity related to copper binding of native prion protein. J Neurochem *76*, 69-76.

Brown, D.R., Hafiz, F., Glasssmith, L.L., Wong, B.S., Jones, I.M., Clive, C., and Haswell, S.J. (2000). Consequences of manganese replacement of copper for prion protein function and proteinase resistance. EMBO J *19*, 1180-1186.

Brown, D.R., Nicholas, R.S., and Canevari, L. (2002). Lack of prion protein expression results in a neuronal phenotype sensitive to stress. J Neurosci Res *67*, 211-224.

Brown, D.R., Qin, K., Herms, J.W., Madlung, A., Manson, J., Strome, R., Fraser, P.E., Kruck, T., von Bohlen, A., Schulz-Schaeffer, W.*, et al.* (1997a). The cellular prion protein binds copper in vivo. Nature *390*, 684-687.

Brown, D.R., Schmidt, B., and Kretzschmar, H.A. (1998). Effects of copper on survival of prion protein knockout neurons and glia. J Neurochem *70*, 1686-1693.

Brown, D.R., Schulz-Schaeffer, W.J., Schmidt, B., and Kretzschmar, H.A. (1997b). Prion protein-deficient cells show altered response to oxidative stress due to decreased SOD-1 activity. Exp Neurol *146*, 104-112.

Brown, D.R., Wong, B.S., Hafiz, F., Clive, C., Haswell, S.J., and Jones, I.M. (1999). Normal prion protein has an activity like that of superoxide dismutase. Biochem J *344 Pt 1*, 1-5.

Brown, L.R., and Harris, D.A. (2003). Copper and zinc cause delivery of the prion protein from the plasma membrane to a subset of early endosomes and the Golgi. J Neurochem *87*, 353-363.

Bueler, H., Aguzzi, A., Sailer, A., Greiner, R.A., Autenried, P., Aguet, M., and Weissmann, C. (1993). Mice devoid of PrP are resistant to scrapie. Cell *73*, 1339-1347.

Bueler, H., Fischer, M., Lang, Y., Bluethmann, H., Lipp, H.P., DeArmond, S.J., Prusiner, S.B., Aguet, M., and Weissmann, C. (1992). Normal development and behaviour of mice lacking the neuronal cell-surface PrP protein. Nature *356*, 577-582.

Bunk, E.C., Konig, H.G., Bonner, H.P., Kirby, B.P., and Prehn, J.H. (2010). NMDA-induced injury of mouse organotypic hippocampal slice cultures triggers delayed neuroblast proliferation in the dentate gyrus: an in vitro model for the study of neural precursor cell proliferation. Brain Res *1359*, 22-32.

Bush, A.I. (2000). Metals and neuroscience. Curr Opin Chem Biol *4*, 184-191.

Calabrese, V., Mancuso, C., Calvani, M., Rizzarelli, E., Butterfield, D.A., and Stella, A.M. (2007). Nitric oxide in the central nervous system: neuroprotection versus neurotoxicity. Nat Rev Neurosci *8*, 766-775.

Carafoli, E. (1985). The homeostasis of calcium in heart cells. J Mol Cell Cardiol *17*, 203-212.

Carafoli, E. (1987). Intracellular calcium homeostasis. Annu Rev Biochem *56*, 395-433.

Carafoli, E., Santella, L., Branca, D., and Brini, M. (2001). Generation, control, and processing of cellular calcium signals. Crit Rev Biochem Mol Biol *36*, 107-260.

Carafoli, E., and Zurini, M. (1982). The Ca2+-pumping ATPase of plasma membranes. Purification, reconstitution and properties. Biochim Biophys Acta *683*, 279-301.

Carleton, A., Tremblay, P., Vincent, J.D., and Lledo, P.M. (2001). Dose-dependent, prion protein (PrP)-mediated facilitation of excitatory synaptic transmission in the mouse hippocampus. Pflugers Arch *442*, 223-229.

Caroni, P., and Carafoli, E. (1981). Regulation of Ca2+-pumping ATPase of heart sarcolemma by a phosphorylation-dephosphorylation Process. J Biol Chem *256*, 9371-9373.

Caughey, B., and Baron, G.S. (2006). Prions and their partners in crime. Nature *443*, 803-810.

Caughey, B., and Raymond, G.J. (1991). The scrapie-associated form of PrP is made from a cell surface precursor that is both protease- and phospholipase-sensitive. J Biol Chem *266*, 18217-18223.

Caughey, B.W., Dong, A., Bhat, K.S., Ernst, D., Hayes, S.F., and Caughey, W.S. (1991). Secondary structure analysis of the scrapie-associated protein PrP 27-30 in water by infrared spectroscopy. Biochemistry *30*, 7672-7680.

Chattopadhyay, M., Walter, E.D., Newell, D.J., Jackson, P.J., Aronoff-Spencer, E., Peisach, J., Gerfen, G.J., Bennett, B., Antholine, W.E., and Millhauser, G.L. (2005). The octarepeat domain of the prion protein binds Cu(II) with three distinct coordination modes at pH 7.4. J Am Chem Soc *127*, 12647-12656.

Chelly, J., Tumer, Z., Tonnesen, T., Petterson, A., Ishikawa-Brush, Y., Tommerup, N., Horn, N., and Monaco, A.P. (1993). Isolation of a candidate gene for Menkes disease that encodes a potential heavy metal binding protein. Nat Genet *3*, 14-19.

Chen, J., Nagayama, T., Jin, K., Stetler, R.A., Zhu, R.L., Graham, S.H., and Simon, R.P. (1998). Induction of caspase-3-like protease may mediate delayed neuronal death in the hippocampus after transient cerebral ischemia. J Neurosci *18*, 4914-4928.

Cherukuri, S., Potla, R., Sarkar, J., Nurko, S., Harris, Z.L., and Fox, P.L. (2005). Unexpected role of ceruloplasmin in intestinal iron absorption. Cell Metab *2*, 309-319.

Chesebro, B., Trifilo, M., Race, R., Meade-White, K., Teng, C., LaCasse, R., Raymond, L., Favara, C., Baron, G., Priola, S.*, et al.* (2005). Anchorless prion protein results in infectious amyloid disease without clinical scrapie. Science *308*, 1435-1439.

Chinnery, P.F., Crompton, D.E., Birchall, D., Jackson, M.J., Coulthard, A., Lombes, A., Quinn, N., Wills, A., Fletcher, N., Mottershead, J.P.*, et al.* (2007). Clinical features and natural history of neuroferritinopathy caused by the FTL1 460InsA mutation. Brain *130*, 110-119.

Choi, B.S., and Zheng, W. (2009). Copper transport to the brain by the blood-brain barrier and blood-CSF barrier. Brain Res *1248*, 14-21.

Choi, Y.B., and Lipton, S.A. (1999). Identification and mechanism of action of two histidine residues underlying high-affinity Zn2+ inhibition of the NMDA receptor. Neuron *23*, 171-180.

Choi, Y.B., and Lipton, S.A. (2000). Redox modulation of the NMDA receptor. Cell Mol Life Sci *57*, 1535-1541.

Choi, Y.B., Tenneti, L., Le, D.A., Ortiz, J., Bai, G., Chen, H.S., and Lipton, S.A. (2000). Molecular basis of NMDA receptor-coupled ion channel modulation by S-nitrosylation. Nat Neurosci *3*, 15-21.

Choquette, D., Hakim, G., Filoteo, A.G., Plishker, G.A., Bostwick, J.R., and Penniston, J.T. (1984). Regulation of plasma membrane Ca2+ ATPases by lipids of the phosphatidylinositol cycle. Biochem Biophys Res Commun *125*, 908-915.

Chua, A.C., and Morgan, E.H. (1997). Manganese metabolism is impaired in the Belgrade laboratory rat. J Comp Physiol B *167*, 361-369.

Chung, R.S., Fung, S.J., Leung, Y.K., Walker, A.K., McCormack, G.H., Chuah, M.I., Vickers, J.C., and West, A.K. (2007). Metallothionein expression by NG2 glial cells following CNS injury. Cell Mol Life Sci *64*, 2716-2722.

Chung, R.S., and West, A.K. (2004). A role for extracellular metallothioneins in CNS injury and repair. Neuroscience *123*, 595-599.

Colling, S.B., Collinge, J., and Jefferys, J.G. (1996). Hippocampal slices from prion protein null mice: disrupted Ca(2+)-activated K+ currents. Neurosci Lett *209*, 49-52.

Collinge, J., Whittington, M.A., Sidle, K.C., Smith, C.J., Palmer, M.S., Clarke, A.R., and Jefferys, J.G. (1994). Prion protein is necessary for normal synaptic function. Nature *370*, 295-297.

Collingridge, G. (1987). Synaptic plasticity. The role of NMDA receptors in learning and memory. Nature *330*, 604-605.

Criado, J.R., Sanchez-Alavez, M., Conti, B., Giacchino, J.L., Wills, D.N., Henriksen, S.J., Race, R., Manson, J.C., Chesebro, B., and Oldstone, M.B. (2005). Mice devoid of prion protein have cognitive deficits that are rescued by reconstitution of PrP in neurons. Neurobiol Dis *19*, 255-265.

Crossgrove, J.S., and Yokel, R.A. (2004). Manganese distribution across the blood-brain barrier III. The divalent metal transporter-1 is not the major mechanism mediating brain manganese uptake. Neurotoxicology *25*, 451-460.

Cui, T., Daniels, M., Wong, B.S., Li, R., Sy, M.S., Sassoon, J., and Brown, D.R. (2003). Mapping the functional domain of the prion protein. Eur J Biochem *270*, 3368-3376.

Cull-Candy, S., Brickley, S., and Farrant, M. (2001). NMDA receptor subunits: diversity, development and disease. Curr Opin Neurobiol *11*, 327-335.

Culotta, V.C., Klomp, L.W., Strain, J., Casareno, R.L., Krems, B., and Gitlin, J.D. (1997). The copper chaperone for superoxide dismutase. J Biol Chem *272*, 23469-23472.

D'Amelio, M., Cavallucci, V., and Cecconi, F. (2010). Neuronal caspase-3 signaling: not only cell death. Cell Death Differ *17*, 1104-1114.

Das, S., Sasaki, Y.F., Rothe, T., Premkumar, L.S., Takasu, M., Crandall, J.E., Dikkes, P., Conner, D.A., Rayudu, P.V., Cheung, W.*, et al.* (1998). Increased NMDA current and spine density in mice lacking the NMDA receptor subunit NR3A. Nature *393*, 377-381.

Davidsson, L., Cederblad, A., Lonnerdal, B., and Sandstrom, B. (1989). Manganese retention in man: a method for estimating manganese absorption in man. Am J Clin Nutr *49*, 170-179.

De Domenico, I., McVey Ward, D., and Kaplan, J. (2008). Regulation of iron acquisition and storage: consequences for iron-linked disorders. Nat Rev Mol Cell Biol *9*, 72-81.

Dening, T.R. (1991). The neuropsychiatry of Wilson's disease: a review. Int J Psychiatry Med *21*, 135-148.

Di Leva, F., Domi, T., Fedrizzi, L., Lim, D., and Carafoli, E. (2008). The plasma membrane Ca2+ ATPase of animal cells: structure, function and regulation. Arch Biochem Biophys *476*, 65-74.

Didonna, A., Sussman, J., Benetti, F., and Legname, G. (2012). The role of Bax and caspase-3 in doppel-induced apoptosis of cerebellar granule cells. Prion *6*, 309-316.

Dingledine, R., Borges, K., Bowie, D., and Traynelis, S.F. (1999). The glutamate receptor ion channels. Pharmacol Rev *51*, 7-61.

DiPolo, R. (1979). Calcium influx in internally dialyzed squid giant axons. J Gen Physiol *73*, 91-113.

Dong, Z., Saikumar, P., Weinberg, J.M., and Venkatachalam, M.A. (2006). Calcium in cell injury and death. Annu Rev Pathol *1*, 405-434.

Erikson, K.M., Syversen, T., Aschner, J.L., and Aschner, M. (2005). Interactions between excessive manganese exposures and dietary iron-deficiency in neurodegeneration. Environ Toxicol Pharmacol *19*, 415-421.

Faller, P., Hasler, D.W., Zerbe, O., Klauser, S., Winge, D.R., and Vasak, M. (1999). Evidence for a dynamic structure of human neuronal growth inhibitory factor and for major rearrangements of its metal-thiolate clusters. Biochemistry *38*, 10158-10167.

Farrant, M., Feldmeyer, D., Takahashi, T., and Cull-Candy, S.G. (1994). NMDA-receptor channel diversity in the developing cerebellum. Nature *368*, 335-339.

Fayyazuddin, A., Villarroel, A., Le Goff, A., Lerma, J., and Neyton, J. (2000). Four residues of the extracellular N-terminal domain of the NR2A subunit control high-affinity Zn2+ binding to NMDA receptors. Neuron *25*, 683-694.

Fischer, P.W., Giroux, A., and L'Abbe, M.R. (1981). The effect of dietary zinc on intestinal copper absorption. Am J Clin Nutr *34*, 1670-1675.

Fleming, R.E., and Gitlin, J.D. (1990). Primary structure of rat ceruloplasmin and analysis of tissue-specific gene expression during development. J Biol Chem *265*, 7701-7707.

Fournier, J.G., Escaig-Haye, F., Billette de Villemeur, T., Robain, O., Lasmezas, C.I., Deslys, J.P., Dormont, D., and Brown, P. (1998). Distribution and submicroscopic immunogold localization of cellular prion protein (PrPc) in extracerebral tissues. Cell Tissue Res *292*, 77-84.

Fournier, J.G., Escaig-Haye, F., and Grigoriev, V. (2000). Ultrastructural localization of prion proteins: physiological and pathological implications. Microsc Res Tech *50*, 76-88.

Frederickson, C.J., Koh, J.Y., and Bush, A.I. (2005). The neurobiology of zinc in health and disease. Nat Rev Neurosci *6*, 449-462.

Fridovich, I. (1974). Superoxide and evolution. Horiz Biochem Biophys *1*, 1-37.

Fridovich, I. (1995). Superoxide radical and superoxide dismutases. Annu Rev Biochem *64*, 97-112.

Fuhrmann, M., Bittner, T., Mitteregger, G., Haider, N., Moosmang, S., Kretzschmar, H., and Herms, J. (2006). Loss of the cellular prion protein affects the Ca2+ homeostasis in hippocampal CA1 neurons. J Neurochem *98*, 1876-1885.

Furukawa, Y., Torres, A.S., and O'Halloran, T.V. (2004). Oxygen-induced maturation of SOD1: a key role for disulfide formation by the copper chaperone CCS. EMBO J *23*, 2872-2881.

Gaggelli, E., Kozlowski, H., Valensin, D., and Valensin, G. (2006). Copper homeostasis and neurodegenerative disorders (Alzheimer's, prion, and Parkinson's diseases and amyotrophic lateral sclerosis). Chem Rev *106*, 1995-2044.

Gahwiler, B.H., Capogna, M., Debanne, D., McKinney, R.A., and Thompson, S.M. (1997). Organotypic slice cultures: a technique has come of age. Trends Neurosci *20*, 471-477.

Garcia, M.L., Murray, K.D., Garcia, V.B., Strehler, E.E., and Isackson, P.J. (1997). Seizure-induced alterations of plasma membrane calcium ATPase isoforms 1, 2 and 3 mRNA and protein in rat hippocampus. Brain Res Mol Brain Res *45*, 230-238.

Gasset, M., Baldwin, M.A., Fletterick, R.J., and Prusiner, S.B. (1993). Perturbation of the secondary structure of the scrapie prion protein under conditions that alter infectivity. Proc Natl Acad Sci U S A *90*, 1-5.

Gibbons, R.A., Dixon, S.N., Hallis, K., Russell, A.M., Sansom, B.F., and Symonds, H.W. (1976). Manganese metabolism in cows and goats. Biochim Biophys Acta *444*, 1-10.

Giese, A., Buchholz, M., Herms, J., and Kretzschmar, H.A. (2005). Mouse brain synaptosomes accumulate copper-67 efficiently by two distinct processes independent of cellular prion protein. J Mol Neurosci *27*, 347-354.

Gitlin, J.D. (2003). Wilson disease. Gastroenterology *125*, 1868-1877.

Giustarini, D., Dalle-Donne, I., Colombo, R., Milzani, A., and Rossi, R. (2008). Is ascorbate able to reduce disulfide bridges? A cautionary note. Nitric Oxide *19*, 252-258.

Goldstein, I.M., Kaplan, H.B., Edelson, H.S., and Weissmann, G. (1979a). Ceruloplasmin. A scavenger of superoxide anion radicals. J Biol Chem *254*, 4040-4045.

Goldstein, I.M., Kaplan, H.B., Edelson, H.S., and Weissmann, G. (1979b). A new function for ceruloplasmin as an acute-phase reactant in inflammation: a scavenger of superoxide anion radicals. Trans Assoc Am Physicians *92*, 360-369.

Gu, Z., Nakamura, T., and Lipton, S.A. (2010). Redox reactions induced by nitrosative stress mediate protein misfolding and mitochondrial dysfunction in neurodegenerative diseases. Mol Neurobiol *41*, 55-72.

Gupta, A., and Lutsenko, S. (2009). Human copper transporters: mechanism, role in human diseases and therapeutic potential. Future Med Chem *1*, 1125-1142.

Haeberle, A.M., Ribaut-Barassin, C., Bombarde, G., Mariani, J., Hunsmann, G., Grassi, J., and Bailly, Y. (2000). Synaptic prion protein immuno-reactivity in the rodent cerebellum. Microsc Res Tech *50*, 66-75.

Haraguchi, T., Fisher, S., Olofsson, S., Endo, T., Groth, D., Tarentino, A., Borchelt, D.R., Teplow, D., Hood, L., Burlingame, A.*, et al.* (1989). Asparagine-linked glycosylation of the scrapie and cellular prion proteins. Arch Biochem Biophys *274*, 1-13.

Hardingham, G.E., and Bading, H. (2003). The Yin and Yang of NMDA receptor signalling. Trends Neurosci *26*, 81-89.

Hardingham, G.E., Fukunaga, Y., and Bading, H. (2002). Extrasynaptic NMDARs oppose synaptic NMDARs by triggering CREB shut-off and cell death pathways. Nat Neurosci *5*, 405-414.

Hardy, P.A., Gash, D., Yokel, R., Andersen, A., Ai, Y., and Zhang, Z. (2005). Correlation of R2 with total iron concentration in the brains of rhesus monkeys. J Magn Reson Imaging *21*, 118-127.

Harris, A.Z., and Pettit, D.L. (2008). Recruiting extrasynaptic NMDA receptors augments synaptic signaling. J Neurophysiol *99*, 524-533.

Harris, Z.L., and Gitlin, J.D. (1996). Genetic and molecular basis for copper toxicity. Am J Clin Nutr *63*, 836S-841S.

Harris, Z.L., Takahashi, Y., Miyajima, H., Serizawa, M., MacGillivray, R.T., and Gitlin, J.D. (1995). Aceruloplasminemia: molecular characterization of this disorder of iron metabolism. Proc Natl Acad Sci U S A *92*, 2539-2543.

Hartter, D.E., and Barnea, A. (1988). Evidence for release of copper in the brain: depolarization-induced release of newly taken-up 67copper. Synapse *2*, 412-415.

Hellman, N.E., Kono, S., Mancini, G.M., Hoogeboom, A.J., De Jong, G.J., and Gitlin, J.D. (2002). Mechanisms of copper incorporation into human ceruloplasmin. J Biol Chem *277*, 46632-46638.

Hentze, M.W., Muckenthaler, M.U., and Andrews, N.C. (2004). Balancing acts: molecular control of mammalian iron metabolism. Cell *117*, 285-297.

Herms, J., Tings, T., Gall, S., Madlung, A., Giese, A., Siebert, H., Schurmann, P., Windl, O., Brose, N., and Kretzschmar, H. (1999). Evidence of presynaptic location and function of the prion protein. J Neurosci *19*, 8866-8875.

Herms, J.W., Tings, T., Dunker, S., and Kretzschmar, H.A. (2001). Prion protein affects Ca2+-activated K+ currents in cerebellar purkinje cells. Neurobiol Dis *8*, 324-330.

Hidalgo, J., Aschner, M., Zatta, P., and Vasak, M. (2001). Roles of the metallothionein family of proteins in the central nervous system. Brain Res Bull *55*, 133-145.

Horiuchi, M., Yamazaki, N., Ikeda, T., Ishiguro, N., and Shinagawa, M. (1995). A cellular form of prion protein (PrPC) exists in many non-neuronal tissues of sheep. J Gen Virol *76 (Pt 10)*, 2583-2587.

Hornshaw, M.P., McDermott, J.R., Candy, J.M., and Lakey, J.H. (1995). Copper binding to the N-terminal tandem repeat region of mammalian and avian prion protein: structural studies using synthetic peptides. Biochem Biophys Res Commun *214*, 993-999.

Howell, G.A., Welch, M.G., and Frederickson, C.J. (1984). Stimulation-induced uptake and release of zinc in hippocampal slices. Nature *308*, 736-738.

Hower, V., Mendes, P., Torti, F.M., Laubenbacher, R., Akman, S., Shulaev, V., and Torti, S.V. (2009). A general map of iron metabolism and tissue-specific subnetworks. Mol Biosyst *5*, 422-443.

Jackson, G.S. (2001). Spontaneous conformational change within the prion protein--implications for disease pathogenesis? Bioessays *23*, 772-774.

Jackson, G.S., Murray, I., Hosszu, L.L., Gibbs, N., Waltho, J.P., Clarke, A.R., and Collinge, J. (2001). Location and properties of metal-binding sites on the human prion protein. Proc Natl Acad Sci U S A *98*, 8531-8535.

Jaffrey, S.R., and Snyder, S.H. (2001). The biotin switch method for the detection of S-nitrosylated proteins. Sci STKE *2001*, pl1.

James, P., Vorherr, T., Krebs, J., Morelli, A., Castello, G., McCormick, D.J., Penniston, J.T., De Flora, A., and Carafoli, E. (1989). Modulation of erythrocyte Ca2+-ATPase by selective calpain cleavage of the calmodulin-binding domain. J Biol Chem *264*, 8289-8296.

Jeong, S.Y., and David, S. (2003). Glycosylphosphatidylinositol-anchored ceruloplasmin is required for iron efflux from cells in the central nervous system. J Biol Chem *278*, 27144-27148.

Jones, C.E., Abdelraheim, S.R., Brown, D.R., and Viles, J.H. (2004). Preferential Cu2+ coordination by His96 and His111 induces beta-sheet formation in the unstructured amyloidogenic region of the prion protein. J Biol Chem *279*, 32018-32027.

Kambe, T., Weaver, B.P., and Andrews, G.K. (2008). The genetics of essential metal homeostasis during development. Genesis *46*, 214-228.

Kanaani, J., Prusiner, S.B., Diacovo, J., Baekkeskov, S., and Legname, G. (2005). Recombinant prion protein induces rapid polarization and development of synapses in embryonic rat hippocampal neurons in vitro. J Neurochem *95*, 1373-1386.

Kardos, J., Kovacs, I., Hajos, F., Kalman, M., and Simonyi, M. (1989). Nerve endings from rat brain tissue release copper upon depolarization. A possible role in regulating neuronal excitability. Neurosci Lett *103*, 139-144.

Keele, N.B., Zinebi, F., Neugebauer, V., and Shinnick-Gallagher, P. (2000). Epileptogenesis up-regulates metabotropic glutamate receptor activation of sodium-calcium exchange current in the amygdala. J Neurophysiol *83*, 2458-2462.

Kenward, A.G., Bartolotti, L.J., and Burns, C.S. (2007). Copper and zinc promote interactions between membrane-anchored peptides of the metal binding domain of the prion protein. Biochemistry *46*, 4261-4271.

Khosravani, H., Zhang, Y., Tsutsui, S., Hameed, S., Altier, C., Hamid, J., Chen, L., Villemaire, M., Ali, Z., Jirik, F.R.*, et al.* (2008a). Prion protein attenuates excitotoxicity by inhibiting NMDA receptors. J Gen Physiol *131*, i5.

Khosravani, H., Zhang, Y., Tsutsui, S., Hameed, S., Altier, C., Hamid, J., Chen, L., Villemaire, M., Ali, Z., Jirik, F.R.*, et al.* (2008b). Prion protein attenuates excitotoxicity by inhibiting NMDA receptors. J Cell Biol *181*, 551-565.

King, J.C. (2011). Zinc: an essential but elusive nutrient. Am J Clin Nutr *94*, 679S-684S.

Klomp, L.W., and Gitlin, J.D. (1996). Expression of the ceruloplasmin gene in the human retina and brain: implications for a pathogenic model in aceruloplasminemia. Hum Mol Genet *5*, 1989-1996.

Knutson, M.D. (2007). Steap proteins: implications for iron and copper metabolism. Nutr Rev *65*, 335-340.

Kono, S., and Miyajima, H. (2006). Molecular and pathological basis of aceruloplasminemia. Biol Res *39*, 15-23.

Kralovicova, S., Fontaine, S.N., Alderton, A., Alderman, J., Ragnarsdottir, K.V., Collins, S.J., and Brown, D.R. (2009). The effects of prion protein expression on metal metabolism. Mol Cell Neurosci *41*, 135-147.

Kramer, M.L., Kratzin, H.D., Schmidt, B., Romer, A., Windl, O., Liemann, S., Hornemann, S., and Kretzschmar, H. (2001). Prion protein binds copper within the physiological concentration range. J Biol Chem *276*, 16711-16719.

Krebs, B., Wiebelitz, A., Balitzki-Korte, B., Vassallo, N., Paluch, S., Mitteregger, G., Onodera, T., Kretzschmar, H.A., and Herms, J. (2007). Cellular prion protein modulates the intracellular calcium response to hydrogen peroxide. J Neurochem *100*, 358-367.

Kristensen, B.W., Noraberg, J., and Zimmer, J. (2001). Comparison of excitotoxic profiles of ATPA, AMPA, KA and NMDA in organotypic hippocampal slice cultures. Brain Res *917*, 21-44.

Kuo, Y.M., Gybina, A.A., Pyatskowit, J.W., Gitschier, J., and Prohaska, J.R. (2006). Copper transport protein (Ctr1) levels in mice are tissue specific and dependent on copper status. J Nutr *136*, 21-26.

L'Abbe, M.R., and Fischer, P.W. (1984). The effects of high dietary zinc and copper deficiency on the activity of copper-requiring metalloenzymes in the growing rat. J Nutr *114*, 813-822.

Lazarini, F., Deslys, J.P., and Dormont, D. (1991). Regulation of the glial fibrillary acidic protein, beta actin and prion protein mRNAs during brain development in mouse. Brain Res Mol Brain Res *10*, 343-346.

Lazzari, C., Peggion, C., Stella, R., Massimino, M.L., Lim, D., Bertoli, A., and Sorgato, M.C. (2011). Cellular prion protein is implicated in the regulation of local Ca2+ movements in cerebellar granule neurons. J Neurochem *116*, 881-890.

Lee, J.Y., Kim, J.H., Palmiter, R.D., and Koh, J.Y. (2003). Zinc released from metallothionein-iii may contribute to hippocampal CA1 and thalamic neuronal death following acute brain injury. Exp Neurol *184*, 337-347.

Levy, J.E., Jin, O., Fujiwara, Y., Kuo, F., and Andrews, N.C. (1999). Transferrin receptor is necessary for development of erythrocytes and the nervous system. Nat Genet *21*, 396-399.

Li, A., Christensen, H.M., Stewart, L.R., Roth, K.A., Chiesa, R., and Harris, D.A. (2007). Neonatal lethality in transgenic mice expressing prion protein with a deletion of residues 105-125. EMBO J *26*, 548-558.

Linden, R., Martins, V.R., Prado, M.A., Cammarota, M., Izquierdo, I., and Brentani, R.R. (2008). Physiology of the prion protein. Physiol Rev *88*, 673-728.

Lipton, S.A., Choi, Y.B., Takahashi, H., Zhang, D., Li, W., Godzik, A., and Bankston, L.A. (2002). Cysteine regulation of protein function--as exemplified by NMDA-receptor modulation. Trends Neurosci *25*, 474-480.

Lipton, S.A., and Rosenberg, P.A. (1994). Excitatory amino acids as a final common pathway for neurologic disorders. N Engl J Med *330*, 613-622.

Liu, L., Jiang, D., McDonald, A., Hao, Y., Millhauser, G.L., and Zhou, F. (2011). Copper redox cycling in the prion protein depends critically on binding mode. J Am Chem Soc *133*, 12229-12237.

Livak, K.J., and Schmittgen, T.D. (2001). Analysis of relative gene expression data using real-time quantitative PCR and the 2(-Delta Delta C(T)) Method. Methods *25*, 402-408.

Lledo, P.M., Tremblay, P., DeArmond, S.J., Prusiner, S.B., and Nicoll, R.A. (1996). Mice deficient for prion protein exhibit normal neuronal excitability and synaptic transmission in the hippocampus. Proc Natl Acad Sci U S A *93*, 2403-2407.

Loftis, J.M., and Janowsky, A. (2003). The N-methyl-D-aspartate receptor subunit NR2B: localization, functional properties, regulation, and clinical implications. Pharmacol Ther *97*, 55-85.

Lovell, M.A. (2009). A potential role for alterations of zinc and zinc transport proteins in the progression of Alzheimer's disease. J Alzheimers Dis *16*, 471-483.

Low, C.M., Zheng, F., Lyuboslavsky, P., and Traynelis, S.F. (2000). Molecular determinants of coordinated proton and zinc inhibition of N-methyl-D-aspartate NR1/NR2A receptors. Proc Natl Acad Sci U S A *97*, 11062-11067.

Lutsenko, S., LeShane, E.S., and Shinde, U. (2007). Biochemical basis of regulation of human copper-transporting ATPases. Arch Biochem Biophys *463*, 134-148.

Madsen, E., and Gitlin, J.D. (2007). Copper and iron disorders of the brain. Annu Rev Neurosci *30*, 317-337.

Maglio, L.E., Perez, M.F., Martins, V.R., Brentani, R.R., and Ramirez, O.A. (2004). Hippocampal synaptic plasticity in mice devoid of cellular prion protein. Brain Res Mol Brain Res *131*, 58-64.

Mallucci, G., Dickinson, A., Linehan, J., Klohn, P.C., Brandner, S., and Collinge, J. (2003). Depleting neuronal PrP in prion infection prevents disease and reverses spongiosis. Science *302*, 871-874.

Mallucci, G.R., Ratte, S., Asante, E.A., Linehan, J., Gowland, I., Jefferys, J.G., and Collinge, J. (2002). Post-natal knockout of prion protein alters hippocampal CA1 properties, but does not result in neurodegeneration. EMBO J *21*, 202-210.

Mani, L., Cheng, F., Havsmark, B., Jonsson, M., Belting, M., and Fransson, L. (2003). Prion, Amyloid - derived Cu(II) Ions, or Free Zn(II) Ions Support S-Nitroso-dependent Autocleavage of Glypican-1 Heparan Sulfate. J Biol Chem *278*, 38956-38965.

Manson, J., West, J.D., Thomson, V., McBride, P., Kaufman, M.H., and Hope, J. (1992). The prion protein gene: a role in mouse embryogenesis? Development *115*, 117-122.

Manson, J.C., Clarke, A.R., Hooper, M.L., Aitchison, L., McConnell, I., and Hope, J. (1994). 129/Ola mice carrying a null mutation in PrP that abolishes mRNA production are developmentally normal. Mol Neurobiol *8*, 121-127.

Manson, J.C., Hope, J., Clarke, A.R., Johnston, A., Black, C., and MacLeod, N. (1995). PrP gene dosage and long term potentiation. Neurodegeneration *4*, 113-114.

Mantovan, M.C., Martinuzzi, A., Squarzanti, F., Bolla, A., Silvestri, I., Liessi, G., Macchi, C., Ruzza, G., Trevisan, C.P., and Angelini, C. (2006). Exploring mental status in Friedreich's ataxia: a combined neuropsychological, behavioral and neuroimaging study. Eur J Neurol *13*, 827-835.

Maret, W. (1994). Oxidative metal release from metallothionein via zinc-thiol/disulfide interchange. Proc Natl Acad Sci U S A *91*, 237-241.

Maret, W. (2000). The function of zinc metallothionein: a link between cellular zinc and redox state. J Nutr *130*, 1455S-1458S.

McCord, J.M., and Fridovich, I. (1969). The utility of superoxide dismutase in studying free radical reactions. I. Radicals generated by the interaction of sulfite, dimethyl sulfoxide, and oxygen. J Biol Chem *244*, 6056-6063.

McLennan, N.F., Brennan, P.M., McNeill, A., Davies, I., Fotheringham, A., Rennison, K.A., Ritchie, D., Brannan, F., Head, M.W., Ironside, J.W.*, et al.* (2004). Prion protein accumulation and neuroprotection in hypoxic brain damage. Am J Pathol *165*, 227-235.

Mercer, J.F., Livingston, J., Hall, B., Paynter, J.A., Begy, C., Chandrasekharappa, S., Lockhart, P., Grimes, A., Bhave, M., Siemieniak, D.*, et al.* (1993). Isolation of a partial candidate gene for Menkes disease by positional cloning. Nat Genet *3*, 20-25.

Miriyala, S., Spasojevic, I., Tovmasyan, A., Salvemini, D., Vujaskovic, Z., St Clair, D., and Batinic-Haberle, I. (2012). Manganese superoxide dismutase, MnSOD and its mimics. Biochim Biophys Acta *1822*, 794-814.

Mitsios, N., Saka, M., Krupinski, J., Pennucci, R., Sanfeliu, C., Miguel Turu, M., Gaffney, J., Kumar, P., Kumar, S., Sullivan, M.*, et al.* (2007). Cellular prion protein is increased in the plasma and peri-infarcted brain tissue after acute stroke. J Neurosci Res *85*, 602-611.

Mittal, B., Doroudchi, M.M., Jeong, S.Y., Patel, B.N., and David, S. (2003). Expression of a membrane-bound form of the ferroxidase ceruloplasmin by leptomeningeal cells. Glia *41*, 337-346.

Miura, T., Sasaki, S., Toyama, A., and Takeuchi, H. (2005). Copper reduction by the octapeptide repeat region of prion protein: pH dependence and implications in cellular copper uptake. Biochemistry *44*, 8712-8720.

Mobley, W.C., Neve, R.L., Prusiner, S.B., and McKinley, M.P. (1988). Nerve growth factor increases mRNA levels for the prion protein and the beta-amyloid protein precursor in developing hamster brain. Proc Natl Acad Sci U S A *85*, 9811-9815.

Momiyama, A., Feldmeyer, D., and Cull-Candy, S.G. (1996). Identification of a native low-conductance NMDA channel with reduced sensitivity to Mg2+ in rat central neurones. J Physiol *494 (Pt 2)*, 479-492.

Monyer, H., Burnashev, N., Laurie, D.J., Sakmann, B., and Seeburg, P.H. (1994). Developmental and regional expression in the rat brain and functional properties of four NMDA receptors. Neuron *12*, 529-540.

Moore, R.C., Lee, I.Y., Silverman, G.L., Harrison, P.M., Strome, R., Heinrich, C., Karunaratne, A., Pasternak, S.H., Chishti, M.A., Liang, Y.*, et al.* (1999). Ataxia in prion protein (PrP)-deficient mice is associated with upregulation of the novel PrP-like protein doppel. J Mol Biol *292*, 797-817.

Moriyoshi, K., Masu, M., Ishii, T., Shigemoto, R., Mizuno, N., and Nakanishi, S. (1991). Molecular cloning and characterization of the rat NMDA receptor. Nature *354*, 31-37.

Moya, K.L., Sales, N., Hassig, R., Creminon, C., Grassi, J., and Di Giamberardino, L. (2000). Immunolocalization of the cellular prion protein in normal brain. Microsc Res Tech *50*, 58-65.

Nakamura, T., and Lipton, S.A. (2011). Redox modulation by S-nitrosylation contributes to protein misfolding, mitochondrial dynamics, and neuronal synaptic damage in neurodegenerative diseases. Cell Death Differ *18*, 1478-1486.

Naslavsky, N., Stein, R., Yanai, A., Friedlander, G., and Taraboulos, A. (1997). Characterization of detergent-insoluble complexes containing the cellular prion protein and its scrapie isoform. J Biol Chem *272*, 6324-6331.

Nishida, N., Tremblay, P., Sugimoto, T., Shigematsu, K., Shirabe, S., Petromilli, C., Erpel, S.P., Nakaoke, R., Atarashi, R., Houtani, T.*, et al.* (1999). A mouse prion protein transgene rescues mice deficient for the prion protein gene from purkinje cell degeneration and demyelination. Lab Invest *79*, 689-697.

Nishihara, E., Furuyama, T., Yamashita, S., and Mori, N. (1998). Expression of copper trafficking genes in the mouse brain. Neuroreport *9*, 3259-3263.

Nose, Y., Kim, B.E., and Thiele, D.J. (2006). Ctr1 drives intestinal copper absorption and is essential for growth, iron metabolism, and neonatal cardiac function. Cell Metab *4*, 235-244.

Oder, W., Grimm, G., Kollegger, H., Ferenci, P., Schneider, B., and Deecke, L. (1991). Neurological and neuropsychiatric spectrum of Wilson's disease: a prospective study of 45 cases. J Neurol *238*, 281-287.

Oesch, B., Westaway, D., Walchli, M., McKinley, M.P., Kent, S.B., Aebersold, R., Barry, R.A., Tempst, P., Teplow, D.B., Hood, L.E.*, et al.* (1985). A cellular gene encodes scrapie PrP 27-30 protein. Cell *40*, 735-746.

Ohgami, R.S., Campagna, D.R., McDonald, A., and Fleming, M.D. (2006). The Steap proteins are metalloreductases. Blood *108*, 1388-1394.

Palmiter, R.D., Cole, T.B., Quaife, C.J., and Findley, S.D. (1996). ZnT-3, a putative transporter of zinc into synaptic vesicles. Proc Natl Acad Sci U S A *93*, 14934-14939.

Paoletti, P., Perin-Dureau, F., Fayyazuddin, A., Le Goff, A., Callebaut, I., and Neyton, J. (2000). Molecular organization of a zinc binding n-terminal modulatory domain in a NMDA receptor subunit. Neuron *28*, 911-925.

Parsons, J.T., Churn, S.B., Kochan, L.D., and DeLorenzo, R.J. (2000). Pilocarpine-induced status epilepticus causes N-methyl-D-aspartate receptor-dependent inhibition of microsomal Mg(2+)/Ca(2+) ATPase-mediated Ca(2+) uptake. J Neurochem *75*, 1209-1218.

Patel, B.N., and David, S. (1997). A novel glycosylphosphatidylinositol-anchored form of ceruloplasmin is expressed by mammalian astrocytes. J Biol Chem *272*, 20185-20190.

Pauly, P.C., and Harris, D.A. (1998). Copper stimulates endocytosis of the prion protein. J Biol Chem *273*, 33107-33110.

Pedersen, P., and Carafoli, E. (1987). Ion motive ATPases. Ubiquity, properties, and significance to cell function. Trends Biochem Sci *12*, 146-150.

Perez-Otano, I., Schulteis, C.T., Contractor, A., Lipton, S.A., Trimmer, J.S., Sucher, N.J., and Heinemann, S.F. (2001). Assembly with the NR1 subunit is required for surface expression of NR3A-containing NMDA receptors. J Neurosci *21*, 1228-1237.

Ponka, P. (1999). Cellular iron metabolism. Kidney Int Suppl *69*, S2-11.

Prestori, F., Rossi, P., Bearzatto, B., Laine, J., Necchi, D., Diwakar, S., Schiffmann, S.N., Axelrad, H., and D'Angelo, E. (2008). Altered neuron excitability and synaptic plasticity in the cerebellar granular layer of juvenile prion protein knock-out mice with impaired motor control. J Neurosci *28*, 7091-7103.

Prusiner, S.B. (1982). Novel proteinaceous infectious particles cause scrapie. Science *216*, 136-144.

Prusiner, S.B. (1991). Molecular biology of prion diseases. Science *252*, 1515-1522.

Prusiner, S.B. (1992). Natural and experimental prion diseases of humans and animals. Curr Opin Neurobiol *2*, 638-647.

Prusiner, S.B. (1994). Biology and genetics of prion diseases. Annu Rev Microbiol *48*, 655-686.

Prusiner, S.B. (2001). Shattuck lecture--neurodegenerative diseases and prions. N Engl J Med *344*, 1516-1526.

Prusiner, S.B., and DeArmond, S.J. (1994). Prion diseases and neurodegeneration. Annu Rev Neurosci *17*, 311-339.

Qian, Z.M., and Wang, Q. (1998). Expression of iron transport proteins and excessive iron accumulation in the brain in neurodegenerative disorders. Brain Res Brain Res Rev *27*, 257-267.

Qin, K., Yang, Y., Mastrangelo, P., and Westaway, D. (2002). Mapping Cu(II) binding sites in prion proteins by diethyl pyrocarbonate modification and matrix-assisted laser desorption ionization-time of flight (MALDI-TOF) mass spectrometric footprinting. J Biol Chem *277*, 1981-1990.

Quaglio, E., Chiesa, R., and Harris, D.A. (2001). Copper converts the cellular prion protein into a protease-resistant species that is distinct from the scrapie isoform. J Biol Chem *276*, 11432-11438.

Rabin, O., Hegedus, L., Bourre, J.M., and Smith, Q.R. (1993). Rapid brain uptake of manganese(II) across the blood-brain barrier. J Neurochem *61*, 509-517.

Rachidi, W., Chimienti, F., Aouffen, M., Senator, A., Guiraud, P., Seve, M., and Favier, A. (2009). Prion protein protects against zinc-mediated cytotoxicity by modifying intracellular exchangeable zinc and inducing metallothionein expression. J Trace Elem Med Biol *23*, 214-223.

Rachidi, W., Vilette, D., Guiraud, P., Arlotto, M., Riondel, J., Laude, H., Lehmann, S., and Favier, A. (2003). Expression of prion protein increases cellular copper binding and antioxidant enzyme activities but not copper delivery. J Biol Chem *278*, 9064-9072.

Radovanovic, I., Braun, N., Giger, O.T., Mertz, K., Miele, G., Prinz, M., Navarro, B., and Aguzzi, A. (2005). Truncated prion protein and Doppel are myelinotoxic in the absence of oligodendrocytic PrPC. J Neurosci *25*, 4879-4888.

Rangel, A., Burgaya, F., Gavin, R., Soriano, E., Aguzzi, A., and Del Rio, J.A. (2007). Enhanced susceptibility of Prnp-deficient mice to kainate-induced seizures, neuronal apoptosis, and death: Role of AMPA/kainate receptors. J Neurosci Res *85*, 2741-2755.

Religa, D., Strozyk, D., Cherny, R.A., Volitakis, I., Haroutunian, V., Winblad, B., Naslund, J., and Bush, A.I. (2006). Elevated cortical zinc in Alzheimer disease. Neurology *67*, 69-75.

Rodolfo, K., Hassig, R., Moya, K.L., Frobert, Y., Grassi, J., and Di Giamberardino, L. (1999). A novel cellular prion protein isoform present in rapid anterograde axonal transport. Neuroreport *10*, 3639-3644.

Rolfs, A., Kvietikova, I., Gassmann, M., and Wenger, R.H. (1997). Oxygen-regulated transferrin expression is mediated by hypoxia-inducible factor-1. J Biol Chem *272*, 20055-20062.

Rossander-Hulten, L., Brune, M., Sandstrom, B., Lonnerdal, B., and Hallberg, L. (1991). Competitive inhibition of iron absorption by manganese and zinc in humans. Am J Clin Nutr *54*, 152-156.

Rossi, D., Cozzio, A., Flechsig, E., Klein, M.A., Rulicke, T., Aguzzi, A., and Weissmann, C. (2001). Onset of ataxia and Purkinje cell loss in PrP null mice inversely correlated with Dpl level in brain. EMBO J *20*, 694-702.

Rumbaugh, G., Prybylowski, K., Wang, J.F., and Vicini, S. (2000). Exon 5 and spermine regulate deactivation of NMDA receptor subtypes. J Neurophysiol *83*, 1300-1306.

Sakaguchi, S., Katamine, S., Nishida, N., Moriuchi, R., Shigematsu, K., Sugimoto, T., Nakatani, A., Kataoka, Y., Houtani, T., Shirabe, S.*, et al.* (1996). Loss of cerebellar Purkinje cells in aged mice homozygous for a disrupted PrP gene. Nature *380*, 528-531.

Sales, N., Hassig, R., Rodolfo, K., Di Giamberardino, L., Traiffort, E., Ruat, M., Fretier, P., and Moya, K.L. (2002). Developmental expression of the cellular prion protein in elongating axons. Eur J Neurosci *15*, 1163-1177.

Sales, N., Rodolfo, K., Hassig, R., Faucheux, B., Di Giamberardino, L., and Moya, K.L. (1998). Cellular prion protein localization in rodent and primate brain. Eur J Neurosci *10*, 2464-2471.

Schlief, M.L., Craig, A.M., and Gitlin, J.D. (2005). NMDA receptor activation mediates copper homeostasis in hippocampal neurons. J Neurosci *25*, 239-246.

Schlief, M.L., and Gitlin, J.D. (2006). Copper homeostasis in the CNS: a novel link between the NMDA receptor and copper homeostasis in the hippocampus. Mol Neurobiol *33*, 81-90.

Schlief, M.L., West, T., Craig, A.M., Holtzman, D.M., and Gitlin, J.D. (2006). Role of the Menkes copper-transporting ATPase in NMDA receptor-mediated neuronal toxicity. Proc Natl Acad Sci U S A *103*, 14919-14924.

Schosinsky, K.H., Lehmann, H.P., and Beeler, M.F. (1974). Measurement of ceruloplasmin from its oxidase activity in serum by use of o-dianisidine dihydrochloride. Clin Chem *20*, 1556-1563.

Sebastiao, A.M., Colino-Oliveira, M., Assaife-Lopes, N., Dias, R.B., and Ribeiro, J.A. (2013). Lipid rafts, synaptic transmission and plasticity: Impact in age-related neurodegenerative diseases. Neuropharmacology *64*, 97-107.

Shmerling, D., Hegyi, I., Fischer, M., Blattler, T., Brandner, S., Gotz, J., Rulicke, T., Flechsig, E., Cozzio, A., von Mering, C.*, et al.* (1998). Expression of amino-terminally truncated PrP in the mouse leading to ataxia and specific cerebellar lesions. Cell *93*, 203-214.

Shyu, W.C., Chen, C.P., Saeki, K., Kubosaki, A., Matusmoto, Y., Onodera, T., Ding, D.C., Chiang, M.F., Lee, Y.J., Lin, S.Z.*, et al.* (2005). Hypoglycemia enhances the expression of prion protein and heat-shock protein 70 in a mouse neuroblastoma cell line. J Neurosci Res *80*, 887-894.

Shyu, W.C., Kao, M.C., Chou, W.Y., Hsu, Y.D., and Soong, B.W. (2000). Heat shock modulates prion protein expression in human NT-2 cells. Neuroreport *11*, 771-774.

Shyu, W.C., Lin, S.Z., Saeki, K., Kubosaki, A., Matsumoto, Y., Onodera, T., Chiang, M.F., Thajeb, P., and Li, H. (2004). Hyperbaric oxygen enhances the expression of prion protein and heat shock protein 70 in a mouse neuroblastoma cell line. Cell Mol Neurobiol *24*, 257-268.

Simons, K., and Ikonen, E. (1997). Functional rafts in cell membranes. Nature *387*, 569-572.

Singh, A., Isaac, A.O., Luo, X., Mohan, M.L., Cohen, M.L., Chen, F., Kong, Q., Bartz, J., and Singh, N. (2009a). Abnormal brain iron homeostasis in human and animal prion disorders. PLoS Pathog *5*, e1000336.

Singh, A., Kong, Q., Luo, X., Petersen, R.B., Meyerson, H., and Singh, N. (2009b). Prion protein (PrP) knock-out mice show altered iron metabolism: a functional role for PrP in iron uptake and transport. PLoS One *4*, e6115.

Singh, A., Mohan, M.L., Isaac, A.O., Luo, X., Petrak, J., Vyoral, D., and Singh, N. (2009c). Prion protein modulates cellular iron uptake: a novel function with implications for prion disease pathogenesis. PLoS One *4*, e4468.

Singh, N., Das, D., Singh, A., and Mohan, M.L. (2010). Prion protein and metal interaction: physiological and pathological implications. Curr Issues Mol Biol *12*, 99-107.

Skripuletz, T., Lindner, M., Kotsiari, A., Garde, N., Fokuhl, J., Linsmeier, F., Trebst, C., and Stangel, M. (2008). Cortical demyelination is prominent in the murine cuprizone model and is strain-dependent. Am J Pathol *172*, 1053-1061.

Solomon, I.H., Huettner, J.E., and Harris, D.A. (2010). Neurotoxic mutants of the prion protein induce spontaneous ionic currents in cultured cells. J Biol Chem *285*, 26719-26726.

Solomon, I.H., Khatri, N., Biasini, E., Massignan, T., Huettner, J.E., and Harris, D.A. (2011). An N-terminal polybasic domain and cell surface localization are required for mutant prion protein toxicity. J Biol Chem *286*, 14724-14736.

Spudich, A., Frigg, R., Kilic, E., Kilic, U., Oesch, B., Raeber, A., Bassetti, C.L., and Hermann, D.M. (2005). Aggravation of ischemic brain injury by prion protein deficiency: role of ERK-1/-2 and STAT-1. Neurobiol Dis *20*, 442-449.

Stahl, N., Borchelt, D.R., and Prusiner, S.B. (1990). Differential release of cellular and scrapie prion proteins from cellular membranes by phosphatidylinositol-specific phospholipase C. Biochemistry *29*, 5405-5412.

Steele, A.D., Lindquist, S., and Aguzzi, A. (2007). The prion protein knockout mouse: a phenotype under challenge. Prion *1*, 83-93.

Stockel, J., Safar, J., Wallace, A.C., Cohen, F.E., and Prusiner, S.B. (1998). Prion protein selectively binds copper(II) ions. Biochemistry *37*, 7185-7193.

Stohr, J., Watts, J.C., Legname, G., Oehler, A., Lemus, A., Nguyen, H.O., Sussman, J., Wille, H., DeArmond, S.J., Prusiner, S.B.*, et al.* (2011). Spontaneous generation of anchorless prions in transgenic mice. Proc Natl Acad Sci U S A *108*, 21223-21228.

Sugihara, H., Moriyoshi, K., Ishii, T., Masu, M., and Nakanishi, S. (1992). Structures and properties of seven isoforms of the NMDA receptor generated by alternative splicing. Biochem Biophys Res Commun *185*, 826-832.

Suh, J.H., Moreau, R., Heath, S.H., and Hagen, T.M. (2005). Dietary supplementation with (R)-alpha-lipoic acid reverses the age-related accumulation of iron and depletion of antioxidants in the rat cerebral cortex. Redox Rep *10*, 52-60.

Takeda, A., Hanajima, T., Ijiro, H., Ishige, A., Iizuka, S., Okada, S., and Oku, N. (1999). Release of zinc from the brain of El (epilepsy) mice during seizure induction. Brain Res *828*, 174-178.

Tao, T.Y., Liu, F., Klomp, L., Wijmenga, C., and Gitlin, J.D. (2003). The copper toxicosis gene product Murr1 directly interacts with the Wilson disease protein. J Biol Chem *278*, 41593-41596.

Tapiero, H., and Tew, K.D. (2003). Trace elements in human physiology and pathology: zinc and metallothioneins. Biomed Pharmacother *57*, 399-411.

Todorich, B., Zhang, X., and Connor, J.R. (2011). H-ferritin is the major source of iron for oligodendrocytes. Glia *59*, 927-935.

Treiber, C., Pipkorn, R., Weise, C., Holland, G., and Multhaup, G. (2007). Copper is required for prion protein-associated superoxide dismutase-I activity in Pichia pastoris. FEBS J *274*, 1304-1311.

Tsenkova, R.N., Iordanova, I.K., Toyoda, K., and Brown, D.R. (2004). Prion protein fate governed by metal binding. Biochem Biophys Res Commun *325*, 1005-1012.

Tsunoo, H., and Sussman, H.H. (1983). Placental transferrin receptor. Evaluation of the presence of endogenous ligand on specific binding. J Biol Chem *258*, 4118-4122.

Vassallo, N., and Herms, J. (2003). Cellular prion protein function in copper homeostasis and redox signalling at the synapse. J Neurochem *86*, 538-544.

Vassiliev, V., Harris, Z.L., and Zatta, P. (2005). Ceruloplasmin in neurodegenerative diseases. Brain Res Brain Res Rev *49*, 633-640.

Vicini, S., Wang, J.F., Li, J.H., Zhu, W.J., Wang, Y.H., Luo, J.H., Wolfe, B.B., and Grayson, D.R. (1998). Functional and pharmacological differences between recombinant N-methyl-D-aspartate receptors. J Neurophysiol *79*, 555-566.

Vlachova, V., Zemkova, H., and Vyklicky, L., Jr. (1996). Copper modulation of NMDA responses in mouse and rat cultured hippocampal neurons. Eur J Neurosci *8*, 2257-2264.

Vulpe, C., Levinson, B., Whitney, S., Packman, S., and Gitschier, J. (1993). Isolation of a candidate gene for Menkes disease and evidence that it encodes a copper-transporting ATPase. Nat Genet *3*, 7-13.

Waggoner, D.J., Drisaldi, B., Bartnikas, T.B., Casareno, R.L., Prohaska, J.R., Gitlin, J.D., and Harris, D.A. (2000). Brain copper content and cuproenzyme activity do not vary with prion protein expression level. J Biol Chem *275*, 7455-7458.

Walter, E.D., Stevens, D.J., Visconte, M.P., and Millhauser, G.L. (2007). The prion protein is a combined zinc and copper binding protein: Zn2+ alters the distribution of Cu2+ coordination modes. J Am Chem Soc *129*, 15440-15441.

Watkins, J.A., Altazan, J.D., Elder, P., Li, C.Y., Nunez, M.T., Cui, X.X., and Glass, J. (1992). Kinetic characterization of reductant dependent processes of iron mobilization from endocytic vesicles. Biochemistry *31*, 5820-5830.

Watt, N.T., and Hooper, N.M. (2003). The prion protein and neuronal zinc homeostasis. Trends Biochem Sci *28*, 406-410.

Watt, N.T., Taylor, D.R., Gillott, A., Thomas, D.A., Perera, W.S., and Hooper, N.M. (2005). Reactive oxygen species-mediated beta-cleavage of the prion protein in the cellular response to oxidative stress. J Biol Chem *280*, 35914-35921.

Watt, N.T., Taylor, D.R., Kerrigan, T.L., Griffiths, H.H., Rushworth, J.V., Whitehouse, I.J., and Hooper, N.M. (2012). Prion protein facilitates uptake of zinc into neuronal cells. Nat Commun *3*, 1134.

Watts, J.C., and Westaway, D. (2007). The prion protein family: diversity, rivalry, and dysfunction. Biochim Biophys Acta *1772*, 654-672.

West, A.K., Chuah, M.I., Vickers, J.C., and Chung, R.S. (2004). Protective role of metallothioneins in the injured mammalian brain. Rev Neurosci *15*, 157-166.

West, A.K., Hidalgo, J., Eddins, D., Levin, E.D., and Aschner, M. (2008). Metallothionein in the central nervous system: Roles in protection, regeneration and cognition. Neurotoxicology *29*, 489-503.

Whittal, R.M., Ball, H.L., Cohen, F.E., Burlingame, A.L., Prusiner, S.B., and Baldwin, M.A. (2000). Copper binding to octarepeat peptides of the prion protein monitored by mass spectrometry. Protein Sci *9*, 332-343.

Wong, B.S., Liu, T., Li, R., Pan, T., Petersen, R.B., Smith, M.A., Gambetti, P., Perry, G., Manson, J.C., Brown, D.R*., et al.* (2001). Increased levels of oxidative stress markers detected in the brains of mice devoid of prion protein. J Neurochem *76*, 565-572.

Yashiro, K., and Philpot, B.D. (2008). Regulation of NMDA receptor subunit expression and its implications for LTD, LTP, and metaplasticity. Neuropharmacology *55*, 1081-1094.

Yokel, R.A., and Crossgrove, J.S. (2004). Manganese toxicokinetics at the blood-brain barrier. Res Rep Health Eff Inst, 7-58; discussion 59-73.

Yokel, R.A., Crossgrove, J.S., and Bukaveckas, B.L. (2003). Manganese distribution across the blood-brain barrier. II. Manganese efflux from the brain does not appear to be carrier mediated. Neurotoxicology *24*, 15-22.

You, H., Tsutsui, S., Hameed, S., Kannanayakal, T.J., Chen, L., Xia, P., Engbers, J.D., Lipton, S.A., Stys, P.K., and Zamponi, G.W. (2012). Abeta neurotoxicity depends on interactions between copper ions, prion protein, and N-methyl-D-aspartate receptors. Proc Natl Acad Sci U S A *109*, 1737-1742.

Zahn, R., Liu, A., Luhrs, T., Riek, R., von Schroetter, C., Lopez Garcia, F., Billeter, M., Calzolai, L., Wider, G., and Wuthrich, K. (2000). NMR solution structure of the human prion protein. Proc Natl Acad Sci U S A *97*, 145-150.

Zakin, M.M., Baron, B., and Guillou, F. (2002). Regulation of the tissue-specific expression of transferrin gene. Dev Neurosci *24*, 222-226.

Zecca, L., Youdim, M.B., Riederer, P., Connor, J.R., and Crichton, R.R. (2004). Iron, brain ageing and neurodegenerative disorders. Nat Rev Neurosci *5*, 863-873.

Zheng, F., Erreger, K., Low, C.M., Banke, T., Lee, C.J., Conn, P.J., and Traynelis, S.F. (2001). Allosteric interaction between the amino terminal domain and the ligand binding domain of NR2A. Nat Neurosci *4*, 894-901.

APPENDIX

Expert Opinion

Gene expression profiling to identify druggable targets in prion diseases

Federico Benetti, Lisa Gasperini, Mattia Zampieri & Giuseppe Legname†
†*Laboratory of Prion Biology, Neurobiology Sector, Scuola Internazionale Superiore di Studi Avanzati-International School of Advanced Studies (SISSA-ISAS), Edificio Q1, Basovizza, Trieste, Italy*

Importance of the field: Despite many recent advances in prion research, the molecular mechanisms by which prions cause neurodegeneration have not been established. In fact, the complexity and the novelty characterizing this class of disorders pose a huge challenge to drug discovery. Pharmacogenomics has recently adopted high-throughput transcriptome analyses to predict potential drug target candidates, with promising results in various fields of medicine.

Areas covered in this review: The present work offers an overview of the transcriptional alterations induced by prion infection in different biological systems. Hereafter, therapeutic approaches are discussed in light of the identified altered processes.

What the reader will gain: This review offers readers a detailed overview on microarray analyses, taking into account their advantages and limitations. Our work can help readers, from many research areas, to design a suitable microarray experiment.

Take home message: So far, drugs acting on the pathways identified by microarray analysis have not been found to be effective in prion diseases therapy. An integration of gene expression profiling, proteomics and physiology should be applied to pursue this aim.

Keywords: drug, gene expression, microarray, prion

Expert Opin. Drug Discov. (2010) 5(2):177-202

1. Introduction

Prion diseases or transmissible spongiform encephalopathies (TSEs) are a class of fatal neurodegenerative disorders characterized by the spongy appearance of brain tissue, synaptic degeneration, microglia and astrocytes activation and neuronal loss [1]. They can be distinguished in sporadic, genetic and infectious disorders. TSEs include: Creutzfeldt-Jakob disease (CJD), Gerstmann-Sträussler-Scheinker syndrome, fatal familial insomnia and kuru in humans, bovine spongiform encephalopathy (BSE) in cattle, scrapie in sheep and goats and chronic wasting disease in elk and deer [2]. Like other neurodegenerative pathologies, such as Alzheimer's disease (AD), Parkinson's disease (PD), amyotrophic lateral sclerosis and Huntington's disease, prion diseases are commonly characterized by abnormal protein aggregates and amyloid deposits. The hypothesis that an infectious proteinaceous particle was responsible of TSE transmissibility was first proposed in the early 1980s by Stanley B. Prusiner [1] and later widely confirmed and accepted [3]. The agent responsible for the onset and propagation of TSE is a pathogenic conformational isoform (PrP^{Sc}) of the cellular prion protein (PrP^{C}) that in humans is encoded by the gene *PRNP*. These two conformational isoforms can

informa healthcare

10.1517/17460440903544449 ISSN 1746-0441

Article highlights.

- Pharmacogenomics has adopted gene expression analysis to predict drug targets.
- In prion biology, gene expression analyses have been performed to compare infected and healthy systems.
- Gene expression analyses using subtractive hybridization approaches have been carried out on both *in vitro* and *in vivo* systems.
- Though the main purpose of gene expression profiling in the prion field is the identification of drug targets, no effective remedies have been found against prion diseases among clinically tested compounds.
- The action mechanisms of some drugs and their efficacy have been correlated with the altered pathways evidenced by microarray analyses.
- In order to select the best target for therapeutic treatments, gene expression profiling must be associated with functional proteomics and physiology.

This box summarises key points contained in the article.

be distinguished in view of their different biochemical properties, such as proteases resistance and insolubility in non-denaturing detergents [1,4,5].

The transmission of the disease is related to the autocatalytic ability of PrP^{Sc} to act as a template converting PrP^{C} into the pathogenic isoform [6,7]. Mutations in the *PRNP* gene favor the misfolding of PrP^{C}, increasing the propensity to the disease onset [8]. Despite the many advances made in recent years, neither the molecular mechanism by which prions determine TSEs nor the physiological function/s of PrP^{C} have been established. Current studies propose prion protein (PrP) involvement in several biological processes such as neuritogenesis [9-13], apoptosis prevention [14-17], protection against oxidative stress [18], cell adhesion [19,20], hormone regulation [21-23], transcriptional regulation [24], myelinogenesis [25] and copper endocytosis [26].

The complexity of this class of neurodegenerative diseases as well as the novelty of their molecular mechanisms pose a huge challenge to biology and drug discovery. Presently, biomarkers for early diagnosis and effective therapeutic treatments have not been identified. Global expression analysis platforms, such as oligonucleotide microarrays, offer unique tools to deal with neurodegenerative disorders. This technology has become robust for both the identification of co-regulated and differentially expressed genes (DEGs) and of novel drug targets [27-29]. Therefore, pharmacogenomics has adopted high-throughput gene expression analysis to predict a flood of potential drug candidates and accelerate drug discovery and development.

Gene expression analysis in the field of prion biology has been mostly used to compare the expression and regulation of genes in healthy and diseased systems. In particular, genome-wide analysis has been carried out to explain the transcriptional changes induced by prion strains at different disease stages. Comprehensive transcriptome profiles of the early disease symptoms might reveal the optimal path for drug discovery, from target to lead compound.

In this paper, we present a comprehensive review of the results obtained investigating the transcriptional changes in different prion-infected systems, and then relate these studies to therapeutic applications.

2. Gene expression profiling using subtractive hybridization approaches

First attempts to study the gene expression modulations induced by scrapie infection with a large-scale approach were performed by Duguid *et al.* [30-32]. The authors analyzed transcriptome variations in scrapie strain 263K-infected hamster brains, performing a subtractive hybridization of cDNA libraries. Their results, confirmed by RNA blotting, evidenced an expression increase of mRNAs encoding glial fibrillary acidic protein (GFAP), metallothionein II (MTII), B-chain of α-crystallin, sulfated glycoprotein 2 (SGP-2), transferrin, β-2 microglobulin and two unknown non-coding sequences.

GFAP is an astrocyte-specific marker. Its deficiency causes Alexander's disease, characterized by progressive failure of central myelination, ataxia, bulbar signs and spasticity and a slowly progressive course [33-38]. Duguid and Trzepacz revealed an upregulation of β-2 microglobulin and both classes of MHC genes as well as the class II-associated invariant chain [39]. MTII selectively binds zinc ions and its regulation strongly depends on the availability of this micro-element, suggesting a dysmetabolism of this metal during prion propagation, as in the case of PD and AD [40,41]. SGP-2 neurobiology encompasses the subjects of cell death, synaptic remodeling and neuroendocrinology [42]. Its upregulation has been also described in AD [42]. Finally, the role of transferrin in neurodegeneration has been demonstrated in patients with macular degeneration [43,44]. Alterations of MTII and transferrin denote a dysmetabolism of micro-elements in prion diseases. Moreover, transcripts previously related to AD, such as SGP-2 and GFAP, highlight possible common mechanisms in both diseases.

The same approach was also applied by Diedrich *et al.* to analyze scrapie-infected mouse brain transcripts [45]. The main mRNA variations, confirmed by *in situ* hybridization and immunocytochemistry on both mouse and AD patient brains, were associated with the upregulation of apolipoprotein E (apoE) and cathepsin D (CD). ApoE and CD upregulation were primarily localized in activated astrocytes. Again, these results confirm neuropathological similarities between prion diseases and AD.

The cDNA library differential screen was performed on scrapie-infected murine neuroblastoma cells [46]. Doh-ura *et al.* identified and confirmed by northern blotting 11 DEGs. Among the annotated ones, chromogranin B, intracisternal A-particle-related retroviral envelope gene, heat shock protein (hsp) 70, ornithine decarboxylase antizyme and ribosomal protein S2 were upregulated, while α-enolase, eIF-4A and hsp90 were downregulated.

More recently, a subtractive suppressive hybridization (SSH) was carried out by Cosseddu *et al.* on mixed midbrain, thalamus, cerebellum and temporal cortex RNAs from a clinically scrapie-affected and healthy sheep brain [47]. The first animal carried out the susceptible scrapie genotype VRQ/VRQ, while the second one had the resistant genotype ARR/ARR. The SSH procedure revealed the following altered transcripts: three short interspersed elements or satellite sheep DNA, the mitochondrial cytochrome c oxidase subunit 1, the brain GTPase-activating protein chimerin 1, the phosphatase 2A catalytic subunit, leucine-rich and fibronectine type III domain containing 5 and the Ser/Thr calcium/calmodulin-dependent protein kinase II α required for hippocampal long-term potentiation and spatial learning.

3. Gene expression profiles on cell cultures

Several works have reported gene expression studies performed on scrapie-infected neuronal cell cultures. Sample homogeneity and higher signal:noise ratio compared to the whole brain allow the identification of tissue specific transcriptional changes. Baker and Manuelidis performed a microarray study on microglia cells isolated from CJD-infected mice brains [48]. The CJD-specificity of DEGs was checked through comparison against lipopolysaccharide-, IFN-γ or protease-resistant PrP-treated microglia cells. These results highlighted the following affected pathways: inflammation, IFN and complement pathways, intercellular communication, chemotaxis and migration, antibody receptor, proteases and protease inhibitors, cell differentiation, lipid metabolism, matrix and cytoskeleton.

Greenwood *et al.* performed a gene-expression profile on murine cell culture models persistently infected with mouse-adapted scrapie strains [49]. They used neuronal origin cells N2a and GT1, which showed a different phenotype in response to prion infection. Both cell types revealed the upregulation of transport proteins, ATP-binding and calcium-binding proteins. However, N2a evidenced an increase in transcripts involved in cytoskeletal functions. The downregulated genes were mainly related to ATP-binding in GT1, while in N2a they were ribosomal-associated genes.

To investigate prion-induced effects on human neuronal cell cultures directly, Martinez and Pascual analyzed the differential gene expression regulation induced by a neurotoxic prion fragment, PrP106-126, on SH-SY5Y neuroblastoma cells [50]. Similar to human post-mortem brain tissues analyses [51], almost 90% of the DEGs were downregulated. The altered biological processes were involved in metabolism, folding and transport of proteins, cell cycle regulation, transcriptional regulation and mitochondrial functions. On the contrary, genes involved in microglia activation as well as inflammation were not highly deregulated in isolated neurons. Although microglia plays a central role in prion pathologies establishment and development, prions could exploit other mechanisms to induce neuronal death and neurodegeneration.

Julius *et al.* evaluated the transcriptional response to persistent RML infection on three distinct murine cell lines: N2aPK1, CAD and GT1 [52]. Surprisingly, they did not find any altered genes and hypothesized that alterations in gene expression represent secondary effects of the infection. Bach *et al.*, by performing microarray analysis on murine N2a cells infected with prion strain 22L, observed upregulated genes of the cholesterol pathway with a subsequent increase of total and free cholesterol levels [53]. Upregulation of cholesterogenic genes – hydroxymethylglutaryl-CoA synthase and reductase, mevalonate kinase, isopentenyl diphosphate isomerase, squalene synthase, cytochrome P450, family 51 and C4-sterol methyl oxidase – was probably due to an increase in the amount and activity of the sterol regulatory element-binding protein Srebp2. In order to test the upregulation of cholesterol pathway on different neuronal cells, the authors analyzed, by using real time PCR, the expression levels of Srebp2, C4-sterol methyl oxidase and low-density lipoprotein receptor in RML-infected GT1 cells. The three genes were found upregulated in this case as well. On the contrary, RML- and 22L-infected BV-2 microglia cells revealed a downregulation of cholesterogenic genes.

4. Gene expression profiles on mouse brain areas

Few studies have been performed on specific mouse brain areas to determine the characteristic effects of prion infection on the different brain regions. Brown *et al.* collected the total hippocampus RNA at the terminal stage of the disease from ME7/CV-infected mice and hybridized it on Clontech Atlas arrays containing >2300 annotated genes [54]. Statistical analysis identified nine genes with differential expression: six previously reported as upregulated by prion infection (GFAP, vimentin, clusterin, CD and complement component 1q α and β polypeptides) and three not previously identified (cystatin C, defender against cell death (DAD) and amino terminal enhancer of split (AES)). DAD and AES only appeared to be downregulated, but the results were not confirmed by real time PCR. Most of the genes identified were involved in microglia activation, a process that occurs in the late stages of the disease. This process probably does not induce neuronal loss, but masks the alteration of its earlier stages. Within the infected hippocampi, CA1 neuronal death occurs between 160 and 180 days post-inoculation (DPI). To elucidate the molecular events causing the neuronal loss, Brown *et al.* analyzed the gene expression profile of ME7-infected murine hippocampus at 170 DPI using Affymetrix high-density oligonucleotide arrays [55]. The hierarchical clustering of the array revealed a clear segregation of control and scrapie-infected samples. Statistical analysis identified 65 up and 13 downregulated genes. The processes mainly affected were oxidative stress-response, endoplasmic reticulum

homeostasis (increased expression of Reticulon 3, calnexin, ER chaperons FK506 binding protein 2), mitochondrial apoptotic pathway (upregulation of the mitochondrial cloride channel mtCLIC4, ring finger protein 7, 2 members of the acidic nuclear phosphoprotein 32 family), protein degradation (induction of proteasome subunit β5, ring finger proteins with ubiquitin E3 ligase activity, α-mannosidase 2 and ATPase, H+ transporting V1 subunit D) and trafficking (upregulation of signal recognition pattern 9, Golgi-localized short coiled-coil protein, VAMP4 and AP1s1), cholesterol and lipid biosynthesis and metabolism (sterol-C5-desaturase, sterol-C4-methyl oxidase, acetyl-CoA acyltransferase 1, sortilin-related receptor, ecithin cholesterol acyltransferase and very-low-density lipoprotein receptor), and transcription and chromatin architecture regulation (for instance, C/EBP δ and IFN consensus sequence binding protein). In the early stages of disease, cholesterol and lipid biosynthesis-related genes were found upregulated in scrapie-infected samples, while appearing downregulated in the later stages [56,57]. The authors related these discrepancies to neuronal tissue loss occurring mainly in the later stages. Surprisingly, only few DEGs were involved in inflammation.

Other brain areas expression profiles were analyzed in the work published by Riemer *et al.* in 2004 [56]. They performed microarray analysis of the total RNA extracted from cortex, medulla and pons of 139A-infected mice identifying 114 DEGs, 86 up and 28 downregulated. Most of the upregulated genes are involved in inflammatory reactions, immune and stress responses. The increased mRNAs were those coding for complement system proteins, enzymes that generate cytotoxic superoxide anion radicals, cathepsins, acute phase proteins (serine proteinase inhibitor 2, α2-macroglobulin and lipocalin 24p3) and transcription factors (CCAAT/enhancer-binding protein δ, IFN consensus sequence binding protein and LRG-21). Interestingly, as shown in the late stage of the disease [56,57], most of the downregulated genes play a significant role in cholesterol biosynthesis.

5. Gene expression profiles on mouse whole brain

To identify DEGs in early and terminal stages of the disease, high-density microarray approaches in whole-brain murine scrapie models have been extensively used. The use of mock-inoculated age-matched mice as controls allows discriminating expression alterations due to aging rather than prion infection. In addition to clinical and late stages of the disease, authors often selected one preclinical time point with minor detectable neuropathological changes. This comparative analysis may reveal biomarkers for prion detection at an early stage.

In 2004, Booth *et al.* studied two strains of mouse-adapted scrapie, ME7 and 79a, to characterize the overall general response to prion infection [58]. Analyzing the whole brain mRNA at the appearance of clinical signs, they were able to select 138 up and 20 downregulated genes. This analysis evidenced a generic fingerprint to damage rather than a prion-specific response. In particular, they observed the upregulation of genes involved in protease/peptideolysis, lysosomal functions, lipid binding, defense and immunity, cell communication, cell death, cell differentiation, cell growth regulation, cell organization and biogenesis, hormone metabolism, ion transport, microtubule-based process and oxygen transport.

To gain deeper insights into the early variations of gene expression, the authors collected samples both at preclinical and clinical disease stages. The time-course study revealed genes involved in the initial acute response to prion agent. Cluster analysis of the 217 DEGs produced four main groups: i) genes upregulated at 21 DPI; ii) genes downregulated at 21 DPI; iii) genes downregulated throughout the course of the disease; and iv) genes upregulated at the midpoint in the disease process. Genes belonging to clusters 1 and 2 evidenced an early disruption of development and differentiation regulation as well as neuronal senescence leading to apoptosis. On the other hand, 50% of the third cluster genes belonged to the hematopoietic system (hemoglobin Y, β-like, hemoglobin-α, NCK-associated protein1) and were proposed as preclinical biomarkers.

The same group published an analysis of the gene expression modifications in the brains of two inbred mice backgrounds, C57BL/6 and VM, infected with three different scrapie strains (22A, ME7 and 79a) [59]. The most represented functional groups in the 'prion-related genes' list were: lipid metabolism, nervous system function and synaptic transmission, cytoskeleton organization and biogenesis, protein biosynthesis and folding, lysosome organization and biogenesis, proteolysis, apoptosis, immune cell activation and inflammatory response. Subsequently, using the Ingenuity Pathways Analysis tool, they identified 22 networks such as tissue development, cell death, endocrine system; behavior, cellular movement, cell cycle; inflammatory disease, connective tissue disorders, infectious disease; cancer, cell death, tumor morphology; and cellular assembly and organization, neurological disease, and tissue morphology. Because astrocytosis is a prominent feature of prion diseases and numerous affected pathways were probably involved in glia origin, the DEGs were annotated in terms of cell-type, comparing astrocytes and microglia versus neurons. Glia-associated DEGs were mainly involved in cell proliferation and growth, cellular migration and inflammation, lysosomal activity, lipid metabolism and transport. The upregulation of these pathways supports the astrocytes activation in the damaged areas of the brain. On the other hand, proteins involved in synaptic functions, signaling pathways, cholesterol metabolism, calcium signaling and long-term potentiation were downregulated in neurons, in agreement with the induced neuronal death during prion disease.

Skinner *et al.* reported the gene expression alterations in brains of C57BL/6 mice infected with three different scrapie

strains: ME7, 22L and RML [60]. Microarray analyses were performed at both preclinical and clinical time points. Over 400 DEGs were detected at the clinical stage of the disease. Bioinformatics analysis revealed the functional categories associated: protein folding and degradation, endosome/lysosome functions, immune response, cytoskeleton organization, metal ion binding, calcium regulation, pumps and ion channels, signaling cascade, transcription/translation, mitochondria functions, carbohydrate processing, lipid metabolism and synapse function. Genes involved in the endosome/lysosome system may function as cofactors in PrP misfolding and accumulation, while the altered gene expressions of the other pathways are probably crucial for microglia activation and neuronal degeneration. At the preclinical stage, only 22 genes were deregulated, revealing no massive brain disruption. To identify prion strain-specific gene patterns, the authors compared among each other mice infected with the three prion isolates. This comparison revealed several genes differentially modulated by the various prion strains, probably underlying distinct infection mechanisms and degeneration processes.

Kretzschmar's group compared the transcriptome of C57BL/6 mice inoculated with two different prion strains (ME7 and RML) [61]. They identified 121 genes common to both prion strains. These genes encode proteins mainly involved in proteolysis, protease inhibition, cell growth and maintenance, immune response, signal transduction, cell adhesion and molecular metabolism. The transcriptional activity generally showed upregulation of these genes from 120 DPI for ME7-inoculated mouse brains and from 90 DPI for RML-inoculated mouse brains. The onset of upregulation was temporally correlated with PrP^{Sc} appearance, glia activation and neuronal cell death. Among the 67 genes upregulated in ME7-infected mice, many were downregulated in RML-inoculated mice. However, none of the genes showing a discordant prion strain-variation were validated through real time PCR. The high percentage of genes involved in the immune response raises the possibility that complement proteins, inflammatory factors and astrocytes associated genes may play a primary role in prion diseases. These results may be related to the later stages of the disease without being essential to prion propagation.

In another study by the same group performing time-course experiments, 430 DEGs were identified [57]. The time-dependent expression profiles revealed a downregulation of cholesterol metabolism-related genes, in addition to an enhanced activation of the immune system and other categories such as translational terminators, cofactors and ubiquinone metabolism. Cholesterol synthesis inhibition suggested a correlation between cholesterol depletion and synaptic degeneration.

To identify pre-symptomatic biomarkers for prion infection diagnosis, Miele *et al.* applied microarray analysis on inbred C57BL/6 mice inoculated with RML prion strain [62]. The authors performed a transcriptional analysis of intraperitoneally prion-infected mouse brains looking for highly upregulated transcripts containing a secretory leader peptide. The microarray analysis revealed 77 DEGs. In particular, α_1-antichymotrypsin was increased in urine and cerebrospinal fluid of prion-affected patients, suggesting its potential use as preclinical biomarker.

In a more recent study, a huge effort to perform a global systematic approach has been carried out. Hwang and coworkers collected >400 Affymetrix chips to monitor the disease progression associated with different mice background (FVB, B6 and B6.I) and prion strains (RML and 301V) [63,64]. A total of 333 DEGs, common to the five prion-mouse combinations, were identified and integrated with the known protein–protein interaction networks. Moreover, transgenic mice expressing different PrP levels were used (Tg4053, $Prnp^{0/+}$ and $Prnp^{0/0}$) and their DEGs investigated. PrP^{C} expression levels affected both the onset of symptoms and the transcriptional regulation. High PrP^{C} content, as in eightfold PrP expressing Tg4053 mice, showed vast transcription alteration associated with earlier onset of symptoms. On the other hand, heterozygous mice ($Prnp^{0/+}$) revealed a transcriptional program similar to wild-type mice during early stages of neuropathological changes and developed the disease later. *Prnp* knockout mice ($Prnp^{0/0}$) did not develop prion disease and, therefore, showed no statistically significant DEGs.

Hwang and collaborators identified a stereotypical set of steps leading to neurodegeneration. Microglia, astrocytes activation and increase of lysosomal protease were detected within 10 weeks from inoculation, followed by alteration in cholesterol, glycosaminoglycan and androgen metabolism, in addition to iron homeostasis and prostaglandin metabolism. Perturbation of androgen metabolism was related to glia activation and neurosteroid metabolism, further linked to cholesterol metabolism. Iron homeostasis and heme metabolism were associated with their potential role in demyelination, while the biosynthesis of protoinflammatory prostlaglandins and leukotrimers was deemed to explain the overproduction of pro-inflammatory metabolites.

Because most DEGs in TSE infection, as in many other brain disorders, are related to neuroinflammation, Moody *et al.* analyzed the transcriptome changes specifically associated with prion neuropathology, adopting a different approach [65]. They compared gene expression profiles of RML-infected and cuprizone-treated mouse brains. Cuprizone is a copper chelator and induces demyelination in the CNS, histopathological lesions, inflammation and glia activation of orally treated mice. The authors analyzed cuprizone-treated mouse brains to highlight the modulations of neuroinflammation-associated RNAs and to identify prion-specific gene expression alterations. Microarray analysis, performed on RML-infected C57BL/6 mice at three time points, revealed 164 DEGs; the majority of them had not been previously identified. Upregulated genes are mainly involved in immune response (probably due to glia proliferation),

response to stimuli, protein modification, intracellular cellular signaling, while downregulated genes belong to the ubiquitin cycle and cellular developmental processes. Cuprizone dose and time exposure were chosen to obtain prion-like histopathological modifications. The transcriptome analysis of cuprizone-treated mice detected 319 DEGs. Upregulated genes are associated with immune response, metabolic processes, apoptosis (probably related to oligodendrocyte demyelination), cell communication, cellular adhesion and localization, while downregulated genes are related to axon ensheathment. Comparing microarray data from both RML- and cuprizone-treated mice, 17 genes resulted to be specific for prion disease. The two major altered pathways in prion disease were: neuropeptide signaling (agouti-related protein and phospholipase C, ε 1) and adipocytokine signaling (agouti-related protein, solute carrier family 2 member 4 and suppressor of citokine signaling).

6. Glycosylation-related gene expression profiles

PrP^C is present in the outer leaf of plasma membranes as un-, mono- or di-glycosylated form. Alterations in the PrP glycopattern have been revealed during prion infection [66]. Barret *et al.* discovered the downregulation of chondroitin sulfate *N*-acetylgalactosaminyltransferase 1 (ChGn) and carbohydrate (*N*-acetylgalactosamine 4-*O*) sulfotransferase 8 (Chst8) genes in scrapie Chandler-infected murine GT1-7 cells [67]. ChGn is involved in the initiation of the synthesis of chondroitin sulfate, while Chst8 in the 4-*O*-sulfation of non-reducing *N*-acetylgalactosamine residues.

Guillerme-Bosselut *et al.* investigated the expression patterns of 165 glycosylation-related genes in the brain and spleen of healthy and 127S ovine strain-affected Tg338 mice, an homozygous transgenic line for the ovine VRQ allele and expressing 8- to 10-fold PrP more than in sheep [68]. Brain and spleen play a role in prion replication and present different glycomes [69,70]. Eight genes encoding for glycosyltransferases and glycosidase were found upregulated in the infected brains. On the contrary, in the spleen there was a dichotomy in glycosyltransferases behavior.

Because prion diseases cause alterations in the extra-cellular matrix [71] and both PrP^C and PrP^{Sc} bind different N-glycans [72], glycosaminoglycan binding sites could represent a potential target for therapeutic treatment.

7. Gene expression profiles on BSE-infected animal brains

Sawiris *et al.* performed microarray analyses on 301V BSE strain-inoculated mouse brains in late stage infection and identified 116 up and 180 downregulated genes [73]. The functional categories mainly affected were: ubiquitin-mediated protein degradation, protein folding, apoptosis, zinc and calcium binding proteins and transcription regulation.

Recently, a time-course transcriptome analysis on BSE orally-infected cattle brains was published revealing 187 DEGs [74]. Among the annotated ones, 46% were upregulated, 35% downregulated and 19% showed complex expression patterns. The most affected categories were: metabolism, transcription and translation, immune response and transport. The higher degree of difference between healthy and BSE-infected brains was at 21 months post-inoculation (MPI). Although some samples did not present any clinical signs at 45 MPI, their gene profiles were highly similar to the infected samples.

8. Gene expression profiles on CJD patients' post-mortem brains

Xiang *et al.* analyzed the transcriptome of sporadic CJD (sCJD)-affected human post-mortem brains [51]. Most of the identified DEGs were downregulated, indicating neuronal dysfunction and degeneration. The major alterations of upregulated pathways include stress and immune responses, as well as cell cycle and death, while downregulated genes encode for protein metabolism, ion transport and synaptic proteins. sCJD brains revealed many similarities to ageing human brains, both in global expression patterns and in DEGs.

9. Drug target identification by gene expression profiling of prion-infected samples

The main purpose of a genome-wide analysis on prion-infected samples is the identification of targets for novel therapeutic approaches. Currently, no effective cures have been found against prion diseases, though several anti-prion compounds have been clinically tested (**Table 1**) [75]. Here, we briefly correlate the action mechanisms of some drugs and their efficacy on the altered pathways evidenced by microarray analyses.

Cholesterol synthesis is one of the most confirmed altered processes in prion-infected samples. The polyene antibiotics – amphotericin B, mepartricin and filipin – interact with cholesterol, inducing alteration of membrane lipid composition, disruption of cell membrane and modification of raft domains that are thought to be the site of PrP^C conversion into PrP^{Sc} [76,77]. As reviewed by Trevitt and Collinge [78] and by Sakaguchi [75], these drugs have shown an anti-prion activity prolonging the incubation time, delaying the disease onset and inhibiting prion propagation in scrapie-infected mouse brains and CJD-infected monkeys. However, the same beneficial effects were not confirmed in CJD patients [79,80]. Other drugs acting on cholesterol, such as statins, were used. Statins decrease cholesterol levels by inhibiting its biosynthesis [81]. Lovastatin and squalestatin were tested on scrapie-infected cells reducing PrP^{Sc} levels [82,83]. The blood-brain barrier permeable simvastatin instead showed weak effects on prion-infected mice [84,85].

Table 1. List of anti-prion compounds, their pathways of intervention and efficacy.

Drug	Pathway	Drug efficacy			References
		In vitro	*In vivo*	In clinical trials	
Drugs acting on altered pathways identified by gene expression analysis					
Pentosan polysulfate	Inflammation	PrP^{Sc} levels reduction	Disease onset delay in mice and hamsters. Incubation time increase in mice. Intra-ventricular administration in mice reduced PrP^{Sc} deposition and pathological changes. Late treatments do not clear pre-existing PrP^{Sc} deposits, but prevent further accumulation	Lifespan prolongation with intraventricularly inoculation. No definite clinical benefit. Weak improvement in eye fixation, verbalization, stimuli response and weight gain. No brain atrophy reduction.	[75,78,80,87]
Polyene antibiotics (methotrexate, amphotericin B, mepartricin and filipin)	Disruption of cell membrane and modification of raft domains	PrP^{Sc} levels reduction	Incubation time prolongation in infected mice and hamster even with late treatment	No significant increase in survival and no clinical status improvement after amphotericin administration.	[75,78-80]
Quinacrine and chloroquine	Lysosomal pathway	PrP^{Sc} levels and propagation reduction	Neither prophylactic nor therapeutic effects in prion-infected mice	Transient and modest improvement in mood or cognitive functions in sCJD and iCJD patients. No benefits in FFI patients. No significant increase in survival. No clinical status improvement.	[75,78,80]
Polyphenolic compounds, minerals and vitamins	Oxidative stress			Responsiveness, myoclonus, apnea and rigidity improvement.	[78,80,91,92]
E-64, E-64d and leupeptin	Lysosomal pathway (cysteine–protease inhibitors)	PrP^{Sc} levels reduction	Neither prophylactic nor therapeutic effects in prion-infected mice		[78,80,86]
Statins	Cholesterol biosynthesis	PrP^{Sc} levels reduction	Weak therapeutic effects on mice: slightly longer incubation time, but indistinguishable levels of prion accumulation and pathological changes		[78,80,82-85]
Pifitrin-α	Apoptosis (p53 inhibitor, caspase-3 decrease).	PrP^{Sc} levels reduction	No improvement in incubation time, astrogliosis and spongiosis		[80,88]

CJD: Creutzfeldt-Jakob disease; FFI: Fatal familial insomnia; GSH: Glutathione; iCJD: Iatrogenic CJD; PrP: Prion protein; PrP^{C}: Cellular prion protein; $PrP^{res.}$: Protease-resistant prion protein; PrP^{Sc}: Pathogenic conformational isoform; sCJD: Sporadic CJD; vCJD: Variant CJD.

Table 1. List of anti-prion compounds, their pathways of intervention and efficacy (continued).

Drug	Pathway	Drug efficacy			References
		In vitro	*In vivo*	In clinical trials	
Flupirtine	Apoptosis and oxidative stress (increases Bcl-2 and GSH levels)			Cognition functions improvement. No significant differences in survival times.	[80,90]
D-penicillamine and clioquinol	Ion homeostasis (copper chelator)	Decrease of copper content and increase of proteinase K sensitivity of PrP^{Sc}	Delay in prion disease onset		[75,95]
Copper	Ion homeostasis	Decrease of PrP^{C} linked to membrane, inhibition of PrP^{res} amplification	Delay in prion disease onset		[75,96,97]
IFN	Inflammation			No changes in CJD patients' condition.	[80]
Drugs acting on not altered pathways in gene expression analysis					
Polyanionic compounds (heteropolyanion-23, dextran sulfate, heparan sulfate mimetics, phosphorothioate oligonucleotides)	PrP^{Sc} degradation stimulation in lysosomes and *de novo* formation blocking	PrP^{Sc} levels reduction	PrP^{Sc} levels reduction in the spleen of scrapie-infected mice. Scrapie onset delay in mice and hamsters. Lifespan prolongation when delivered into the brain or when peripherally administered before infection or before inoculated prions reach the CNS		[75,78]
Tetracycline and doxycyclin	Amyloid destabilization and fibrils resorption	Brain homogenate infectivity reduction; revertion of PrP^{Sc} purified from vCJD patients	Disease onset delay and absence of histopathological features by scrapie and drug concomitant administration		[75,78]
Tetrapyrroles (porphyrines and phtalocyanins)	PrP^{Sc} binding and conformational change	Reduction PrP^{Sc} levels and propagation prevention	Incubation time prolongation when prophylactically applied. Disease onset delay after intraperitoneal infection, not after intracerebral infection and not upon late stage treatment		[78,80]

CJD: Creutzfeldt-Jakob disease; FFI: Fatal familial insomnia; GSH: Glutathione; iCJD: Iatrogenic CJD; PrP: Prion protein; PrP^{C}: Cellular prion protein; PrP^{res}: Protease-resistant prion protein; PrP^{Sc}: Pathogenic conformational isoform; sCJD: Sporadic CJD; vCJD: Variant CJD.

Table 1. List of anti-prion compounds, their pathways of intervention and efficacy (continued).

Drug	Pathway	Drug efficacy			References
		In vitro	*In vivo*	In clinical trials	
Imatinib mesilate	Cell signaling (tyrosine kinase inhibition)	PrP^{Sc} levels reduction by stimulation of prion degradation in lysosomes	Very slight prolongation of the incubation time upon early treatment. No significant improvement detected with late treatment		[75]
Cytidine-5-diphosphocoline, bromoenol lactone, aristolochic acid, arachidonyl trifluoromethyl ketone	Cell signaling (free fatty acid and lysophospholipid production)	PrP^{Sc} levels reduction			[75]
SL327	Cell signaling (MAPK kinase 1/2)	PrP^{Sc} levels reduction by degradating or preventing the *de novo* synthesis of prion			[75]
Suramin	Protein misfolding, oligomerization and degradation	PrP^{Sc} levels reduction; decrease of PrP^{C} surface levels and induction of PrP aggregation in uninfected cells	Modest incubation time increase in hamsters and mice		[78]
Polycationic compounds	Disaggregation and β-sheet content decrease; strain and sequence-dependent proteolytic susceptibility increase	PrP^{Sc} levels reduction; prevention of *de novo* PrP^{Sc} formation; clearance of cells infectivity to mice	Splenic PrP^{Sc} reduction; incubation time prolongation		[78]
Acyclovir	Antiviral			No changes in CJD patients' condition.	[80]

CJD: Creutzfeldt-Jakob disease; FFI: Fatal familial insomnia; GSH: Glutathione; iCJD: Iatrogenic CJD; PrP: Prion protein; PrP^{C}: Cellular prion protein; PrP^{res}: Protease-resistant prion protein; PrP^{Sc}: Pathogenic conformational isoform; sCJD: Sporadic CJD; vCJD: Variant CJD.

Table 1. List of anti-prion compounds, their pathways of intervention and efficacy (continued).

Drug	Pathway	Drug efficacy			References
		In vitro	*In vivo*	In clinical trials	
Amantadine	Antiviral			No changes in clinical symptoms and no differences in survival. Transient and weak improvement in wakefulness, cognition, communication and rigidity.	[80]
Vidarabine	Antiviral			Transient improvement of all neurological symptoms and decrease of involuntary movement.	[80]
Clomipramine and venlafaxine	Antidepressant			No changes in CJD patients' condition.	[80]
Levetiracetam	Anticonvulsant			Marked myoclonus reduction. Patient still alive at the time of the report.	[80]
Topiramate	Anticonvulsant			Decrease of myoclonus and rigidity; movement and communication improvement. Patient still alive at the time of the report, but probably the disease was misdiagnosed.	[80]

CJD: Creutzfeldt-Jakob disease; FFI: Fatal familial insomnia; GSH: Glutathione; iCJD: Iatrogenic CJD; PrP: Prion protein; PrP^{C}: Cellular prion protein; PrP^{res}: Protease-resistant prion protein; PrP^{Sc}: Pathogenic conformational isoform; sCJD: Sporadic CJD; vCJD: Variant CJD.

Table 2. List of DEGs collected from reviewed publications.

Gene symbol	Gene name	No. of citations
CTSS	Cathepsin s	12
CTSH	Cathepsin h	10
GFAP	Glial fibrillary acidic protein	10
C1QA	Complement component 1, q subcomponent, alpha polypeptide	9
C1QB	Complement component 1, q subcomponent, beta polypeptide	9
HEXB	Hexosaminidase b	9
ABCA1	Atp-binding cassette, sub-family a (abc1), member 1	8
B2M	Beta-2 microglobulin	8
FCER1G	Fc receptor, ige, high affinity i, gamma polypeptide	8
GRN	Granulin	8
IFIT3	Interferon-induced protein with tetratricopeptide repeats 3	8
LY86	Lymphocyte antigen 86	8
APOD	Apolipoprotein d	7
CD53	Cd53 antigen	7
CD68	Cd68 antigen	7
CLU	Clusterin	7
CNN3	Calponin 3, acidic	7
CST3	Cystatin c	7
CST7	Cystatin f (leukocystatin)	7
DBI	Diazepam binding inhibitor	7
DHRS1	Dehydrogenase/reductase (sdr family) member 1	7
FCGR2B	Fc receptor, igg, low affinity iib	7
H2-D1	Histocompatibility 2, d region locus 1	7
LAPTM5	Lysosomal-associated protein transmembrane 5	7
LGALS3BP	Lectin, galactoside-binding, soluble, 3 binding protein	7
SERPINA3N	Serine (or cysteine) peptidase inhibitor, clade a, member 3n	7
TYROBP	Tyro protein tyrosine kinase binding protein	7
VIM	Vimentin	7
CD52	Cd52 antigen	6
CD9	Cd9 antigen	6
CTSC	Cathepsin c	6
FXYD1	Fxyd domain-containing ion transport regulator 1	6
HMGCS1	3-hydroxy-3-methylglutaryl-coenzyme a synthase 1	6
MPEG1	Macrophage expressed gene 1	6
S100A6	S100 calcium binding protein a6 (calcyclin)	6
SGK	Serum/glucocorticoid regulated kinase	6
SOX9	Sry-box containing gene 9	6
AQP4	Aquaporin 4	5
C4B	Complement component 4b (childo blood group)	5
CAPG	Capping protein (actin filament), gelsolin-like	5
CCL9	Chemokine (c-c motif) ligand 9	5
CD84	Cd84 antigen	5
CEBPD	Ccaat/enhancer binding protein (c/ebp), delta	5
CHI3L1	Chitinase 3-like 1	5

Cited genes have been found in at least three studies.

Table 2. List of DEGs collected from reviewed publications (continued).

Gene symbol	Gene name	No. of citations
CSF1R	Colony stimulating factor 1 receptor	5
CTSD	Cathepsin d	5
CTSZ	Cathepsin z	5
CXCL10	Chemokine (c-x-c motif) ligand 10	5
CYBA	Cytochrome b-245, alpha polypeptide	5
EGR1	Early growth response 1	5
H2-K1	Histocompatibility 2, k1, k region	5
HPGD	Hydroxyprostaglandin dehydrogenase 15 (nad)	5
IFITM3	Interferon induced transmembrane protein 3	5
ITGB2	Integrin beta 2	5
LAMP2	Lysosomal membrane glycoprotein 2	5
LMNA	Lamin a	5
MDH1	Malate dehydrogenase 1, nad (soluble)	5
MSR2	Macrophage scavenger receptor 2	5
NUPR1	Nuclear protein 1	5
OSMR	Oncostatin m receptor	5
PRDX6	Peroxiredoxin 6	5
SC4MOL	Sterol-c4-methyl oxidase-like	5
SLC25A18	Solute carrier family 25 (mitochondrial carrier), member 18	5
SPARC	Secreted acidic cysteine rich glycoprotein	5
TRF	Transferrin	5
A2M	Alpha-2-macroglobulin	4
ALDOC	Aldolase 3, c isoform	4
ANXA3	Annexin a3	4
APOE	Apolipoprotein e	4
AU020206	Expressed sequence au020206	4
BCL2A1A	B-cell leukemia/lymphoma 2 related protein a1a	4
BLNK	B-cell linker	4
C1QC	Complement component 1, q subcomponent, c chain	4
C3AR1	Complement component 3a receptor 1	4
CD14	Cd14 antigen	4
CD48	Cd48 antigen	4
CD86	Cd86 antigen	4
CLEC7A	C-type lectin domain family 7, member a	4
CRYAB	Alpha crystallin B chain	4
CTSB	Cathepsin b	4
CTSL	Cathepsin l	4
DNAJA1	Dnaj (hsp40) homolog, subfamily a, member 1	4
FCGR3	Fc receptor, igg, low affinity iii	4
FYB	Fyn binding protein	4
GP49A	Glycoprotein 49 a	4
GPNMB	Glycoprotein (transmembrane) nmb	4
HBA-A1	Hemoglobin alpha, adult chain 1	4
HMGCR	3-hydroxy-3-methylglutaryl-coenzyme a reductase	4
IDI1	Isopentenyl-diphosphate delta isomerase	4

Cited genes have been found in at least three studies.

Table 2. List of DEGs collected from reviewed publications (continued).

Gene symbol	Gene name	No. of citations
IRF8	Interferon regulatory factor 8	4
ITGAX	Integrin alpha x	4
LCN2	Lipocalin 2	4
LDLR	Low density lipoprotein receptor	4
LGALS3	Lectin, galactose binding, soluble 3	4
LILRB4	Leukocyte immunoglobulin-like receptor, subfamily b, member 4	4
LYZS	Lysozyme	4
MSN	Moesin	4
NEFL	Neurofilament, light polypeptide	4
NFKBIA	Nuclear factor of kappa light chain gene enhancer in b-cells inhibitor, alpha	4
PLEK	Pleckstrin	4
PSMB8	Proteosome (prosome, macropain) subunit, beta type 8 (large multifunctional peptidase 7)	4
PTPRC	Protein tyrosine phosphatase, receptor type, c	4
PYCARD	Pyd and card domain containing	4
RAB31	Riken cdna 1700093e07 gene	4
RPH3A	Rabphilin 3a	4
S100A4	S100 calcium binding protein a4	4
SPP1	Secreted phosphoprotein 1	4
TLR2	Toll-like receptor 2	4
TNFRSF1A	Tumor necrosis factor receptor superfamily, member 1a	4
TRIM30	Tripartite motif protein 30	4
TTC3	Tetratricopeptide repeat domain 3	4
TTR	Transthyretin	4
ABHD4	Abhydrolase domain containing 4	3
ACTA2	Actin, alpha 2, smooth muscle, aorta	3
ACTB	Actin, beta, cytoplasmic	3
ADAM23	A disintegrin and metallopeptidase domain 23	3
ALDH1A1	Aldehyde dehydrogenase family 1, subfamily a1	3
ATP1B1	Atpase, na+/k+ transporting, beta 1 polypeptide	3
ATP1B2	Atpase, na+/k+ transporting, beta 2 polypeptide	3
ATP6V1A	Atpase, h+ transporting, lysosomal v1 subunit a	3
BC032204	Expressed sequence c79673	3
BCL2A1D	B-cell leukemia/lymphoma 2 related protein a1d	3
C3	Complement component 3	3
CALM3	Calmodulin 1	3
CAMK2B	Calcium/calmodulin-dependent protein kinase ii, beta	3
CAR8	Carbonic anhydrase 8	3
CCL12	Chemokine (c-c motif) ligand 12	3
CCL3	Chemokine (c-c motif) ligand 3	3
CCL6	Chemokine (c-c motif) ligand 6	3
CCNC	Cyclin c	3
CD44	Cd44 antigen	3
CSF1	Colony stimulating factor 1 (macrophage)	3
CTLA2B	Cytotoxic t lymphocyte-associated protein 2 beta	3
CTNNB1	Catenin (cadherin associated protein), beta 1	3

Cited genes have been found in at least three studies.

Table 2. List of DEGs collected from reviewed publications (continued).

Gene symbol	Gene name	No. of citations
CTSA	Protective protein for beta-galactosidase	3
CTSK	Cathepsin k	3
CX3CR1	Chemokine (c-x3-c) receptor 1	3
CYBB	Cytochrome b-245, beta polypeptide	3
D12ERTD647E	Dna segment, chr 12, erato doi 647, expressed	3
DDR1	Discoidin domain receptor family, member 1	3
EIF5A	Eukaryotic translation initiation factor 5a	3
EXT2	Exostoses (multiple) 2	3
FCGR1	Fc receptor, igg, high affinity i	3
GBP2	Guanylate nucleotide binding protein 2	3
GJA1	Gap junction membrane channel protein alpha 1	3
GLUL	Glutamate-ammonia ligase (glutamine synthetase)	3
GNB4	Guanine nucleotide binding protein, beta 4	3
GNG5	Guanine nucleotide binding protein (g protein), gamma 5 subunit	3
GSTM1	Glutathione s-transferase, mu 1	3
GUSB	Beta-glucuronidase structural	3
HIST1H1C	Histone 1, h1c	3
HRSP12	Heat-responsive protein 12	3
HSPB1	Heat shock protein 1	3
IFI30	Interferon gamma inducible protein 30	3
IGFBP5	Insulin-like growth factor binding protein 5	3
IIGP1	Interferon inducible gtpase 1	3
ITGB5	Integrin beta 5	3
LPL	Lipoprotein lipase	3
LYN	Yamaguchi sarcoma viral (v-yes-1) oncogene homolog	3
LYZ	P lysozyme structural	3
MAFB	V-maf musculoaponeurotic fibrosarcoma oncogene family, protein b (avian)	3
MAN2B1	Mannosidase 2, alpha b1	3
MBP	Myelin basic protein	3
MCOLN1	Mucolipin 1	3
MS4A6D	Membrane-spanning 4-domains, subfamily a, member 6d	3
MT2	Metallothionein 2	3
MTAP4	Microtubule-associated protein 4	3
MYH11	Myosin, heavy polypeptide 11, smooth muscle	3
NCALD	Neurocalcin delta	3
NCF1	Neutrophil cytosolic factor 1	3
NEFM	Neurofilament 3, medium	3
NTRK2	Neurotrophic tyrosine kinase, receptor, type 2	3
OASL2	2′′-5′ oligoadenylate synthetase-like 2	3
PARP3	Poly (adp-ribose) polymerase family, member 3	3
PCMT1	Protein-l-isoaspartate (d-aspartate) o-methyltransferase 1	3
PDLIM4	Pdz and lim domain 4	3
PHPT1	Phosphohistidine phosphatase 1	3
PLEKHB2	Riken cdna 2310009m15 gene	3
PMP22	Peripheral myelin protein	3

Cited genes have been found in at least three studies.

Table 2. List of DEGs collected from reviewed publications (continued).

Gene symbol	Gene name	No. of citations
PROS1	Protein s (alpha)	3
PTBP1	Polypyrimidine tract binding protein 1	3
PTPN6	Protein tyrosine phosphatase, non-receptor type 6	3
PTPRZ1	Protein tyrosine phosphatase, receptor type z, polypeptide 1	3
QK	Quaking	3
RAB1	Rab1, member ras oncogene family	3
RALGDS	Ral guanine nucleotide dissociation stimulator	3
RASA2	Ras p21 protein activator 2	3
RGS2	Regulator of g-protein signaling 2	3
RNASE4	Ribonuclease, rnase a family 4	3
RPL4	Ribosomal protein l4	3
RUNX1	Runt related transcription factor 1	3
S100B	S100 protein, beta polypeptide, neural	3
SGPP1	Sphingosine-1-phosphate phosphatase 1	3
SLC11A1	Solute carrier family 11 (proton-coupled divalent metal ion transporters), member 1	3
SLC1A3	Solute carrier family 1 (glial high affinity glutamate transporter), member 3	3
SLC4A4	Solute carrier family 4 (anion exchanger), member 4	3
SOCS3	Suppressor of cytokine signaling 3	3
SORL1	Sortilin-related receptor, ldlr class a repeats-containing	3
SUCLA2	Succinate-coenzyme a ligase, adp-forming, beta subunit	3
TCFCP2L1	Riken cdna 4932442m07 gene	3
TIMP1	Tissue inhibitor of metalloproteinase 1	3
TM2D1	Tm2 domain containing 1	3
TMSB4X	Thymosin, beta 4, x chromosome	3
TOB2	Transducer of erbb2, 2	3
TREM2	Triggering receptor expressed on myeloid cells 2c	3
TRPC4	Transient receptor potential cation channel, subfamily c, member 4	3
TSC22D4	Riken cdna 1700023b23 gene	3
UCHL5	Ubiquitin carboxyl-terminal esterase l5	3
UCP2	Uncoupling protein 2 (mitochondrial, proton carrier)	3
VAMP1	Vesicle-associated membrane protein 1	3

Cited genes have been found in at least three studies.
DEG: Differentially expressed gene.

Lysosomes are potential sites for PrP^{Sc} conversion and their activity is altered during prion infection, as revealed by microarray analyses. Therefore, the lysosomal pathway represents a potential drug target. Tricyclic compounds, such as quinacrine and chloroquine, are lysosomotropic factors. Though modest improvements have been registered in CJD patients, preclinical and clinical quinacrine tests gave controversial results [75,78,80]. Several DEGs are also involved in proteolysis. Cysteine preotease inhibitors have been tested on infected cells reducing PrP^{Sc} levels [86].

The immune response and the inflammation are altered processes in prion disorders. Pentosan polysulfate, an anti-inflammatory drug, competes with endogenous glycosaminoglycans for the interaction with PrP^{C} and/or PrP^{Sc}, preventing the conversion and decreasing neuronal death [26,75,78,80,87].

Another crucial pathway in neurodegeneration, confirmed by microarray experiments, concerns apoptosis. Pifitrin-α a p53 inhibitor, causes the decrease of caspase-3. Although infected cells treated with Pifitrin-α showed a dose-dependent decrease of prion levels, *in vivo* studies did not evidence improvements in incubation time, astrogliosis and spongiosis [88]. Flupirtine, a non-opioid analgesic anti-apoptotic drug, has also been tested on CJD patients. It increases the Bcl-2 and glutathione synthetase expression levels [89]. Flupirtine administration to CJD patients brought some benefits to

Table 3. List of altered pathways obtained using Kyoto encyclopedia of genes and genomes and gene ontology.

Pathway	Count	p Value	Genes
Innate and adaptive inflammatory host defenses	38	0.0421	CYBB, MSN, CTNNB1, NCF1, CYBA, ACTB, NFKBIA, PTPN6, FCGR2B, LYN, BLNK, PTPN6, FCGR3, TYROBP, ITGB2, H2-D1, CD48, FCER1G, CCL3, CX3CR1, TNFRSF1A, CSF1R, CCL9, CCL12, CSF1, CCL6, CXCL10, OSMR, B2M, CTSL, H2-K1, IFI30, CTSB, CTSS,SPP1, CD14, CD86, TLR2
Hematopoietic cell lineage	6	0.0366	CSF1R, FCGR1, CD14, CSF1, CD44, CD9
Alzheimer's disease	6	0.0003	APOE, C1QC, LPL, C1QB, C1QA, A2M
Complement and coagulation cascades	7	0.0046	C1QC, C3, C1QB, C4B, C1QA, A2M, C3AR1
Biosynthesis of steroids	3	0.0938	HMGCR, IDI1, SC4MOL
Response to stress	37	4.8E-11	DNAJA1, HSPB1, RUNX1, C4B, CRYAB, FCER1G, NCF1, CXCL10, CD9, FCGR2B, TNFRSF1A, FCGR3, FCGR1, CD14, CCL12, CD44, C1QA, CTSB, LY86, APOE, PYCARD, C1QC, CLEC7A, PROS1, S100B, GJA1, NEFL, C1QB, C3, TLR2, C3AR1, TSC22D4, CCL3, SPP1, SERPINA3N, SGK, PRDX6
Proteolysis	22	0.0006	ABHD4, PYCARD, CTSA, C1QC, CTSL, S100B, PSMB8, C1QB, C3, C4B, C3AR1, CTSS, CTSD, UCHL5, CTSZ, CTSC, TIMP1, CTSK, C1QA, CTSH, CTSB, ADAM23
Cell differentiation	39	0.00111	TM2D1, MYH11, BCL2A1A, BCL2A1D, EIF5A, EXT2, LYZS, LYZ, SOX9, CSF1, RUNX1, FCER1G, SGPP1, TCFCP2L1, PTPRZ1, TNFRSF1A, FCGR3, FCGR1, EGR1, S100A6, APOE, PYCARD, NFKBIA, CTNNB1, NEFM, ALDH1A1, S100B, GJA1, NEFL, LYN, IRF8, NTRK2, PTPRC, QK, SPP1, TIMP1, MAFB, SGK, CLU
Alcohol metabolic process	12	0.0008	APOE, SORL1, ALDOC, LDLR, MDH1, HMGCR, IDI1, MAN2B1, SC4MOL, SGPP1, HMGCS1, ABCA1,
Vesicle-mediated transport	15	0.0016	SORL1, CTNNB1, CLEC7A, C3, FCER1G, MCOLN1, ABCA1, RAB1, FCGR2B, LDLR, FCGR3, NCALD, FCGR1, RPH3A, VAMP1
Lipid metabolic process	18	0.0034	APOE, ABHD4, SORL1, GRN, HMGCR, IDI1, NCF1, SC4MOL, SGPP1, ABCA1, QK, LDLR, TNFRSF1A, HPGD, LPL, HMGCS1, HEXB, PRDX6
Regulation of apoptosis	14	0.0050	APOE, TM2D1, PYCARD, BCL2A1A, BCL2A1D, S100B, ALDH1A1, SOX9, NEFL, FCER1G, PTPRC, SPP1, FCGR3, FCGR1
Biological adhesion	17	0.0106	CD84, ITGAX, CLEC7A, CTNNB1, PROS1, DDR1, ATP1B2, SOX9, CSF1, CD9, ITGB5, GPNMB, SPP1, BC032204, ITGB2, CD44, ADAM23
Ion homeostasis	8	0.0125	APOE, PTPRC, MT2, S100B, TRF, SLC4A4, C3AR1, HEXB
Response to chemical stimulus	18	0.0002	APOE, NFKBIA, MT2, LYN, HSPB1, TLR2, FCER1G, CXCL10, C3AR1, CCL3, SPP1, FCGR3, CCL9, CCL12, ITGB2, CCL6, CTSB, PRDX6

cognitive functions, less deterioration in the dementia tests, but no differences in survival [80,90].

Transcriptome analysis of prion-infected samples identified some DEGs playing a role in oxidative stress, a crucial pathway in neuronal cell death. Antioxidant compounds – polyphenolic molecules, coenzyme Q-10, vitamins, NADH, minerals and others – decrease PrP^{Sc} propagation in infected cells [91]. Administration of these compounds to CJD patients revealed clinical improvements, including responsiveness, myoclonus, apnoeic episodes and rigidity [80,92].

10. Expert opinion

Microarray technology has been demonstrated to be a useful tool to simultaneously monitor the expression levels of thousands of genes and to study the effects of treatments, diseases and biological processes on gene expression. In particular, gene expression profiling can be used to identify altered transcripts in response to pathogens, such as prions, and to select potential targets for novel therapeutic approaches.

Although the reviewed studies demonstrate scarce reproducibility between different laboratories and manufacturers, several overlapping genes and metabolic pathways were found (**Tables 2** and **3**). This heterogeneity may be due to various aspects: different biological systems – cell cultures, mouse brain areas or mouse whole brains, sheep and CJD patient post-mortem brains – and genetic background of the host; prion strain and titer used for inoculation as well as the inoculation method; microarray platforms, working strategy and algorithms for analysis and statistical thresholds for significance selection (**Table 4**).

Table 4. List of the reviewed references.

Authors	Year	Biological system		Technology	Disease stage	Biological processes
		Host tissue/cell line	Prion strain			
Duguid *et al.* [30]	1988	Syrian hamster brain	263K	cDNA library subtractive hybridization	Late clinical stage	Astrocyte activation, ion-binding proteins, stress response
Duguid *et al.* [31]	1989	Syrian hamster brain	263K	cDNA library subtractive hybridization	Late clinical stage	Lipid transport, iron transport
Duguid and Dinauer [32]	1990	Syrian hamster brain	263K	cDNA library subtractive hybridization	Late clinical stage	Inflammatory response
Diedrich *et al.* [45]	1991	C57BL/6 mouse brain	22L	cDNA library differential screening	Late clinical stage	Lipid transport, protein degradation
Doh-ura *et al.* [46]	1995	Murine neuroblastoma cells N2a	Persistent infection with scrapie	cDNA library differential screening		Protein folding and degradation, heparin-binding proteins
Cosseddu *et al.* [47]	2007	Romanov sheep midbrain, thalamus, cerebellum, temporal cortex	Scrapie	Subtractive suppressive hybridization	Clinical stage	Cell growth and division, spatial learning, signal cascade, mitochondrial functions, vescicular transport pathways
Baker and Manuelidis [48]	2003	Microglia cells (~ 95% CD11b+ cells) from mouse brain	Fukuoka strain of CJD	Mouse 1.2 II expression array (Clonotech)		Inflammation, intercellular communication, chemotaxis and migration, antibody receptors proteases and protease inhibitors, cell differentiation, lipid metabolism, matrix and cytoskeleton
Greenwood *et al.* [49]	2005	Murine neuroblastoma cell (N2a, GT1)	Persistent infection with RML-Chandler	DNA-chip, probes from the Lion Bioscience mouse array-TAG clone set.		Transport proteins, ATP-binding and calcium-binding proteins

*Prion-specific altered pathways, resulting from the comparison between RML- and cuprizone-treated mice.

BMAP: Brain Molecular Anatomy Project; BSE: Bovine spongiform encephalopathy; CJD: Creutzfeldt-Jakob disease; DPI: Days post-inoculation; EST: Expressed sequence tag; GAG : Glycosaminoglycan; GPI: Glycophosphatidylinositol; MPI: Months post-inoculation; sCJD: Sporadic CJD.

Table 4. List of the reviewed references (continued).

Authors	Year	Biological system		Technology	Disease stage	Biological processes
		Host tissue/cell line	Prion strain			
Martinez and Pascual [50]	2007	Human neuroblastoma cells (SH-SY5Y)	Neurotoxix prion fragment (PrP106 – 126)	Affymetrix U133A Plus 2.0 human genome array		Protein metabolism, folding and transport, in cell cycle regulation, transcriptional regulation and mitochondrial functions
Julius *et al.* [52]	2008	Murine neuroblastoma cells (N2aPK1, CAD, GT1)	RML	Affymetrix MOE430A and MOE430B chips		No altered processes
Bach *et al.* [53]	2009	Murine neuroblastoma cell (N2a)	22L	Home-made array containing 20,000 cDNA mouse array-TAG		Cholesterol biosynthesis
Brown *et al.* [54]	2004	C57BLxVM/Dk mouse hippocampus	ME7	Clontech Atlas Mouse 1.2 Array and Atlas Mouse 1.2 Array II	Terminal stage	Microglia activation, lysosomal activation, apoptosis regulation
Brown *et al.* [55]	2005	C57BLxVM/Dk mouse hippocampus	ME7	Affymetrix MG-U74Av2	170 DPI (early stage)	Oxidative stress-response, endoplasmic reticulum homeostasis, mitochondrial apoptotic pathway, protein degradation and trafficking, cholesterol and lipid biosynthesis and metabolism, transcription and chromatin architecture regulation
Riemer *et al.* [56]	2004	C57BL/6 mouse cortex, medulla, pons	139A	Affymetrix MG-U74Av3	Terminal stage	Inflammatory reactions, immune response and stress response, complement system proteins, enzymes that generate cytotoxic superoxide anion radicals, cathepsins, acute phase proteins, transcription factors, cholesterol biosynthesis

*Prion-specific altered pathways, resulting from the comparison between RML- and cuprizone-treated mice.

BMAP: Brain Molecular Anatomy Project; BSE: Bovine spongiform encephalopathy; CJD: Creutzfeldt-Jakob disease; DPI: Days post-inoculation; EST: Expressed sequence tag; GAG : Glycosaminoglycan; GPI: Glycophosphatidylinositol; MPI: Months post-inoculation; sCJD: Sporadic CJD.

Table 4. List of the reviewed references (continued).

Authors	Year	Biological system		Technology	Disease stage	Biological processes
		Host tissue/cell line	Prion strain			
Booth *et al.* [58]	2004	C57BL/6 mouse brain	ME7 and 79a	BMAP 3′ EST library cDNA array	Clinical signs appearance Time course (20 DPI, 100 DPI, end point)	Protese/peptideolysis, lysosomal functions, lipid binding, defence and immunity, cell communication, cell death, cell differentiation, cell growth regulation, cell organization and biogenesis, hormone metabolism, ion transport, microtubule-based process, oxygen transport, hematopoietic system
Sorensen *et al.* [59]	2008	C57BL/6 mouse brain VM mouse brain	22L, ME7 and 79a 22L, ME7 and 79a	BMAP 3′ EST library cDNA array	Onset of clinical symptoms	Lipid metabolism, nervous system function, synaptic transmission, cytoskeleton organization and biogenesis, protein biosynthesis and folding, lysosome organization and biogenesis, proteolysis, apoptosis, immune cell activation and inflammatory response
Skinner *et al.* [60]	2006	C57BL/10 mouse brain	ME7, 22L and RML-Chandler	BMAP library cDNA array	104 and 146 DPI	Protein folding and degradation, endosome/lysosome functions, immune response, cytoskeleton organization, metal ion binding, calcium regulation, pumps and ion channels, signaling cascade, transcription/translation, mitochondrial functions, carbohydrate processing, lipid metabolism and synapse function
Xiang *et al.* [61]	2004	C57BL/6 mouse brain	ME7	Mouse expression array 430A Affymetrix	30, 60, 90, 120 DPI and terminal stage	Proteolysis, protease inhibition, cell growth and maintenance, immune response, signal transduction, cell adhesion and molecular metabolism

*Prion-specific altered pathways, resulting from the comparison between RML- and cuprizone-treated mice.

BMAP: Brain Molecular Anatomy Project; BSE: Bovine spongiform encephalopathy; CJD: Creutzfeldt-Jakob disease; DPI: Days post-inoculation; EST: Expressed sequence tag; GAG : Glycosaminoglycan; GPI: Glycophosphatidylinositol; MPI: Months post-inoculation; sCJD: Sporadic CJD.

Table 4. List of the reviewed references (continued).

Authors	Year	Biological system		Technology	Disease stage		Biological processes
		Host tissue/cell line	Prion strain				
Xiang *et al.* [57]	2007	C57BL/6 mouse brain	ME7 and RML	Mouse expression array 430A Affymetrix	30, 60, 90, 120 DPI and terminal stage		Cholesterol metabolism, immune system, translational terminators, cofactors and ubiquinone metabolism
Miele *et al.* [62]	2008	C57BL/6 mouse brain	RML	Affymetrix MOE430A and MOE430B	145 DPI		Serine-type endopeptidase inhibitors in acute phase response
Hwang *et al.* [63]	2009				Harvest interval	End point	Microglia and astrocytes activation, lysosomal protease, cholesterol, GAG and androgen metabolism, iron homeostasis, heme metabolism, prostaglandin and androgen metabolism
		C57BL/6J mouse brain	RML	Affymetrix GeneChip Mouse Genome 430 2,0 array	2 weeks	23 weeks	
			301V		4 weeks	41 weeks	
		C57BL/6.I-1 mouse brain	RML		4 weeks	48 weeks	
			301V		2 weeks	18 weeks	
		FVB/Ncr mouse brain	RML		2 weeks	22 weeks	
		FVB-Tg(PrP-A)4053 mouse brain	RML		1 weeks	8 weeks	
		(FVB x FVB.129-*Prnp*$^{tm\ 1\ Zrch}$)F1 (0/+)	RML		4 weeks	56 weeks	
		Prnp0/+ mouse brain	RML		4 weeks	28 or 51 weeks	
Moody *et al.* [65]	2009	C57BL/6 mouse brain	RML	Affymetrix GeneChip Mouse Genome 430 2,0 array	108, 158, a98 DPI		Neuropeptide signaling, adipocytokine signaling*
Barret *et al.* [67]	2005	Murine neuroblastoma cell (N2a, GT1)	Persistent infection with RML-Chandler	Home-made array containing 165 DNA hybridization units specific of the main murine glycosylation-related genes			Chondroitin sulfate synthesis, 4-*O*-sulfation of non-reducing *N*-acetylgalactosamine residues

*Prion-specific altered pathways, resulting from the comparison between RML- and cuprizone-treated mice.

BMAP: Brain Molecular Anatomy Project; BSE: Bovine spongiform encephalopathy; CJD: Creutzfeldt-Jakob disease; DPI: Days post-inoculation; EST: Expressed sequence tag; GAG : Glycosaminoglycan; GPI: Glycophosphatidylinositol; MPI: Months post-inoculation; sCJD: Sporadic CJD.

Table 4. List of the reviewed references (continued).

Authors	Year	Biological system		Technology	Disease stage	Biological processes
		Host tissue/cell line	Prion strain			
Guillerme-Bosselut *et al.* [68]	2009	C57BL/6 (tg338, overexpressing PrP^{VRQ}) mouse brain	127S	Home-made array containing 165 DNA hybridization units specific of the main murine glycosylation-related genes	60 DPI	GM2 ganglioside degradation, sialic acid residue transfer, synthesis of glycan structures involved in the inflammatory response, glycosyltransferase activity, GPI biosynthesis, α-series gangliosides synthesis
Sawiris *et al.* [73]	2007	VM mouse brain	301V BSE	m17k Array	Onset of all BSE symptoms	Ubiquitin-mediated protein degradation, protein folding, apoptosis, zinc-binding proteins, calcium ion binding, transcription regulation
Tang *et al.* [74]	2009	Friesian or Holstein–Friesian cattle brain stem	BSE	Affymetrix bovine genome geneChips	6, 21, 27, 36, 39, 45 MPI	Metabolism, transcription and translation, immune response and transport
Xiang *et al.* [51]	2005	Human frontal cortex	sCJD	Affymetrix HGU133A arrays	Post mortem	Stress and immune response, cell cycle, cell death, protein metabolism, ion transport and synaptic functions

*Prion-specific altered pathways, resulting from the comparison between RML- and cuprizone-treated mice.

BMAP: Brain Molecular Anatomy Project; BSE: Bovine spongiform encephalopathy; CJD: Creutzfeldt-Jakob disease; DPI: Days post-inoculation; EST: Expressed sequence tag; GAG : Glycosaminoglycan; GPI: Glycophosphatidylinositol; MPI: Months post-inoculation; sCJD: Sporadic CJD.

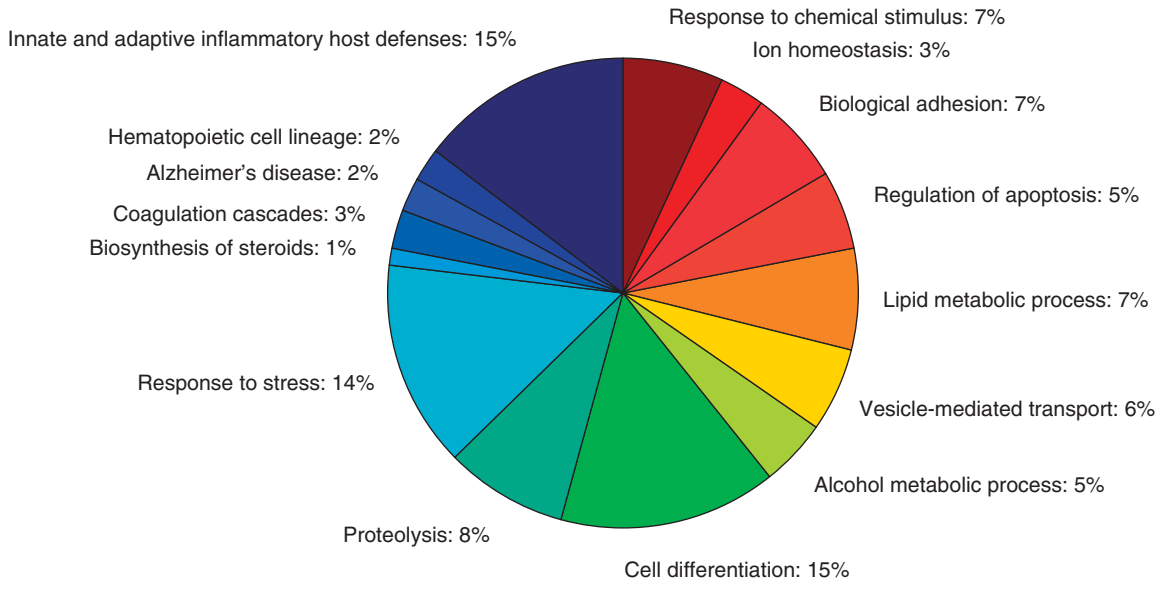

Figure 1. Pie chart of the most altered metabolic pathways, as reported in Table 3.

Several drugs have been tested for their anti-prion activity. These compounds, as reported above, act on cholesterol biosynthesis, lysosomal activity, immune response and inflammation and play a role against oxidative stress (**Table 1**). Although these drugs operate on the pathways identified by microarray analyses (**Figure 1**), so far, no effective cures have been found against prion diseases.

Genes belonging to a metabolic or biological process often share enzymatic reactions with other pathways, such as ApoE and ApoD. ApoE holds roles in lipid metabolic process, regulation of apoptosis, ion homeostasis, response to chemical stimuli and stress, cell differentiation and alcohol metabolic process. ApoD occurs in the macromolecular complex with lecithin–cholesterol acyltransferase, transports and binds bilin and other ligands. Moreover, ApoD inhibits translocation of phosphorylated MAPKs into the nucleus [93], altering the MAPK-dependent transcriptional regulation. Because MAPK pathways are altered during prion infection [94] and cellular protein–protein networks are complex, the trigger remains still unknown. In addition, drugs acting on cholesterol biosynthesis can disrupt the lipid raft domains, altering both protein locations and synaptic functions, and cause significant injuries.

Metal ion homeostasis is yet another altered pathway during prion infection. Almost all physiological processes are governed by metal ions – calcium, sodium, magnesium, manganese, iron, copper and zinc – through allosteric and prosthetic regulations, or electrostatic interactions. Alterations of their homeostasis affect ATP production, action potential, protein synthesis and metabolism, vesicle transport, osmotic pressure and apoptosis. Incorporation of metal ions into apo-proteins takes place in organs other than the brain, such as the liver. Metal ions dysmetabolism prompts the coexistence of multi-factorial events during neurodegeneration.

Many drugs used to cure prion diseases through their direct action on altered pathways manifest important effects on unaltered pathways (**Table 5**). Statins showed weak therapeutic effects on mice inhibiting endogenous cholesterol production. They also affect related pathways such as Ras- and Rho-signaling as well as ubiquinone. D-penicillamine used as copper chelator acts as an immunosuppressor by reducing numbers of T-lymphocytes, inhibiting macrophage function, decreasing IL-1, decreasing rheumatoid factor and preventing collagen from crosslinking. Quinacrine also acts on histamine metabolism, muscarinic acetylcholine receptor M1 and arachidonic acid 5-lipoxygenase. ApoE and ApoD are involved in several other disorders such as PD and AD. The commonalities among prion diseases and PD and AD disorders highlight either similar neurodegenerative molecular mechanisms or similar pathological secondary events. To establish suitable drug targets for prion disorders, a more stringent and specific approach is requested. Comparative analyses of altered pathways of prion diseases, PD and AD could expose characteristic gene targets.

Microarray analyses on prion-infected samples evaluate the transcriptional variations following the onset of prion pathology. Because many ligands are required to maintain proteins in an active form, gene expression profile *per se* is not sufficient to fully understand the molecular mechanisms involved in neurodegeneration. Are those altered genes translated in an active form? How does metal ions deregulation affect overall enzymatic activities.

In order to select the best target for therapeutic treatments, gene expression profiling has to be associated with functional proteomics and physiology. For instance, it is worth noting

Table 5. List of drug targets in prion diseases and their side effects on unaltered pathways.

Drug	Target pathway altered in prion disease	Examples of target pathway not altered in prion disease
Polyene antibiotics (methotrexate, amphotericin B, mepartricin and filipin)	Lipid raft conformation alteration	Methotrexate: DNA replication, DNA repair and cell cycles alteration Amphotericin B: permeability alteration in mammalian cells also Mepartricin: estrogen biosynthesis
Quinacrine	Lysosomal pathway	Histamine metabolism (histamine methyltransferase inhibition); arachidonic acid balance deregulation that induces oxidative stress and neuroinflammation (phospholipase-A2 inhibition)
Chloroquine	Lysosomal pathway	Lymphocyte proliferation and phospholipase A inhibition, enzymes release from lysosomes, reactive oxygen species release from macrophages, IL-1 production
Leupeptin	Lysosomal pathway (cysteine–protease inhibitors)	Ion homeostasis, integrin signaling pathway, PTP1B signaling, T-cell apoptosis, cdk5 deregulation in Alzheimer's disease
Statins	Cholesterol biosynthesis inhibition	Ras- and Rho-signaling as well as ubiquinone
Pifitrin-α	Apoptosis (p53 inhibition, caspase-3 decrease)	Interference with heat shock and glucocorticoid receptor signaling
D-Penicillamine	Ion homeostasis (copper chelator)	T-lymphocytes reduction, macrophage function inhibition, IL-1 and rheumatoid factor decrease and collagen crosslinking prevention

that most of known enzymatic chains have a negative feedback regulatory mechanism. Rational drug design should be addressed to restore or modulate the endogenous enzymatic activity instead of replacing its products.

New experiments focused on understanding of the molecular reasons behind pathways or protein activity alterations must be performed. Therefore, once an altered pathway is discovered, it will be crucial to analyze the physiological state of all its components, assess the damage and design specific drugs restoring its functionality.

The similarity in symptoms, as for AD and PD, and multi-factorial events require a multi-disciplinary approach to neurodegenerative diseases. While microarray analyses can highlight altered genes and biological pathways, proteomics and physiology ought to confirm such alterations, and, therefore, ensure the identification of the best drug targets. However, to achieve synergistic outcomes from a multi-disciplinary approach to neurodegenerative disorders treatments, new breakthrough bioinformatics tools capable of integrating and interpreting large amounts of information will represent a much sought after endeavor in the coming years.

Acknowledgements

The authors thank G Furlan for English editing of the manuscript.

Declaration of interest

This work was supported by grants from Italian Institute of Technology, SISSA-ISAS Unit to F Benetti and G Legname, and from Compagnia di San Paolo and Ministero della Salute to G Legname.

Bibliography

1. Prusiner SB. Prions. Proc Natl Acad Sci USA 1998;95(23):13363-83
2. Doherr MG. Brief review on the epidemiology of transmissible spongiform encephalopathies (TSE). Vaccine 2007;25(30):5619-24
3. Legname G, Baskakov IV, Nguyen HO, et al. Synthetic mammalian prions. Science 2004;305(5684):673-6
4. Hill AF, Antoniou M, Collinge J. Protease-resistant prion protein produced in vitro lacks detectable infectivity. J Gen Virol 1999;80(Pt 1):11-4
5. Cohen FE, Prusiner SB. Pathologic conformations of prion proteins. Annu Rev Biochem 1998;67:793-819
6. Telling GC, Parchi P, DeArmond SJ, et al. Evidence for the conformation of the pathologic isoform of the prion protein enciphering and propagating prion diversity. Science 1996;274(5295):2079-82
7. Laurent M. Autocatalytic processes in cooperative mechanisms of prion diseases. FEBS Lett 1997;407(1):1-6
8. Telling GC, Haga T, Torchia M, et al. Interactions between wild-type and mutant prion proteins modulate neurodegeneration in transgenic mice. Genes Dev 1996;10(14):1736-50
9. Kanaani J, Prusiner SB, Diacovo J, et al. Recombinant prion protein induces rapid polarization and development of synapses in embryonic rat hippocampal neurons in vitro. J Neurochem 2005;95(5):1373-86
10. Lopes MH, Hajj GN, Muras AG, et al. Interaction of cellular prion and stress-inducible protein 1 promotes neuritogenesis and neuroprotection by distinct signaling pathways. J Neurosci 2005;25(49):11330-9
11. Santuccione A, Sytnyk V, Leshchyns'ka I, Schachner M. Prion protein recruits its neuronal receptor NCAM to lipid rafts to activate p59fyn and to enhance neurite outgrowth. J Cell Biol 2005;169(2):341-54
12. Steele AD, Emsley JG, Ozdinler PH, et al. Prion protein (PrPc) positively regulates neural precursor proliferation during developmental and adult mammalian neurogenesis. Proc Natl Acad Sci USA 2006;103(9):3416-21
13. Chen S, Mange A, Dong L, et al. Prion protein as trans-interacting partner for neurons is involved in neurite outgrowth and neuronal survival. Mol Cell Neurosci 2003;22(2):227-33
14. Bounhar Y, Zhang Y, Goodyer CG, LeBlanc A. Prion protein protects human neurons against Bax-mediated apoptosis. J Biol Chem 2001;276(42):39145-9
15. Roucou X, Giannopoulos PN, Zhang Y, et al. Cellular prion protein inhibits proapoptotic Bax conformational change in human neurons and in breast carcinoma MCF-7 cells. Cell Death Differ 2005;12(7):783-95
16. Shyu WC, Chen CP, Saeki K, et al. Hypoglycemia enhances the expression of prion protein and heat-shock protein 70 in a mouse neuroblastoma cell line. J Neurosci Res 2005;80(6):887-94
17. Mitteregger G, Vosko M, Krebs B, et al. The role of the octarepeat region in neuroprotective function of the cellular prion protein. Brain Pathol 2007;17(2):174-83
18. Milhavet O, Lehmann S. Oxidative stress and the prion protein in transmissible spongiform encephalopathies. Brain Res Brain Res Rev 2002;38(3):328-39
19. Schmitt-Ulms G, Legname G, Baldwin MA, et al. Binding of neural cell adhesion molecules (N-CAMs) to the cellular prion protein. J Mol Biol 2001;314(5):1209-25
20. Sales N, Rodolfo K, Hassig R, et al. Cellular prion protein localization in rodent and primate brain. Eur J Neurosci 1998;10(7):2464-71
21. Sanchez-Alavez M, Conti B, Moroncini G, Criado JR. Contributions of neuronal prion protein on sleep recovery and stress response following sleep deprivation. Brain Res 2007;1158:71-80
22. Sanchez-Alavez M, Criado JR, Klein I, et al. Hypothalamic-pituitary-adrenal axis disregulation in PrPC-null mice. Neuroreport 2008;19(15):1473-7
23. Tobler I, Gaus SE, Deboer T, et al. Altered circadian activity rhythms and sleep in mice devoid of prion protein. Nature 1996;380(6575):639-42
24. Rachidi W, Chimienti F, Aouffen M, et al. Prion protein protects against zinc-mediated cytotoxicity by modifying intracellular exchangeable zinc and inducing metallothionein expression. J Trace Elem Med Biol 2009;23(3):214-23
25. Nishida N, Tremblay P, Sugimoto T, et al. A mouse prion protein transgene rescues mice deficient for the prion protein gene from purkinje cell degeneration and demyelination. Lab Invest 1999;79(6):689-97
26. Caughey B, Brown K, Raymond GJ, et al. Binding of the protease-sensitive form of PrP (prion protein) to sulfated glycosaminoglycan and congo red [corrected]. J Virol 1994;68(4):2135-41
27. Yang Y, Adelstein SJ, Kassis AI. Target discovery from data mining approaches. Drug Discov Today 2009;14(3-4):147-54
28. di Bernardo D, Thompson MJ, Gardner TS, et al. Chemogenomic profiling on a genome-wide scale using reverse-engineered gene networks. Nat Biotechnol 2005;23(3):377-83
29. Gardner TS, di Bernardo D, Lorenz D, Collins JJ. Inferring genetic networks and identifying compound mode of action via expression profiling. Science 2003;301(5629):102-5
30. Duguid JR, Rohwer RG, Seed B. Isolation of cDNAs of scrapie-modulated RNAs by subtractive hybridization of a cDNA library. Proc Natl Acad Sci USA 1988;85(15):5738-42
31. Duguid JR, Bohmont CW, Liu NG, Tourtellotte WW. Changes in brain gene expression shared by scrapie and Alzheimer disease. Proc Natl Acad Sci USA 1989;86(18):7260-4
32. Duguid JR, Dinauer MC. Library subtraction of in vitro cDNA libraries to identify differentially expressed genes in scrapie infection. Nucleic Acids Res 1990;18(9):2789-92
33. Brenner M, Johnson AB, Boespflug-Tanguy O, et al. Mutations in GFAP, encoding glial fibrillary acidic protein, are associated with Alexander disease. Nat Genet 2001;27(1):117-20
34. Rodriguez D, Gauthier F, Bertini E, et al. Infantile Alexander disease: spectrum of GFAP mutations and genotype-phenotype correlation. Am J Hum Genet 2001;69(5):1134-40
35. Aoki Y, Haginoya K, Munakata M, et al. A novel mutation in glial fibrillary acidic protein gene in a patient with Alexander disease. Neurosci Lett 2001;312(2):71-4

36. Sawaishi Y, Yano T, Takaku I, Takada G. Juvenile Alexander disease with a novel mutation in glial fibrillary acidic protein gene. Neurology 2002;58(10):1541-3

37. Stumpf E, Masson H, Duquette A, et al. Adult Alexander disease with autosomal dominant transmission: a distinct entity caused by mutation in the glial fibrillary acid protein gene. Arch Neurol 2003;60(9):1307-12

38. Brockmann K, Meins M, Taubert A, et al. A novel GFAP mutation and disseminated white matter lesions: adult Alexander disease? Eur Neurol 2003;50(2):100-5

39. Duguid J, Trzepacz C. Major histocompatibility complex genes have an increased brain expression after scrapie infection. Proc Natl Acad Sci USA 1993;90(1):114-7

40. Ebadi M, Iversen PL, Hao R, et al. Expression and regulation of brain metallothionein. Neurochem Int 1995;27(1):1-22

41. Karin M. Metallothioneins: proteins in search of function. Cell 1985;41(1):9-10

42. May PC, Finch CE. Sulfated glycoprotein 2: new relationships of this multifunctional protein to neurodegeneration. Trends Neurosci 1992;15(10):391-6

43. Stamatos C, Squicciarini J, Fine RE. Chick embryo spinal cord neurons synthesize a transferrin-like myotrophic protein. FEBS Lett 1983;153(2):387-90

44. Chowers I, Wong R, Dentchev T, et al. The iron carrier transferrin is upregulated in retinas from patients with age-related macular degeneration. Invest Ophthalmol Vis Sci 2006;47(5):2135-40

45. Diedrich JF, Minnigan H, Carp RI, et al. Neuropathological changes in scrapie and Alzheimer's disease are associated with increased expression of apolipoprotein E and cathepsin D in astrocytes. J Virol 1991;65(9):4759-68

46. Doh-ura K, Perryman S, Race R, Chesebro B. Identification of differentially expressed genes in scrapie-infected mouse neuroblastoma cells. Microb Pathog 1995;18(1):1-9

47. Cosseddu GM, Andreoletti O, Maestrale C, et al. Gene expression profiling on sheep brain reveals differential transcripts in scrapie-affected/not-affected animals. Brain Res 2007;1142:217-22

48. Baker CA, Manuelidis L. Unique inflammatory RNA profiles of microglia in Creutzfeldt-Jakob disease. Proc Natl Acad Sci USA 2003;100(2):675-9

49. Greenwood AD, Horsch M, Stengel A, et al. Cell line dependent RNA expression profiles of prion-infected mouse neuronal cells. J Mol Biol 2005;349(3):487-500

50. Martinez T, Pascual A. Identification of genes differentially expressed in SH-SY5Y neuroblastoma cells exposed to the prion peptide 106-126. Eur J Neurosci 2007;26(1):51-9

51. Xiang W, Windl O, Westner IM, et al. Cerebral gene expression profiles in sporadic Creutzfeldt-Jakob disease. Ann Neurol 2005;58(2):242-57

52. Julius C, Hutter G, Wagner U, et al. Transcriptional stability of cultured cells upon prion infection. J Mol Biol 2008;375(5):1222-33

53. Bach C, Gilch S, Rost R, et al. Prion-induced activation of cholesterogenic gene expression by Srebp2 in neuronal cells. J Biol Chem 2009;284(45):31260-9

54. Brown AR, Webb J, Rebus S, et al. Identification of up-regulated genes by array analysis in scrapie-infected mouse brains. Neuropathol Appl Neurobiol 2004;30(5):555-67

55. Brown AR, Rebus S, McKimmie CS, et al. Gene expression profiling of the preclinical scrapie-infected hippocampus. Biochem Biophys Res Commun 2005;334(1):86-95

56. Riemer C, Neidhold S, Burwinkel M, et al. Gene expression profiling of scrapie-infected brain tissue. Biochem Biophys Res Commun 2004;323(2):556-64

57. Xiang W, Hummel M, Mitteregger G, et al. Transcriptome analysis reveals altered cholesterol metabolism during the neurodegeneration in mouse scrapie model. J Neurochem 2007;102(3):834-47

58. Booth S, Bowman C, Baumgartner R, et al. Identification of central nervous system genes involved in the host response to the scrapie agent during preclinical and clinical infection. J Gen Virol 2004;85(Pt 11):3459-71

59. Sorensen G, Medina S, Parchaliuk D, et al. Comprehensive transcriptional profiling of prion infection in mouse models reveals networks of responsive genes. BMC Genomics 2008;9:114

60. Skinner PJ, Abbassi H, Chesebro B, et al. Gene expression alterations in brains of mice infected with three strains of scrapie. BMC Genomics 2006;7:114

61. Xiang W, Windl O, Wunsch G, et al. Identification of differentially expressed genes in scrapie-infected mouse brains by using global gene expression technology. J Virol 2004;78(20):11051-60

62. Miele G, Seeger H, Marino D, et al. Urinary alpha1-antichymotrypsin: a biomarker of prion infection. PLoS One 2008;3(12):e3870

63. Hwang D, Lee IY, Yoo H, et al. A systems approach to prion disease. Mol Syst Biol 2009;5:252

64. Gehlenborg N, Hwang D, Lee IY, et al. The Prion Disease Database: a comprehensive transcriptome resource for systems biology research in prion diseases. Database 2009, doi: 10.1093/database/bap011

65. Moody LR, Herbst AJ, Yoo HS, et al. Comparative prion disease gene expression profiling using the prion disease mimetic, cuprizone. Prion 2009;3(2):99-109

66. Russelakis-Carneiro M, Saborio GP, Anderes L, Soto C. Changes in the glycosylation pattern of prion protein in murine scrapie. Implications for the mechanism of neurodegeneration in prion diseases. J Biol Chem 2002;277(39):36872-7

67. Barret A, Forestier L, Deslys JP, et al. Glycosylation-related gene expression in prion diseases: PrPSc accumulation in scrapie infected GT1 cells depends on beta-1,4-linked GalNAc-4-SO4 hyposulfation. J Biol Chem 2005;280(11):10516-23

68. Guillerme-Bosselut F, Forestier L, Jayat-Vignoles C, et al. Glycosylation-related gene expression profiling in the brain and spleen of scrapie-affected mouse. Glycobiology 2009;19(8):879-89

69. Aguzzi A, Heikenwalder M. Pathogenesis of prion diseases: current status and future outlook. Nat Rev Microbiol 2006;4:765-75

70. Comelli EM, Head SR, Gilmartin T, et al. A focused microarray approach to functional glycomics: transcriptional regulation of the glycome. Glycobiology 2006;16(2):117-31

71. Costa C, Tortosa R, Vidal E, et al. Central nervous system extracellular matrix changes in a transgenic mouse model of bovine spongiform encephalopathy. Vet J 2009;182(2):306-14

72. Ritchie MA, Gill AC, Deery MJ, Lilley K. Precursor ion scanning for detection and structural characterization of heterogeneous glycopeptide mixtures. J Am Soc Mass Spectrom 2002;13(9):1065-77

73. Sawiris GP, Becker KG, Elliott EJ, et al. Molecular analysis of bovine spongiform encephalopathy infection by cDNA arrays. J Gen Virol 2007;88(Pt 4):1356-62

74. Tang Y, Xiang W, Hawkins SA, et al. Transcriptional changes in the brains of cattle orally infected with the bovine spongiform encephalopathy agent precede detection of infectivity. J Virol 2009;83(18):9464-73

75. Sakaguchi S. Recent developments in therapeutics for prion disease. Expert Opin Ther Patents 2008;18(1):35-9

76. Brajtburg J, Elberg S, Bolard J, et al. Interaction of plasma proteins and lipoproteins with amphotericin B. J Infect Dis 1984;149(6):986-97

77. Pocchiari M, Casaccia P, Ladogana A. Amphotericin B: a novel class of antiscrapie drugs. J Infect Dis 1989;160(5):795-802

78. Trevitt CR, Collinge J. A systematic review of prion therapeutics in experimental models. Brain 2006;129(Pt 9):2241-65

79. Masullo C, Macchi G, Xi YG, Pocchiari M. Failure to ameliorate Creutzfeldt-Jakob disease with amphotericin B therapy. J Infect Dis 1992;165(4):784-5

80. Stewart LA, Rydzewska LH, Keogh GF, Knight RS. Systematic review of therapeutic interventions in human prion disease. Neurology 2008;70(15):1272-81

81. Sviridov D, Nestel P, Watts G. Statins and metabolism of high density lipoprotein. Cardiovasc Hematol Agents Med Chem 2007;5(3):215-21

82. Taraboulos A, Scott M, Semenov A, et al. Cholesterol depletion and modification of COOH-terminal targeting sequence of the prion protein inhibit formation of the scrapie isoform. J Cell Biol 1995;129(1):121-32

83. Bate C, Salmona M, Diomede L, Williams A. Squalestatin cures prion-infected neurons and protects against prion neurotoxicity. J Biol Chem 2004;279(15):14983-90

84. Mok SW, Thelen KM, Riemer C, et al. Simvastatin prolongs survival times in prion infections of the central nervous system. Biochem Biophys Res Commun 2006;348(2):697-702

85. Kempster S, Bate C, Williams A. Simvastatin treatment prolongs the survival of scrapie-infected mice. Neuroreport 2007;18(5):479-82

86. Doh-Ura K, Iwaki T, Caughey B. Lysosomotropic agents and cysteine protease inhibitors inhibit scrapie-associated prion protein accumulation. J Virol 2000;74(10):4894-7

87. Caughey B, Raymond GJ. Sulfated polyanion inhibition of scrapie-associated PrP accumulation in cultured cells. J Virol 1993;67(2):643-50

88. Engelstein R, Grigoriadis N, Greig NH, et al. Inhibition of P53-related apoptosis had no effect on PrP(Sc) accumulation and prion disease incubation time. Neurobiol Dis 2005;18(2):282-5

89. Perovic S, Schroder HC, Pergande G, et al. Effect of flupirtine on Bcl-2 and glutathione level in neuronal cells treated in vitro with the prion protein fragment (PrP106-126). Exp Neurol 1997;147(2):518-24

90. Otto M, Cepek L, Ratzka P, et al. Efficacy of flupirtine on cognitive function in patients with CJD: a double-blind study. Neurology 2004;62(5):714-8

91. Kocisko DA, Baron GS, Rubenstein R, et al. New inhibitors of scrapie-associated prion protein formation in a library of 2000 drugs and natural products. J Virol 2003;77(19):10288-94

92. Drisko JA. The use of antioxidants in transmissible spongiform encephalopathies: a case report. J Am Coll Nutr 2002;21(1):22-5

93. Soiland H, Soreide K, Janssen EA, et al. Emerging concepts of apolipoprotein D with possible implications for breast cancer. Cell Oncol 2007;29(3):195-209

94. Nordstrom E, Fisone G, Kristensson K. Opposing effects of ERK and p38-JNK MAP kinase pathways on formation of prions in GT1-1 cells. FASEB J 2009;23(2):613-22

95. Sigurdsson EM, Brown DR, Alim MA, et al. Copper chelation delays the onset of prion disease. J Biol Chem 2003;278(47):46199-202

96. Hijazi N, Shaked Y, Rosenmann H, et al. Copper binding to PrPC may inhibit prion disease propagation. Brain Res 2003;993(1-2):192-200

97. Orem NR, Geoghegan JC, Deleault NR, et al. Copper (II) ions potently inhibit purified PrPres amplification. J Neurochem 2006;96(5):1409-15

Affiliation

Federico Benetti[1,2] PhD, Lisa Gasperini[3], Mattia Zampieri[4] & Giuseppe Legname[†5,6,7] PhD

[†]Author for correspondence

[1]Post doc, Laboratory of Prion Biology, Neurobiology Sector, Scuola Internazionale Superiore di Studi Avanzati-International School of Advanced Studies (SISSA-ISAS), Edificio Q1, Basovizza, Trieste, Italy

[2]Post doc, Italian Institute of Technology, SISSA-ISAS Unit, Trieste, Italy

[3]PhD student, Laboratory of Prion Biology, Neurobiology Sector, Scuola Internazionale Superiore di Studi Avanzati-International School of Advanced Studies (SISSA-ISAS), Edificio Q1, Basovizza, Trieste, Italy

[4]PhD student, Functional Analysis Sector, Scuola Internazionale Superiore di Studi Avanzati-International School of Advanced Studies (SISSA-ISAS), Trieste, Italy

[†5]Associate Professor, Laboratory of Prion Biology, Neurobiology Sector, Scuola Internazionale Superiore di Studi Avanzati-International School of Advanced Studies (SISSA-ISAS), Edificio Q1, Basovizza, Trieste, Italy

Tel: +39 040 375 6515; Fax: +39 040 375 6502; E-mail: legname@sissa.it

[6]Associate Professor, Italian Institute of Technology, SISSA-ISAS Unit, Trieste, Italy

[7]Associate Professor, ELETTRA Laboratory, Sincrotrone Trieste S.C.p.A, Trieste, Italy

Molecular and Cellular Neuroscience 47 (2011) 28–35

Contents lists available at ScienceDirect

Molecular and Cellular Neuroscience

journal homepage: www.elsevier.com/locate/ymcne

Aged PrP null mice show defective processing of neuregulins in the peripheral nervous system

Stefano Benvegnù [a], Lisa Gasperini [a], Giuseppe Legname [a,b,c,*]

[a] Laboratory of Prion Biology, Neurobiology Sector, Scuola Internazionale Superiore di Studi Avanzati (SISSA), via Bonomea 265, I-34136 Trieste, Italy
[b] ELETTRA Laboratory, Sincrotrone Trieste S.C.p.A., S.S. 14 Km 163.5, I-34149 Basovizza (TS), Trieste, Italy
[c] Italian Institute of Technology, SISSA Unit, via Bonomea 265, I-34136 Trieste, Italy

ARTICLE INFO

Article history:
Received 18 November 2010
Revised 1 February 2011
Accepted 10 February 2011
Available online 17 February 2011

Keywords:
Prion protein
Neuregulin
Aging
Nervous system

ABSTRACT

A prion, a protease-resistant conformer of the cellular prion protein (PrP^C), is the causative agent of transmissible spongiform encephalopathies or prion diseases. While this property is well established for the aberrantly folded protein, the physiological function of PrP^C remains elusive. Among different putative functions, the non-pathogenic protein isoform PrP^C is involved in several cellular processes. Here, we show that PrP^C regulates the cleavage of neuregulin-1 proteins (NRG1). Neuregulins provide key axonal signals that regulate several processes, including glial cells proliferation, survival and myelination. Interestingly, mice devoid of PrP^C ($Prnp^{0/0}$) were recently shown to have a late-onset demyelinating disease in the peripheral nervous system (PNS) but not in the central nervous system (CNS). We found that NRG1 processing is developmentally regulated in the PNS and, by comparing wildtype and $Prnp^{0/0}$ mice, that PrP^C influences NRG1 processing in old, but not in young, animals. In addition, we found that also the processing of neuregulin-3, another neuregulin family member, is altered in the PNS of $Prnp^{0/0}$ mice. These differences in neuregulin proteins processing are not paralleled in the CNS, thus suggesting a different cellular function for PrP^C between the CNS and the PNS.

Introduction

Prion diseases are fatal neurodegenerative diseases whose etiology is linked to the conversion of the cellular form of the prion protein (PrP), PrP^C, to a protease-resistant aberrant conformer, denoted as prion (Prusiner, 1982). Prion diseases include Creutzfeldt–Jakob disease, fatal familial insomnia and kuru in humans; bovine spongiform encephalopathy and scrapie in cows and sheep, respectively; and chronic wasting disease in free-ranging cervids including deer, elk and moose. The physiological function of PrP^C still remains enigmatic, although several putative roles have been proposed for different cellular functions, including synaptic activity (Herms et al., 1999), neurite outgrowth (Kanaani et al., 2005; Santuccione et al., 2005), neuroprotection (Bounhar et al., 2001) and maintenance of myelinated sheet (Radovanovic et al., 2005). Recently, mice lacking the PrP-encoding gene ($Prnp^{0/0}$) were shown to have a late-onset peripheral demyelinating polyneuropathy (Bremer et al., 2010) not observed in the central nervous system (CNS) of the same $Prnp^{0/0}$ mice.

Myelination and myelin maintenance are different physiological processes which require distinct axonal molecular signals acting on glial cells and supporting them at different developmental stages. One of the most studied molecular signals is mediated by neuregulin-1 proteins (NRG1) (Newbern and Birchmeier, 2010). The NRG1 contain an epidermal growth factor (EGF)-like domain that signals through the binding of ErbB receptor tyrosine kinases (Mei and Xiong, 2008). The best-defined function of NRG1 is the control of myelination in the peripheral nervous system (PNS), where NRG1 are essential for neuronal and glial survival (Garratt et al., 2000b; Jessen and Mirsky, 2005; Nave and Salzer, 2006). On the other hand, NRG1 role in the myelination of the CNS have not yet been established and, despite *in vitro* data, neuregulin protein family (NRG) signaling seems to be dispensable for CNS myelination *in vivo*, at least during postnatal stages (Brinkmann et al., 2008). This suggests that NRG1 may function differently in the PNS and CNS.

Gene transcripts encoding at least 14 different NRG1 isoforms have been identified (Fischbach and Rosen, 1997). The most common NRG1 isoforms in the nervous system are synthesized as transmembrane pro-proteins and are classified according to their different N-terminal domains (Falls, 2003). NRG1 type I and type II possess N-terminal

Abbreviations: PrP, prion protein; PrP^C, cellular form of the PrP; TSE, transmissible spongiform encephalopathy; APP, amyloid precursor protein; BACE1, β-site of APP cleaving enzyme-1; NRG, neuregulin protein family; NRG1, neuregulin-1 proteins; NRG1-FL, full length neuregulin-1 pro-proteins; NRG1-CTF, carboxy-terminal fragment of neuregulin-1 after proteolytic cleavage; NRG1-NTF, amino-terminal fragment of neuregulin-1 after proteolytic cleavage; NRG3, neuregulin-3; CHAPS, 3-[(3-cholamidopropyl)dimethylammonio]-1-propanesulfonate; HRP, horseradish peroxidase; Fab, recombinant antibody antigen-binding fragment.

* Corresponding author at: Scuola Internazionale Superiore di Studi Avanzati (SISSA), via Bonomea 265, 34136 Trieste, Italy. Fax: +39 040 3787 702.
E-mail address: legname@sissa.it (G. Legname).

1044-7431/$ – see front matter © 2011 Elsevier Inc. All rights reserved.
doi:10.1016/j.mcn.2011.02.005

immunoglobulin-like domains, while NRG1 type III is characterized by a cysteine-rich domain, which functions as a second transmembrane domain (Buonanno and Fischbach, 2001). Neuregulin-1 pro-proteins undergo protease-mediated proteolytic cleavage in the stalk region (Burgess et al., 1995; Lu et al., 1995; Loeb et al., 1998). Thus, NRG1 types I and II are released from the cell surface and may function as paracrine signals, while NRG1 type III remains tethered to the cell membrane after cleavage and may act as a juxtacrine signal (Nave and Salzer, 2006). In any case, the EGF-like signaling domain (present in all NRG1-isoforms) is required and sufficient for binding and activation of the ErbB transmembrane receptor tyrosine kinases (Holmes et al., 1992; Lu et al., 1995).

The proteolytic cleavage of NRG1 is catalyzed by different membrane proteases, including members of the ADAM proteases family, like ADAM17/TACE (Loeb et al., 1998; Montero et al., 2007) and ADAM19 (Yokozeki et al., 2007), and the β-site of amyloid precursor protein (APP) cleaving enzyme, (β-secretase, BACE1) (Hu et al., 2006; Willem et al., 2006). The BACE1 knockout mice show a deficit in NRG1 processing in their nervous system and display a peripheral neuropathy similar to that observed in mice lacking NRG1/ErbB signaling (Garratt et al., 2000b; Michailov et al., 2004; Taveggia et al., 2005). Thus, the physiological BACE1-mediated processing of NRG1 seems to be a key trophic instruction for the normal development and maintenance of myelin physiology, at least in the PNS. As PrP^C is known to interact and regulate BACE1 activity (Parkin et al., 2007), we were led to investigate whether PrP^C could influence the physiological NRG1 processing, both in the CNS and in the PNS. We found that PrP^C positively influences the processing of NRG1 in the old, but not young, PNS of the mouse. Aged $Prnp^{0/0}$ mice show indeed a significant reduction in the levels of NRG1 cleaved fragments, in contrast to their wildtype littermates. We could also confirm an influence of PrP^C on the cleavage of neuregulin-3 (NRG3), another BACE1 substrate and member of the NRG. This influence of PrP^C on neuregulins processing, however, is not detectable in the CNS. Hence, our results suggest that the influence of PrP^C on the cleavage of NRG1 (and NRG3) is limited to the PNS of aged mice. These findings point at different functional roles of PrP^C in the CNS and in the PNS and confirm an involvement of PrP^C in peripheral myelin maintenance during aging processes.

Results

NRG1 processing is developmentally regulated in sciatic nerves

The NRG1 proteins are one of the major axonal cues acting as myelination-promoting factor during PNS development (Garratt et al., 2000a; Jessen and Mirsky, 2005; Nave and Salzer, 2006; Newbern and Birchmeier, 2010). Alteration in the processing of NRG1 has been linked to deficit in correct myelination mechanisms (Hu et al., 2006; Willem et al., 2006), thus showing that the resulting cleaved fragments, rather than the full length pro-proteins, are the active key instruction for a physiological myelination process. In order to analyze the processing of NRG1 during PNS development and maturation, we undertook a time-course analysis of NRG1 expression in total protein extracts from mouse sciatic nerves at different ages (postnatal days P15, P30, P90 and P120) (Fig. 1A). The anti-NRG1 antibody sc-348 that we used recognizes an epitope specific to the most common cytoplasmic tail variant in the NRGs expressed in the nervous system (Wen et al., 1994). In Western blot analyses, two main proteins at ~140 kDa and ~100 kDa were labeled in sciatic nerve protein extracts with both the cytoplasmic tail antibody (sc-348) (Fig. 1A) and the NRG1 N-terminal antibody sc-28916 (data not shown). Labeling of these proteins by antibodies directed against both the N-terminal ectodomain and cytoplasmic domain epitope points that these are NRG1 pro-proteins. Additionally, two ~65- and ~55-kDa proteins were labeled by the cytoplasmic tail antibody, indicating that these proteins are C-terminal fragments (CTFs) resulting from stalk cleavage of the pro-proteins. The reason why there are C-terminal fragments with two different electrophoretic mobilities is unknown. However, the pro-protein and C-terminal fragment sizes that we observed are consistent with previous analyses of NRG1 processing (Burgess et al., 1995; Carroll et al., 1997; Loeb et al., 1998; Savonenko et al., 2008).

We found that, during this time course, the levels of full length NRG1 pro-proteins (NRG1-FL) significantly decrease with age to very low detectable levels, while the levels of the cleaved C-terminal fragments of NRG1 (NRG1-CTFs) significantly increase up to stage P90, reaching then a steady-state level (Fig. 1B) which persists at least till 1 year of age (data not shown). This finding suggests that active processing of NRG1 is taking place and increasing during postnatal development, and once the PNS reaches full maturation, NRG1 bioactive cleaved fragments are constantly produced during adulthood.

NRG1 cleavage is altered in the PNS of aged, but not young, $Prnp^{0/0}$ mice

Mice lacking PrP ($Prnp^{0/0}$ mice, (Bueler et al., 1992)) were recently shown to manifest a late-onset peripheral demyelinating polyneuropathy (Bremer et al., 2010). As the deficit in the proteolytic fragments of NRG1 has been linked to a loss of myelin homeostasis (Hu et al., 2006; Willem et al., 2006), we compared the levels of NRG1-CTFs in the sciatic nerves of wildtype mice and of their $Prnp^{0/0}$ littermates at different ages. According to the authors of this work (Bremer et al., 2010), we could not identify any significant difference in NRG1 processing during early postnatal development, at P15 (Fig. 2A) and at P30 (Fig. 2B). However, by increasing the age of the animals under investigation, we could find a decreasing level of NRG1-CTFs at 5 months of age (P150) in $Prnp^{0/0}$ mice yet not reaching statistical significance (Fig. 2 C). Finally, when we analyzed 1-year-old mice sciatic nerves, we found significant lower levels of the NRG1-CTFs in $Prnp^{0/0}$ mice compared to their wildtype counterpart (Fig. 2D). Thus, during early postnatal PNS development $Prnp^{0/0}$ and wildtype mice show no differences in NRG1 processing; in contrast, with aging, $Prnp^{0/0}$ mice show a chronically defective processing of NRG1 protein.

PrP^C stimulates ectodomain shedding of NRG1 in cell cultures

We have identified that the lack of PrP^C in sciatic nerves reduces the levels of NRG1-cleaved fragments. In order to verify whether high levels of PrP^C, on the contrary, could enhance the production of NRG1 cleaved fragments, we took advantage of N2a and N2a-CL3 cell lines. N2a-CL3 cell line consists of N2a cells stably transfected with full-length mouse PrP^C (Ghaemmaghami et al., 2010) to express higher level of PrP^C than normal N2a cells. We confirmed the higher levels of PrP^C in cell lysates of N2a-CL3 cells compared to N2a cells (Fig. 3A). Then, we checked for NRG1 levels in cell lysates and in the conditioned medium. We took advantage of the sc-28916 antibody, raised against the N-terminal domain of NRG1, in the perspective that the functional bioactive EGF-like containing ectodomain, after proteolytic cleavage of NRG1 pro-protein, could be detectable also in the extracellular environment. We could observe that, in N2a-CL3 cell lysates, compared to N2a cell lysates, there was a significant lower amount of total NRG1-FL, in contrast to a higher amount of the NRG1-N-terminal fragment (NRG1-NTF, ~70 kDa) (Fig. 3A and B). The size of the NRG1-NTF detected in our Western blots is consistent with previous studies on cell cultures, brain and spinal cord samples (Sandrock et al., 1995; Bermingham-McDonogh et al., 1996; Carroll et al., 1997; Wang et al., 2001). We then checked in the conditioned medium (CM) of N2a and N2a-CL3 cells for the presence of NRG1-NTF and we could identify a significant higher amount of NRG1-NTF in the conditioned medium of N2a-CL3 cells compared to the conditioned

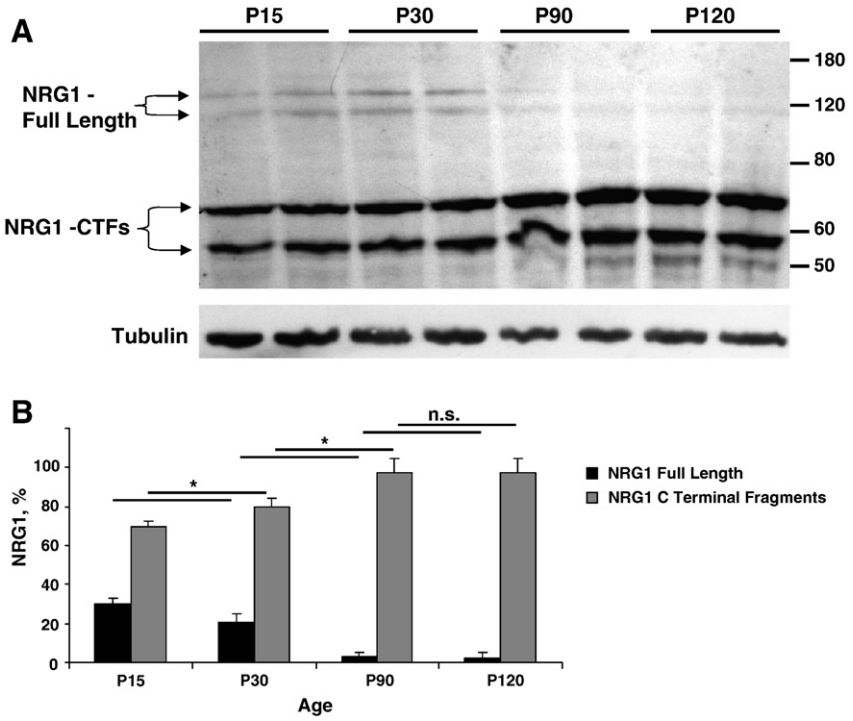

Fig. 1. The processing of NRG1 proteins is developmentally regulated in the sciatic nerve. (A) Sciatic nerves were excised from mice at different developmental stage ($n=4$, for each age) and protein extract (50 μg/lane) was analyzed for NRG1 content. We used an anti-NRG1-C-terminal antibody, by which we can recognize full length NRG1 pro-proteins and C-terminal fragments after cleavage (NRG1-CTFs). (B) Quantification of the Western blot; values of NRG1 full length and of NRG1-C-terminal fragments were normalized on beta-tubulin levels, and expressed as percentage of total neuregulin protein. Values are expressed as mean ± SD; $^{*}p \leq 0.05$; n.s. = not statistically significant.

medium of N2a cells (Figs. 3A and C). These results suggest that high levels of PrP^{C} potentiate NRG1 cleavage in intracellular compartments and that, after this processing, the NRG1 N-terminal fragment is released in the extracellular environment.

$Prnp^{0/0}$ mice show a defective cleavage also of NRG3

The protein PrP^{C} was previously shown to regulate BACE1-mediated cleavage of APP, a molecule that plays a central role in the

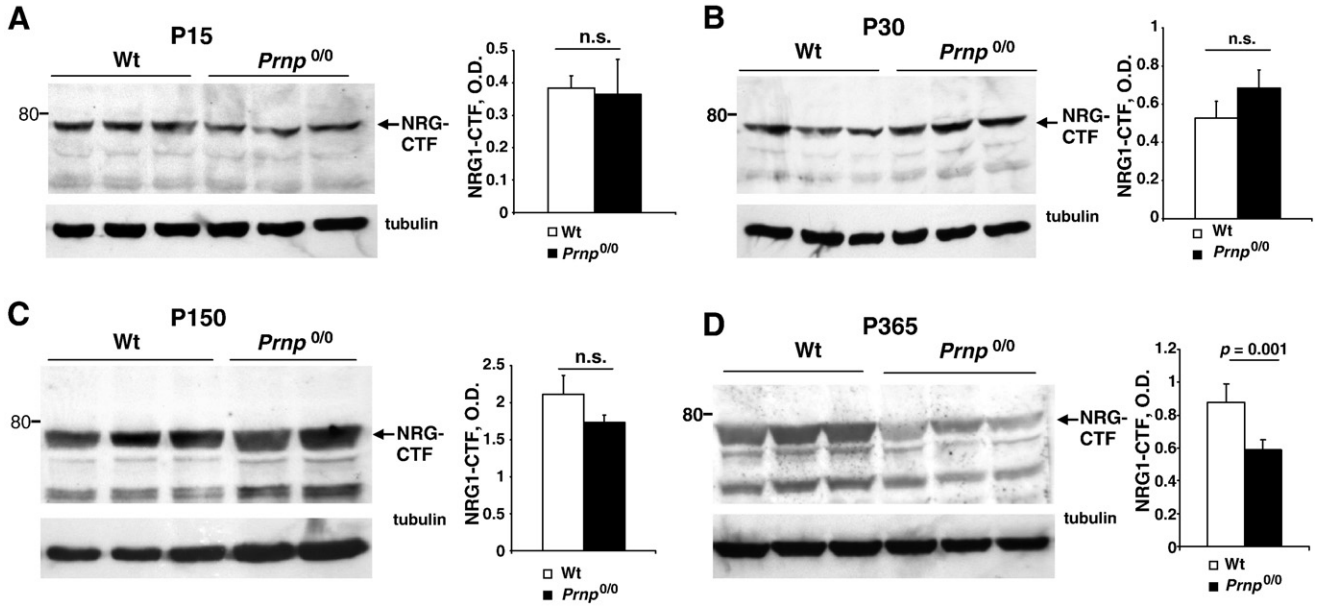

Fig. 2. The proteolytic cleavage of NRG1 is affected in aged, but not young, $Prnp^{0/0}$ mice sciatic nerves. Comparison between protein extracts of sciatic nerves of P15 (A), P30 (B), P150 (C), and P365 mice (D) from wildtype (Wt) and $Prnp^{0/0}$ mice. (A) Western blot of sciatic nerve protein extracts of P15 $Prnp^{0/0}$ ($n=3$) and Wt ($n=5$) mice using an antibody recognizing the C-terminal fragments after cleavage (NRG-CTFs) of NRG1. Quantification of the NRG-CTFs was normalized to the expression levels of beta-tubulin (right panel). (B) Western blot of sciatic nerve protein extracts of P30 $Prnp^{0/0}$ ($n=3$) and Wt ($n=3$) mice using an antibody recognizing the C-terminal fragments after cleavage (NRG-CTFs) of NRG1. Quantification of the NRG-CTFs was normalized to the expression levels of beta-tubulin (right panel). (C) Western blot of sciatic nerve protein extract of P150 $Prnp^{0/0}$ ($n=3$) and Wt ($n=4$) mice using an antibody recognizing the C-terminal fragments after cleavage (NRG-CTFs) of NRG1. Quantification of the NRG-CTFs was normalized to the expression levels of beta-tubulin (right panel). (D) Western blot of sciatic nerve protein extract of P365 $Prnp^{0/0}$ ($n=5$) and Wt ($n=9$) mice using an antibody recognizing the C-terminal fragments after cleavage (NRG-CTFs) of NRG1. Quantification of the NRG-CTFs was normalized to the expression levels of beta-tubulin (right panel). Values are expressed as mean ± SD; n.s. = not statistically significant.

pathogenesis of Alzheimer's disease (AD) (Parkin et al., 2007). As BACE1 is known to cleave other different substrates, we were prompted to verify whether PrP^C could regulate the cleavage of other BACE1 substrates. The protein NRG3 is another member of the NRG (Zhang et al., 1997) and was shown to share the same BACE1 cleavage site of NRG1 and to be directly processed by BACE1 (Hu et al., 2008). Thus, we investigated whether the levels of NRG3 could also change between wildtype and $Prnp^{0/0}$ mice sciatic nerves. Similarly to the brains and sciatic nerves of BACE1 null mice (Hu et al., 2008), we found a significant accumulation of unprocessed full length NRG3 in the sciatic nerves of $Prnp^{0/0}$ mice, when compared to their wildtype counterpart (Fig. 4). Thus, we could observe that also NRG3 processing is affected in the PNS of mice lacking PrP.

Fyn and ERK kinases signaling pathways are not affected in sciatic nerves of $Prnp^{0/0}$ mice

In neuregulin canonical signaling pathways, mature cleaved NRG1 proteins bind to and induce dimerization of ErbB receptors, which in turn activate auto-phosphorylation of the receptors themselves and the subsequent downstream activation of intracellular signaling pathways (Mei and Xiong, 2008). Among these, the extracellular signal-regulated kinase (ERK) (Si et al., 1996; Tansey et al., 1996) and Fyn kinase (Bjarnadottir et al., 2007) pathways can be activated. Moreover, PrP^C was also shown to signal through the same signaling pathways (Mouillet-Richard et al., 2000; Toni et al., 2006). In addition, Fyn kinase is known to regulate CNS (Umemori et al., 1994) and, recently, also PNS myelination (Hossain et al., 2010). Nevertheless, Bremer et al. (2010) could not detect any alteration of Akt and ERK kinases phosphorylation during PNS myelination (ages P10 and P30). The convergence of these signaling pathways led us to investigate whether there could be an aberrant activation of Fyn or ERK kinases in aged $Prnp^{0/0}$ mice compared to their wildtype counterpart. However, we also could not find any alteration of ERK or Fyn kinases activation in the sciatic nerves between aged wildtype and $Prnp^{0/0}$ mice (Fig. 5). This finding suggests that these signaling pathways are still active in aged $Prnp^{0/0}$ mice as in physiologically myelinated nerves and thus are not influenced by the lack of PrP^C or by a deficit in NRG1 processing.

Neuregulins processing is not altered in the CNS of $Prnp^{0/0}$ mice

We found a correlation between the lack of PrP^C and a defective processing of NRG1 and NRG3 in the PNS (sciatic nerves) of aged animals. In order to verify whether this processing was defective also in the CNS, we analyzed the levels of NRG1 and NRG3 in hippocampal homogenate from 1-year-old wildtype and $Prnp^{0/0}$ mice. We failed to detect any difference in expression and processing of NRG1 and NRG3 in the hippocampus between wildtype and $Prnp^{0/0}$ mice (Fig. 6). Thus, we can conclude that the lack of PrP^C influences neuregulins processing only in the PNS of aged mice, whereas in the CNS this influence is not effective.

Discussion

The physiological function of PrP^C is still under intense investigation. The protein PrP^C has been shown to influence several important aspects of cell biology, including cell adhesion, neurite outgrowth, protection against oxidative stress, and myelin homeostasis (reviewed by Aguzzi et al. (2008)). Recently, $Prnp^{0/0}$ mice were shown to manifest a late-onset chronic demyelinating polyneuropathy (Bremer et al., 2010). Interestingly, this phenotype was evident only in the PNS of aged $Prnp^{0/0}$ mice. Moreover, the demyelination was recovered by expression of axonal PrP^C and not by glial expression. This suggests an axonal trophic support, mediated by PrP^C neuronal expression, acting *in trans* to Schwann cells for a physiological myelin homeostasis. Thus, we were prompted to investigate for a neuron-specific key element that could be regulated by PrP^C and is involved in myelin homeostasis. PrP^C was previously shown to interact and regulate the β-site of APP cleaving enzyme (β-secretase BACE1) (Parkin et al., 2007). The protease BACE1 is preferentially expressed by neurons (Rossner et al., 2001), and interestingly, BACE1 null mice show myelin defects in the CNS and the PNS (Hu et al., 2006; Willem et al., 2006). These defects were bona fide

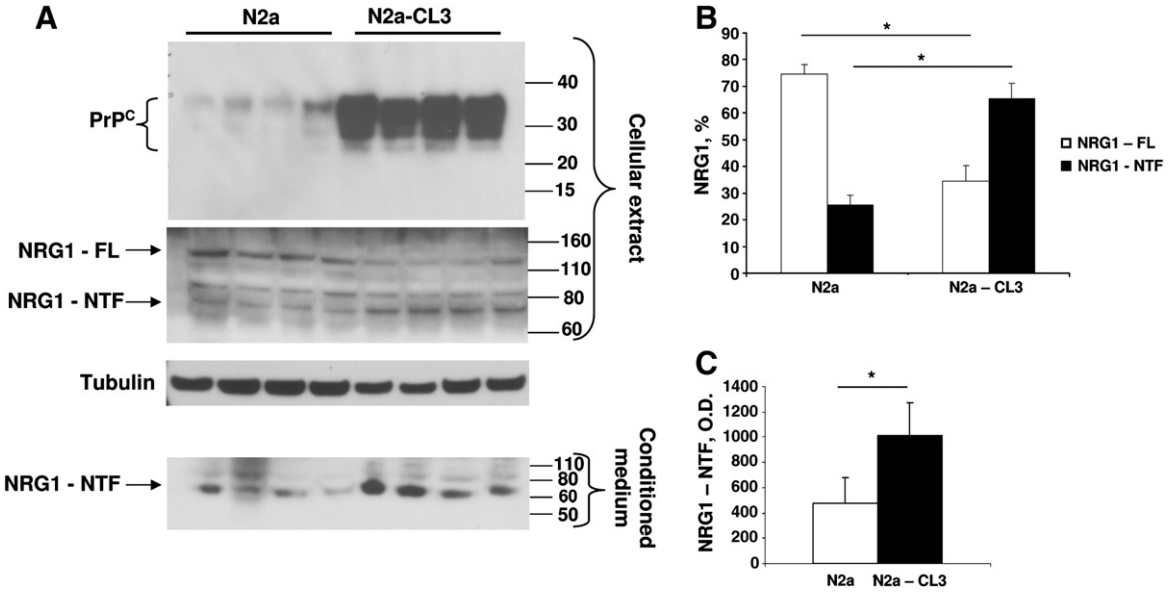

Fig. 3. The shedding of NRG1 ectodomain is enhanced by overexpression of PrP^C in cell lines. N2a and N2a-CL3 cells stably overexpressing PrP^C were cultured in serum-free medium, and cellular extract and conditioned medium were prepared and analyzed for the levels of NRG1 using an antibody recognizing full length (NRG1-FL) and the N-terminal fragment on NRG1 after cleavage (NRG1-NTF). (A) Western blots of cell lysates and conditioned medium from N2a and N2a-CL3. We confirmed the overexpression of PrP^C in N2a-CL3 cell lysates, compared to N2a cell lysates (upper panel). Cell lysates of N2a-CL3 cells show a reduced level of NRG1-FL and a concomitant increased level of NRG1-NTF, if compared to N2a cell lysates (central panel). Conditioned media were also analyzed for the levels of NRG1-NTF (lower panel). (B) Quantification of NRG1-FL and NRG1-NTF in the cell lysates of N2a (left) and N2a-CL3 (right) cells. Values were normalized to the levels of beta-tubulin, and expressed as percentage of total NRG1 protein. (C) Quantification of the NRG1-NTF in the conditioned medium of N2a (white column) and N2a-CL3 (black column) cells. Values are expressed as mean ± SD; $^*p \leq 0.05$.

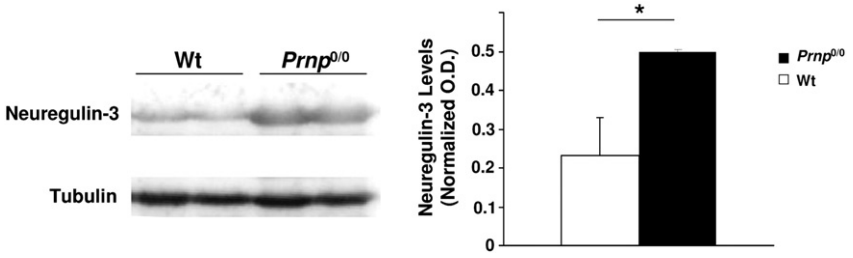

Fig. 4. Unprocessed NRG3 accumulates in the sciatic nerves of *Prnp*$^{0/0}$ mice. Sciatic nerve protein extracts of 1-year-old wildtype (Wt) ($n=9$) and *Prnp*$^{0/0}$ ($n=5$) mice were investigated for the levels of full length NRG3. The amount of full length NRG3 was analyzed quantitatively and normalized to the expression level of beta-tubulin (right panel). Values are expressed as mean ± SD; $^{*}p \leq 0.05$.

linked to a lack of processing of NRG1 proteins, which are BACE1 substrates and key regulators of PNS myelination (Mei and Xiong, 2008; Newbern and Birchmeier, 2010). Thus, we investigated whether, besides regulating BACE1 activity in the cleavage of APP (Parkin et al., 2007), PrP^{C} could also regulate the cleavage of other BACE1 substrates, i.e., neuregulins.

Here we demonstrate that *Prnp*$^{0/0}$ mice show a defective processing of NRG1. However, this defect in NRG1 processing is time- and tissue-definite. Indeed, we could highlight a difference in NRG1 processing only in aged *Prnp*$^{0/0}$ mice compared to their wildtype counterpart, whereas in young animals we could not find any difference between the two genotypes. This finding hints that during the first postnatal development, i.e., during the initial PNS myelination process, PrP^{C} role for neuregulin processing is dispensable, whereas it starts to exert its effects and to be relevant in adult and aged animals. This is suggestive of a physiological role of PrP^{C} for NRG1 processing during the aging of an animal. Moreover, *Prnp*$^{0/0}$ mice showed altered NRG1 cleavage only in their PNS, whereas they did not show any difference, if compared to their wildtype counterpart, in NRG1 processing in the CNS at any age of investigation. The molecule PrP^{C} thus seems to fulfill different functions between CNS and PNS, at least for NRG1 processing and, in turn, possibly for myelin homeostasis.

In order to verify whether PrP^{C} could directly stimulate the cleavage of NRG1, we used N2a cells stably over-expressing full-length mouse PrP^{C} and identified an increase of NRG1-N-terminal cleaved fragment both in the cell lysates and in the conditioned medium. This suggests that the cleavage of NRG1, stimulated by PrP^{C} expression, occurs in intracellular compartments, for example in the endosomal system, and then the cleaved fragment is released in the cell medium, probably through a subsequent move of the cleaved fragment to the protein secretory pathway. The protease BACE1 is known to cleave its substrate APP in the endosomal pathway and then the cleaved fragment is released in the extracellular medium via the secretory pathway (Koo and Squazzo, 1994; Thinakaran et al., 1996; Tomita et al., 1998; Marlow et al., 2003). This suggests the need of acidic compartments (i.e., endosomes and/or late Golgi) for BACE1 activity. This finding hints that BACE1-mediated cleavage of NRG1 may require the same endocytosis/recycling process as for BACE1-mediated APP processing.

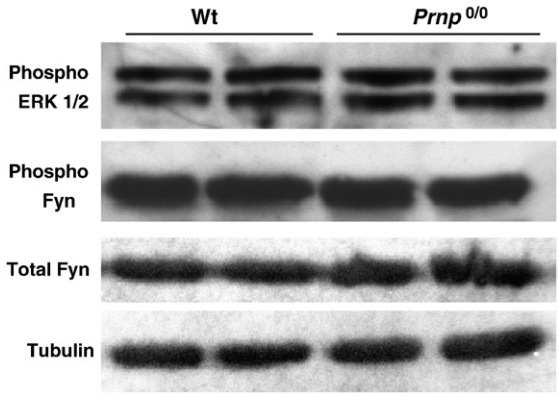

Fig. 5. ERK and Fyn kinases signaling pathways are not altered in the sciatic nerves of *Prnp*$^{0/0}$ mice. Western blot of protein extracts from sciatic nerves of 1-year-old wildtype (Wt) ($n=9$) and *Prnp*$^{0/0}$ ($n=5$) mice. The levels of total Fyn protein, of phosphorylated Fyn and phosphorylated ERK proteins do not significantly change between wildtype and *Prnp*$^{0/0}$ mice.

We also identified altered processing of NRG3 in *Prnp*$^{0/0}$ mice. NRG3 is another member of the NRG, possesses a similar structural organization to NRG1, and also activates ErbB receptor (Zhang et al., 1997). Like NRG1, NRG3 is also substrate of BACE1, and after proteolytical cleavage it was proposed to bind Schwann cells ErbB receptors (Hu et al., 2008). We could detect a difference in processing also for NRG3 only in the PNS of *Prnp*$^{0/0}$ mice and not in the CNS if compared to wildtype animals. Hence, PrP^{C} can stimulate the processing of neuregulins only in the PNS and not in the CNS.

We also investigated whether two intracellular signaling pathways, i.e., ERK and Fyn kinases, linked both to PrP^{C} and neuregulins signaling, could be altered in the sciatic nerves of *Prnp*$^{0/0}$ mice, but we could not highlight any difference from their wildtype counterpart in the activation of these two signaling cascades. This suggests that other signaling pathways may be affected by the lack of PrP^{C} and the defective neuregulin processing. Further studies need to investigate other intracellular cascades related to both PrP^{C} and neuregulin signaling (for example, the PI3K pathway (Li et al., 2001; Roffe et al., 2010)).

The age-dependent effect of PrP^{C} on neuregulin processing may be associated to different cellular mechanisms. Lipid rafts are dynamic and highly ordered sterol- and sphingolipid-enriched domains that can concentrate selected subsets of proteins and serve as a platform for cellular processes, including cell signaling, protein sorting and trafficking, and extracellular/membrane protein proteolysis (Simons and Toomre, 2000; Ledesma et al., 2003; Helms and Zurzolo, 2004; Hancock, 2006). Rafts are continuously endocytosed from cellular plasma membrane via the endocytic pathway, and either recycled back to the plasma membrane or returned to the Golgi apparatus (Puri et al., 1999; Mukherjee and Maxfield, 2000). Neuregulin (Frenzel and Falls, 2001), PrP^{C} (Vey et al., 1996) and BACE1 (Riddell et al., 2001) are all enriched in lipid rafts domains. Moreover, targeting BACE1 lumenal domain to lipid rafts by the addition of a glycophosphatidylinositol anchor was shown to increase BACE1-mediated APP processing (Cordy et al., 2003). This hints at lipid rafts as functional compartment for BACE1 activity. Besides, PrP^{C} was shown to exert its regulation on BACE1-mediated APP cleavage only when correctly localized to lipid rafts domain (Parkin et al., 2007). Although from our experiments we cannot draw a direct functional link between PrP^{C} and the regulation of BACE1, our findings suggest that PrP^{C} could physiologically influence also the BACE1-mediated neuregulins cleavage and this occurring in an endocytosis/secretory pathway-dependent manner. Lipid rafts however do not maintain the same protein and lipid composition: with aging and in pathological condition (like in AD), the ratio between cholesterol, sphingolipid and phospholipid changes (Prinetti et al., 2001; Palestini et al., 2002; Martin et al., 2010). This in

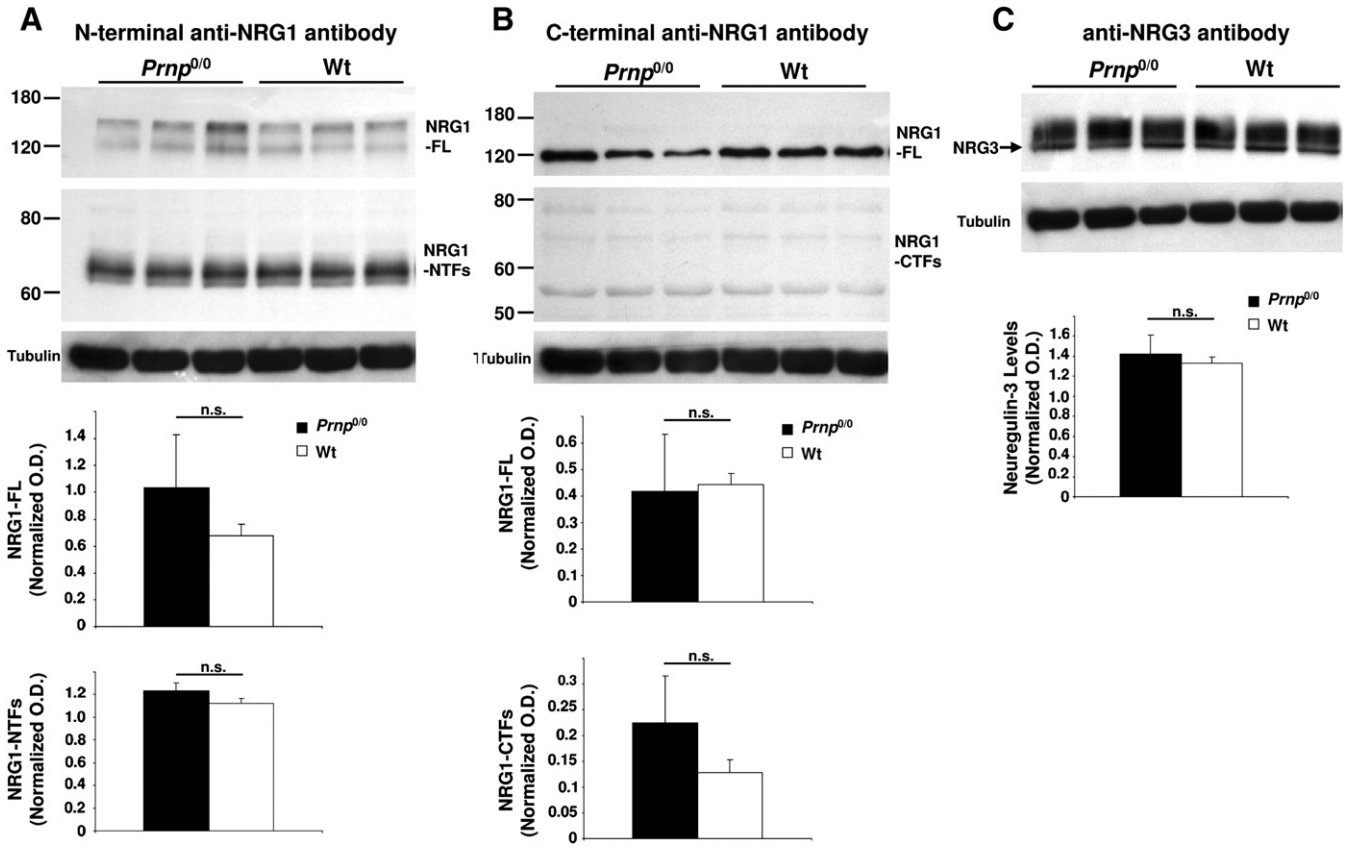

Fig. 6. Processing of NRG1 and NRG3 is not altered in the hippocampus of *Prnp*$^{0/0}$ mice. Hippocampal homogenates from 1-year-old wildtype (Wt) ($n=3$) and *Prnp*$^{0/0}$ ($n=3$) mice were analyzed for the levels of NRG1 proteins using antibody against the N-terminus of NRG1 (A) against the C-terminus of NRG1 (B) or against full length NRG3 (C). The Western blot showed no significant difference in expression or processing of both NRG1 and NRG3 proteins between wildtype and *Prnp*$^{0/0}$ mice hippocampi. Quantification of the Western blot: values of NRG1 full length, NRG1 terminal fragments and NRG3 were normalized on beta-tubulin levels (lower panels). Values are expressed as mean ± SD; $^{*}p \leq 0.05$.

turn may affect the affinity of certain proteins for these microdomains. As a consequence of this, the protein composition of the lipid rafts may dramatically change, and this can consequently modify their properties as "signaling scaffolds" during different cellular life stages. Hence, we may suggest that, during early postnatal development, the lack of PrP^{C} in lipid rafts and the specific protein/lipid composition may not destabilize BACE1-mediated NRGs processing, whereas by changing the biochemical composition of the rafts, i.e., with adulthood and aging, the lack of PrP^{C} could instead destabilize lipid rafts-mediated BACE1–NRGs interaction. This in turn could lead to the observed altered NRGs processing. In this perspective, PrP^{C} may be a crucial key element in lipid rafts protein homeostasis, composition and in physiological signaling processes during lifetime, and particularly during aging.

Moreover, the possible age-dependent influence of PrP^{C} on BACE1-mediated neuregulin cleavage may be also due to the opposite dynamic expression levels between PrP^{C} and BACE1 throughout the lifespan of the animal. Indeed, PrP^{C} levels were shown to increase during postnatal development then reaching a *plateau* of expression in adulthood (Sales et al., 2002), whereas BACE1 levels are high during development and then decrease to a low levels in adult animals (Willem et al., 2006). Thus, PrP influence could be minimal during early development when PrP^{C} low levels of expression overlap the high levels of BACE1; on the contrary, in adult animals, the minimal expression of BACE1 could be strongly influenced by the high levels of PrP^{C}. Accordingly, in *Prnp*$^{0/0}$ mice BACE1 activity may not be affected by the lack of PrP^{C} in young animals, while on the contrary it can be effectively altered during adulthood and aging of the animals.

The mechanisms responsible for the tissue-dependent influence of PrP^{C} on neuregulin processing also are not clear and need further investigation. We detected altered NRGs processing only in the PNS of aged *Prnp*$^{0/0}$ mice and not in their CNS. This can suggest that some compensatory mechanism for neuregulin processing may occur in the CNS, whereas it is not effective in the PNS.

Pharmacological inhibition of BACE1 in adult mice brain was shown to induce significant Aβ-peptide lowering, but it was without any major effect on brain NRG1 processing (Sankaranarayanan et al., 2008). The same study suggests differences in BACE1-mediated NRG1 processing only in early development in the brain, as aged (2-years-old) BACE1 null mice show identical full-length NRG1 and NRG-NTF levels to their wildtype counterpart. Therefore, BACE1 inhibition in the brain showed to have an effective impact on the lowering of APP processing and no alteration on NRG1 processing. Similarly, PrP^{C} was shown to inhibit BACE1-mediated APP processing in the brain (Parkin et al., 2007), whereas in our present study we could not detect any role for PrP^{C} on NRG1 processing in the CNS of aged mice. These independent findings are suggestive of a different PrP^{C} influence on BACE1 processing activity between the CNS and the PNS.

Taken together, our findings are indicative of the occurrence of different age-dependent and tissue-dependent cellular mechanisms for the regulation of neuregulins processing. We envision that future studies on NRGs processing and cleavage need to take into deep account the different ages and tissues of the animals under investigation, in order to describe a correct spatial and dynamic frame of neuregulins processing and biological action.

Conclusions

In summary, our study points at PrP^{C} as a positive regulator of NRGs processing. This effect was manifest as age-dependent (only in

aged, but not in young mice) and tissue-dependent (only in the PNS, but not in the CNS). Our results suggest that PrP^C could exert different functions, during development and aging, between the CNS and the PNS, at least as regards neuregulin processing and possibly myelin homeostasis. In turn, this finding could shed new light on the etiology of the peripheral demyelinating neuropathy affecting aged mice null for the PrP (Bremer et al., 2010).

Experimental methods

Animals

C57/B6 wildtype, mixed B6/129 wildtype, B6/129 *Prnp*$^{0/0}$ (Bueler et al., 1992), FVB wildtype and FVB *Prnp*$^{0/0}$ (Lledo et al., 1996) mice were used in these experiments. All experiments were carried out in accordance with European regulations [European Community Council Directive, November 24, 1986 (86/609/EEC)] and were approved by the local authority veterinary service. After animal sacrifice, tissues were immediately dissected and processed for protein analysis.

Protein analysis

Mouse hippocampi and sciatic nerves were dissected and immediately frozen in ice-cold lysis buffer (50 mM Tris–HCl pH 7.5, 150 mM NaCl, 1 mM EDTA, 0.5% CHAPS, 10% glycerol) containing proteases inhibitors (Inhibitor complete mini, Roche Diagnostics Corp., Mannheim, Germany) and stored at −80 °C or immediately homogenized. Hippocampal samples were further cleared by centrifugation at +4 °C, 2000*g*, 10 min. For sciatic nerves of P15 and P30 wildtype and *Prnp*$^{0/0}$ mice, nerves from 2 animals were pooled together in each sample, while for older mice each sample included sciatic nerves from a single animal. Total protein content was determined by the bicinchoninic acid (BCA) assay (Pierce), and the same amount of proteins for each sample (50 μg) was separated either on gradient SDS–PAGE gels (NuPAGE® Novex 4-12%, Invitrogen) or on 8% homemade SDS–PAGE gels, and transferred to PVDF membrane.

Antibodies

We used the following primary antibodies: NRG1 C-Terminal epitope, C-20 (sc-348, Santa Cruz Biotechnology); NRG1 N-terminal epitope, H-210 (sc-28916, Santa Cruz Biotechnology); NRG3, H-70 (sc-67002, Santa Cruz Biotechnology); Anti-PrP antibody HRP-conjugated Fab D13 (Williamson et al., 1998); anti total non-phosphorylated Fyn, phosphorylated Fyn and phosphorylated ERK kinases [Src Family Antibody #2109, phospho-Src Family (Tyr416) antibody #2101, and phospho-p44/42 Map Kinase (Thr202/Tyr204) Ab #9101, Cell Signaling Technology].

Cell culture

N2a and N2a-CL3 cells, stably transfected with and overexpressing full-length mouse PrP^C, were cultured as previously described (Ghaemmaghami et al., 2010). Briefly, all cell lines were maintained in Modified Eagle's Medium (MEM) supplemented with 10% vol/vol fetal bovine serum, 1% penicillin–streptomycin, and 1% GlutaMAX (Invitrogen) at 37 °C in a humidified atmosphere with 5% CO_2.

Preparation of cytosolic extracts and conditioned medium proteins

Cells were grown almost to confluency in 10-cm diameter tissue culture plates (Corning). Cells were then washed with PBS (3×) and maintained in serum-depleted MEM for 40 h. Conditioned medium was then removed, spun at 10,000*g*, 10 min, 4 °C to remove cell debris, and then precipitated with 5 volumes of cold acetone. Samples were incubated at least 2 h at −20 °C, and then spun at 5000*g*, 20 min, 4 °C. Protein pellets were then air dried and resuspended in Laemmli buffer.

The cell layer remaining in the plate after the incubation period in serum-free MEM was washed with PBS (3×) and lysed with 500 μL of cold lysis buffer (10 mm Tris–HCl, pH 8.0, 150 mm NaCl, 0.5% sodium deoxycholate, 0.5% Nonidet P-40). Cell lysates were then centrifuged at 10,000*g*, 5 min, 4 °C to remove cell debris. The supernatant was collected and the total protein concentration was measured by using the bicinchoninic acid assay (Pierce). The conditioned medium and cell lysates were normalized for total protein based on the cell lysate protein concentrations, boiled for 5 min, electrophoresed on gradient SDS–PAGE gels (NuPAGE® Novex 4–12%, Invitrogen) and transferred to PVDF membrane.

Data and statistical analysis

Image analysis was carried out with Quantity One® software v 4.6.2 (Bio-Rad). In each gel, bands were detected, background was subtracted and protein bands quantities were defined with the dedicated functions. We took advantage of the "Volume analysis" tool provided with the software. For the analysis, we used the adjusted volume parameter, corresponding to the band volume [i.e., the sum of the intensities of the pixels inside the volume boundary × area of a single pixel (in mm^2)] minus the background volume. Each value was then normalized against the b-tubulin value of the same biological sample. Then, normalized results were analyzed with Student's *t* test, with a cutoff value of $p \leq 0.05$.

Acknowledgments

This work was supported by grants from the Compagnia di San Paolo and Italian Ministry of Health to GL. We are grateful to Prof. Stephen J. DeArmond and Dr. Misol Ahn, Institute for Neurodegenerative Disease (IND), University of California, San Francisco, for their advice and help with this study.

References

Aguzzi, A., Baumann, F., Bremer, J., 2008. The prion's elusive reason for being. Annu. Rev. Neurosci. 31, 439–477.
Bermingham-McDonogh, O., McCabe, K.L., Reh, T.A., 1996. Effects of GGF/neuregulins on neuronal survival and neurite outgrowth correlate with erbB2/neu expression in developing rat retina. Development 122, 1427–1438.
Bjarnadottir, M., Misner, D.L., Haverfield-Gross, S., Bruun, S., Helgason, V.G., Stefansson, H., Sigmundsson, A., Firth, D.R., Nielsen, B., Stefansdottir, R., Novak, T.J., Stefansson, K., Gurney, M.E., Andresson, T., 2007. Neuregulin1 (NRG1) signaling through Fyn modulates NMDA receptor phosphorylation: differential synaptic function in NRG1 +/− knock-outs compared with wild-type mice. J. Neurosci. 27, 4519–4529.
Bounhar, Y., Zhang, Y., Goodyer, C.G., LeBlanc, A., 2001. Prion protein protects human neurons against Bax-mediated apoptosis. J. Biol. Chem. 276, 39145–39149.
Bremer, J., Baumann, F., Tiberi, C., Wessig, C., Fischer, H., Schwarz, P., Steele, A.D., Toyka, K.V., Nave, K.A., Weis, J., Aguzzi, A., 2010. Axonal prion protein is required for peripheral myelin maintenance. Nat. Neurosci. 13, 310–318.
Brinkmann, B.G., Agarwal, A., Sereda, M.W., Garratt, A.N., Muller, T., Wende, H., Stassart, R.M., Nawaz, S., Humml, C., Velanac, V., Radyushkin, K., Goebbels, S., Fischer, T.M., Franklin, R.J., Lai, C., Ehrenreich, H., Birchmeier, C., Schwab, M.H., Nave, K.A., 2008. Neuregulin-1/ErbB signaling serves distinct functions in myelination of the peripheral and central nervous system. Neuron 59, 581–595.
Bueler, H., Fischer, M., Lang, Y., Bluethmann, H., Lipp, H.P., DeArmond, S.J., Prusiner, S.B., Aguet, M., Weissmann, C., 1992. Normal development and behaviour of mice lacking the neuronal cell-surface PrP protein. Nature 356, 577–582.
Buonanno, A., Fischbach, G.D., 2001. Neuregulin and ErbB receptor signaling pathways in the nervous system. Curr. Opin. Neurobiol. 11, 287–296.
Burgess, T.L., Ross, S.L., Qian, Y.X., Brankow, D., Hu, S., 1995. Biosynthetic processing of neu differentiation factor. Glycosylation trafficking, and regulated cleavage from the cell surface. J. Biol. Chem. 270, 19188–19196.
Carroll, S.L., Miller, M.L., Frohnert, P.W., Kim, S.S., Corbett, J.A., 1997. Expression of neuregulins and their putative receptors, ErbB2 and ErbB3, is induced during Wallerian degeneration. J. Neurosci. 17, 1642–1659.
Cordy, J.M., Hussain, I., Dingwall, C., Hooper, N.M., Turner, A.J., 2003. Exclusively targeting beta-secretase to lipid rafts by GPI-anchor addition up-regulates beta-site processing of the amyloid precursor protein. Proc. Natl Acad. Sci. USA 100, 11735–11740.
Falls, D.L., 2003. Neuregulins: functions, forms, and signaling strategies. Exp. Cell Res. 284, 14–30.

Fischbach, G.D., Rosen, K.M., 1997. ARIA: a neuromuscular junction neuregulin. Annu. Rev. Neurosci. 20, 429–458.
Frenzel, K.E., Falls, D.L., 2001. Neuregulin-1 proteins in rat brain and transfected cells are localized to lipid rafts. J. Neurochem. 77, 1–12.
Garratt, A.N., Britsch, S., Birchmeier, C., 2000a. Neuregulin, a factor with many functions in the life of a Schwann cell. Bioessays 22, 987–996.
Garratt, A.N., Voiculescu, O., Topilko, P., Charnay, P., Birchmeier, C., 2000b. A dual role of erbB2 in myelination and in expansion of the Schwann cell precursor pool. J. Cell Biol. 148, 1035–1046.
Ghaemmaghami, S., Ullman, J., Ahn, M., St Martin, S., Prusiner, S.B., 2010. Chemical induction of misfolded prion protein conformers in cell culture. J. Biol. Chem. 285, 10415–10423.
Hancock, J.F., 2006. Lipid rafts: contentious only from simplistic standpoints. Nat. Rev. Mol. Cell Biol. 7, 456–462.
Helms, J.B., Zurzolo, C., 2004. Lipids as targeting signals: lipid rafts and intracellular trafficking. Traffic 5, 247–254.
Herms, J., Tings, T., Gall, S., Madlung, A., Giese, A., Siebert, H., Schurmann, P., Windl, O., Brose, N., Kretzschmar, H., 1999. Evidence of presynaptic location and function of the prion protein. J. Neurosci. 19, 8866–8875.
Holmes, W.E., Sliwkowski, M.X., Akita, R.W., Henzel, W.J., Lee, J., Park, J.W., Yansura, D., Abadi, N., Raab, H., Lewis, G.D., et al., 1992. Identification of heregulin, a specific activator of p185erbB2. Science 256, 1205–1210.
Hossain, S., Fragoso, G., Mushynski, W.E., Almazan, G., 2010. Regulation of peripheral myelination by Src-like kinases. Exp. Neurol. 226, 47–57.
Hu, X., He, W., Diaconu, C., Tang, X., Kidd, G.J., Macklin, W.B., Trapp, B.D., Yan, R., 2008. Genetic deletion of BACE1 in mice affects remyelination of sciatic nerves. FASEB J. 22, 2970–2980.
Hu, X., Hicks, C.W., He, W., Wong, P., Macklin, W.B., Trapp, B.D., Yan, R., 2006. Bace1 modulates myelination in the central and peripheral nervous system. Nat. Neurosci. 9, 1520–1525.
Jessen, K.R., Mirsky, R., 2005. The origin and development of glial cells in peripheral nerves. Nat. Rev. Neurosci. 6, 671–682.
Kanaani, J., Prusiner, S.B., Diacovo, J., Baekkeskov, S., Legname, G., 2005. Recombinant prion protein induces rapid polarization and development of synapses in embryonic rat hippocampal neurons in vitro. J. Neurochem. 95, 1373–1386.
Koo, E.H., Squazzo, S.L., 1994. Evidence that production and release of amyloid beta-protein involves the endocytic pathway. J. Biol. Chem. 269, 17386–17389.
Ledesma, M.D., Da Silva, J.S., Schevchenko, A., Wilm, M., Dotti, C.G., 2003. Proteomic characterisation of neuronal sphingolipid-cholesterol microdomains: role in plasminogen activation. Brain Res. 987, 107–116.
Li, Y., Tennekoon, G.I., Birnbaum, M., Marchionni, M.A., Rutkowski, J.L., 2001. Neuregulin signaling through a PI3K/Akt/Bad pathway in Schwann cell survival. Mol. Cell. Neurosci. 17, 761–767.
Lledo, P.M., Tremblay, P., DeArmond, S.J., Prusiner, S.B., Nicoll, R.A., 1996. Mice deficient for prion protein exhibit normal neuronal excitability and synaptic transmission in the hippocampus. Proc. Natl Acad. Sci. USA 93, 2403–2407.
Loeb, J.A., Susanto, E.T., Fischbach, G.D., 1998. The neuregulin precursor proARIA is processed to ARIA after expression on the cell surface by a protein kinase C-enhanced mechanism. Mol. Cell. Neurosci. 11, 77–91.
Lu, H.S., Hara, S., Wong, L.W., Jones, M.D., Katta, V., Trail, G., Zou, A., Brankow, D., Cole, S., Hu, S., et al., 1995. Post-translational processing of membrane-associated neu differentiation factor proisoforms expressed in mammalian cells. J. Biol. Chem. 270, 4775–4783.
Marlow, L., Cain, M., Pappolla, M.A., Sambamurti, K., 2003. Beta-secretase processing of the Alzheimer's amyloid protein precursor (APP). J. Mol. Neurosci. 20, 233–239.
Martin, M., Dotti, C.G., Ledesma, M.D., 2010. Brain cholesterol in normal and pathological aging. Biochim. Biophys. Acta 1801, 934–944.
Mei, L., Xiong, W.C., 2008. Neuregulin 1 in neural development, synaptic plasticity and schizophrenia. Nat. Rev. Neurosci. 9, 437–452.
Michailov, G.V., Sereda, M.W., Brinkmann, B.G., Fischer, T.M., Haug, B., Birchmeier, C., Role, L., Lai, C., Schwab, M.H., Nave, K.A., 2004. Axonal neuregulin-1 regulates myelin sheath thickness. Science 304, 700–703.
Montero, J.C., Rodriguez-Barrueco, R., Yuste, L., Juanes, P.P., Borges, J., Esparis-Ogando, A., Pandiella, A., 2007. The extracellular linker of pro-neuregulin-alpha2c is required for efficient sorting and juxtacrine function. Mol. Biol. Cell 18, 380–393.
Mouillet-Richard, S., Ermonval, M., Chebassier, C., Laplanche, J.L., Lehmann, S., Launay, J. M., Kellermann, O., 2000. Signal transduction through prion protein. Science 289, 1925–1928.
Mukherjee, S., Maxfield, F.R., 2000. Role of membrane organization and membrane domains in endocytic lipid trafficking. Traffic 1, 203–211.
Nave, K.A., Salzer, J.L., 2006. Axonal regulation of myelination by neuregulin 1. Curr. Opin. Neurobiol. 16, 492–500.
Newbern, J., Birchmeier, C., 2010. Nrg1/ErbB signaling networks in Schwann cell development and myelination. Semin. Cell Dev. Biol. 21, 922–928.
Palestini, P., Botto, L., Guzzi, F., Calvi, C., Ravasi, D., Masserini, M., Pitto, M., 2002. Developmental changes in the protein composition of sphingolipid- and cholesterol-enriched membrane domains of rat cerebellar granule cells. J. Neurosci. Res. 67, 729–738.
Parkin, E.T., Watt, N.T., Hussain, I., Eckman, E.A., Eckman, C.B., Manson, J.C., Baybutt, H.N., Turner, A.J., Hooper, N.M., 2007. Cellular prion protein regulates beta-secretase cleavage of the Alzheimer's amyloid precursor protein. Proc. Natl Acad. Sci. USA 104, 11062–11067.
Prinetti, A., Chigorno, V., Prioni, S., Loberto, N., Marano, N., Tettamanti, G., Sonnino, S., 2001. Changes in the lipid turnover, composition, and organization, as sphingolipid-enriched membrane domains, in rat cerebellar granule cells developing in vitro. J. Biol. Chem. 276, 21136–21145.
Prusiner, S.B., 1982. Novel proteinaceous infectious particles cause scrapie. Science 216, 136–144.
Puri, V., Watanabe, R., Dominguez, M., Sun, X., Wheatley, C.L., Marks, D.L., Pagano, R.E., 1999. Cholesterol modulates membrane traffic along the endocytic pathway in sphingolipid-storage diseases. Nat. Cell Biol. 1, 386–388.
Radovanovic, I., Braun, N., Giger, O.T., Mertz, K., Miele, G., Prinz, M., Navarro, B., Aguzzi, A., 2005. Truncated prion protein and Doppel are myelinotoxic in the absence of oligodendrocytic PrPC. J. Neurosci. 25, 4879–4888.
Riddell, D.R., Christie, G., Hussain, I., Dingwall, C., 2001. Compartmentalization of beta-secretase (Asp2) into low-buoyant density, noncaveolar lipid rafts. Curr. Biol. 11, 1288–1293.
Roffe, M., Beraldo, F.H., Bester, R., Nunziante, M., Bach, C., Mancini, G., Gilch, S., Vorberg, I., Castilho, B.A., Martins, V.R., Hajj, G.N., 2010. Prion protein interaction with stress-inducible protein 1 enhances neuronal protein synthesis via mTOR. Proc. Natl Acad. Sci. USA 107, 13147–13152.
Rossner, S., Apelt, J., Schliebs, R., Perez-Polo, J.R., Bigl, V., 2001. Neuronal and glial beta-secretase (BACE) protein expression in transgenic Tg2576 mice with amyloid plaque pathology. J. Neurosci. Res. 64, 437–446.
Sales, N., Hassig, R., Rodolfo, K., Di Giamberardino, L., Traiffort, E., Ruat, M., Fretier, P., Moya, K.L., 2002. Developmental expression of the cellular prion protein in elongating axons. Eur. J. Neurosci. 15, 1163–1177.
Sandrock Jr., A.W., Goodearl, A.D., Yin, Q.W., Chang, D., Fischbach, G.D., 1995. ARIA is concentrated in nerve terminals at neuromuscular junctions and at other synapses. J. Neurosci. 15, 6124–6136.
Sankaranarayanan, S., Price, E.A., Wu, G., Crouthamel, M.C., Shi, X.P., Tugusheva, K., Tyler, K.X., Kahana, J., Ellis, J., Jin, L., Steele, T., Stachel, S., Coburn, C., Simon, A.J., 2008. In vivo beta-secretase 1 inhibition leads to brain Abeta lowering and increased alpha-secretase processing of amyloid precursor protein without effect on neuregulin-1. J. Pharmacol. Exp. Ther. 324, 957–969.
Santuccione, A., Sytnyk, V., Leshchyns'ka, I., Schachner, M., 2005. Prion protein recruits its neuronal receptor NCAM to lipid rafts to activate p59fyn and to enhance neurite outgrowth. J. Cell Biol. 169, 341–354.
Savonenko, A.V., Melnikova, T., Laird, F.M., Stewart, K.A., Price, D.L., Wong, P.C., 2008. Alteration of BACE1-dependent NRG1/ErbB4 signaling and schizophrenia-like phenotypes in BACE1-null mice. Proc. Natl Acad. Sci. USA 105, 5585–5590.
Si, J., Luo, Z., Mei, L., 1996. Induction of acetylcholine receptor gene expression by ARIA requires activation of mitogen-activated protein kinase. J. Biol. Chem. 271, 19752–19759.
Simons, K., Toomre, D., 2000. Lipid rafts and signal transduction. Nat. Rev. Mol. Cell Biol. 1, 31–39.
Tansey, M.G., Chu, G.C., Merlie, J.P., 1996. ARIA/HRG regulates AChR epsilon subunit gene expression at the neuromuscular synapse via activation of phosphatidylinositol 3-kinase and Ras/MAPK pathway. J. Cell Biol. 134, 465–476.
Taveggia, C., Zanazzi, G., Petrylak, A., Yano, H., Rosenbluth, J., Einheber, S., Xu, X., Esper, R.M., Loeb, J.A., Shrager, P., Chao, M.V., Falls, D.L., Role, L., Salzer, J.L., 2005. Neuregulin-1 type III determines the ensheathment fate of axons. Neuron 47, 681–694.
Thinakaran, G., Teplow, D.B., Siman, R., Greenberg, B., Sisodia, S.S., 1996. Metabolism of the "Swedish" amyloid precursor protein variant in neuro2a (N2a) cells. Evidence that cleavage at the "beta-secretase" site occurs in the golgi apparatus. J. Biol. Chem. 271, 9390–9397.
Tomita, S., Kirino, Y., Suzuki, T., 1998. Cleavage of Alzheimer's amyloid precursor protein (APP) by secretases occurs after O-glycosylation of APP in the protein secretory pathway. Identification intracellular compartments which APP cleavage occurs without using toxic agents that interfere protein metabolism. J Biol Chem 273, 6277–6284.
Toni, M., Spisni, E., Griffoni, C., Santi, S., Riccio, M., Lenaz, P., Tomasi, V., 2006. Cellular prion protein and caveolin-1 interaction in a neuronal cell line precedes Fyn/Erk 1/2 signal transduction. J. Biomed. Biotechnol. 2006, 69469.
Umemori, H., Sato, S., Yagi, T., Aizawa, S., Yamamoto, T., 1994. Initial events of myelination involve Fyn tyrosine kinase signalling. Nature 367, 572–576.
Vey, M., Pilkuhn, S., Wille, H., Nixon, R., DeArmond, S.J., Smart, E.J., Anderson, R.G., Taraboulos, A., Prusiner, S.B., 1996. Subcellular colocalization of the cellular and scrapie prion proteins in caveolae-like membranous domains. Proc. Natl Acad. Sci. USA 93, 14945–14949.
Wang, J.Y., Miller, S.J., Falls, D.L., 2001. The N-terminal region of neuregulin isoforms determines the accumulation of cell surface and released neuregulin ectodomain. J. Biol. Chem. 276, 2841–2851.
Wen, D., Suggs, S.V., Karunagaran, D., Liu, N., Cupples, R.L., Luo, Y., Janssen, A.M., Ben-Baruch, N., Trollinger, D.B., Jacobsen, V.L., et al., 1994. Structural and functional aspects of the multiplicity of Neu differentiation factors. Mol. Cell. Biol. 14, 1909–1919.
Willem, M., Garratt, A.N., Novak, B., Citron, M., Kaufmann, S., Rittger, A., DeStrooper, B., Saftig, P., Birchmeier, C., Haass, C., 2006. Control of peripheral nerve myelination by the beta-secretase BACE1. Science 314, 664–666.
Williamson, R.A., Peretz, D., Pinilla, C., Ball, H., Bastidas, R.B., Rozenshteyn, R., Houghten, R.A., Prusiner, S.B., Burton, D.R., 1998. Mapping the prion protein using recombinant antibodies. J. Virol. 72, 9413–9418.
Yokozeki, T., Wakatsuki, S., Hatsuzawa, K., Black, R.A., Wada, I., Sehara-Fujisawa, A., 2007. Meltrin beta (ADAM19) mediates ectodomain shedding of Neuregulin beta1 in the Golgi apparatus: fluorescence correlation spectroscopic observation of the dynamics of ectodomain shedding in living cells. Genes Cells 12, 329–343.
Zhang, D., Sliwkowski, M.X., Mark, M., Frantz, G., Akita, R., Sun, Y., Hillan, K., Crowley, C., Brush, J., Godowski, P.J., 1997. Neuregulin-3 (NRG3): a novel neural tissue-enriched protein that binds and activates ErbB4. Proc. Natl Acad. Sci. USA 94, 9562–9567.